INSTITUTE
FOR
AEROSPACE STUDIES

UNIVERSITY OF TORONTO

NUMERICAL RECONSTRUCTION OF PART OF AN ACTUAL BLAST-WAVE FLOW FIELD TO AGREE WITH AVAILABLE EXPERIMENTAL DATA

by

S. C. M. Lau and J. J. Gottlieb

AUGUST 1984

UTIAS Technical Note No. 251
CN ISSN 0082-5263

NUMERICAL RECONSTRUCTION OF PART OF AN ACTUAL BLAST-WAVE FLOW FIELD TO AGREE WITH AVAILABLE EXPERIMENTAL DATA

by

S. C. M. Lau and J. J. Gottlieb

Submitted November 1983

UTIAS Technical Note No. 251

Acknowledgements

Many thanks are extended to Professor J. M. Dewey and Mr. D. J. McMillin of the University of Victoria for providing much detailed experimental data on TNT explosions for convenient utilization in the present research work. The interest, encouragement and additional experimental information both on TNT and ANFO explosions provided by Mr. N. H. Ethridge of the United States Army Ballistic Research Laboratory are also very much appreciated.

A debt of gratitude is also owed to Dr. T. Saito, who gave considerable advice and enlightenment in regard to the application of the random-choice method.

Many thanks are also extended to Mr. H. S. I. Sadek for his assistance in collecting and interpreting required experimental data. He also assisted in verifying the numerical simulations against experimental data, and for this we are very thankful.

It is also our pleasure to acknowledge Professor I. I. Glass of UTIAS for his interest in my work. His helpful suggestions and comments are greatly appreciated.

Financial assistance in the form of a student scholarship for the first author from the University of Toronto (Open Master Fellowship) is gratefully acknowledged. Additional financial assistance, especially for the extensive numerical computations, under a contract to the second author from the Defence Research Establishment Suffield, Ralston, Alberta, Canada, is acknowledged with many thanks.

Abstract

A new method of solution is presented and validated for the numerical reconstruction of a certain part of an actual blast-wave flow field of interest for planar, cylindrical and spherical explosions, away from the explosion source where the blast-wave has become sufficiently weak that real-gas effects are unimportant. This method involves, essentially, a trial-and-error process of constructing the best possible path of a fluid particle or equivalent piston at the upstream side of the flow field of interest such that the resulting flow field constructed numerically in front of the equivalent moving piston agrees as well as possible with all available although limited experimental data. For this study, the relatively new random-choice method has been suitably modified to easily handle the numerical computations of the nonstationary flow in front of the moving piston. Finally, the present method is used to reconstruct the flow field for past TNT and ANFO surface explosions, for which the blast-wave amplitudes are less than about 1 MPa. These new results are presented in convenient graphical and tabular form, scaled for the case of a 1-kg TNT surface explosion or its equivalent in a standard atmosphere, so that they can be utilized readily for different sized explosions at the same or other atmospheric conditions.

Table of Contents

Notation

a	speed of sound
C	contact surface
$\vec{C}$	compression wave
C^+	positive-sloped characteristic line
C_d	drag coefficient
C_v	heat capacity per unit mass at constant volume
e	total energy per unit volume $[p/(\gamma-1) + \rho u^2/2]$
F	vector of terms dependent on G in Eq. 1
G	solution vector in Eq. 1
I	vector of inhomogeneous or source terms in Eq. 1
k	denotes $[(\alpha+1)\rho_2(u_3-u_2)^2]/[(\alpha-1)^2 p_2]$
L	characteristic length
M	Mach number u/a
p	static pressure
$\bar{p}$	normalized static pressure p/p_1 used in appendix A
r	radial distance
$\bar{r}$	normalized radius $r/\bar{R}$ used in appendix A
r_0	initial radius of a fluid particle
r_p	radial distance of a fluid particle
Δr	radial distance between adjacent grid points
R	gas constant
$\bar{R}$	characteristic radius specified for a particular problem
Re	Reynolds number $\rho Lu/\mu$
$\vec{R}$	rarefaction wave
$\vec{R}_h$	head of a rarefaction wave

Notation (continued)

$\vec{R}_t$	tail of a rarefaction wave
S_r	Sachs's scaling factor for distance
S_t	Sachs's scaling factor for time
$\vec{S}$	shock- or blast-wave front
t	time
$\bar{t}$	normalized time $a_1 t/\bar{R}\sqrt{\gamma}$ used in appendix A
t_a	time of arrival of shock wave at a certain radius r
Δt	time interval of a full time step in the numerical computations
Δt^*	time interval of a half time step in the numerical computations
T	static temperature
u	flow or particle velocity
$\bar{u}$	normalized flow velocity $u\sqrt{\gamma}/a_1$ used in appendix A
V	piston velocity
W	mass of an explosive charge in kilogram
W_0	standard TNT mass of 1 kilogram
x	planar distance
Δx	planar distance between adjacent grid points
α	denotes $(\gamma+1)/(\gamma-1)$
γ	ratio of the specific heats for a perfect gas
μ	coefficient of viscosity
Δp	overpressure of a shock- or blast-wave
ρ	static density
η	geometric parameter in Eq. 1, where it is equal to 1, 2 or 3 for planar, cylindrical or spherical geometries, respectively

Subscripts

0 denotes standard atmospheric conditions (p_0 = 101.33 kPa, T_0 = 288.15 K, a_0 = 340.3 m/s)

1 denotes ambient conditions in the quiescent gas ahead of the shock or blast wave

2 denotes the flow conditions ahead of the shock or rarefaction wave generated by the motion of a piston

3 denotes the flow conditions behind of the shock or rarefaction wave generated by the motion of a piston

1. INTRODUCTION

1.1 Background Information

Blast waves from nuclear and chemical explosions have been an interesting subject of much intensive gasdynamic research during the past fifty years. Initial work in obtaining the analytical solution for strong blast waves from a point-source explosion (without counterpressure) was done independently in the 1940s by von Neumann in the United States [1], Sedov in the Soviet Union [2 & 3] and Taylor in England [4]. Sedov also obtained the solutions for strong blast waves from both line-source and sheet-source explosions. Other work of relevance can be found in Refs. 5 and 6. By resorting to numerical methods the assumption of strong blast waves or negligible counterpressure was relaxed during the 1950s, and numerical solutions for the blast wave from a point-source explosion with counterpressure were then obtained by Goldstine and von Neumann [7], Brode [8] and Korobeinikov [9]. Approximate analytical solutions of much interest were also found by Sakurai [10] and Bach and Lee [11]. These studies ignored all of the detailed explosion characteristics of nuclear and chemical charges, as well as real-gas effects. However, since the 1950s, the nature of the detonation and the effects of the real gases have been incorporated in the best numerical codes for more realistic predictions of blast-wave flow fields (e.g., see Refs. 12 to 21).

Most of the initial research on predicting blast waves from explosions was done to provide a good understanding and characterization of the physics of such phenomena. However, the driving force behind this research was to develop the capability of assessing blast-wave effects on military and civilian structures, equipment and personnel. The development of a prediction capability for blast waves and their effects was accompanied by an experimental program that involved measurements of both the blast-wave flow properties and responses of military and civilian structures and equipment. Nuclear tests were originally conducted during the 1940s and 1950s, mainly for weapons development but also for studying blast-wave effects [22 & 23]. With the advent of the ban on the atmospheric testing of nuclear weapons in 1961, large-scale chemical explosions having a yield of up to 500 tons of trinitrotoluene (TNT) have since been used to simulate as well as possible a nuclear-blast environment for component and full-scale testing purposes [24]. Such experiments with interesting names like SAILOR HAT (1965), PRAIRIE HAT (1968), DIAL PACK (1970), MIXED COMPANY (1972), DICE THROW (1976), MISERS BLUFF (1979), MISTY CASTLE (1981) and DIRECT COURSE (1983) are still continuing today, and they are providing valuable information on the effects of blast waves on structures and equipment.

In field trials involving large chemical explosions for simulating a nuclear-blast environment, the structure, equipment or simply target to be tested is located at a suitable test site away from the explosive charge, where the blast wave has a certain desired shape, amplitude and positive-overpressure amplitude (see Fig. 1). To correlate response and damage data of the target with various blast-wave flow properties, and also to confirm theoretical and empirical calculations of target response, it is necessary to have a thorough and accurate knowledge of all of the flow properties of the incident blast wave on the target at the test site [25]. For example, if a prediction technique for the dynamic drag response of a simple structure is to be confirmed, then a large number of flow parameters is needed. The flow velocity u and sound speed a define the flow Mach number M (u/a); and the density ρ, particle velocity u,

characteristic length L, and dynamic viscosity μ (which depends only on temperature T) define the Reynolds number Re ($\rho Lu/\mu$). These two numbers (M, Re) allow the drag coefficient C_d to be selected from previously known experimental data. This empirical coefficient C_d and dynamic pressure $\rho u^2/2$ can then be used as input data for a structural response calculation, which in turn yields the detailed motion of the structure [26 & 27]. Finally, the validity of the prediction technique can be assessed by comparing the predicted motion and measured response data [26 & 27].

The blast-wave flow properties at a particular test site can, of course, be predicted by employing one of the more suitable numerical computer codes mentioned previously [12 to 21]. However, such numerical computations are very involved, because a sophisticated model of the charge detonation process and an accurate equation of state for real gases are required. Further, the numerical modelling should include the turbulent mixing of the detonation products with the surrounding air and the resulting afterburning, radiation losses from the high temperature gases, energy losses due to ground cratering (if applicable), and a means of reducing accumulating numerical errors. In order to get meaningful results, these codes also require the use of high-speed computers with their associated high computational cost. Such sophisticated computer codes and high-speed digital computers are not readily available to and even usable by a typical researcher. Furthermore, the predicted blast-wave flow properties at the test site are generally not in good agreement with available but limited measured data taken during the test. For example, the predicted and measured peak overpressures and positive-overpressure durations of the blast wave can differ by typically 10% and 20%, respectively. This is disturbing and unacceptable to the structural engineer or researcher in charge of the structural test at the test site. To overcome this problem, some of the computer codes employ empirical or so-called "fudge" factors to improve the agreement between the predicted and measured flow properties. As a consequence, the computer calculations then become more of a numerical simulation of the available experimental results than a "bona fide" prediction.

Although one might initially think that sufficient experimental data on blast-wave flow properties for structural response tests have been gathered at test sites over the past thirty years, this is not true. Early instrumentation was not sufficiently well developed to get good quality field measurements, and even today some instrumentation cannot give reliable results from field trials. More importantly, however, is that sufficient instrumentation is simply just not available today to record at a test site of interest the consistent set of blast-wave flow properties needed for structural response predictions. Limited experimental data of good quality are, of course, available [28 to 36]. The consistency and accuracy of some of these results for explosions of TNT and ANFO (ammonium nitrate mixed with fuel oil) are apparent from the recent work of Sadek and Gottlieb [37]. Available experimental information can be used, of course, to partially verify numerical predictions of the blast-wave flow field, but they are generally insufficient for defining the blast-wave loading on most structures.

1.2 Description of Problem

From the remarks made in the preceding section, it should be obvious that there is a need for a good, simple method of predicting both accurately and easily a consistent set of blast-wave flow properties at the test site in an explosion field trial for testing structures and equipment. Such a simple

possible method that is relatively easy to use would have to dispense with the complex details of a detonating and expanding charge, real-gas effects, and doing both tedious and time-consuming numerical computations in a step-by-step manner from the charge all the way out and probably beyond the particular test site. If these details could be eliminated, then other equivalent information would certainly have to be included as a replacement, otherwise the flow field at the test site could not be determined realistically. One obvious form of the equivalent information might be the available, but limited, experimental results taken at the test site during the field trial. Then the method would consist, essentially, of numerically reconstructing only a part of the entire blast-wave flow field, at the test site which is away from the charge, to agree as well as possible with all available experimental information.

The advantages of such a possible method are fairly obvious but given here for completeness. Firstly, blast-wave flow-field computations would now be fewer and more quickly done, because the required spatial extent of the flow field would be smaller, being confined to a certain narrow spatial region containing the test site. Secondly, the complexities of including the details of the detonation and expansion of the charge would be eliminated. Thirdly, the flow-field computations at the test site where the blast wave is sufficiently weak such that real-gas effects are negligible would at each time step be much simpler and faster, because the air would be treated simply as a thermally and calorically perfect gas. Finally, the numerical computations needed to obtain the desired consistent set of flow properties at the test site would likely be sufficiently simple and quick to perform that most researchers could do them easily on a normally available high-speed digital computer like an IBM-3033 or a CDC-6600. It is worth mentioning, however, that the computed flow field by such a method would be only as accurate as the available experimental information on which it is based.

If the blast-wave flow field can be successfully reconstructed numerically to agree with available experimental data, it should be noted here that the results of such a method would be a numerical simulation rather than a numerical prediction. However, this type of numerical simulation would be more reasonable than that obtained by using any of the previously mentioned computer codes [12 to 21] which make use of empirical or "fudge" factors to get better agreement with experimental data.

1.3 Previous Studies

The idea of reconstructing the blast-wave flow field at a test site to agree with available experimental data is not new. Because of the need for such flow-field reconstructions, as mentioned in the previous section, a number of different methods have been developed and tested during the past thirty years. These will now be reviewed briefly in this section.

The earliest and crudest approximate method involved obtaining, from a single reliable time history of the overpressure at the test site, all of the other blast-wave flow properties [22]. In this method the flow past the test site was first assumed to be isentropic, such that the overpressure could be used directly with simple, standard isentropic equations to yield the rest of the thermodynamic properties consisting of the density, temperature and sound speed. Then, the particle velocity and dynamic pressure were assumed to be directly proportional to the overpressure and the square of the overpressure, respectively. The first assumption made to obtain the thermodynamic properties

is reasonable only for weak blast waves having a peak overpressure less than about 100 kPa, and the second assumption to obtain the dynamic flow properties is almost never reasonable. Additional details of this approximate method and an assessment of its accuracy are given in Ref. 25.

It is worth mentioning that this approximate method was not presented in Ref. 22 as a practical means of obtaining realistic blast-wave flow properties at a test site. Rather, it was given there more to illustrate the shape of the various flow property signatures and their approximate interrelationships. It is unfortunate that such a simple and inaccurate method was adopted in so many studies of the drag coefficient of cylinders and the drag response of simple and complex structures during the 1970s [26 & 38 to 54], and that the particular empirical relationship used for the viscosity of air as a function of temperature was also inaccurate [55].

The method developed by Makino and Shear [56] for obtaining the blast-wave flow properties at a particular test site has a solid theoretical founding. They start the flow-field reconstruction from a known segment of a shock path or trajectory (blast-wave front) that includes the test site (see Fig. 2). The analytical shock trajectory in terms of radius versus time that is used in the calculations is based on a curve fit to experimental shock arrival times at a series of increasing distances from the explosion center. This shock trajectory is then used as a boundary with known conditions from which to commence the numerical computations for the reconstruction of the flow field behind the blast-wave front. The flow-field reconstruction is initially done numerically with the tedious method of characteristics, in Lagrangian rather than Eulerian coordinates.

The size of the reconstructed flow field is limited to a triangular like region bounded by the shock trajectory, a particle path and a positive-sloped characteristic line, as depicted on Fig. 2. This region is limited in size even when the shock trajectory is extended indefinitely to an infinite radius, because at large radii the positive-sloped characteristic lines and the weak blast-wave trajectory tend to the same slope or speed (ambient speed of sound). The limitation on region size is the major disadvantage of this method. Even when an abnormally long segment of the shock trajectory is known experimentally, only a small part - about one third - of the required flow field can be reconstructed to obtain the blast-wave flow properties.

The method of Makino and Shear [56] was suitably extended by Gottlieb and Ritzel [25], such that a larger region of the flow field could be computed (see Fig. 3). Although the numerical calculations were done in Eulerian instead of Lagrangian coordinates, the tedious method of characteristics was also employed. The blast-wave flow field behind the known shock trajectory (region 1 in Fig. 3) was computed first, as in the previous method, by starting at the known shock boundary and reconstructing the flow field away from it. Then, by employing an additional time history of the overpressure measured at the test site as new information, the flow field was extended to later times (region 2 in Fig. 3). Sufficiently long time histories of the flow properties at the test site could then be obtained from the flow-field computations. Note that in this method the segment of the shock trajectory needs to be known only at radii preceding the test site, whereas in the previous method a much longer segment was required that included the test site.

Three main disadvantages of this method are briefly outlined here for interest. Firstly, the method of characteristics is tedious to apply with as

many as thirteen separate cells required in the computations. Secondly, some characteristics of the same family sometimes crossed and this problem was very difficult to handle numerically. Although such crossings of characteristics normally indicate the presence of a shock wave imbedded in the flow field, they were sometimes due simply to numerical inaccuracies. Finally, the method could not handle imbedded shocks in a realistic manner, unless an additional sophisticated computational procedure was developed.

Another method that is very original in its approach to reconstructing the blast-wave flow field from available experimental data is that due to Dewey [30, 34 & 36]. During the explosion, the motion of numerous small particle tracers in the form of smoke trails or puffs are photographed with a high-speed camera. The lengthy reduction of this photographic information yields numerous particle paths in the flow field, as well as their associated flow velocities and accelerations. Furthermore, a subsequent analysis based on the gasdynamic equations of motion was developed by Dewey for reconstructing all of the other blast-wave flow properties from this original measured data. Good results have already been obtained from TNT explosion trials [30, 34 & 36] and also from a propane-oxygen explosion [57]. The success of this fairly sophisticated method is dependent on conducting good photographic measurements of numerous particle tracers in the blast-wave flow in an explosion field trial.

Finally, another sophisticated method for reconstructing the blast-wave flow field at a specific test site was also developed by Celmins [58], which is based partly on much earlier theoretical work by Makino [59]. In this method, numerous time histories of the overpressure measured at different radii during an explosion trial were used in conjunction with the governing flow equations, to reconstruct numerically the flow field from these measurements. The success of this method depends mainly on having available numerous good quality overpressure measurements from the field trial.

The last two methods by Dewey and Celmins are well founded and worthwhile. However, these methods are presently set up to deal exclusively with either measured particle paths or measured overpressure-time histories. In the case of some explosion trials, however, measured particle paths are simply not available or sufficiently numerous (e.g., for ANFO explosions), and measured overpressure signatures might also not be sufficiently numerous. Consequently, there is still a need for a method to reconstruct the blast-wave flow field from all types of available experimental information, whether it be particle paths, overpressure signatures, density signatures or shock trajectories, as well as any combination of these measurements. It would be beneficial if this new method was even simpler to use than the previously mentioned methods and yet just as accurate for the reconstruction of the blast-wave flow field.

1.4 Current Study

In the present study a new method of solution is both introduced and validated for reconstructing numerically only one part of an actual blast-wave flow field at a particular test site, to agree with only one type or all types of available experimental data. This method is applicable to reconstructing planar, cylindrical and spherical explosion flow fields, although spherical explosions are of prime interest here. The new method is relatively easy to understand and apply, as the reader will observe later, and reconstructed flow fields are just as accurate as those from the two past reconstruction methods of Dewey [30, 34 & 36] and Celmins [58].

The concept and solution procedure for the present method are now outlined briefly. This method involves a trial-and-error process of selecting a piston path at the upstream side of the test site and then computing the flow field in front of the moving piston, at the test site (see Fig. 4), such that the computed flow-field properties are in the best possible agreement with all available but limited experimental or other useful information. The first step is to initially guess a suitable piston path that would hopefully simulate as closely as possible the path or trajectory of one fluid particle in an explosion of interest (see Fig. 4). The second step is to numerically construct the flow field that would occur in front of this moving piston. The third step is to compare the calculated flow properties from the flow field to all available experimental data from an explosion trial at the test site and note the various types of disagreement. The fourth step would be to judiciously modify the piston path to improve the agreement between the numerically computed and experimental results. The last step is then repeated as many times as desired until the best possible agreement is obtained, or the experimental results are simulated as well as possible. In this trial-and-error manner, the blast-wave flow field at a test site is reconstructed.

Based on past theoretical shock-tube and blast-wave studies (e.g., see Refs. 1 to 6, 12 & 14, and 60 & 61), it is obvious that the one-dimensional flow fields in front of a particle path and a moving piston having identical motions are also theoretically identical (see Fig. 4). Consequently, the flow field ahead of a particle path can theoretically be reproduced by a computation of the flow field in front of a moving piston that precisely replicates this particle path. These are the basic concepts on which the present method of using a piston motion and experimental data for the reconstruction of blast-wave flow fields are based. Unfortunately, particle paths from actual explosions on which piston motions might be based for reconstructing actual blast-wave flow fields are generally not available. However, other types of experimental information are normally available, and this information is usually more extensive but still very limited. This is the main reason why the piston path must be initially guessed and eventually established from a trail-and-error method, along with the blast-wave flow field, such that the latter agrees as well as possible with all available experimental or other useful information.

It is worth reiterating here that experimental information, if accurate, contains all of the real-life effects of explosions, including, for example, the detonation process, real gases with dissociation and ionization, energy losses due to radiation, and also energy losses due to ground cratering. If a numerical simulation of available experimental information can be achieved by the present or another method, then the resulting computed flow field will also contain these effects, as is desired. This is one of the main advantages of a numerical simulation of experimental data over a purely numerical prediction, especially when the analysis for a numerical prediction can include real-life effects in only an approximate manner, which almost always leads to imprecise numerical predictions.

The material presented in this report regarding the reconstruction of a blast-wave flow field to agree with experimental data is organized in the following manner. The analysis and solution procedure for this problem involving the construction of flow fields in front of moving pistons with the random-choice method are given first in chapter 2. The analysis and resulting computer program are then validated in chapter 3, by reconstructing nonstationary flow fields for certain piston motions for which known solutions are available (to provide the valuable confirmations). Reconstructed flow fields are then

presented for both TNT and ANFO surface explosions in chapter 4. These results are given in convenient graphical and tabular form, scaled for the case of a 1-kg TNT surface explosion or its equivalent in a standard atmosphere, such that they can be utilized easily for different sized explosions at the same or other atmospheric conditions. The concluding remarks and references finally follow in chapters 5 and 6, respectively.

2. ANALYSIS AND SOLUTION PROCEDURE

In order to determine the nonstationary flow field in front of a moving piston, for the present study, the general equations of motion for an inviscid, nonheat-conducting, compressible gas are needed. These equations are the same, of course, as those normally used for numerical computations of blast-wave flow fields. In vector notation, the continuity, momentum and energy equations for one-dimensional planar, cylindrical and spherical flows are given by [62 & 63]

$$\frac{\partial}{\partial t}[G] + \frac{\partial}{\partial r}[F(G)] = -I(G), \qquad (1)$$

where

$$G = \begin{bmatrix} \rho \\ \rho u \\ e \end{bmatrix}, \quad F(G) = \begin{bmatrix} \rho u \\ \rho u^2 + p \\ u(e + p) \end{bmatrix}, \quad I(G) = \frac{(\eta - 1)}{r} \begin{bmatrix} \rho u \\ \rho u^2 \\ u(e + p) \end{bmatrix}$$

In these expressions, p, ρ, u, e, r and t denote static pressure, density, flow velocity, total energy per unit volume, radial distance and time, respectivity. The total energy e is given by $e = p/(\gamma-1) + \rho u^2/2$, where the first term is the internal energy (from $\rho C_v T$), the second term is kinetic energy, and the symbol γ denotes the ratio of the specific heats of the gas. Also, η equals 1, 2 or 3 for flows with planar, cylindrical or spherical symmetry, respectively. This means that the flow field has been assumed implicitly to be one dimensional, which is a common assumption adopted for studies of the present type. For example, for chemical explosive charges located away from reflecting surfaces and a hemispherical or even spherical charge located right at the ground or other reflecting surface, the blast-wave flow field at a relatively short but practical distance away from the explosion center is for all practical purposes one dimensional or radial [30, 34 & 36].

In the present study the flow field is reconstructed away from the explosion center, where the blast-wave pressure and temperature are sufficiently low that real-gas effects are unimportant. As a consequence, the continuity, momentum and energy equations can be closed by using a simple, well-known equation of state for a perfect gas. Hence, $p = \rho RT$, where R and T denote the gas constant and static temperature, respectively. Furthermore, the sound-speed relation $a^2 = \gamma RT = \gamma p/\rho$ is also employed implicitly in this study, in order to relate the sound speed a to the temperature T.

The set of partial differential equations given by Eq. 1 can be solved by using the method of characteristics, finite-difference methods and the relatively new random-choice method (RCM). The RCM is employed in the present work

because it is particularly well suited for solving one-dimensional nonstationary flow problems involving shock-wave and contact-surface discontinuities. In this method, both shock waves and contact surfaces are well defined with sharp fronts, unlike the results from finite-difference methods in which they are smeared over many grid zones, because of the use of artificial viscosity terms added explicitly to the equations and/or the implicit presence of numerical viscosity.

It is worth mentioning that the RCM was invented by Glimm [64] and first used practically for solving nonstationary planar flow problems by Chorin [65]. The operator-splitting technique introduced to the RCM by Sod [66], in order that the solution for one-dimensional planar flows could be extended to include both cylindrical and spherical flows, is also used in the present study. Note that the RCM is a first-order, explicit numerical scheme that repeatedly solves a Riemann or shock-tube problem between grid points, to get the solution at the next time level. Although the details of this method can be found in Ref. 64 to 66 and Ref. 17, a brief description of the RCM is included herein, in order that modifications to be introduced later in this section will become more understandable.

The mesh or grid layout in the time-distance or physical plane for the RCM solution procedure is shown in Fig. 5a. At each time level the grid points are distributed uniformly along the distance axis, with a regular spacing of Δx or Δr between adjacent grid points. However, the grid points do alternate in location from one time level to the next, being at the midpoints between successive grid points of the previous time level. As a result of this alternating grid system, computations made from one time level to the next are done in a so-called half time step, and computations made for two consecutive half time steps are said to be done for a full time step. The full time step has a time interval of Δt. Each half time step Δt^* should be controlled by the so-called Courant-Friedrichs-Lewy stability criterion [61 & 62], which restricts the half time step such that any type of wave cannot travel more than one-half of a grid zone ($\Delta x/2$) in the time Δt^*, to ensure numerical stability in the computations. However, for simplicity and mostly for a savings in computational cost from not always checking the Courant-Friedrichs-Lewy criterion at each grid computation, the time interval for the second half time step is normally forced to be equal to that for the first half time step. Because this technique does not cause any apparent difficulties with numerical stability in the computations, it is also used in the present numerical work. Note that, because of the stability criterion, the time interval Δt from one full time step to the next will generally be different.

When a complete set of initial conditions are specified at each of two grid points, on time level t (see Fig. 5a), a Riemann or shock-tube problem can be established and solved analytically for a planar flow [64 & 65]. Initial conditions for the RCM solution normally consist of knowing the pressure, density and flow velocity at each grid point for the first time level. The particular solution and its details are not repeated here, but they can be found in Refs. 64 and 65, as well as Ref. 17. However, the shock-tube wave pattern consisting of a shock wave, contact surface and rarefaction wave are depicted in Fig. 5b. These waves and the contact surface separate growing quasi-steady or steady flow regions (i.e., regions 1, 2, 3 and 5 in Fig. 5b). Region 4 is a simple nonstationary region within the rarefaction-wave fan.

When the flow properties are determined from the shock-tube solution for each of the five states, the flow properties can then be assigned to the inter-

mediary grid point at the next time level. This assignment of flow properties to the intermediary grid point involves a fairly simple random sampling procedure [64 & 65], giving the random-choice method its name. By choosing a random-number between -1/2 and +1/2 from a uniform distribution, the flow properties from one of the five states is selected for assignment to the intermediary grid point at the next time level [64 & 65]. Because the random-number algorithm can affect the smoothness or quality of the computed results [67], sometimes in a drastic manner, the van der Corput algorithm which is recommended in Ref. 67 is adopted for this study.

For the case of computations involving both cylindrical and spherical flows, the planar solution is always completed first. This initial solution is approximate, and it must then be corrected for the change in area, by using the operator-splitting technique [66]. Note that this correction should be made at the end of each half time step, not just over a full time step; otherwise, the computed results will normally be inaccurate and not meaningful. The general solution procedure involves solving the shock-tube problem between successive grid points at one time level, in an ordered sequence from left to right or vice versa across the flow field. When this is done and the flow properties are all known at the next time level, the process is then repeated from one time level to the next.

At the two outer extremities of the flow field, boundary conditions must be specified for the outermost grid points at alternate time levels. Closed and open ended flow fields, corresponding to closed ducts with solid reflecting walls and continuous ducts with the same trends in area, respectively, which are normally encountered in duct or pipe flows, are easily specified boundary conditions [17]. However, other boundary conditions like that for a subsonic flow field open to the atmosphere and for a moving piston in a flow field are more difficult to specify properly. The latter boundary condition for a moving piston is fundamental to the current study, and details of the incorporation of this boundary condition in the RCM for the present study is now documented here in detail. This boundary condition will be of interest to all RCM work that involves piston motions or nonstationary piston-driven flows.

For the motion of a piston in a planar duct the elemental wave patterns needed for the RCM solution are depicted in Fig. 6. For the specific case when the piston velocity (V) exceeds the flow velocity (u_2) ahead of the piston (at the right grid point), a shock wave must then exist between the piston and this grid point, as shown in Fig. 6a. For the other specific case when the piston velocity is smaller than the flow velocity at the right grid point, a rarefaction wave must then exist between the piston and this grid point, as shown in Fig. 6b. Note that these two elemental wave patterns for the motion of a piston are simply complementary portions of the elemental wave pattern for the Riemann or shock-tube problem shown in the previous figure.

In order to handle the first case of a piston preceded by a shock wave in the RCM solution, the flow properties consisting of the flow velocity u_3, pressure p_3, and density ρ_3 in state 3 (Fig. 6a) between the shock wave and piston are required. These properties have to be computed from the known piston velocity V and known flow conditions consisting of the flow velocity u_2, pressure p_2 and density ρ_2 in state 2 (Fig. 6a) ahead of the shock wave. Because the piston path given by x(t) or r(t) is specified in the present problem, the piston velocity (V = dx/dt or dr/dt) is also known. As a consequence, the flow velocity u_3 then equals the piston velocity V. From a knowledge of the piston or flow velocity behind the shock wave and the known flow conditions

in front of it, the well-known Rankine-Hugoniot equations [62 & 63] can be manipulated to give the pressure

$$p_3 = p_2 [(1 + k\alpha/2) + \sqrt{k(1 + \alpha + k\alpha^2/4)}] , \qquad (2)$$

where

$$\alpha = (\gamma+1)/(\gamma-1) \qquad \text{and} \qquad k = [(\alpha+1)\rho_2 (u_3 - u_2)^2] / [(\alpha-1)^2 p_2] .$$

The density

$$\rho_3 = \rho_2 [1 + \alpha p_3/p_2] / [\alpha + p_3/p_2] \qquad (3)$$

then follows directly from the Rankine-Hugoniot relations.

In order to handle the other case of a piston with a rarefaction wave in the RCM solution, similar flow properties in state 3 (Fig. 6b) between the piston and the rarefaction-wave tail must be determined in terms of the specified piston velocity and similar known conditions in state 2 in front of the rarefaction-wave head. As before, the particle velocity u_3 equals the known piston velocity V. From a knowledge of the flow velocity u_3 and the known conditions (u_2, p_2 and ρ_2) in front of the rarefaction wave, the isentropic equations for a rarefaction wave [62 & 63] can be expressed as

$$p_3 = p_2 [1 + (\gamma - 1)(u_3 - u_2) / 2a_2]^{2\gamma/(\gamma-1)} \qquad (4)$$

and

$$\rho_3 = \rho_2 \left(\frac{p_3}{p_2}\right)^{1/\gamma} \qquad (5)$$

to get the pressure and density in state 3.

For the case of piston motions with either a shock or rarefaction wave, the flow properties p_2, ρ_2 and u_2 in state 2 for the RCM are those for the right grid point according to Fig. 6. The solution for p_3, ρ_3 and u_3 in state 3 from Eqs. 2 to 5 can now be assigned for convenience in the RCM to the left grid point, the one circled in Fig. 6. By doing this the initial conditions for an elemental shock-tube problem between these two adjacent grid points are established. Then the flow properties at the intermediary grid point at the next time level can be found simply by using standard algorithms already coded into the RCM computer program for solving the shock-tube problem. The resulting solution that is then returned by the standard RCM algorithms will have a contact surface (or piston path) with the correct originally specified velocity. If the first case of a piston with a shock wave is under consideration (Fig. 6a), the shock-tube wave pattern will consist of a shock wave of the correct strength and a rarefaction wave that is simply a Mach wave (with no strength), which is the desired pattern. If the second case of a piston path with a rarefaction wave is under consideration (Fig. 6b), the shock-tube wave pattern will then consist of a rarefaction wave of the correct strength and a shock wave that is a simple Mach wave (with no strength), which is again the

desired pattern. Hence, the standard RCM algorithms provide the required solutions corresponding to the originally specified piston velocity and the known conditions at the right grid point.

With some special considerations taken into account before each half time step, therefore, the boundary condition for a specified piston motion through the flow field can be handled fairly easily. Rightward and leftward moving piston paths are depicted in Fig. 7, and the flow field to be calculated is on the right-hand side of the piston path. Based on the previous work, special considerations come into play at each time level or half time step to get the flow properties at the circled grid point that lies immediately to the left of or behind the piston path. Flow properties at all grid points farther to the left of the circled ones (behind the piston path) are not required. Finally, in the usual RCM solution procedure, the flow properties at each time level for the planar flow case can be corrected if necessary for flows that are not planar but are either cylindrically or spherically symmetric.

For a number of nonstationary flow problems that involve piston-driven flows, the piston path may be known or specified. If this is the case, therefore, the flow field can be computed directly by employing the RCM with the piston boundary condition presented earlier. However, the piston path is not known in advance for many problems, including the case of the reconstruction of part of the blast-wave flow field from an explosion to agree with available experimental data. In such cases the computation of the flow field can be much more difficult and also more challenging. The logic involved in the present study for reconstructing only a part of the blast-wave flow field to agree with experimental data at a test site in an explosion is now outlined.

The first step is to simply guess a piston path that is located between the explosion center and the test site, on the upstream side of the flow field. This initial guess of the piston path $x(t)$ or $r(t)$ includes the initial distance-time coordinates, initial slope or piston velocity, and profile or shape, as illustrated in Fig. 8a. Previous theoretical and experimental knowledge, as well as practical experience with the present method, would be very beneficial, of course, but it is not absolutely essential. In the present study, the guessed path is initially specified with approximately twelve to fifteen discrete distance-time coordinates. These coordinate points are normally spaced closer together where the piston path is believed to have a higher curvature or velocity. Furthermore, the coordinate points are distributed fairly smoothly without jaggedness along the piston path (see Fig. 8a), based on a quick subjective assessment, unless the piston path is expected to have an abrupt kink or change in slope resulting from a sudden change in piston velocity.

The second step is to spline a continuous curve through the coordinate points (Fig. 8a), to get an analytical function for the piston path, which will in turn easily yield the path velocity and acceleration by differentiation. In the present study, a cubic spline based on a piecewise continuous third-order polynomial is employed, and its logic and computer-program listing are given in Ref. 68. However, similar and probably equivalent cubic splines with the same and other boundary conditions are also available in the International Mathematical and Statistical Libraries (IMSL), and also many standard mathematically oriented engineering text books (e.g., see Ref. 69).

Two boundary conditions are required at each end of the cubic spline. These are the coordinate position and the slope of the curve at both ends. At the initial end of the splined curve (see Fig. 8a), both the coordinate point

and the slope are chosen to agree with experimental or other data. The slope or piston velocity is normally set equal to the measured flow velocity. (For an experimentally or other known shock trajectory, the particle velocity would normally be obtained by using the Rankine-Hugoniot relations.) At the other end the coordinate point is initially guessed, and the slope or velocity is set equal to an initially undetermined constant, by specifying that the second time derivative or acceleration is zero.

The following points regarding cubic splines are worth mentioning here. A cubic spline passes through every coordinate point specified for the piston path, and it does this with a minimum of curvature. Any interpolation between splined points is done readily. A continuous splined curve could be made to include a slope discontinuity (other than the initial one), corresponding to a sudden change in piston velocity; however, a highly curved part of the path (without a discontinuity) will essentially accomplish the same result. Hence, a shock wave can be easily produced in the flow field by the cubic-splined piston motion, if coordinate points are put close together with very rapid or discontinuous curvature, and a shock wave imbedded in the flow field can be handled. The technique of using coordinate points with the cubic spline to represent the piston path is much more flexible, or has the capability of more degrees of freedom, than that employing some specifically selected analytical function like a polynomial curve.

The third step consists of computing as much of the flow field in front of the specified or guessed piston path as desired (Fig. 8b). This is done in the manner described previously in this section, by using the RCM with the piston boundary condition.

The fourth step is to compare some of the computed flow-field properties to all available experimental or other useful information. The various types of disagreement and the magnitudes of the differences should be noted at this stage. The assessment of the disagreement could be either qualitative or quantitative (or both). A quantitative assessment would, of course, be the best approach; however, this would require some or possibly a lot of additional analysis. For example, a least-squares indicator for all of the differences between the computed and available data might be needed. This indicator would no doubt change from one example to to the next, because the type of available data would also probably change with each new example. For simplicity in the present study, only a qualitative or subjective assessment of the disagreement is utilized. This generally involved looking at many differences between the computed and all available information, which were displayed conveniently in graphical form. Such a form is easier to digest than a table of numbers.

The final step is to modify the initial piston path and repeat all steps after the first (Fig. 8c). The piston path should be modified in such a manner that the disagreement between computed flow properties and all available comparison information is reduced, as compared to the previous case. This step is then repeated as many times as desired, until the best possible agreement is obtained. In this trial-and-error approach, only a few coordinate points near the beginning of the piston path are normally adjusted first, and these are changed only slightly, in order to discover the trend of their effects on the flow-field properties and the resulting disagreement with available comparison data. The type and degree of modification to the coordinate points is generally quite obvious fairly quickly, and the trial-and-error process to a final acceptable solution is not unduly tedious. In the above manner, the available experimental or other information can be simulated numerically.

The analysis presented in this chapter has been embodied in a FORTRAN VII computer program or code. This program can predict planar, cylindrical and spherical flow fields in front of a moving piston whose path is specified in advance. The listing of this computer program is given in appendix A not only for interest but also for future reference and use. This FORTRAN VII program has been developed to run on a Perkin-Elmer 32-bit computer with a 3250 central processor and a high-speed PRINTRONIX printer and VERSATEC V-80 plotter. It is used to generate all of the results that are given in the next two chapters.

3. VALIDATION OF ANALYSIS AND COMPUTER PROGRAM

The analysis and computer program are validated in this chapter, first by reconstructing flow fields in front of moving pistons and then by comparing the results from these computations to those from either exact analytical solutions or previous numerical ones for such piston motions. This is done here for five different examples of piston motions, which are listed as follows:

a) constant-velocity piston motion to produce a shock wave,

b) constant-velocity piston motion to produce a centered rarefaction wave,

c) accelerating piston motion to produce a focussed compression wave,

d) accelerating piston motion to produce a noncentered rarefaction wave,

e) constant-velocity spherical piston motion to produce a shock wave.

The first four examples (a to d) are all for the case of planar piston and wave motions, whereas the final example (e) is for piston and wave motions that are spherical. The last example is included so that the operator-splitting technique is employed at least once. Exact analytical solutions for the first four examples can be found either in Refs. 60, 62 and 63 or obtained from the theory presented therein. The solution for the last example is the numerical solution of two coupled differential equations of fairly simple form, whose derivation was given first by Taylor [70], for the self-similar shock-wave flow field in front of an expanding spherical piston.

For each example the compressible gas is perfect air with a specific-heat ratio of 1.400. Before the piston and wave motions commence, the air is taken to be quiescent (with no initial motion or flow velocity) and at standard atmospheric conditions (p_0 = 101.33 kPa, T_0 = 288.15 K, and a_0 = 340.29 m/s). Finally, for the RCM computations of the flow field, note that the number of grid zones per meter of flow field is 360 for the first example (a), 180 for the second example (b), 400 for both the third and fourth examples (c and d), and 200 for the last example (e). The number of grid points employed in the RCM computations for each example are sufficiently numerous to get good quality results; that is, the numerical noise or randomness introduced into the numerical results by the RCM is reduced to an acceptably low level.

Example 1: Constant-Velocity Piston Motion to Produce a Shock Wave

In this first problem the piston is pushed into quiescent air at a constant velocity of 143.8 m/s, or at a Mach number of 0.423. This would theoretically produce a simple flat-topped shock wave (see Figs. 9 and 10), with a

shock Mach number of 1.285 and strength or pressure ratio of 1.760, according to the Rankine-Hugoniot relations. The computed results from the RCM with the piston boundary condition are virtually the same for this simple test problem, which is just one of the elemental wave patterns shown earlier (Fig. 6a). The main reason for making a test case of this first example is to verify that this elemental wave pattern and its flow properties can be reproduced correctly by the modified RCM. This is an essential step before undertaking more complex problems.

Graphical results are presented to illustrate this good agreement. Two comparisons of computations by the Rankine-Hugoniot equations and the RCM are given, one for shock trajectories in Fig. 9 and the other for shock-wave pressures in Fig. 10. The spatial distribution of pressure was taken at a time of 0.70 ms, corresponding to the dashed horizontal line in Fig. 9. A very slight wandering of the RCM computed shock trajectory from the predicted straight line is noticeable in the results, which is normal for the RCM computations, because the random number has an effect on how the shock wave propagates from one grid zone to the next. The shock-wave pressures calculated by the Rankine-Hugoniot equations and RCM, which are compared in Fig. 10, match identically, because the Rankine-Hugoniot equations are used without alteration in the RCM. Similar results were obtained for similar spatial distributions of density, temperature and flow velocity, which are not shown here for brevity. The comparisons given here, however, illustrate that the analysis and computer program give excellent results for this simple problem, as should be expected.

Example 2: Constant-Velocity Piston Motion to Give a Centered Rarefaction Wave

In this second problem the piston is pulled away from the quiescent air at a constant velocity of -431.4 m/s, or a Mach number of -1.277. For this case of a suddenly accelerated piston to a constant velocity, this would theoretically produce a very simple centered rarefaction wave behind the piston (see Figs. 11 and 12), with a strength or pressure ratio across the wave of 0.129, as predicted by the well-known method of characteristics. The computed results from the RCM with the piston boundary condition are once again virtually the same for this simple test problem, which is again just one of the elemental wave patterns shown earlier (Fig. 6b). The reason for making a test case of this second example is the same as that for the first one, in order to verify that this elemental wave pattern and all of its flow properties can be reproduced correctly by the modified RCM. This is again essential before undertaking more complex problems.

Graphical results are presented to illustrate this good agreement. Two comparisons of computations by the method of characteristics and the RCM are included here, one for the motions of both the head and tail of the centered rarefaction wave in Fig. 11 and the other for the spatial distribution of the flow velocity through the rarefaction wave in Fig. 12. The spatial profile of the flow velocity was taken at a time of 0.70 ms, corresponding directly to the dashed horizontal line in Fig. 11. The two sets of calculated results from the method of characteristics and RCM can be seen to be in good agreement. The agreement here is in fact even better than that for comparisons of similar work involving shock-tube problems presented in Ref. 17, which is attributed to the present use of the van der Corput random-number algorithm, which has been shown to be a better random-number generator for the RCM [67]. Similar results were obtained for the pressure, density and temperature distributions, which are not shown here for brevity. Such comparisons illustrate that the analysis and com-

puter program again give excellent results for such a simple problem, as one might expect.

Example 3: Accelerated Piston Motion to Produce a Focussed Compression Wave

In this problem the piston is accelerated uniformly from rest to a constant velocity of 368.4 m/s at a time of 0.70 ms, with a constant acceleration. This type of piston motion produces a focusing compression wave ahead of the piston, with a theoretical pressure ratio of 3.94, which theoretically focusses at a certain time (1.445 ms) and distance (0.5 m) in front of the piston (see Fig. 13), as predicted by the results given in Ref. 60. A shock wave with a theoretical pressure ratio of 3.85, which moves to the right, replaces the focussed compression wave, and a contact surface follows behind this shock wave. A fairly weak rarefaction wave with a theoretical pressure ratio of only 0.977 is also produced, and it propagates in the opposite direction and eventually collides with the piston. Furthermore, after the piston velocity becomes constant, a region of quasi-steady or steady flow occurs between the focusing compression wave and the piston.

Comparisons of results from the RCM and the combined method of characteristics and Rankine-Hugoniot equations [60] are now given in Figs. 13 to 15. From the results presented in Fig. 13 it can be seen that the RCM predicts the motions of the focussed compression wave and the resulting shock wave and contact surface very well. Details of the flow only in the vicinity of the focal point are not predicted clearly, however, because the flow with steep gradients in this region is modelled with too few grid points. Consequently, the smooth steepening of the focussed compression is predicted by the RCM to be a series of steep-fronted shocks before the focus, and one steep-fronted shock wave emerges just before the focus. As a result, the weak rarefaction wave is not centered but spread out. It cannot be recognized in the numerical results of the RCM, partly for this reason and partly because it is simply a weak wave.

The other two results given in Figs. 14 and 15 are for the time histories of the sound speed and flow velocity, respectively, taken at a fixed distance of 0.278 m from the origin of the piston motion, corresponding to the dashed vertical line in Fig. 13. These results are a further illustration of the good agreement between the predictions by the RCM and method of characteristics for this problem. Such graphical results illustrate that the analysis and computer program again give good results.

Example 4: Accelerated Piston Motion to Produce a Noncentered Rarefaction Wave

In this fourth problem the piston is accelerated uniformly from rest to a constant velocity of -368.4 m/s at a time of 0.70 ms, with a constant acceleration. This type of piston motion produces a noncentered rarefaction wave behind the piston (see Fig. 16), with a theoretical pressure ratio of 0.433, as given by the method of characteristics.

Comparisons of results from the RCM and method of characteristics are now given in Figs. 16 to 18. From the results shown in Fig. 16 it can be seen that the RCM predicts the motions of the head and tail of the noncentered rarefaction wave very well. The other two results given in Figs. 17 and 18 are for the spatial distributions of the sound speed and flow velocity, respectively, taken at a fixed time of 1.10 ms from the start of the piston motion, corres-

ponding to the dashed horizontal line in Fig. 16. These results illustrate the good agreement between the predictions by the RCM and method of characteristics for this problem. Such graphical results again demonstrate that the analysis and computer program give good results.

Example 5: Constant-Velocity Spherical Piston Motion to Produce a Shock Wave

In this final problem, a spherical piston is pushed outward into quiescent air at a constant velocity of 178.0 m/s, or at a Mach number of 0.523. This would theoretically produce an outward moving shock wave in front of this expanding spherical piston (see Fig. 19), with a constant strength or pressure ratio of 1.035 [70]. However, the flow properties between the shock-wave front and piston are nonuniform, although spatial distributions at various increasing times are self similar [70].

The comparison in Fig. 19 of the shock trajectories calculated by the RCM and Taylor's solution [70] show good agreement. Further good agreement for the spatial distributions of pressure and flow velocity are shown in Figs. 20 and 21, respectively. Each set of two spatial distributions in each figure was obtained at different time levels of 1.4 and 2.1 ms, respectively, corresponding to the dashed horizontal lines sketched in Fig. 19. Note that these two spatial distributions at two different times are self similar [70], and the RCM solution also shows this self similarity. Such graphical results demonstrate once again that the analysis and computer program give good predictions of nonstationary flows in front of moving pistons with specified paths.

4. NUMERICAL RESULTS AND DISCUSSION

In this chapter, the blast-wave flow fields from both TNT and ANFO explosions are reconstructed with the modified RCM, by using the trial-and-error method of establishing a suitable piston path described in chapter 2, such that the reconstructed flow field agrees as well as possible with all available experimental information at a specific test site in the explosion.

It is important to realize that blast-wave flow fields from explosions of different sizes of the same explosive do not necessarily have to be reconstructed for each explosion of a different size. This is so because blast-wave flow properties in the form of shock trajectories, time histories at a fixed distance, and spatial distributions at a fixed time can generally be scaled simply and accurately from one explosion size to another of the same explosive, by using Sachs's well-known scaling laws [71]. This is especially true for blast-wave flow properties farther away from the explosive charge, where the amplitude of the blast wave is less than about 10 MPa and real-gas effects are unimportant [28]. Consequently, all reconstructed blast-wave flow fields for TNT and ANFO will be presented here for the specific case of a surface explosion of 1 kg of TNT or its equivalent. These reconstructed flow-field results, which will be given in graphical and tabular form, can then be utilized easily by scaling them to those conditions required for a different sized explosion of the same explosive at the same or different atmospheric conditions.

Sachs's scaling laws [71] are given here for convenient reference and also completeness. They are a direct extension of Hopkinson's purely geometric scaling laws, which are based on charge size only [72], in that Sachs included the additional effects on scaling of different ambient pressures and tempera-

tures (or sound speeds). The scaling factor for distance S_r and the scaling factor for time S_t are simply

$$S_r = \left[\frac{W}{W_o} \frac{p_0}{p_1} \right]^{1/3} \tag{6}$$

and

$$S_t = \frac{a_0}{a_1} S_r , \tag{7}$$

where W is the charge mass in kilograms of TNT or its equivalent, W_o is the standard TNT mass of 1 kg or its equivalent, and the subscripts 0 and 1 on the pressure (p) and sound speed (a) denote standard atmospheric and local ambient conditions, respectively. Standard atmospheric conditions are p_0 = 101.33 kPa, T_0 = 288.15 K, and a_0 = 340.29 m/s.

The validity of these scaling laws and the method in which they are used can be found in Refs. 28 and 37. Furthermore, the scaling factors S_r and S_t that are used in the present study to scale available experimental information from actual TNT and ANFO explosions to the specific case of a 1 kg TNT surface or hemispherical explosion or its equivalent at standard atmospheric conditions are listed in table 1. Note that the sizes of the actual explosions of TNT and ANFO and the local ambient conditions are also given in this table.

Case 1: TNT Explosion

The blast-wave flow field for a 1-kg TNT explosion in a standard atmosphere is reconstructed with the RCM in the spatial region from 1 to 10 m from the explosion center, over which the peak overpressure of the blast wave decays from 1000 kPa to only 10 kPa. For this case the number of grid zones per meter of flow field is 140, or 1260 grid zones is used between 1 and 10 meters. This flow field is reconstructed to agree as well as possible with different types of scaled experimental information for a number of different sized explosions of TNT. The types of experimental information that are utilized from different sized explosions are itemized as follows:

a) a shock trajectory in equational form from Ref. 37, which was obtained from an empirical curve fit to measured arrival times of the shock- or blast-wave front at various different radii from the center of a 20-ton TNT surface explosion [29] and two 500-ton TNT surface explosions named SNOWBALL and SAILOR HAT [30 & 73],

b) thirty-five particle paths or trajectories measured by means of high-speed photography of smoke trails or tracers at various different radii from the center of a 500-ton surface explosion named SNOWBALL [30 & 73],

c) twenty particle paths or trajectories measured by means of high-speed photography of smoke trails or tracers at various different radii from the center of a 500-ton surface explosion named SAILOR HAT [30 & 73],

d) twenty time histories of overpressure measured with piezoelectric pressure transducers at various different radii from the center of a 20-ton TNT surface explosion that were made by American researchers [29],

e) twenty-one time histories of overpressure measured with piezoelectric pressure gages at various different radii from the center of a 20-ton TNT surface explosion that were made by British researchers [29],

f) eigthteen time histories of overpressure measured with piezoelectric pressure gages at various different radii from the center of a 20-ton TNT surface explosion that were made by Canadian researchers [29],

g) six time histories of density measured with specially designed beta-ray density gages at various different radii from the center of a 100-ton TNT surface explosion [34].

If the reader is interested in more details or information regarding the experimental measurements and the different sized explosions, they can be obtained directly from the original references and also from Ref. 37.

The piston path is specified by fourteen independent distance and time coordinate points in the physical plane and joined by a smooth cubic spline, as explained in chapter 2. After the blast-wave flow is reconstructed by the RCM to match as well as possible all available experimental information just mentioned, the final fourteen coordinates for the piston path are obtained. These final points are listed in table 2, along with the initial slope of the spline through these points. They can be used for future reference to reconstruct the flow field, without having to repeat the trial-and-error process.

The reconstructed blast-wave flow field for the 1-kg TNT explosion is now shown in the physical plane in Fig. 22. This flow field lies in front of the piston path, and it contains the blast-wave front trajectory and thirty-five particle paths. These particle paths are initially stationary ahead of the blast-wave front and have a predominantly outward motion behind it. The flow field is terminated at a distance of 10 m by using a continuous boundary condition (not a reflecting wall). It is also terminated eventually in time by a C^+ characteristic line, which is really a weak disturbance created in the solution by the RCM for convenience. It is created by inserting a slight kink in the piston path, and this is the signal that is used to indicate that the earlier part of the flow field is based on available experimental information and the latter part is not. Hence, the flow field predicted at later times is meaningless, because it is artificially created for a guessed but unverified piston motion, and this part of the flow field is not shown for this reason. Note that the initial positions of the numerically reconstructed particle paths shown in Fig. 22 correspond directly to those for the measurements made in the 500-ton TNT explosion trial called SNOWBALL [30 & 73].

The reconstruction of the blast-wave flow field is based partly on the previous knowledge of a blast- or shock-wave front trajectory in the form of an empirical curve fit to experimental data [37]. The percentage error between the location of the reconstructed shock trajectory and that from the empirical curve is shown in the topmost inset in the figure. The error is fairly small all the way along the trajectory. Another convenient indicator of the quality of the reconstruction is the shock-front pressure, which can be obtained from the RCM reconstruction and the empirical curve [37]. The percentage error in the shock-front pressure ratio is shown in the bottom inset. The error is a little larger in this case, but it is typically still below 3%.

The reconstruction of the flow field is also based partly on thirty-five particle paths measured in a 500-ton TNT explosion trial called SNOWBALL [30 &

73]. The reconstructed particle paths based on the measured ones were already shown in Fig. 22. In order to illustrate how well the reconstructed particle paths agree with the experimental ones, two types of graphical information are presented in Fig. 23 (a to g), which consists of seven consecutive pages of results. On the left hand side of each page the percentage error in the particle-path location is given. On the right hand side a direct comparison is made between the reconstructed flow velocity along the particle path and the corresponding flow velocity obtained from the slope or velocity of the particle path. These corresponding results on the left and right hand side are given for all thirty-five particle paths. Both the errors in the particle paths and flow-velocity profiles are plotted in terms of the displacement $r_p - r_0$ of the fluid-particle path, where r_p is the instantaneous fluid-particle location and r_0 is its initial position before the blast wave arrives. Hence, they should not be mistakenly confused with spatial distributions at a fixed time. Furthermore, the initial position of the particle path r_0 and the time of arrival t_a of the blast-wave front at this location are both given as insets in the graphs. It can be seen that this set of results is arranged in the order of increasing radius or decreasing amplitude of the flow velocity. Finally, it can also be observed that the reconstructed flow-velocity field is in good agreement with this available experimental data.

Twenty particle paths are also available from another 500-ton TNT explosion trial called SAILOR HAT [30 & 73], and a comparison of these measurements with the reconstructed blast-wave flow field is also presented here. The same reconstructed flow field given initially in Fig. 22 is given again in Fig. 24, with one main difference. The reconstructed particle paths shown in this new figure are now different; their initial positions now correspond directly to those for the measurements made in the trial called SAILOR HAT.

A comparison of reconstructed and measured results for the twenty particle paths is now presented in Fig. 25 (a to d), which consists of four pages of results. On the left hand side of each page the percentage error in the particle-path location is given. On the right hand side a direct comparison is made between the reconstructed flow velocity along the particle path and the corresponding flow velocity obtained from the slope or velocity of the particle path. Although the reconstructed particle-path locations are in good agreement, as found for the previous results in Fig. 23, some of the reconstructed flow-velocity profiles are not in as good agreement as that for the previous results. If better agreement between the reconstructed and measured flow-velocities was forced to occur for this later set of results, then the agreement deteriorated not only for the earlier set of results but also for the present particle-path locations. Suitable compromises led to the presently accepted reconstructed blast-wave flow field, which is in fact quite good and believed to be the best possible at the present time.

The reconstruction of the flow field is also based partly on fifty-nine time histories of overpressure, which were measured in a 20-ton TNT surface explosion trial by British, American and Canadian researchers [29]. Comparisons of only four of these measured overpressure signatures with the corresponding ones from the reconstructed flow field are given in Fig. 26, mainly for brevity and also because these four cases are typical of most of the results. Although the peak overpressures of the reconstructed and measured signatures agree fairly well for all of the signatures, the agreement in shape is not always so good, as illustrated by the second set of results in Fig. 26. In a few cases the disagreement in shape was found to be very bad, even worse than shown, and in these cases it was assumed that these overpressure measurements

were basically incorrect. Hence, such cases were disregarded in the numerical simulation process. However, the numerical simulation of the measured overpressure signatures was in general very good, being better for weaker blast waves at larger radii.

If better agreement between some of the reconstructed and measured overpressure signatures was forced to occur during the flow-field reconstruction process, then it was found that the agreement between other reconstructed and measured overpressure signatures deteriorated. Furthermore, the good agreement between the reconstructed and measured particle paths and flow velocities also deteriorated. For the latter case it was then felt that the two different sets of experimental results were slightly inconsistent and one set would therefore have to be given more credit or weight. In consideration of the poor quality of piezoelectric transducers and pressure measurements at the time of the explosion trial (1961), it was thought that the set of measured particle paths were more reliable than the measured overpressure signatures. Consequently, any disagreement between the reconstructed and measured overpressure signatures was not given as much weight in the flow-field reconstruction.

The reconstruction of the flow field is also based partly on six time histories of the density measured during a 100-ton TNT surface explosion trial [34]. The comparison of four of these density signatures with those from the reconstructed flow field by the RCM appears in Fig. 27. The agreement is in general fairly good, especially for the amplitude and shape of the first half of the signature.

Time histories of the blast-wave flow properties at a fixed radius or an experimental test site in an explosion are important to engineers and researchers doing explosion experiments in field trials. For this reason, graphical and tabulated data for the reconstructed blast-wave flow field of a 1-kg TNT surface explosion by the RCM are now presented in this form. Ten sets of overpressure, sound-speed, density and flow-velocity signatures are presented in Fig. 28 (a to j), for different radial locations from about 1 to 10 m. The specific radius r is given in each figure as an inset, along with the time of arrival t_a of the blast-wave front at this particular radius. Over this range of distances the peak blast-wave overpressure decays from about 1 to 0.01 MPa.

These signatures clearly show the amplitudes, positive-phase durations and wave shapes at various distances from the explosion center, as well as how they change with increasing distance. For example, the exponential like decay with time behind the blast-wave front in higher-amplitude signatures closer to the explosion center changes with increasing distance to become almost linear for the lower amplitude signatures farther away. The positive-phase duration for the overpressure, sound speed, density and flow velocity at one specific location can be very different, especially when the blast wave is stronger. In some cases the sound speed does not even decay to its ambient value at later times (see Figs. 28a to 28d). The duration of the flow velocity is normally substantially longer that that of the overpressure, even for the weakest blast wave shown here. Note that the durations of all four signatures become equal only for very weak blast waves, when they are sound waves, and the amplitude is less than about 1.5 kPa.

It is interesting to observe that for strong blast waves the sound-speed signature does not decay to the ambient value (see Figs. 28a to 28d), as the others do, whereas it appears to do this for weaker blast waves (see Figs. 28e to 28j). This is not something new but is rather characteristic of one-dimen-

sional explosion calculations [8, 12 to 14]. As a blast-wave front moves outward from the explosion center and diminishes in amplitude, it leaves behind a decreasing entropy field with increasing distance. Consequently, when a fluid particle nearer to the explosion expands nearly isentropically back toward atmospheric pressure, both its temperature and sound speed remain higher than the ambient values because of its higher entropy, and the density is correspondingly smaller. This can be observed in the results shown in Figs. 28a to 28d.

Some of the reconstructed blast-wave signatures shown in Fig. 28 (a to j) contain random numerical noise or are slightly jagged in appearance. This could also have been noticed in previous reconstructed results. Such noise is characteristic of calculated results from the RCM [17 & 67]. It can normally be reduced by employing a larger number of grid points to represent the flow field for the computations, if this is desired. However, the use of more grid points increases the number of numerical computations and associated computational costs, and this was not deemed necessary for the present study.

Although the graphical time histories of the blast-wave flow properties from the 1-kg TNT surface explosion aptly illustrate the physical trends of the results, tables of numerical values of the flow properties are generally more useful to the engineer or researcher. For this reason, tabulated time histories of the overpressure, sound speed, density and flow velocity at a fixed radius or an experimental test site in an explosion are presented in appendix B. Thirty-three sets of these signatures are given, to cover in small steps the distance range from about 1 to 10 m from the explosion center, for which the peak blast-wave overpressure decays from about 1 to 0.01 MPa. Note that all of the other flow properties like the temperature, flow Mach number, Reynolds number per unit length and dynamic pressure can be obtained directly from these tabulated values by using simple well-known equations.

Case 2: ANFO Explosion

The blast-wave flow field for a 1-kg TNT equivalent ANFO surface explosion in a standard atmosphere is reconstructed with the RCM in the spatial region from 1 to 10 m from the explosion center, over which the peak overpressure of the blast wave decays from about 2000 kPa to only 10 kPa. For this case the number of grid zones per meter of reconstructed flow field is simply 140. This flow field is reconstructed to agree as well as possible with two different types of scaled experimental information, both from a 628-ton ANFO explosion called DICE THROW [32 & 33]. The two types of experimental information that are utilized from this explosion are itemized as follows:

a) a shock trajectory in equational form from Ref. 37, which was obtained from an empirical curve fit to measured arrival times of the shock- or blast-wave front at various different radii from the center of the 628-ton ANFO surface explosion [32 & 33],

b) seventeen time histories of overpressure measured with piezoelectric pressure transducers at various different radii from the center of the 628-ton ANFO surface explosion [32].

c) sixty-one time histories of overpressure measured with piezoelectric pressure transducers at various different radii from the center of the 628-ton ANFO surface explosion [33].

If the reader is interested in more details or information regarding the experimental measurements and the different sized explosions, they can be obtained directly from the original references and also from Ref. 37. It is unfortunate that particle-trajectory measurements were never obtained for ANFO explosions, such that they could have been advantageously utilized in the present study.

The piston path is specified by fifteen independent distance and time coordinate points in the physical plane and joined by a smooth cubic spline, as explained in chapter 2. After the blast-wave flow is reconstructed by the RCM to match as well as possible all available experimental information just mentioned, the final fifteen coordinates for the piston path are obtained. These final points are listed in table 3, along with the initial slope of the spline through these points. They can be used for future reference to reconstruct the flow field, without having to repeat the trial-and-error process.

The reconstructed blast-wave flow field for the 1-kg TNT equivalent ANFO surface explosion is now shown in the physical plane in Fig. 29. Although the flow field shown extends only out to about 8 m, the flow field was originally terminated at a distance of 10 m by using a continuous boundary condition (not a reflecting wall). It is also terminated eventually in time by a C^+ characteristic line, which is really a weak disturbance created in the solution by the RCM for convenience, as described previously for the case of TNT.

The reconstruction of the blast-wave flow field is based partly on the previous knowledge of a blast- or shock-wave front trajectory in the form of an empirical curve fit to experimental data [37]. The percentage error between the location of the reconstructed shock trajectory and that from the empirical curve is shown in the topmost inset in the figure. The error is fairly small all the way along the trajectory. Another convenient indicator of the quality of the reconstruction is the shock-front pressure, which can be obtained from the RCM reconstruction and the empirical curve [37]. The percentage error in the shock-front pressure ratio is shown in the bottom inset. The error is a little larger in this case, but it is typically still below 4%.

The reconstruction of the flow field is also based partly on seventy-eight experimental time histories of the overpressure. Comparisons of only thirteen of these measured overpressure signatures with the corresponding ones from the reconstructed flow field are shown in Fig. 30 (a to d), which consists of four consecutive pages of results. It can be seen that the agreement is very good. Similar agreement was obtained for other comparisons from Refs. 32 and 33, which are not shown here for brevity.

It is worth mentioning here that measured overpressure signatures are not always consistent. Measurements at the same radius but different and even similar angular positions, for example, reveal that their amplitudes can differ by 20%, their positive-overpressure durations can differ by as much as 30%, and the signature shapes can also be somewhat different. Variations of this sort are readily apparent from the signatures shown in Refs. 32 and 33. This is the main reason for most of the differences in the reconstructed and measured overpressure signatures that are compared in Fig. 30. Considering the variability in the measured signatures, the differences are in fact quite small. This is partly because some of the overpressure measurements that were obviously of questionable quality were culled out of the group to be used for the flow-field reconstruction. In consideration that seventy-eight selected measurements were used in the blast-wave flow-field reconstruction, it is felt that the resulting reconstruction for the 1-kg TNT equivalent ANFO explosion is quite good.

Time histories of the blast-wave flow properties at a fixed radius or an experimental test site in an explosion are important to engineers and researchers doing explosion measurements in field trials. For this reason, graphical and tabulated data for the reconstructed blast-wave flow field of a 1-kg TNT equivalent ANFO surface explosion by the RCM are now presented in this form, as was done for the case of TNT. Eight sets of overpressure, sound-speed, density and flow-velocity signatures are presented in Fig. 31 (a to h), for different radial locations from about 1 to 10 m. The specific radius is given in each figure as an inset, along with the time of arrival of the blast-wave front at this particular radius. Over this range of distances the peak blast-wave overpressure decays from about 2 to 0.01 MPa.

These signatures clearly show the amplitudes, positive-phase durations and wave shapes at various distances from the explosion center, as well as how they change with increasing distance. These results are very similar to those for the previous case of TNT, and most of the comments made for the previous case are also applicable here.

Although the graphical time histories of the blast-wave flow properties from the 1-kg TNT equivalent ANFO surface explosion aptly illustrate the physical trends of the results, tables of numerical values of the flow properties are generally more useful to the engineer or researcher. For this reason, as for the case of TNT, tabulated time histories of the overpressure, sound speed, density and flow velocity at a fixed radius or an experimental test site in an explosion are presented in appendix C. Thirty-nine sets of these signatures are given, to cover in small steps the distance range from about 1 to 10 m from the explosion center, for which the peak blast-wave overpressure decays from about 2 to 0.01 MPa. Note that all of the other flow properties like the temperature, flow Mach number, Reynolds number per unit length and dynamic pressure can be obtained directly from these tabulated values by using simple well-known equations.

5. CONCLUDING REMARKS

The present new method of establishing a suitable piston path by trial and error for the numerical reconstruction of part of a blast-wave flow field, away from the explosion center at an experimental test site, to agree as well as possible with all available but limited experimental information, has been demonstrated to be highly feasible and very useful. Flow fields for both TNT and ANFO were reconstructed successfully by this method, and extensive flow-field properties for these two explosions were presented in both graphical and tabular form for future reference. These flow properties are given in scaled form, for a 1-kg TNT surface explosion and a 1-kg TNT equivalent ANFO surface explosion in a standard atmosphere, which can easily be scaled for the cases of different sized TNT and ANFO explosions in the same or different atmospheres.

Flow properties of this nature can now be employed in a variety of ways. For example, they are valuable for the following:

a) determination of the flow properties of a blast wave incident on an experimental test site in an explosion trial, where military and civilian structures, vehicles and equipment are being tested,

b) determination of the flow properties of a blast wave from a possible accidental explosion that is incident on civilian structures, vehicles

and equipment, for which an assessment is needed of blast-wave damage effects and survivability,

c) reevaluation of past drag coefficients of free-flight cylinders in blast waves, for which the cylinder motion was known accurately by accelerometers and high-speed photography, but the blast-wave flow properties were inadequately known in the past,

d) reevaluation of the drag response due to blast-wave flows of flexible, cantilevered structures like whipmast and polemast antenna of naval ships.

Note that the flow properties for TNT explosions have already been used in the assessment of blast-wave effects on a commerical nuclear power plant and those for ANFO are presently being used to reevaluate the drag coefficient of cylinders in blast-wave flows.

The blast-wave flow-field reconstruction is done for only a part of the flow field, away from the explosion center. However, the reconstructed part of the flow field does not have to be small or limited in spatial extent, but it can be rather large and cover a considerable spatial region. For example, no problems were encountered in the reconstruction of flow fields for a 1-kg TNT explosion or a 1-kg TNT equivalent ANFO explosion that covered a distance from 1 to 10 m, for which the peak blast-wave overpressure decayed from about 2 MPa to only 0.01 MPa. All that is really needed as input is good experimental information that can be used as the basis for the reconstruction.

Reconstructions of blast-wave flow fields in the present study involved numerical computations. These were done with the random-choice method (RCM), which was modified to include a moving piston boundary condition. The details of this boundary condition were presented, and it worked very well in the RCM. Furthermore, the RCM was found to be excellent for constructing flow fields in front of moving pistons.

The best methods currently available for reconstructing blast-wave flow fields to agree with experimental information are as follows:

a) Dewey's method [30, 34 & 36] which involves fitting a surface to numerous measured particle paths and calculating the other flow-field properties with a suitable analysis,

b) Celmins's method [58] which involves fitting a surface to numerous overpressure signatures by using a least-squares technique and simultaneously computing the other flow-field properties with a suitable analysis,

c) the present method which involves the establishment of a piston path and flow field in front of this piston by a trial-and-error process.

Other past methods by Makino [56] and Gottlieb and Ritzel [25], which involve the tedious method of characteristics and reconstruct the flow field in reverse from a specified shock trajectory only, or by utilizing this trajectory with a single additional overpressure signature, are simply not as good, for obvious reasons, as mentioned in the introduction. The present method is more flexible and generally better for reconstructing blast-wave flow fields than the methods of both Dewey and Celmins, because it bases the reconstruction on all available

experimental information, not just on measured particle paths or measured overpressure signatures. Furthermore, the present method can handle embedded shock waves in the flow field being computed with very little added difficulty, which none of the previous methods can do without the incorporation of much additional sophistication. However, part of the gain in increased flexibility involves paying the price of being stuck with a trial-and-error process of establishing an acceptable piston path and reconstructed blast-wave flow field in front of it. Finally, it is worth mentioning that, if only measured particle paths are available for reconstructing the blast-wave flow field, then the present method and Dewey's would very likely produce equivalent quality flow fields, but the method of Dewey would produce this flow field with more ease. Finally, if overpressure signatures were the only available experimental information, then the same remarks would also apply regarding the present method and Celmins's technique.

6. REFERENCES

1. J. von Neumann, "The Point Source Solution", first published in the NDRC, Division B Report No. AM-9, June 30, 1941; then in "Shock Hydrodynamics and Blast Waves" (H. A. Bethe, K. Fuchs, J. von Neumann, R. Peierls, and W. G. Penney, Eds.), Report No. AECD-2860, 1944; revised version in "Blast Waves" (H. A. Bethe, Ed.), LASL Report No. LA-2000, Los Alamos Scientific Laboratory, New Mexico, U.S.A., pp. 27-55, 1957; reprinted in the collected works of John von Neumann (A. H. Taub, Ed.), "Theory of Games, Astrophysics, Hydrodynamics and Meteorology", Vol. VI, pp. 219-237, Pergamon Press, New York, New York, U.S.A., 1963.

2. L. I. Sedov, "Rasprostraneniye Sil'nykh Vzryvnykh Voln" (Propagation of Intense Blast Waves), Priklednaya Matematika i Mekhanika (Applied Mathematics and Mechanics), Moscow, U.S.S.R., Vol. 10, No. 2, 1946.

3. L. I. Sedov, "Rasprostraneniye Sil'nykh Vzryvnykh Voln", revised version in "Similarity and Dimensional Methods in Mechanics", fourth printing, Gostekhizdat, Moscow, U.S.S.R., 1947; translated by M. Friedman and edited by M. Holt, Academic Press, New York, New York, U.S.A., 1959.

4. Sir Geoffrey Taylor, "The Formation of a Blast Wave by a Very Intense Explosion", first published in British Report RC-210, June 27, 1941; revised version in Proceedings of the Royal Society of London, Vol. A201, part I, pp. 159-174, part II, pp. 175-186, March 1950.

5. K. P. Stanyukovich, "Unsteady Motion of Continuous Media", Gostekhizdat, Moscow, U.S.S.R., 1955; English translation edited by M. Holt, Pergamon Press, Vol. XIII, New York, New York, U.S.A., 1960.

6. K. P. Stanyukovich, "Application of Particular Solutions for Equations of Gasdynamics to the Study of Blast and Shock Waves", Report of the Soviet Academy of Sciences, Moscow, U.S.S.R., Vol. 52, No. 7, 1946.

7. H. Goldstine and J. von Neumann, "Blast Wave Calculation", Communications of Pure and Applied Mathematics, Vol. 8, pp. 327-353, 1955; reprinted in the collected works of John von Neumann (A. H. Taub, Ed.), "Theory of Games, Astrophysics, Hydrodynamics and Meteorology", Vol. VI, pp. 368-412, Pergamon Press, New York, New York, U.S.A., 1963.

8. H. L. Brode, "Numerical Solutions of Spherical Blast Waves", Journal of Applied Physics, Vol. 26, No. 6, pp. 766-775, 1955.

9. V. P. Korobeinikov, N. S. Mil'nikova, and Ye. V. Ryazanov, "The Theory of the Point Explosion", Fizmatgiz, Moscow, 1961; English translation, U.S. Department of Commerce, JPRS (14, 334), CSO No. 6961-N, Washington, D.C., 1962.

10. A. Sakurai, "Blast Wave Theory", "Blast Development in Fluid Dynamics" (M. Holt, Ed.), Academic Press, New York, New York, U.S.A., Vol. I, pp. 309-375, 1965.

11. G. G. Bach and J. H. S. Lee, "An Analytic Solution for Blast Waves", AIAA Journal, Vol. 8, No. 2, pp. 271-275, 1970.

12. H. L. Brode, "A Calculation of the Blast Wave from a Spherical Charge of TNT", Report No. RM-1965, Rand Corporation, Santa Monica, California, U.S.A., 1957.

13. H. L. Brode, "Blast Waves from a Spherical Charge", Physics of Fluid, Vol. 2, No. 2, pp. 217-229, March-April 1959.

14. H. L. Brode, "Point Source Explosion in Air", Report No. RM-1824-AEC, Rand Corporation, Santa Monica, California, U.S.A., 1956.

15. P. Colella and H. M. Glaz, "Numerical Modelling of Inviscid Shocked Flows of Real Gases", Proceedings of the Eighth International Conference of Numerical Methods in Fluid Mechanics, (E. Krause, Ed.), pp. 175-182, Aachen, West Germany, 1982.

16. D. L. Lehto and R. A. Larson, "Long Range Propagation of Spherical Shock Waves from Explosions in Air", NOL Report No. NOLTR 69-88, United States Naval Ordnance Laboratories, Write Oak, Maryland, U.S.A., 1969.

17. T. Saito and I. I. Glass, "Application of Random Choice Method to Problems in Shock and Detonation-Wave Dynamics", UTIAS Report No. 240, University of Toronto Institute for Aerospace Studies, Downsview, Ontario, Canada, October 1979.

18. M. Fry, J. Titsworth, A. Kuhl, D. Book, J. Boris, and M. Picone, "Shock Capturing Using Flux-Corrected Transport Algorithms with Adaptive Gridding", Thirteenth International Symposium on Shock Tubes and Waves, pp. 376-384, edited by C. E. Treanor and J. G. Hall, Niagra Falls, New York, New York, U.S.A., State University of New York Press, U.S.A. 1981.

19. J. P. Boris and D. L. Book, "Flux-Corrected Transport: I. SHASTA, A Fluid Transport Algorithm that Works", Journal of Computational Physics, Vol. 11, 1973. See also "Solution of Continuity Equations by Method of Flux-Corrected Transport", "Methods of Computational Physics" (J. Killeen, Ed.), Vol. 16, Academic Press, New York, New York, U.S.A., 1976.

20. D. L. Book, "Two Dimensional FCT Model of Low Altitude Nuclear Effects", United States NRL Memorandum Report No. 4362, Naval Research Laboratory, Washington, D.C., 1981.

21. W. A. Whitaker, E. A. Nawrocki, C. E. Needham, and W. W. Troutman, "Theoretical Calculations of the Phenomenology of HE Detonations", AFWL Report No. AFWL-TR-66-141, Vols. 1 and 2, U.S. Air Force Weapons Laboratory, Albuquerque, New Mexico, U.S.A., November 1966.

22. S. Glasstone (Ed.), "The Effect of Nuclear Weapons", United States Department of Defence and Atomic Energy Commission, Washington, D.C., 1957; revised in 1962; subsequent revision in 1977 with P. J. Dolan (Ed.), but this last revision does not contain the list of nuclear tests.

23. H. L. Brode, "The Real Thing: Blast Waves from Atmospheric Nuclear Explosions", Proceedings of the Twelfth International Symposium on Shock Tubes and Waves, Jerusalem, 16-19 July, 1979, pp. 31-47 of the book of proceedings "Shock Tubes and Waves" (A. Lifshitz and J. Rom, Eds.), The Magnes Press, The Hebrew University, Jerusalem, Israel, 1980.

24. See the proceedings of the eight international symposia on "Military Applications of Blast Simulation", 1967-1983.

25. J. J. Gottlieb and D. V. Ritzel, "Flow Properties of a Spherical Blast Wave", Proceedings of the Sixth Internation Symposium on Military Applications of Blast Simulation, Vol. 1, pp. 1.4-1 to 1.4-29, held on 25-29 June 1979 in Cahors, France, and sponsored by the Centre d'Etude de Gramat, Gramat, France.

26. G. V. Price, "Numerical Simulation of the Air Blast Response of Tapered Cantilever Beams (U)", DRES Suffield Report No. 447, Defence Research Establishment Suffield, Ralston, Alberta, Canada, November 1977.

27. Y. S. Kim and P. R. Ukrainetz, "Drag Loading on a Circular Cylinder from an Air Blast Wave (U)", DRES Suffield Report No. 392, Defence Research Establishment Suffield, Ralston, Alberta, Canada, November 1971.

28. W. E. Baker, "Explosion in Air", University of Texas Press, Austin, Texas, U.S.A., 1973.

29. Anon., "Scientific Observations on the Explosion of a 20-ton TNT Charge (U)", DRES Suffield Report No. 203, Vol. 2, Defence Research Establishment Suffield, Ralston, Alberta, Canada, September 1961.

30. John M. Dewey, "The Properties of a Blast Wave Obtained from an Analysis of the Particle Trajectories", Proceedings of the Royal Society, Series A, Vol. 324, pp. 275-299, 1971.

31. J. H. B. Anderson, "Canadian Air Blast Measurements from Operation Distant Plain - Event 2A (U)", DRES Suffield Technical Note No. 270, Defence Research Establishment Suffield, Ralston, Alberta, Canada, April 1970.

32. F. H. Winfield, "Event DICE THROW, Canadian Air Blast Measurements (U)", DRES Suffield Technical Note No. 451, Defence Research Establishment Suffield, Ralston, Alberta, Canada, March 1977.

33. G. D. Teel, "Free-Field Air Blast Definition - Even DICE THROW", Proceedings of the Dice Throw Symposium, Vol. 1, held on 21-23 June 1977 in California, U.S.A., and sponsored by the Defence Nuclear Agency, Washington, D.C.

34. John M. Dewey, "The Air Velocity and Density in Blast Waves from TNT Explosions (U)", DRES Suffield Report No. 207, Defence Research Establishment Suffield, Ralston, Alberta, Canada, March 1964.

35. H. J. Goodman, "Compiled Free-Air Blast Data on Bare Spherical Pentolite", BRL Report No.1092, U.S. Army Ballistic Research Laboratory, Aberdeen Proving Ground, Maryland, U.S.A., February 1960.

36. John M. Dewey, "The Air Velocity in Blast Waves from TNT Explosions", Proceedings of the Royal Society, Series A, Vol. 279, pp. 366-385, 1964.

37. H. S. I. Sadek and J. J. Gottlieb, "Initial Decay of Flow Properties of Planar, Cylindrical and Spherical Blast Waves", UTIAS Technical Note No. 244, University of Toronto Institute for Aerospace Studies, Downsview, Ontario, Canada, October 1983.

38. S. B. Mellsen, "Drag Measurement on Cylinders by the Free Flight Method - Operation PRAIRIE FLAT (U)", Suffield Technical Note No. 249, Defence Research Establishment Suffield, Ralston, Alberta, Canada, January 1969.

39. S. B. Mellsen, "Correlation of Drag Measurements in Operation PRAIRIE FLAT with Known Steady Flow Values (U)", DRES Suffield Memorandum No. 12/69, Defence Research Establishment Suffield, Ralston, Alberta, Canada, April 1969.

40. S. B. Mellsen, "Aerodynamic Drag Measurements and Flow Studies on a Circular Cylinder in a Shock Tube (U)", DRES Suffield Memorandum No. 7/69, Defence Research Establishment Suffield, Ralston, Alberta, Canada, May, 1969.

41. S. B. Mellsen, "Drag of Free Flight Cylinders in a Blast Wave", The Shock and Vibration Bulletin, Bulletin 40, part 2, pp. 83-99, December 1969.

42. S. B. Mellsen, "Measurement of Drag on Cylinders by the Free Flight Method - Event DIAL PACK (U)", DRES Suffield Technical Paper No. 382, Defence Research Establishment Suffield, Ralston, Alberta, Canada, December 1971.

43. S. B. Mellsen, "Drag Measurements in Event DIAL PACK", The Shock and Vibration Bulletin, Bulletin 42, part 4, pp. 157-173, January 1972.

44. S. B. Mellsen, "Drag on Cylinders in a 20 to 25 millisecond Blast Wave (U)", DRES Suffield Memorandum No. 114/71, Defence Research Establishment Suffield, Ralston, Alberta, Canada, July 1972.

45. R. Naylor and S. B. Mellsen, "Unsteady Drag from Free-Field Blast Waves (U)", DRES Suffield Memorandom No. 42/71, Defence Research Establishment Suffield, Ralston, Alberta, Canada, January 1973.

46. S. B. Mellsen, "Measurement of Drag on Cylinders by the Free Flight Method - Event MIXED COMPANY (U)", DRES Suffield Technical Paper No. 419, Defence Research Establishment Suffield, Ralston, Alberta, Canada, March 1974.

47. A. W. M. Gibb and D. A. Hill, "Free-Flight Measurement of the Drag Forces on Cylinders - Event DICE THROW", Proceedings of the DICE THROW Symposium, June 21-23, 1977, DNA Report No. DNA-4377P-2, Vol. 2, Defence Nuclear Agency, Washington, D.C., July 1977.

48. A. W. M. Gibb and D. A. Hill, "Free-Flight Measurement of the Drag Forces on Cylinders in Event DICE THROW (U)", DRES Suffield Technical Paper No. 453, Defence Research Establishment Suffield, Ralston, Alberta, Canada, February 1979.

49. B. R. Long, "The Analysis of Shipboard Lattice Antenna Masts under Air Blast and Underwater Shock Loading: part III - Final Report (U)", DRES Suffield Technical Paper No. 431, Defence Research Establishment Suffield, Ralston, Alberta, Canada, June 1975.

50. G. V. Price and C. G. Coffey, "Blast Response of 35-ft Fiberglass Whip Antenna - Event DICE THROW", Proceedings of the DICE THROW Symposium, June 21-23, 1977, DNA Report No. DNA-4377P-2, Vol. 2, Defence Nuclear Agency, Washinton, D.C., July 1977.

51. C. G. Coffey and G. V.Price, "Blast Response of UHF Polemast Antenna - Event DICE THROW", Proceedings of the DICE THROW Symposium, June 21-23, 1977, DNA Report No. DNA-4377P-2, Vol. 2, Defence Nuclear Agency, Washington, D.C., July 1977.

52. C. G. Coffey and G. V. Price, "Blast Response of UHF Polemast Antenna - Event DICE THROW (U)", DRES Suffield Technical Paper No. 449, Defence Research Establishment Suffield, Ralston, Alberta, Canada, November 1977.

53. R. Geminder and R. W. Hicks, "Analytical and Empirical Study of Shipboard Antenna Masts Subjected to a Blast Environment: Vol. I, II and III", MRI Report No. MRI-C2230-TR-1, Mechanics Research Incorporated, Los Angeles, California, U.S.A., November 1969.

54. R. W. Hicks and R. Geminder, "Calculated Strains in Antenna Mast Located at 19 psi Subjected to the 'DIAL PACK' Blast Environment", MRI Report No. MRI-2422, Mechanics Research Incorporated, Los Angeles, California, U.S.A., December 1970.

55. J. J. Gottlieb and D. V. Ritzel, "A Semi-Empirical Equation for the Viscosity of Air (U)", DRES Suffield Technical Note No. 454, Defence Research Establishment Suffield, Ralston, Alberta, Canada, July 1979.

56. R. C. Makino and R. E. Shear, "Unsteady Spherical Flow Behind a known Shock Line", BRL Report No. 1154, U.S. Army Ballistic Research Laboratory, Aberdeen Proving Ground, Maryland, U.S.A., November 1961.

57. J. M. Dewey and D. J. McMillin, "The Properties of a Blast Wave Produced by a Large-Scale Detonable Gas Explosion", Proceedings of the Seventh International Symposium on Military Applications of Blast Simulation, Vol. 1, pp. 6.6-1 to 6.6-18, held on the 13-17 July 1981 in Medicine Hat, Alberta, sponsored by the Defence Research Establishment Suffield, Ralston, Alberta, Canada.

58. A. Celmins, "Reconstruction of a Blast Field from Selected Pressure Observations," Proceedings of the Seventh International Symposium on Military Applications of Blast Simulation, Vol. 1, pp. 2.5-1 to 2.5-17, held on the 13-17 July 1981 in Medicine Hat, Alberta, sponsored by the Defence Research Establishment Suffield, Ralston, Alberta, Canada.

59. R. C. Makino, "An Approximation Method in Blast Calculations", BRL Memorandum Report No. 1034, U.S. Army Ballistic Research Laboratory, Aberdeen Proving Ground, Maryland, U.S.A., February 1956.

60. I. I. Glass and J. G. Hall, "Shock Tubes", section 18 of the "Handbook of Supersonic Aerodynamics", NAVORD Report No. 1488 (Vol. 6), U.S. Government Printing Office, Washington, D. C., December 1959.

61. I. I. Glass, "Aerodynamics of Blasts", Canadian Aeronautical Journal, Vol. 7, No. 3, pp. 109-135, 1961. Also, UTIA Review No. 17, University of Toronto Institute for Aerospace Studies, Downsview, Ontario, Canada, 1960.

62. R. Courant and K. O. Friedrichs, "Supersonic Flow and Shock Waves", Interscience Publishers (a division of John Wiley and Sons), New York, New York, U.S.A., 1948.

63. J. A. Owczarek, "Fundamentals of Gasdynamics", International Textbook Company, Scranton, Pennslyvania, U.S.A., 1964.

64. J. Glimm, "Solution in the Large for Nonlinear Hyperblic Systems of Equations", Communications of Pure and Applied Mathematics, Vol. 18, pp. 697-715, 1965.

65. J. A. Chorin, "Random Choice Solution of Hyperbolic System", Journal of Computational Physics, Vol. 22, part 4, pp.517-533, 1976.

66. G. A. Sod, "A Numerical Study of Converging Cylindrical Shock", Journal of Fluid Mechanics, Vol. 83, part 4, pp. 785-794, 1977.

67. O. Igra, J. J. Gottlieb, and T. Saito, "An Analytical and Numerical Study of the Interaction of Rarefaction Waves with Area Changes in Ducts - Part 2: Area Enlargements", UTIAS Report No. 273, University of Toronto Institute for Aerospace Studies, Downsview, Ontario, Canada, to be printed in 1984.

68. G. E. Forsythe, M. A. Malcolm and C. B. Moler, "Computer Methods for Mathematical Computation", Prentice-Hall, Englewood Cliffs, New Jersey, U.S.A., 1977.

69. E. Kreyszig, "Advanced Engineering Mathematics", fourth edition, John Wiley and Sons, New York, New York, U.S.A., 1979.

70. G. I. Taylor, "The Air Wave Surrounding an Expanding Sphere", Proceedings of the Royal Society, Series A, Vol. 186, pp. 273-292, 1946.

71. R. G. Sachs, "The Dependence of Blast on Ambient Pressure and Temperature", BRL Report No. 446, United States Army Ballistic Research Laboratory, Aberdeen Proving Ground, Maryland, U.S.A., 1950.

72. B. Hopkinson, British Ordnance Board Minutes 13565, Great Britian, 1915.

73. J. M. Dewey and D. J. McMillin, by private correspondence the authors were very thankful to obtain raw and processed experimental data for all shock and particle trajectories and taken in the 500-ton TNT surface explosion trials called SNOWBALL and SAILOR HAT.

TABLE 1. AMBIENT CONDITIONS AND SCALING FACTORS FOR SURFACE EXPLOSION TRIALS

Explosion Trial	Equivalent Mass of TNT (tons)	Ambient Pressure (kPa)	Ambient Sound Speed at 1 m above Ground (m/s)	Scaling Factor for Distance S_r	Scaling Factor for Time S_t
20 tons of TNT	20	93.35	348.26	27.00	26.38
100 tons of TNT	100	94.04	388.91	46.06	40.32
500 tons of TNT (Snowball)	500	93.76	345.89	78.85	77.59
500 tons of TNT (Sailor Hat)	500	100.87	346.59	76.95	75.55
628 tons of ANFO (Dice Throw)	500	85.01	337.23	81.46	82.21

Table 2

List of the distance and time coordinates used for the piston path in the reconstruction of the blast-wave flow field for a 1-kg TNT surface explosion in a standard atmosphere.

(The initial slope of the cubic spline through these coordinate points is 920.49 m/s.)

Distance r (m)	Time t (ms)
1.0040	0.4788
1.0855	0.5737
1.1726	0.6954
1.2715	0.8693
1.3435	1.0431
1.3985	1.2170
1.4625	1.4775
1.5145	1.7385
1.5770	2.1732
1.6225	2.6078
1.6540	3.0424
1.6725	3.4771
1.6830	3.9117
1.6875	4.3463

Table 3

List of the distance and time coordinates used for the piston path in the reconstruction of the blast-wave flow field for a 1-kg TNT equivalent ANFO surface explosion in a standard atmosphere.

(The initial slope of the cubic spline through these coordinate points is 1205.25 m/s.)

Distance r (m)	Time t (ms)
1.0740	0.3931
1.1675	0.4781
1.2465	0.5650
1.3075	0.6519
1.3715	0.7823
1.4280	0.9562
1.4840	1.2170
1.5190	1.4776
1.5455	1.8255
1.5585	2.1732
1.5605	2.6078
1.5500	3.0424
1.5355	3.4771
1.5150	3.9117
1.4875	4.3463

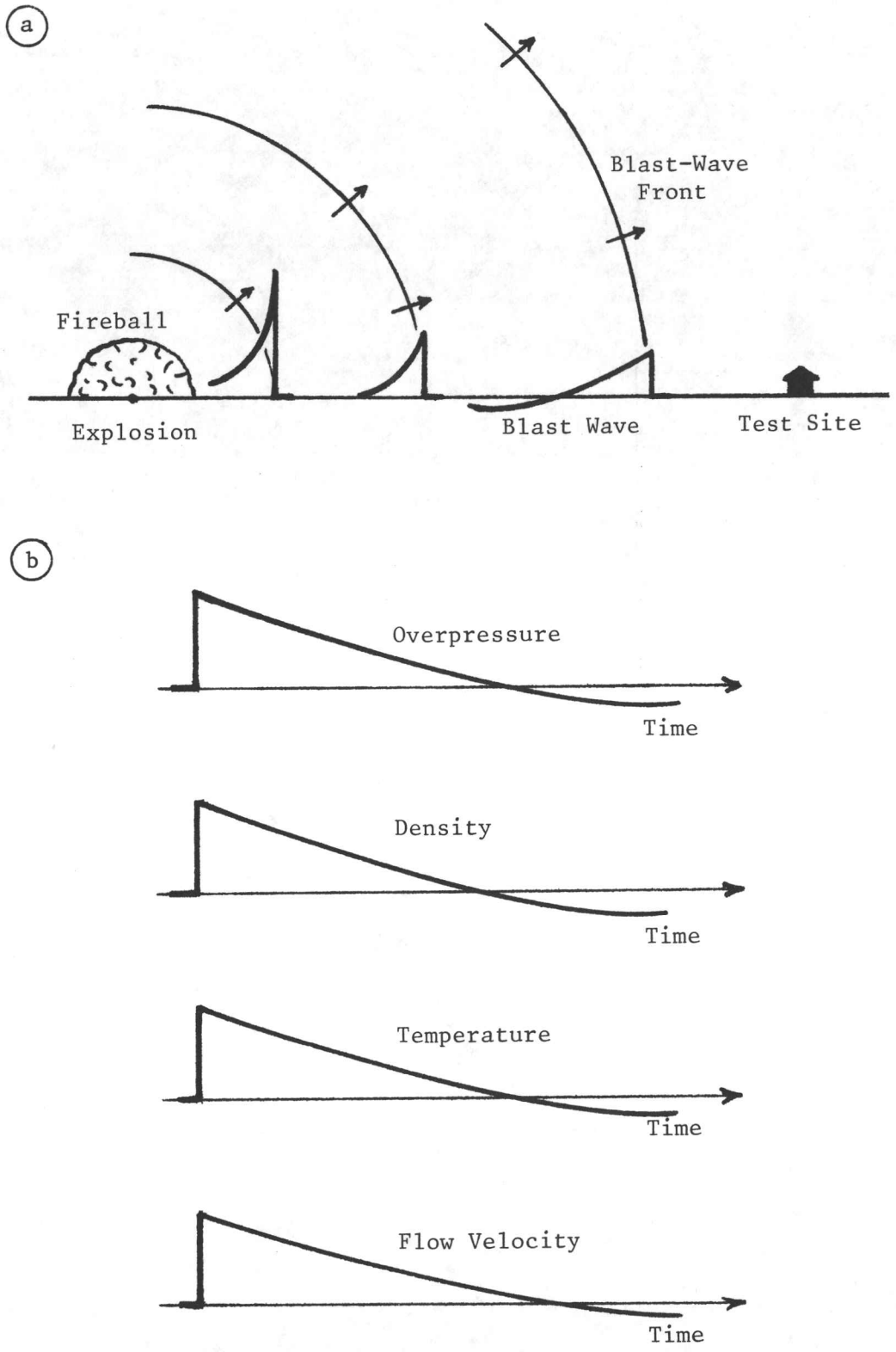

Fig. 1. Schematic diagrams of the blast wave from an explosion (a) and the resulting time histories of overpressure, density, temperature and flow velocity (b) at the test site.

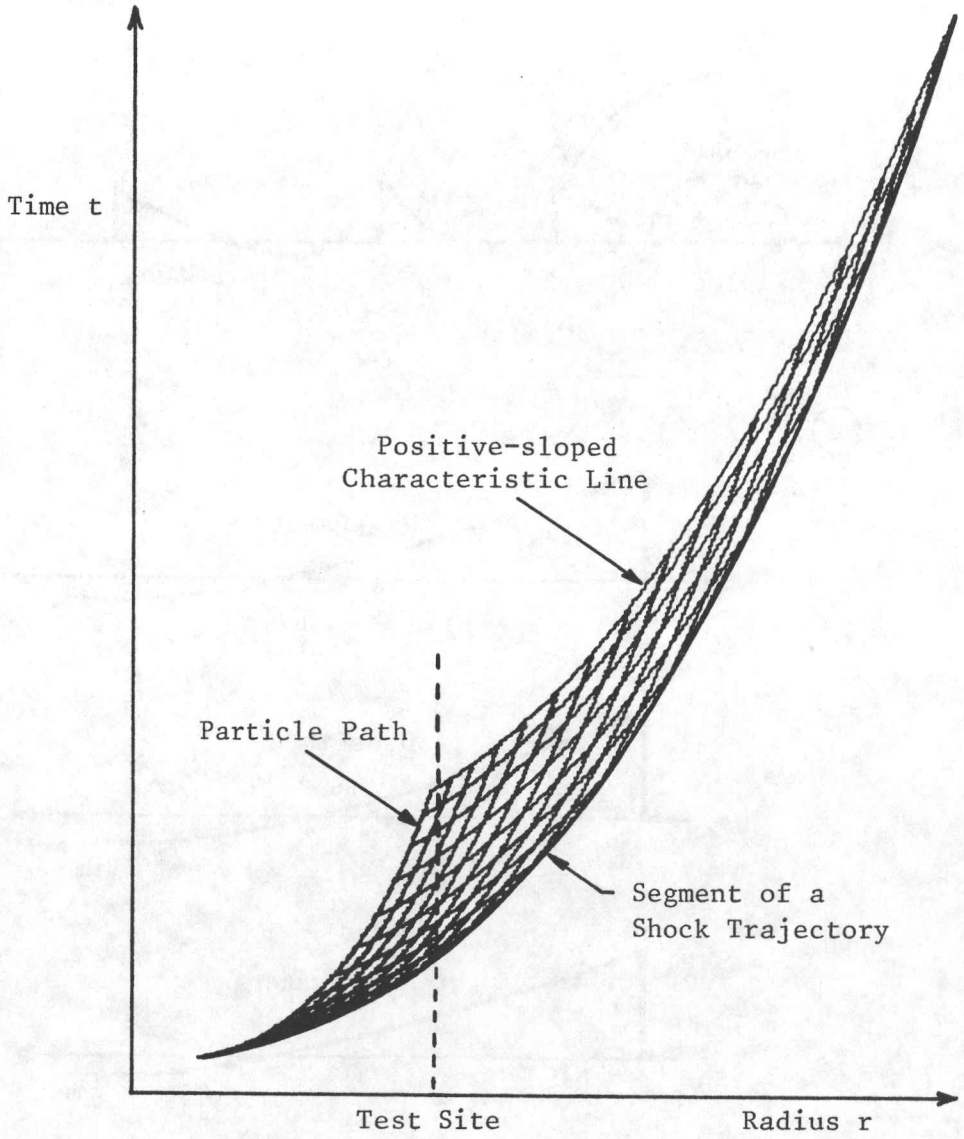

Fig. 2. Illustration of the reconstructed region of a blast-wave flow field behind a segment of a known shock trajectory.

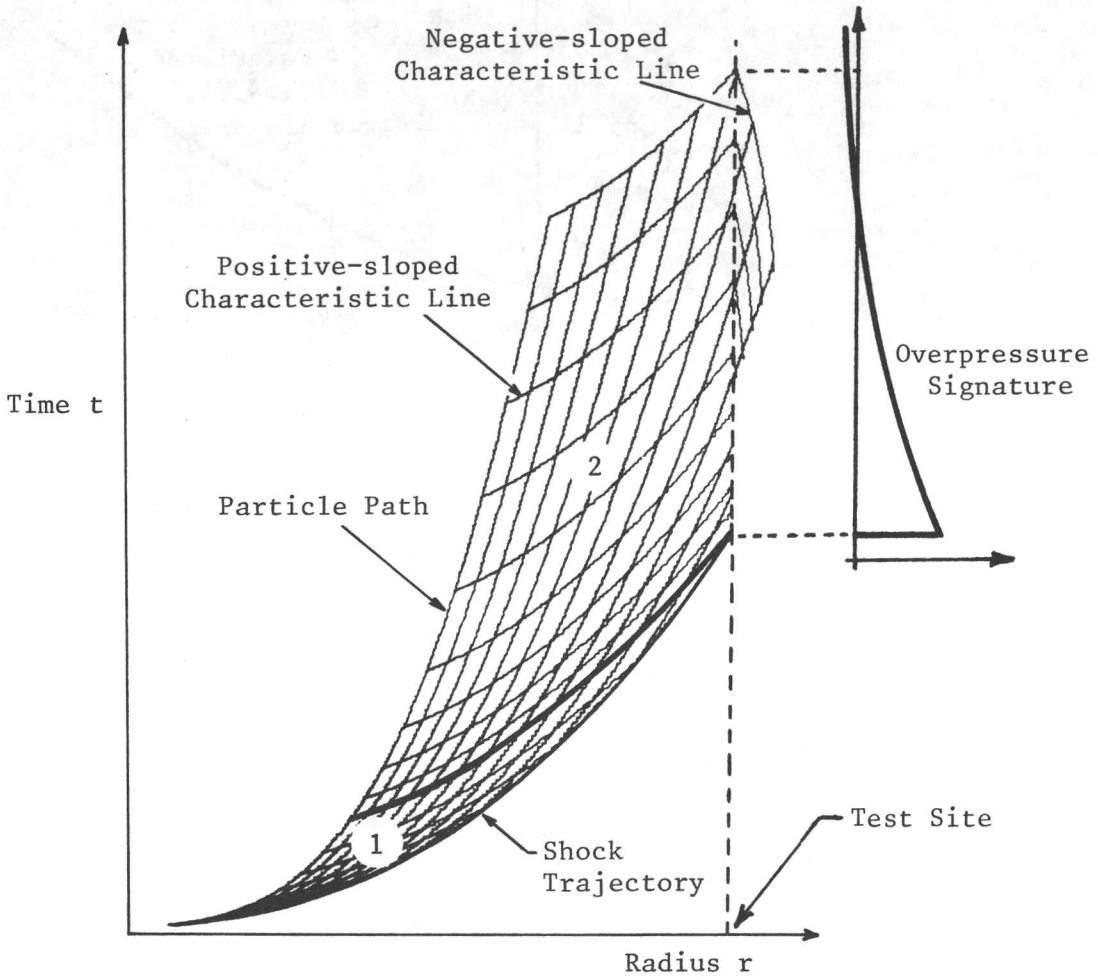

Fig. 3. Illustration of the reconstructed region of a blast-wave flow field behind a segment of a known shock trajectory and extended in time by using an overpressure-time signature measured at the test site.

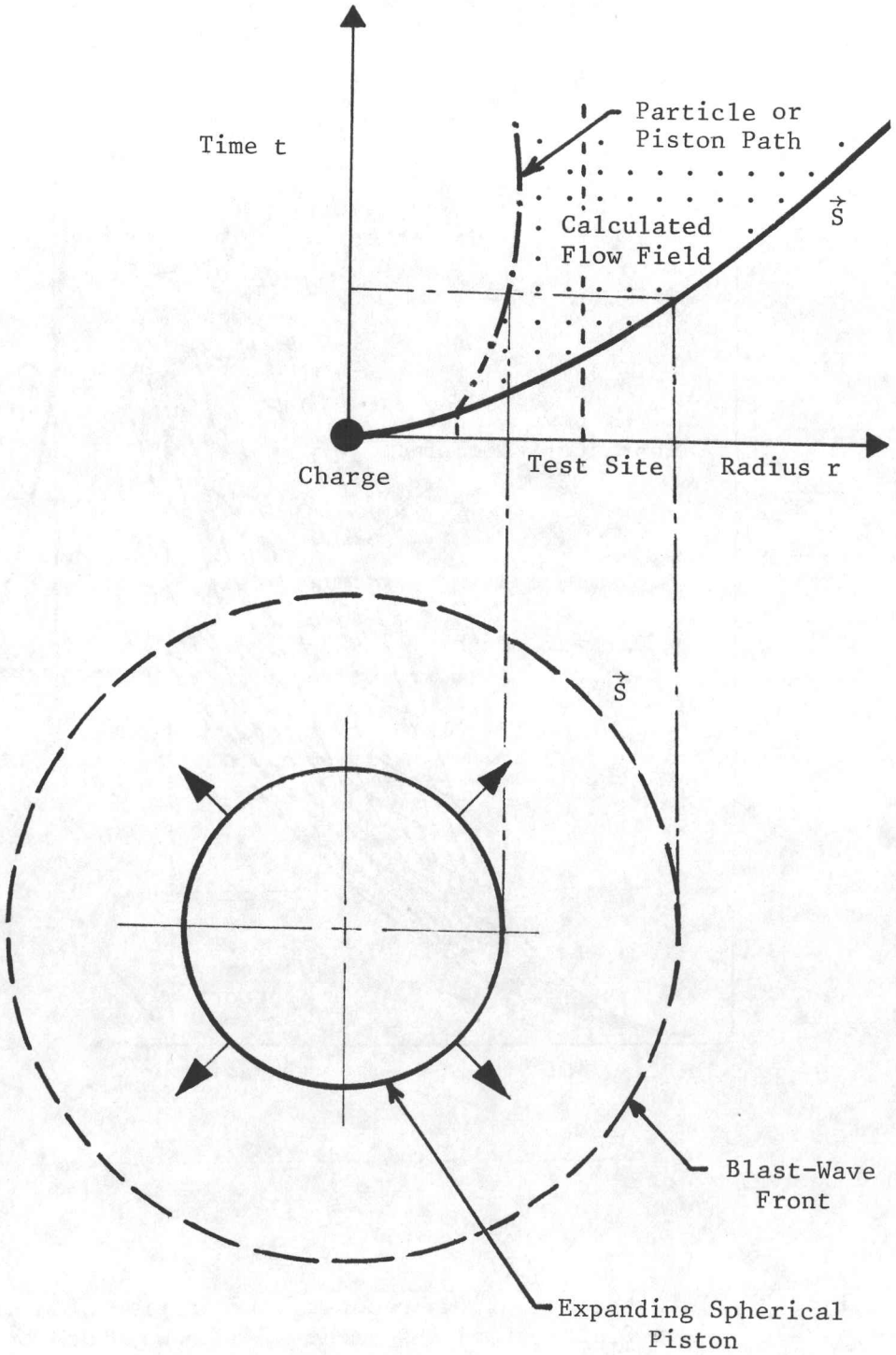

Fig. 4. Explosion flow field produced by an expanding spherical piston.

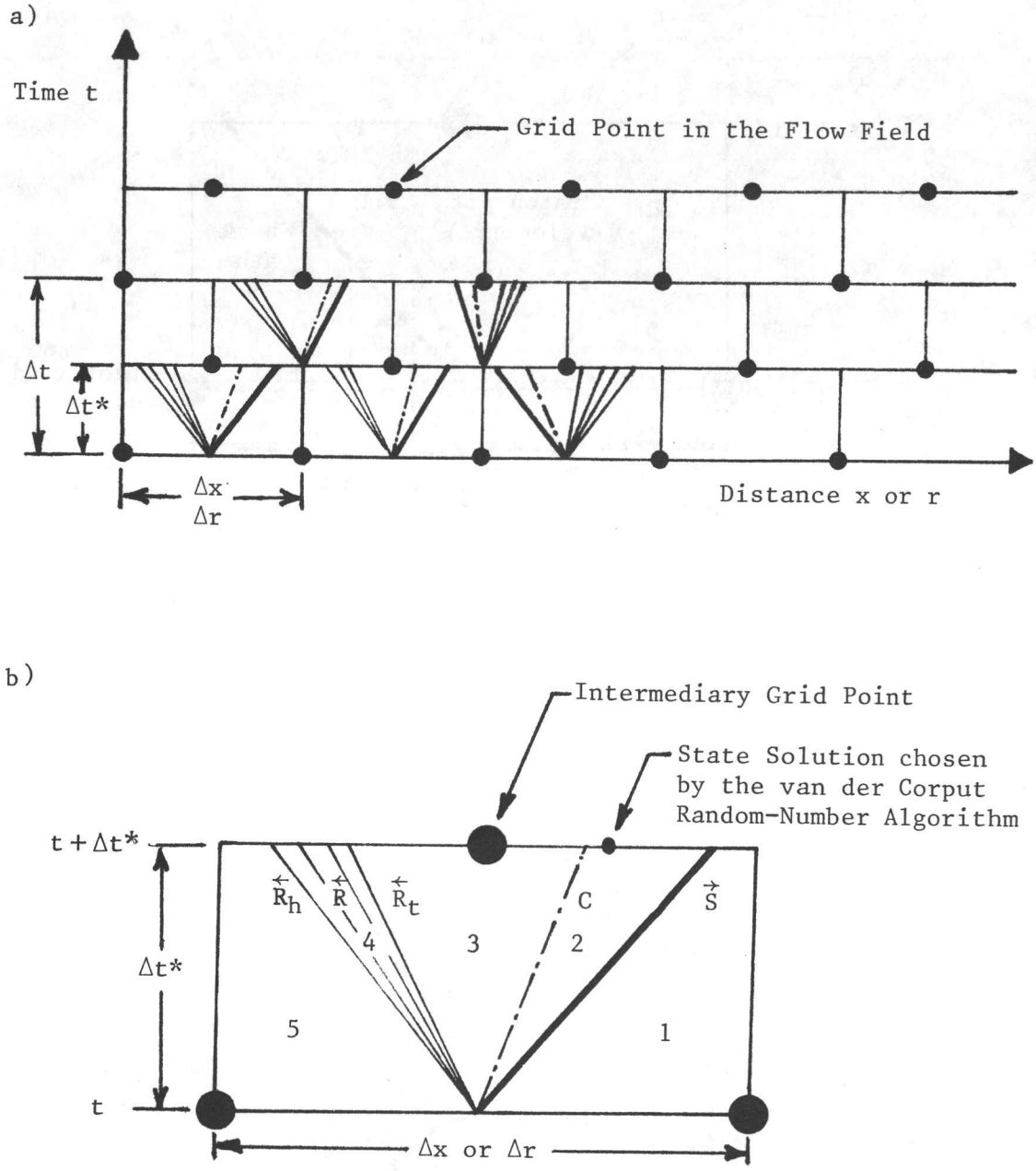

Fig. 5. Illustration of the grid layout for the flow field (a) and the wave pattern for the solution of the shock-tube problem between two consecutive grid points (b).

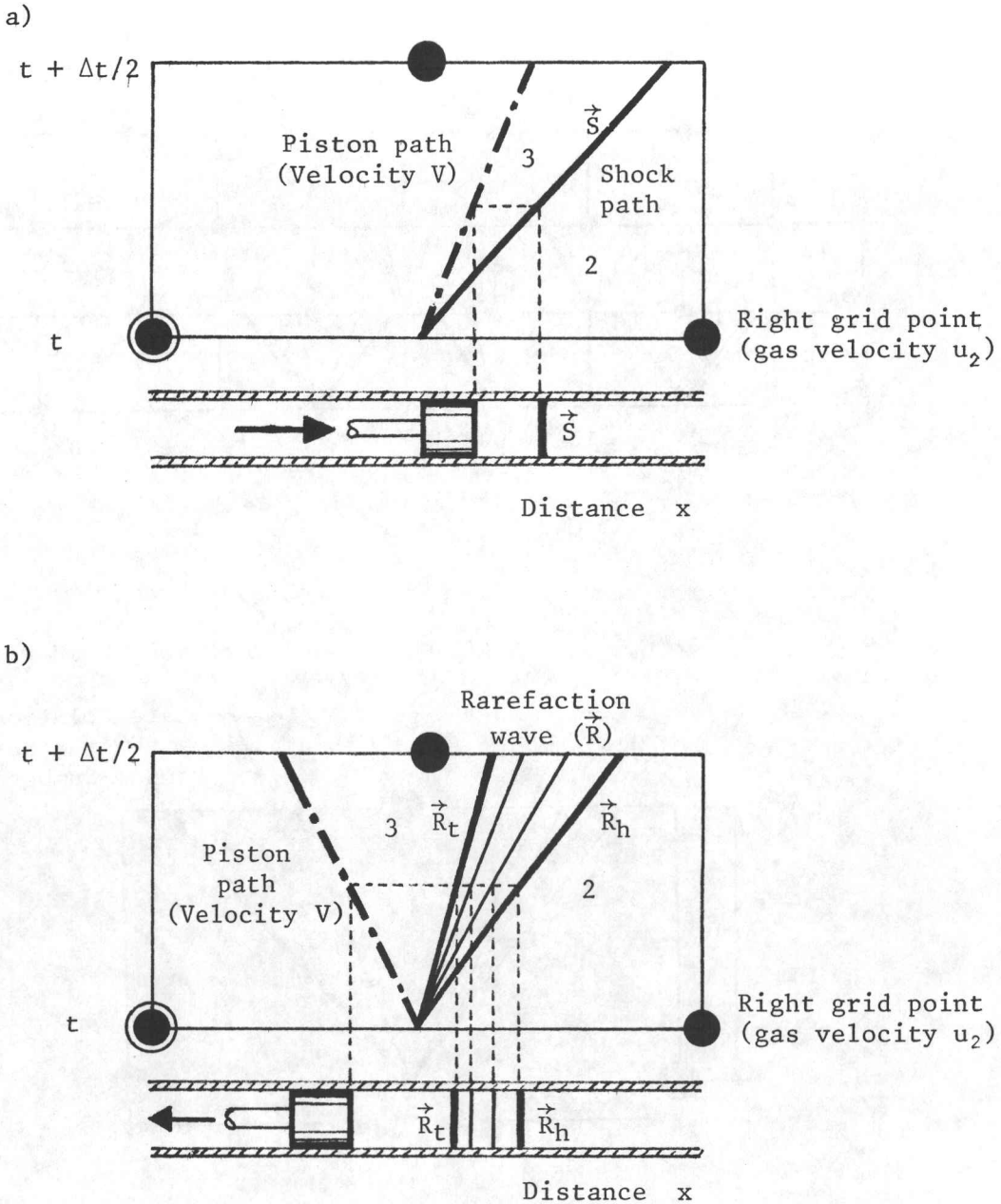

Fig. 6. Illustrations of the elemental wave patterns needed for the solution by the RCM for piston motions for which (a) the piston velocity exceeds the gas velocity ($V > u_2$) (b) the gas velocity exceeds the piston velocity ($u_2 > V$)

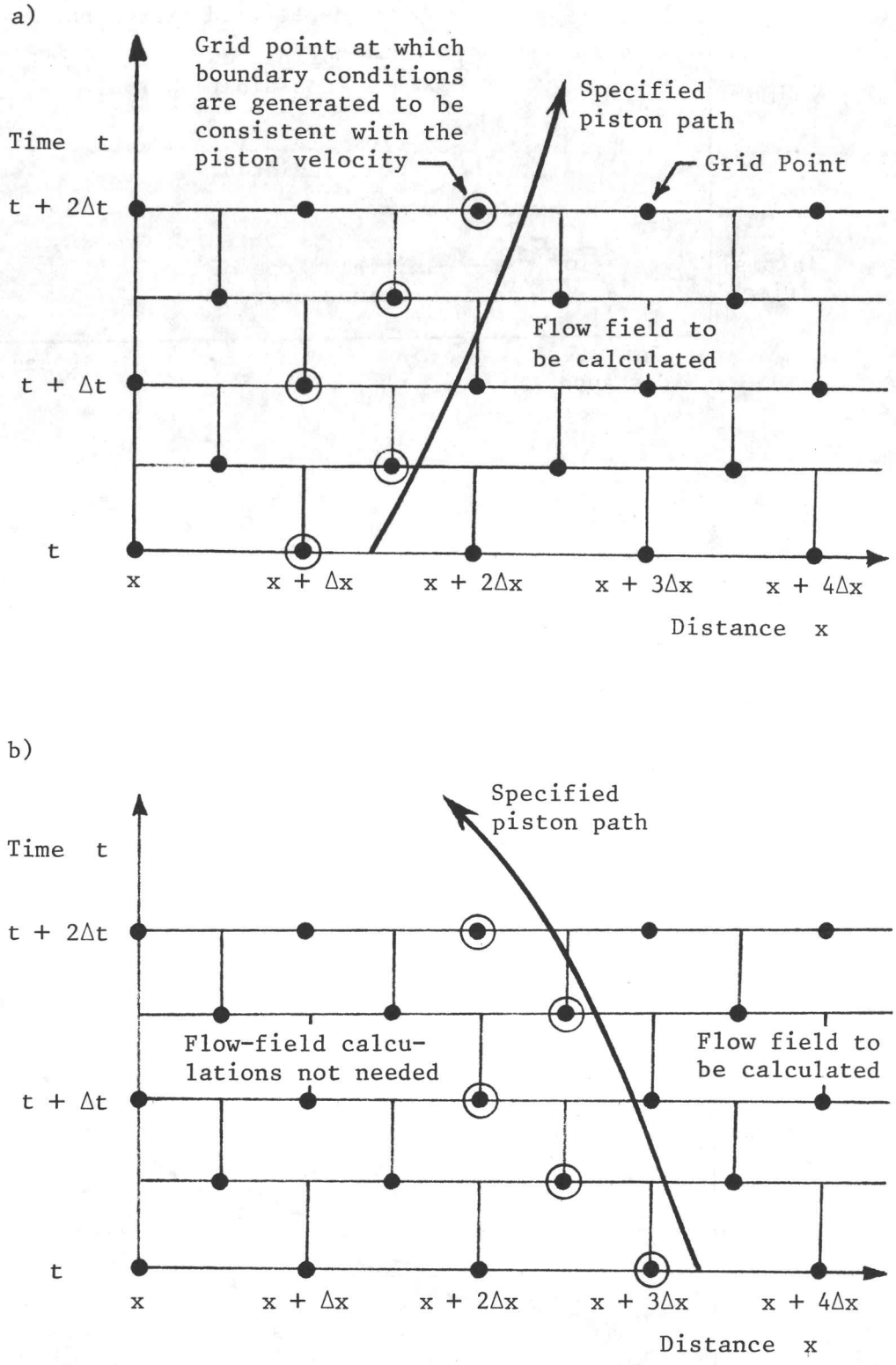

Fig. 7. Illustrations of the grid layout for flow-field computations by the RCM for a specified piston path which slopes to the right (a) and left (b).

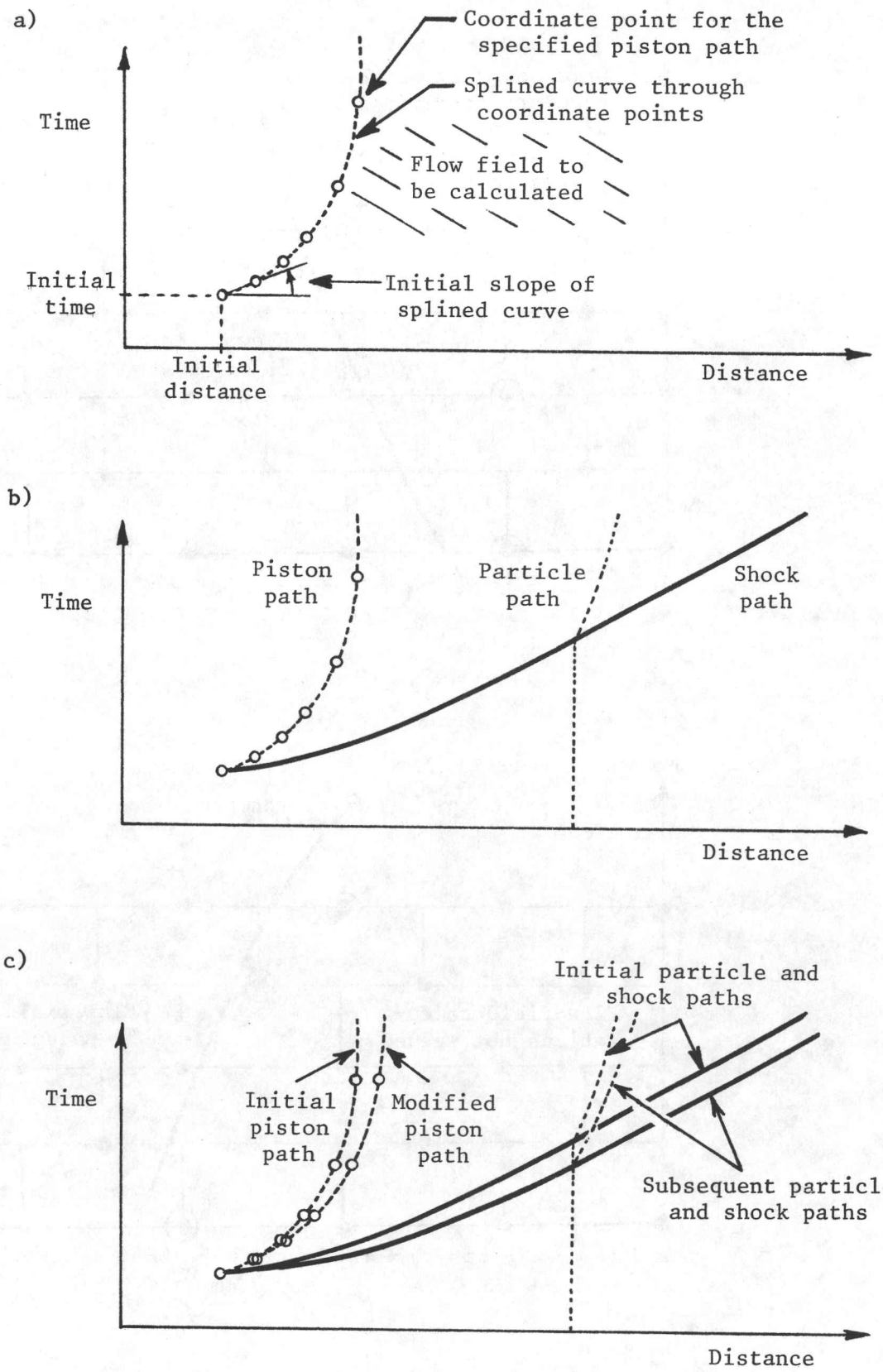

Fig. 8. Illustration of the initial guess of the coordinate points for the piston path and the splined curve (a), resulting prediction of the flow field in front of the moving piston (b), and the first modification to the piston path that gives the modified flow field.

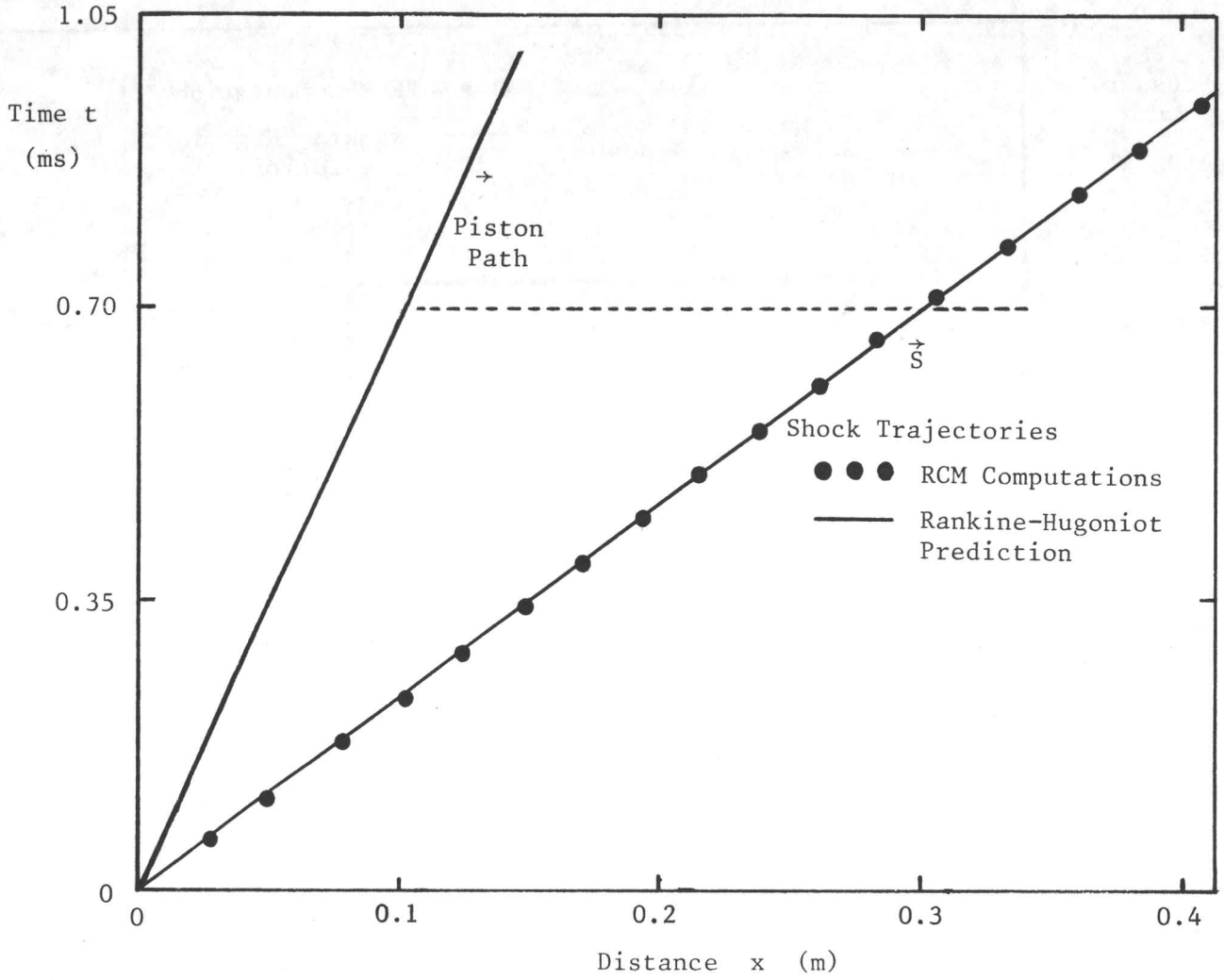

Fig. 9. Comparison of shock trajectories computed by both the RCM and the Rankine-Hugoniot equations, for a specified linear piston path with a constant piston velocity of 143.8 m/s. The shock Mach number from the Rankine-Hugoniot prediction is 1.285.

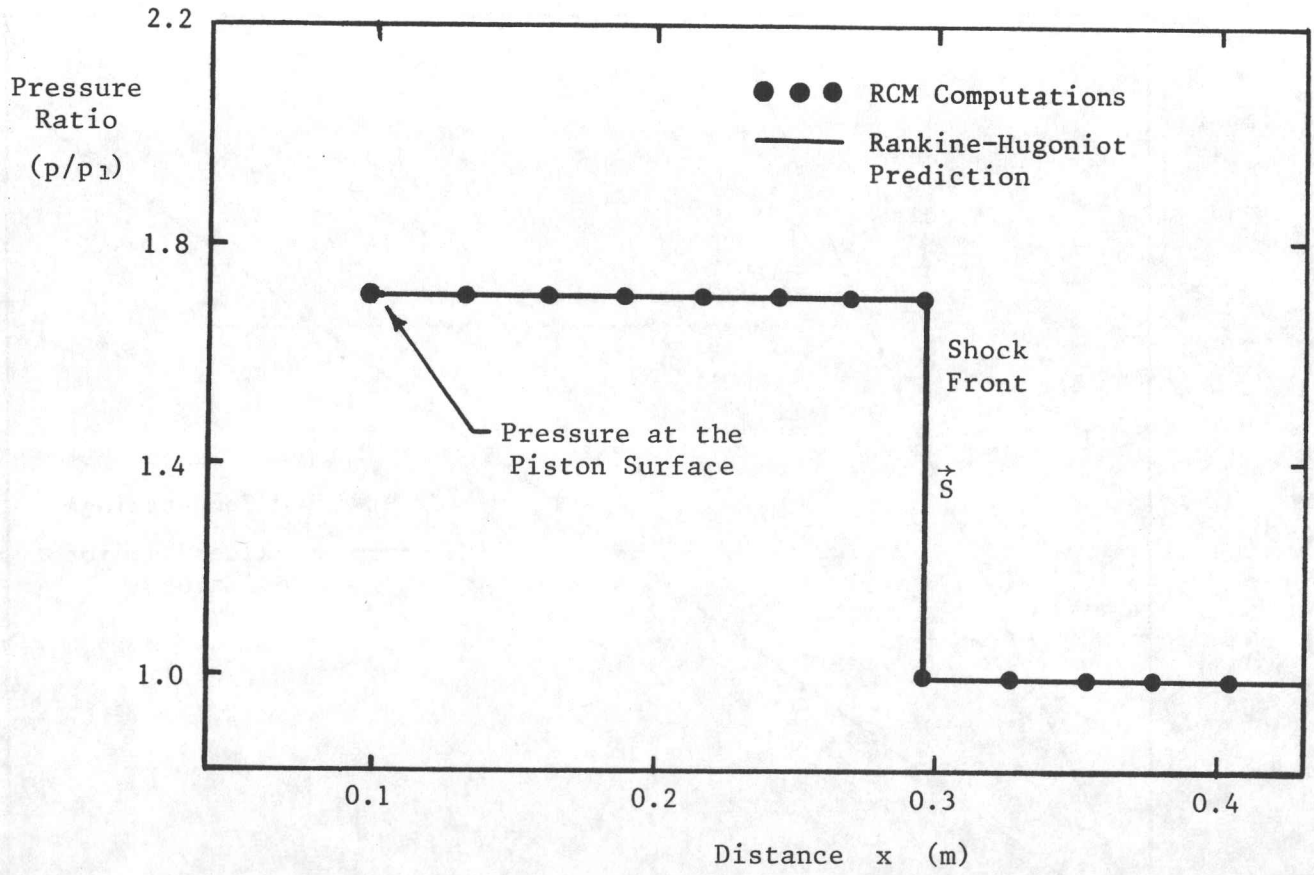

Fig. 10. Comparison of shock-wave pressures computed by both the RCM and the Rankine-Hugoniot equations, for a specified linear piston path shown in Fig. 9 with a constant velocity of 143.8 m/s. The shock pressure ratio from the Rankine-Hugoniot prediction is 1.760.

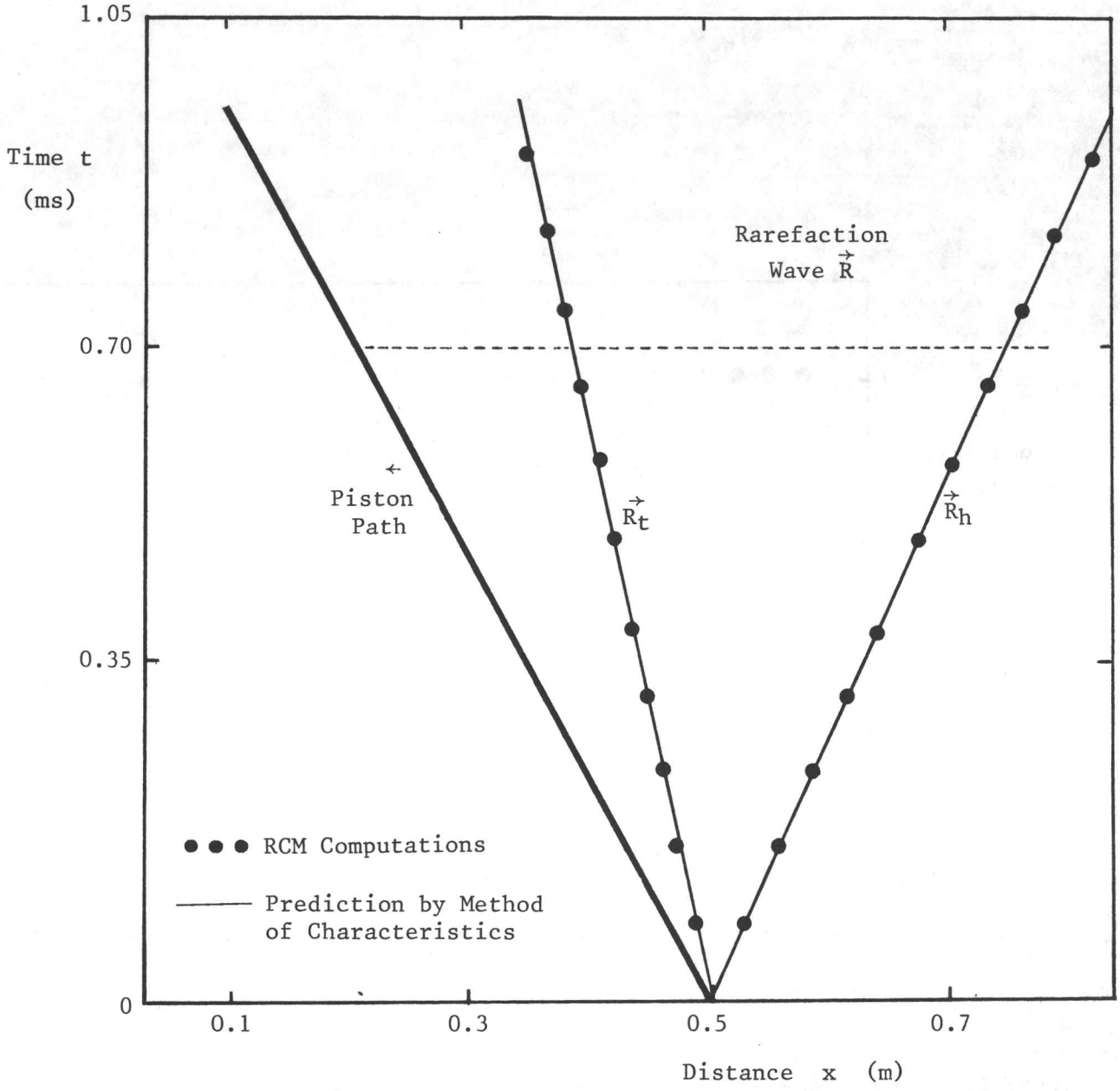

Fig. 11. Comparison of locations of both the rarefaction-wave head and tail, as calculated by the method of characteristics and the RCM, for the case of a suddenly accelerated piston to a constant velocity of -431.4 m/s. The pressure ratio across the centered rarefaction wave produced by this piston motion is 0.129.

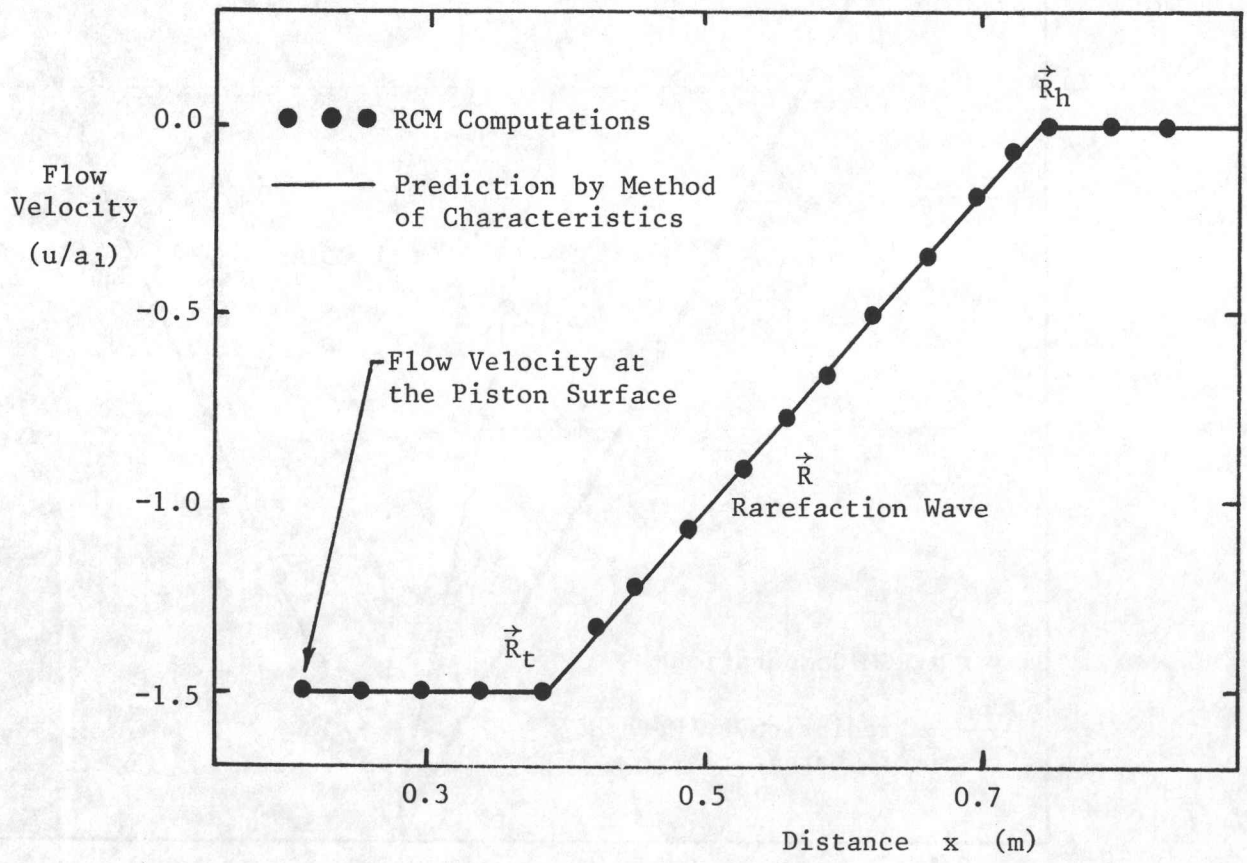

Fig. 12. Comparison of spatial distributions of the flow velocity through the rarefaction wave, as calculated by the method of characteristics and the RCM, for the case of a suddenly accelerated piston to a constant velocity of -431.4 m/s.

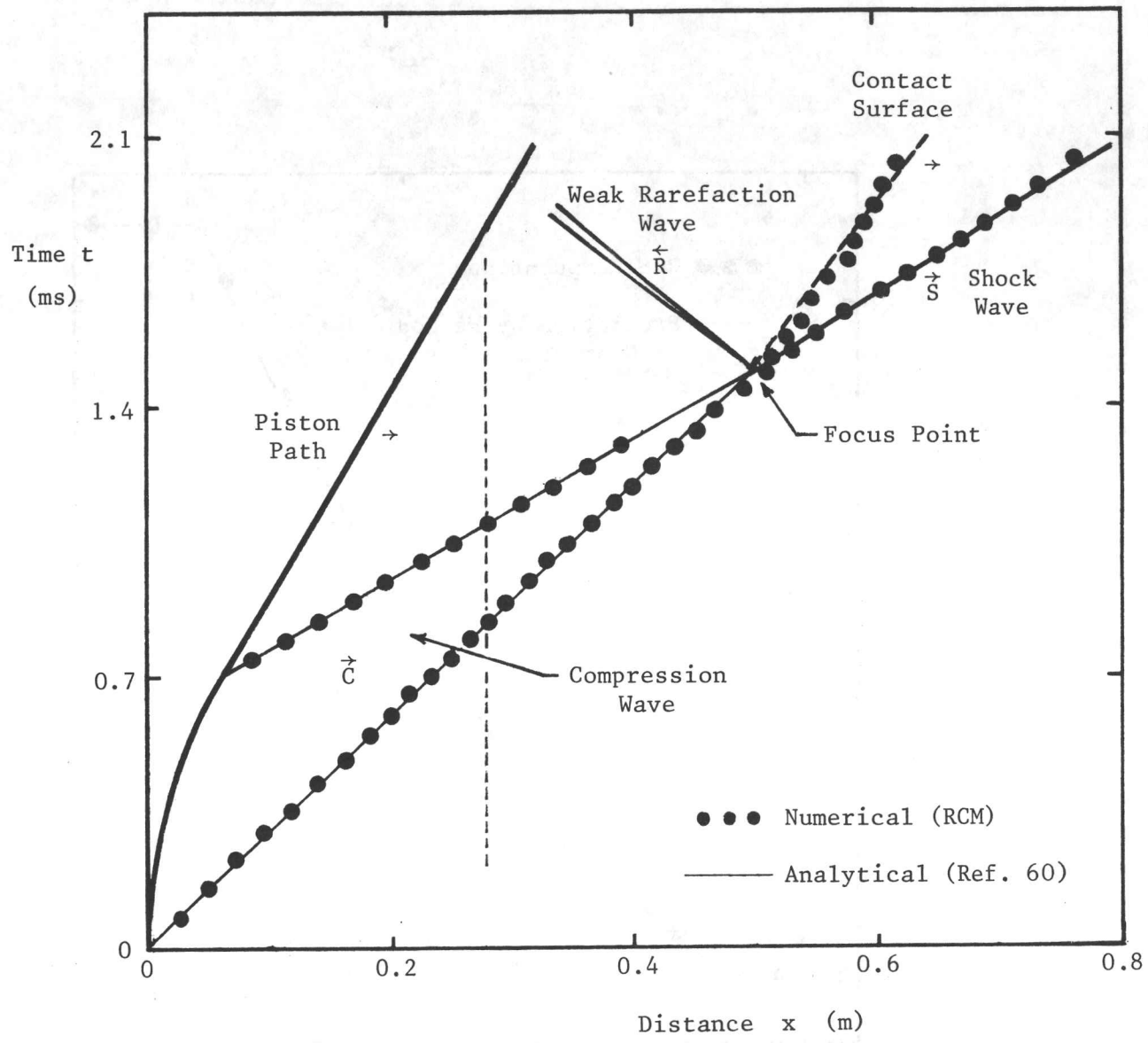

Fig. 13. Comparison of analytical (Ref. 60) and numerical (RCM) results for the case of an accelerated piston motion that produces a focussed compression wave with a resulting shock wave.

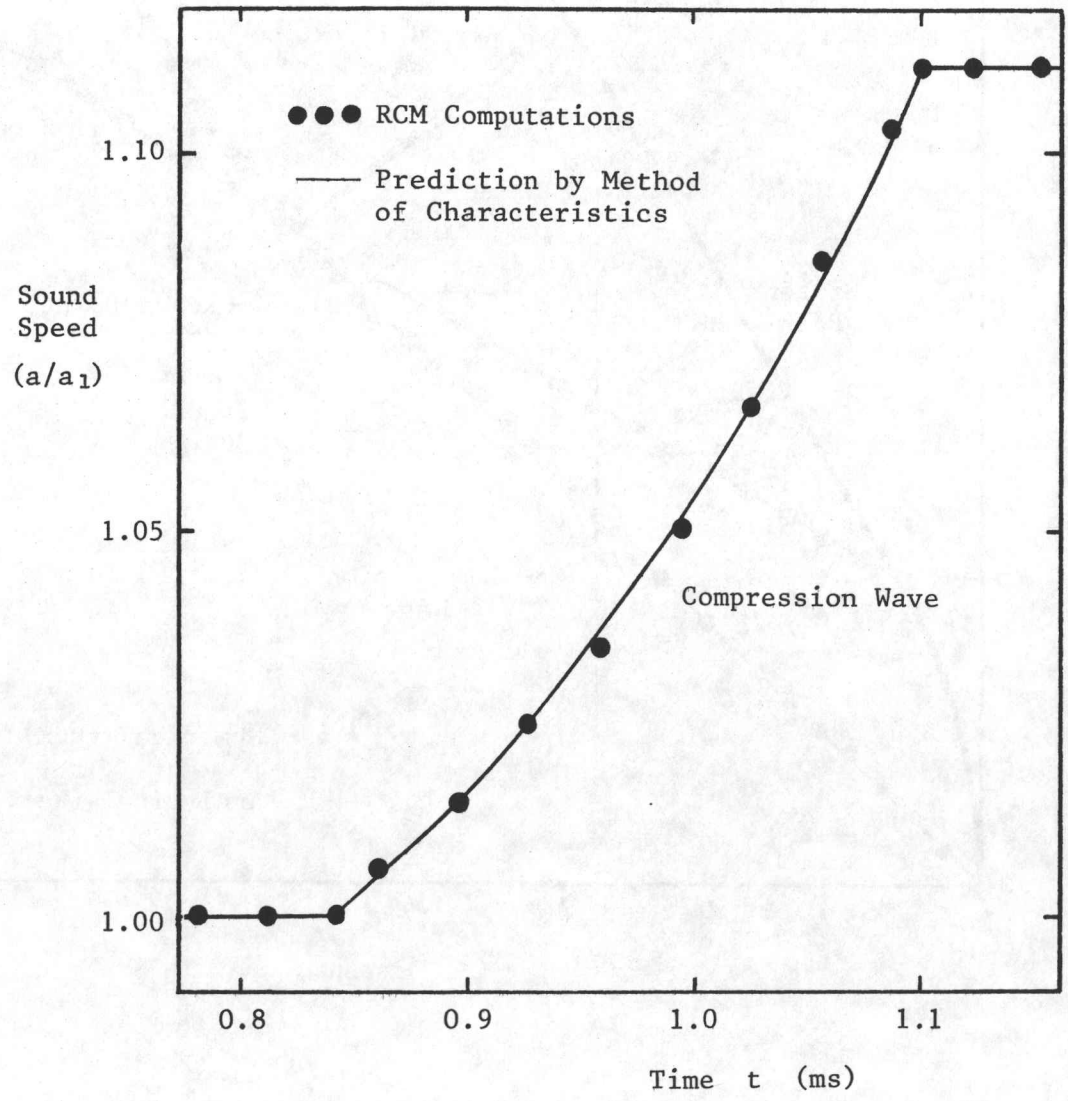

Fig. 14. Comparison of RCM and method-of-characteristics computations for the time history of the sound speed through the focusing compression wave.

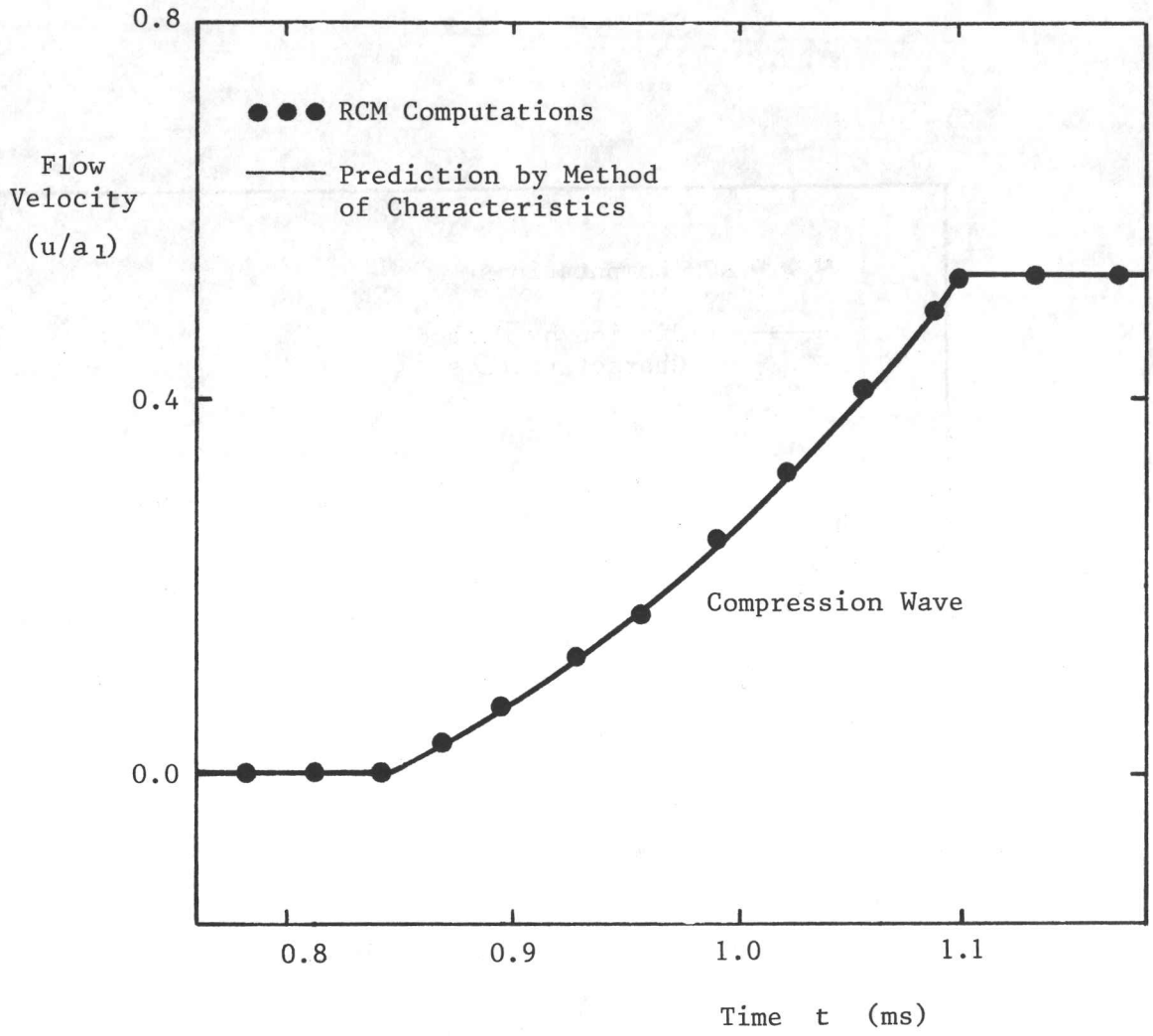

Fig. 15. Comparison of RCM and method-of-characteristics computations for the time history of the flow velocity through the focusing compression wave.

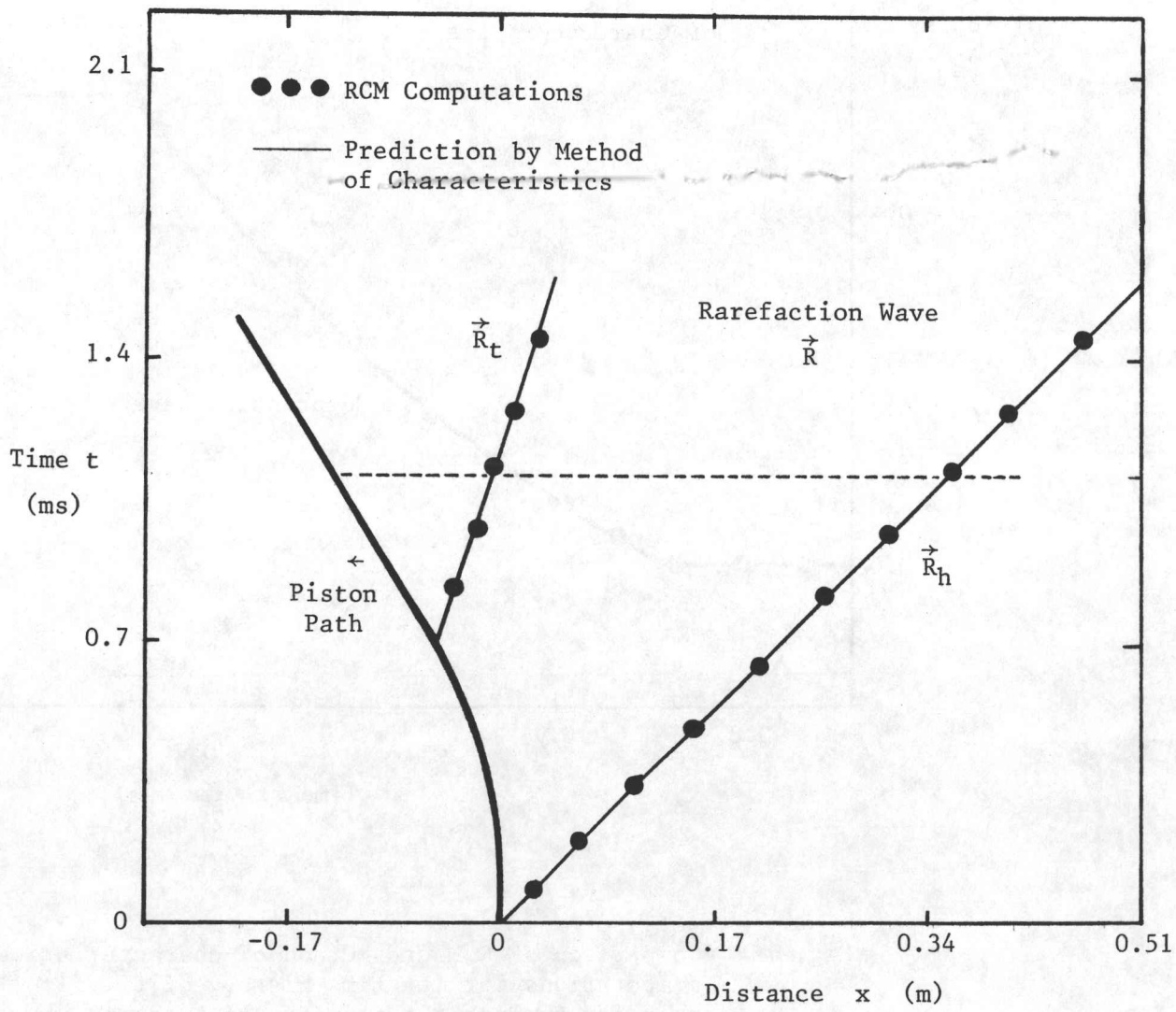

Fig. 16. Comparison of RCM and method-of-characteristics calculations for the locations of the head and tail of a noncentered rarefaction wave with a pressure ratio of 0.433 formed behind an accelerating piston.

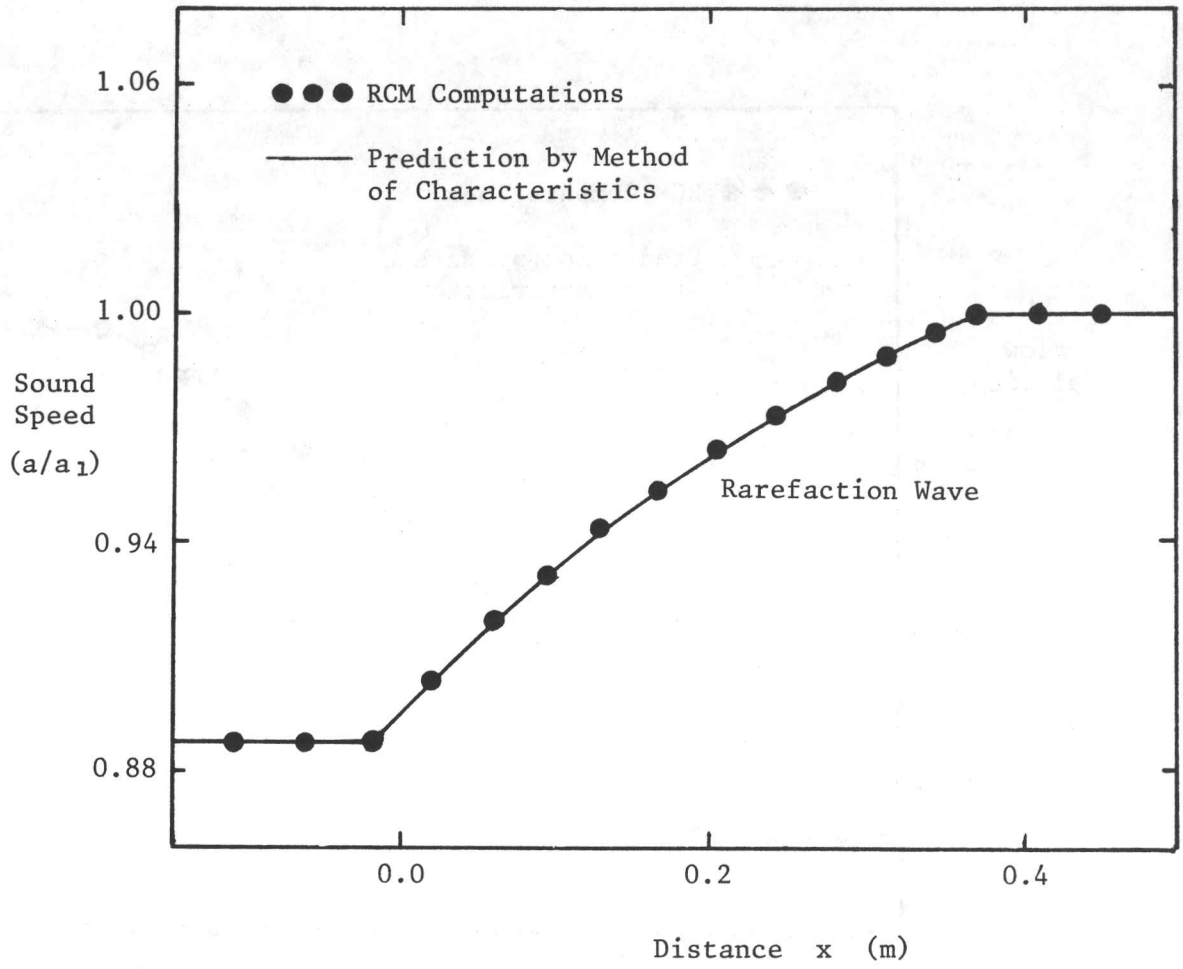

Fig. 17. Comparison of RCM and method-of-characteristics calculations for the spatial distribution of sound speed through the noncentered rarefaction wave formed behind an accelerating piston.

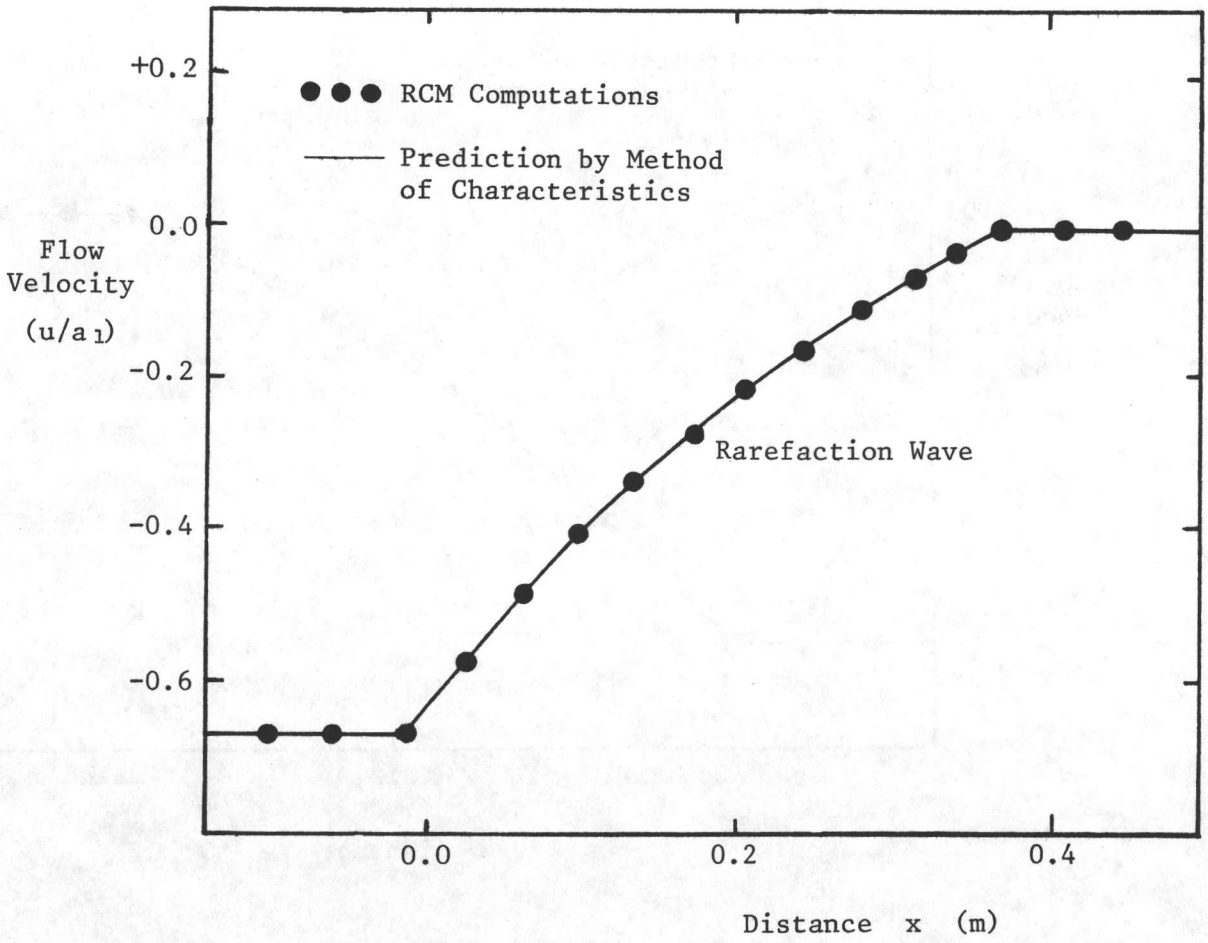

Fig. 18. Comparison of RCM and method-of-characteristics calculations for the spatial distribution of flow velocity through the noncentered rarefaction wave formed behind an accelerating piston.

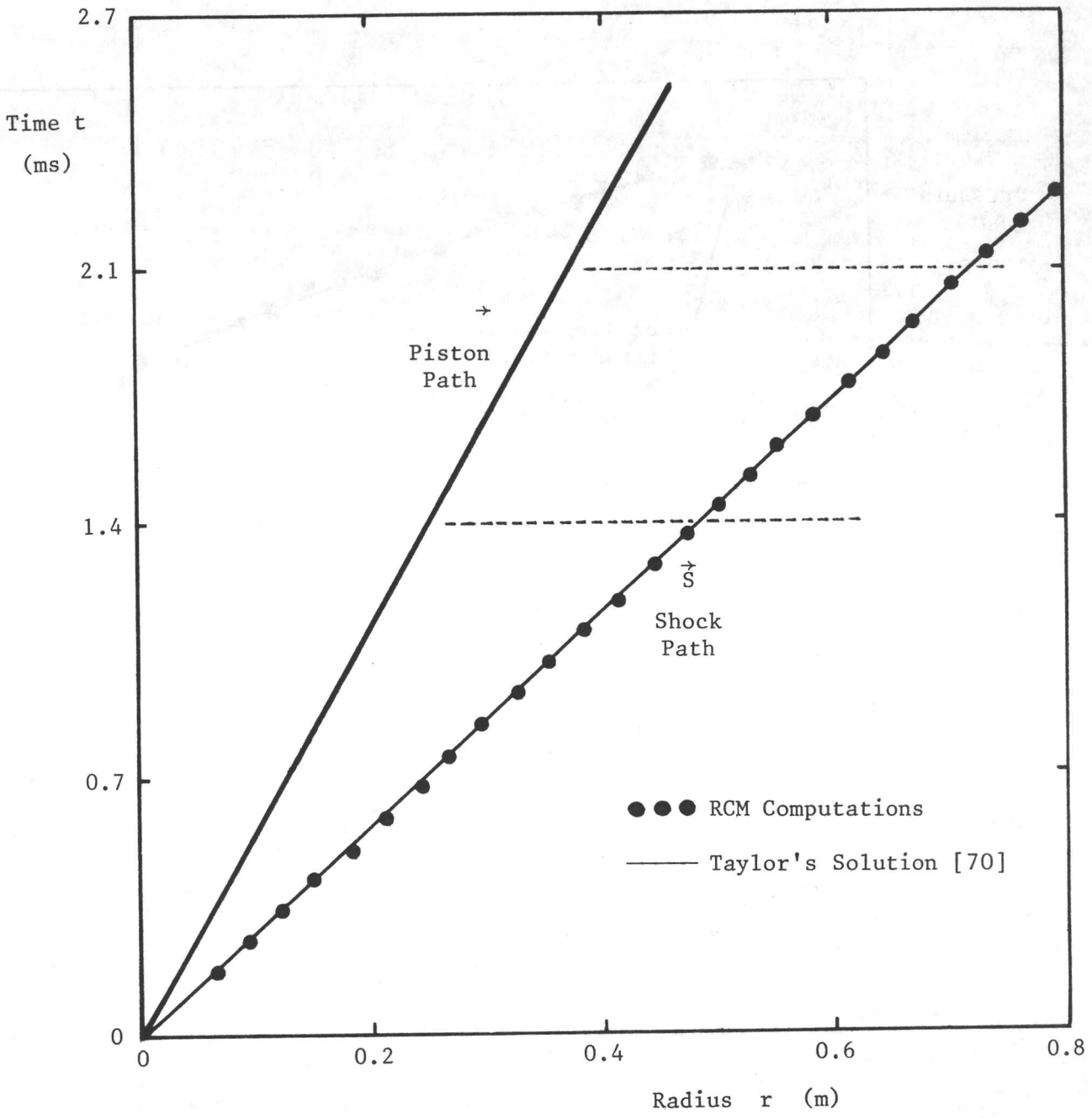

Fig. 19. Comparison of shock trajectories from the RCM and Taylor's solution, for the case of an expanding spherical piston with a constant velocity of 178.0 m/s. The pressure ratio of the shock-wave front is 1.035.

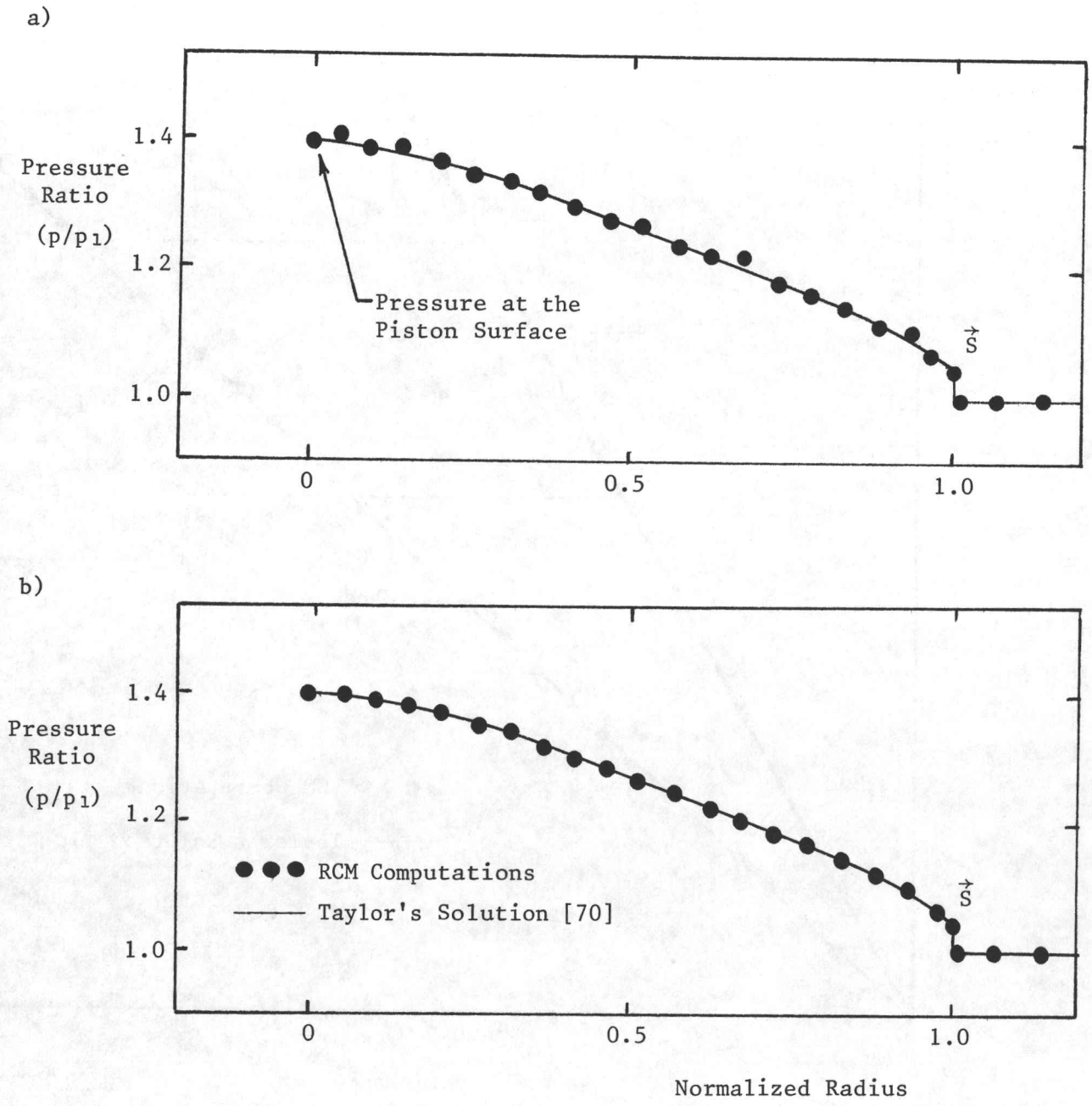

Fig. 20. Comparison of results from the RCM and Taylor's solution for spatial distributions of pressure between an expanding spherical piston and the shock-wave front, at two different times corresponding to 1.4 ms (a) and 2.1 ms (b).

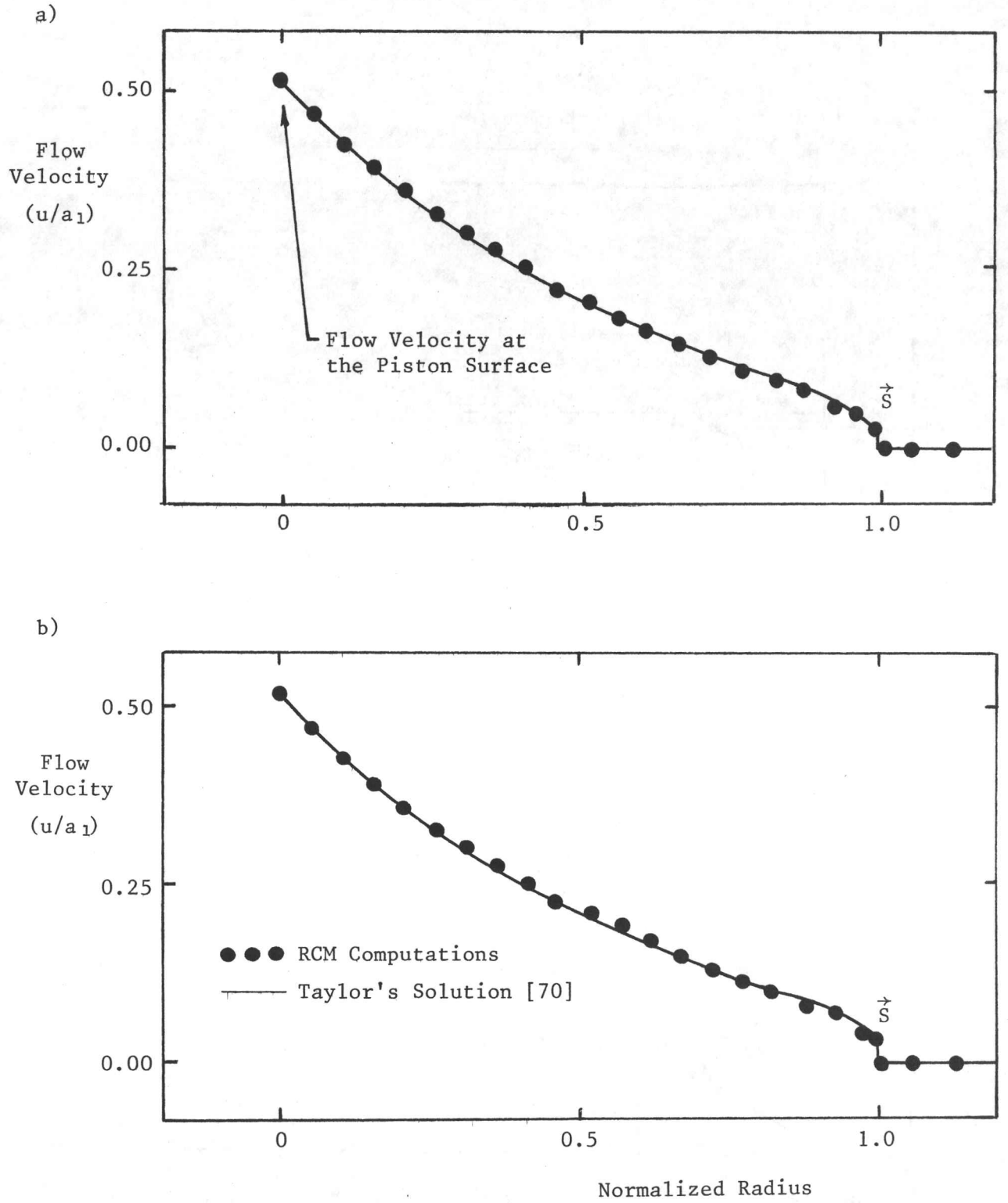

Fig. 21. Comparison of results from the RCM and Taylor's solution for spatial distributions of flow velocity between an expanding spherical piston and the shock-wave front, at two different times corresponding to 1.4 ms (a) and 2.1 ms (b).

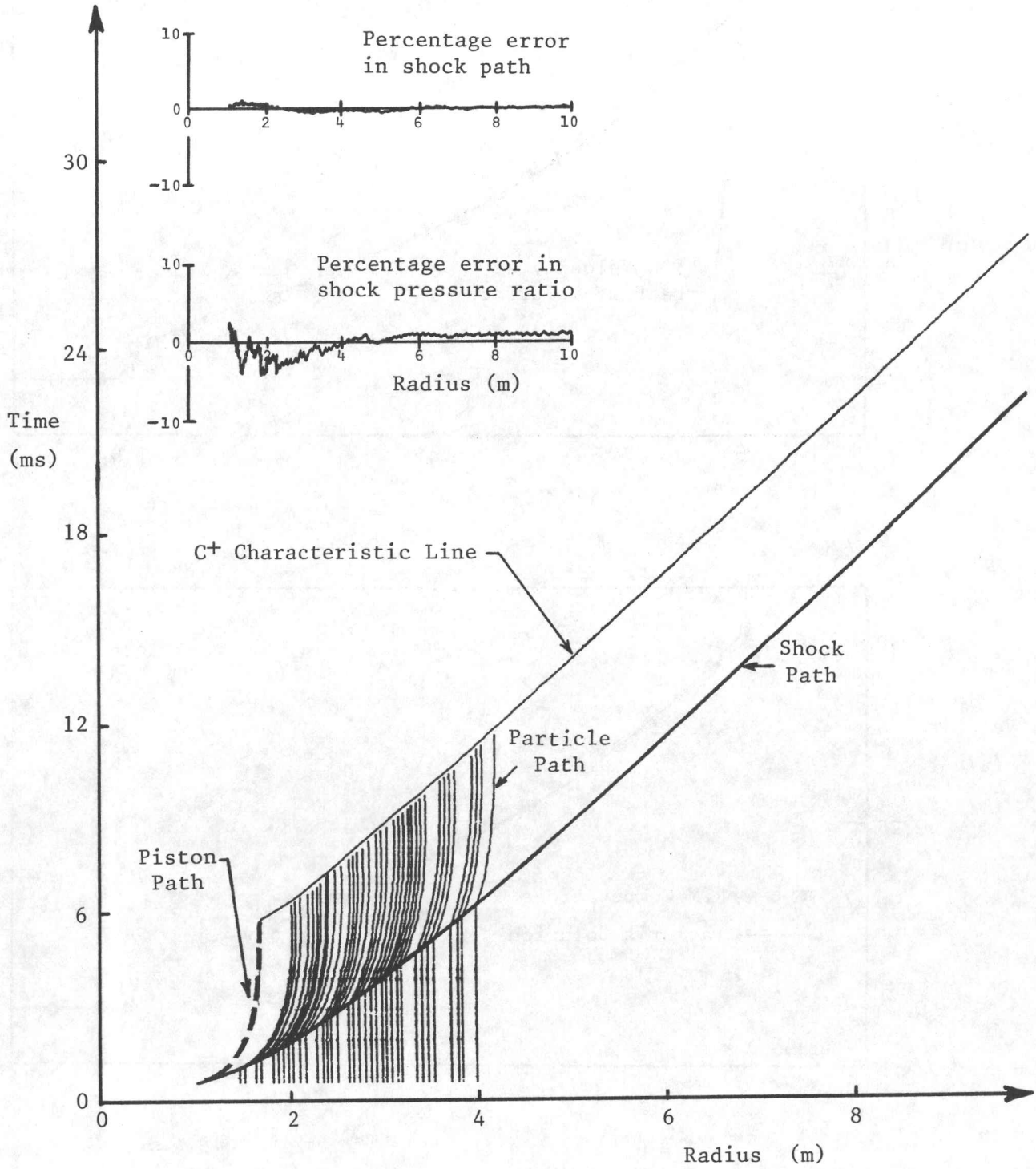

Fig. 22. The reconstructed blast-wave flow field for a 1-kg TNT surface explosion in a standard atmosphere, showing in the physical plane the piston path and many particle paths between the shock trajectory and a C^+ characteristic line. These particle paths have the same initial positions as those measured in a 500-ton TNT explosion called SNOWBALL.

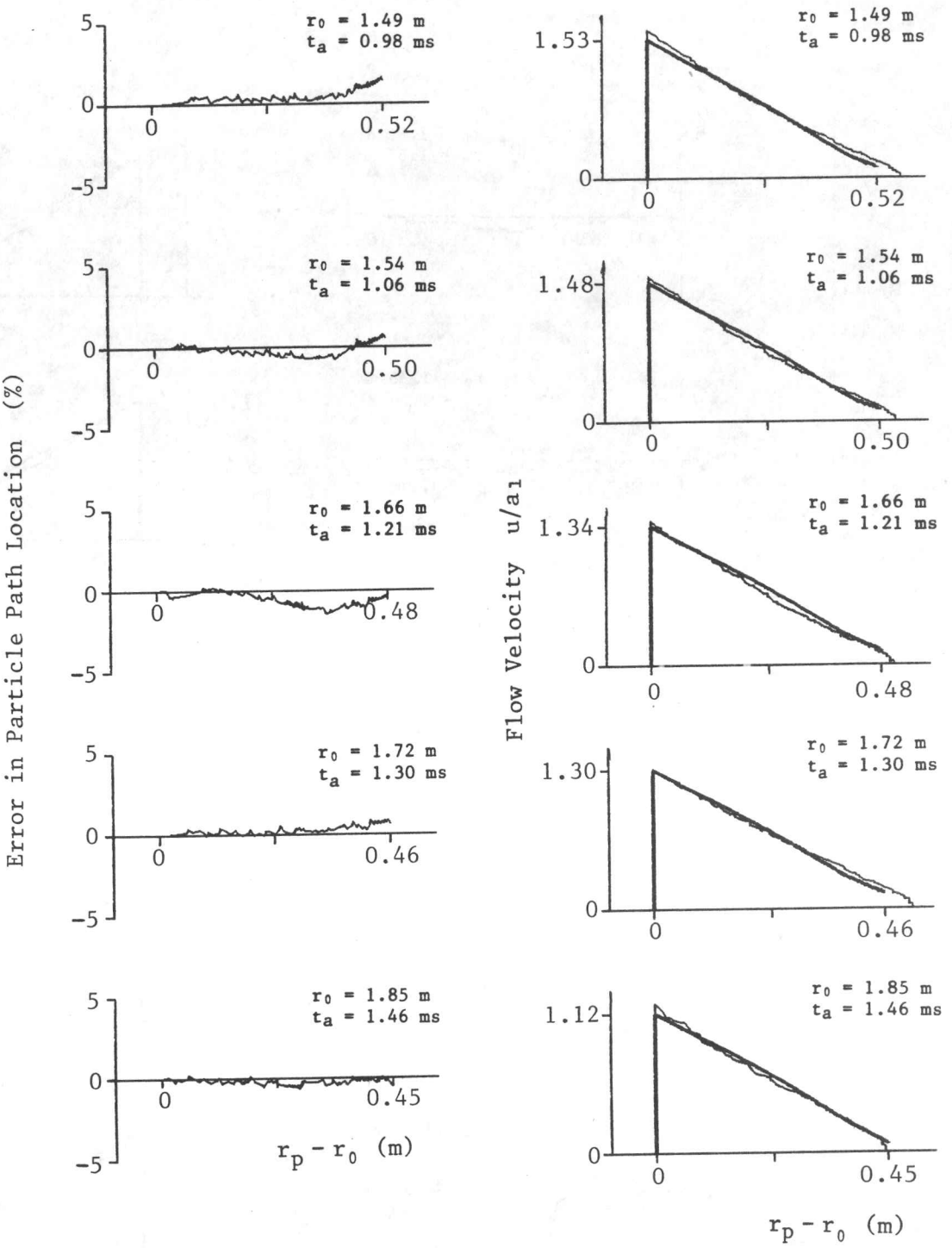

Fig. 23a. Percentage error between reconstructed and measured particle paths (left side), and comparison between reconstructed (~~~~) and measured (——) flow velocities of a particle path (right side). The measured results are from particle paths from the 500-ton TNT explosion trial called SNOWBALL.

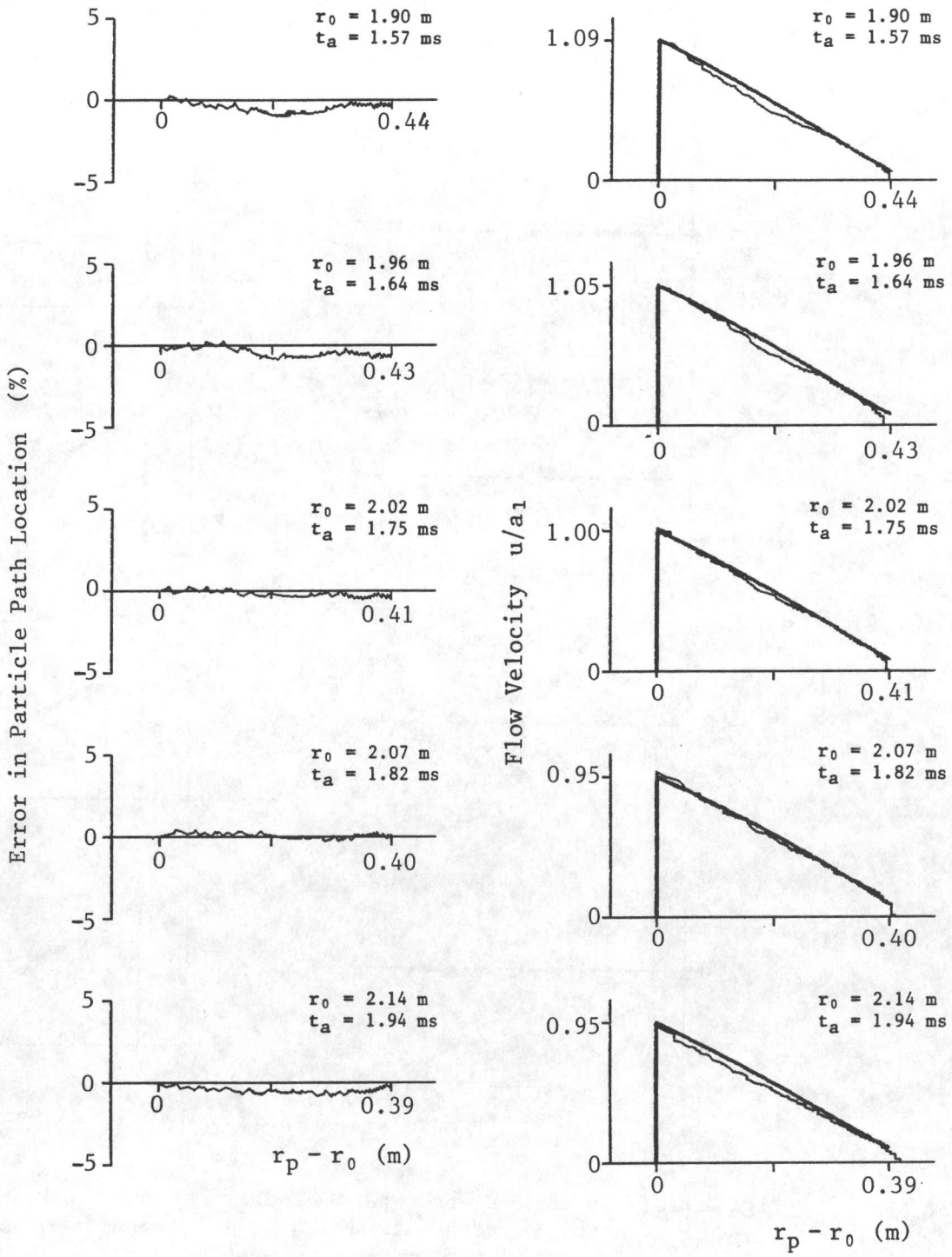

Fig. 23b. Percentage error between reconstructed and measured particle paths (left side), and comparison between reconstructed (~~~~) and measured (——) flow velocities of a particle path (right side). The measured results are from particle paths from the 500-ton TNT explosion trial called SNOWBALL.

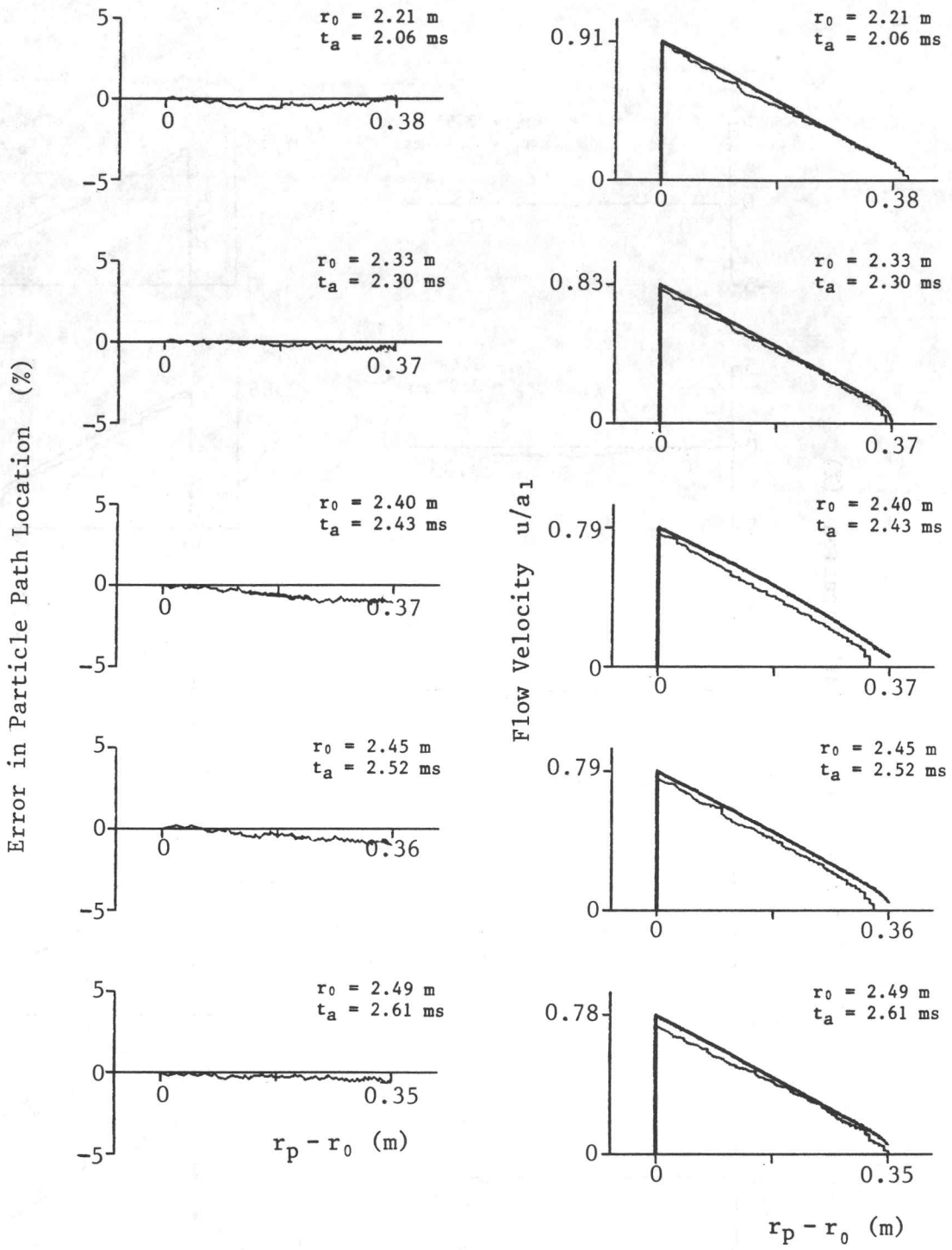

Fig. 23c. Percentage error between reconstructed and measured particle paths (left side), and comparison between reconstructed (wavy line) and measured (——) flow velocities of a particle path (right side). The measured results are from particle paths from the 500-ton TNT explosion trial called SNOWBALL.

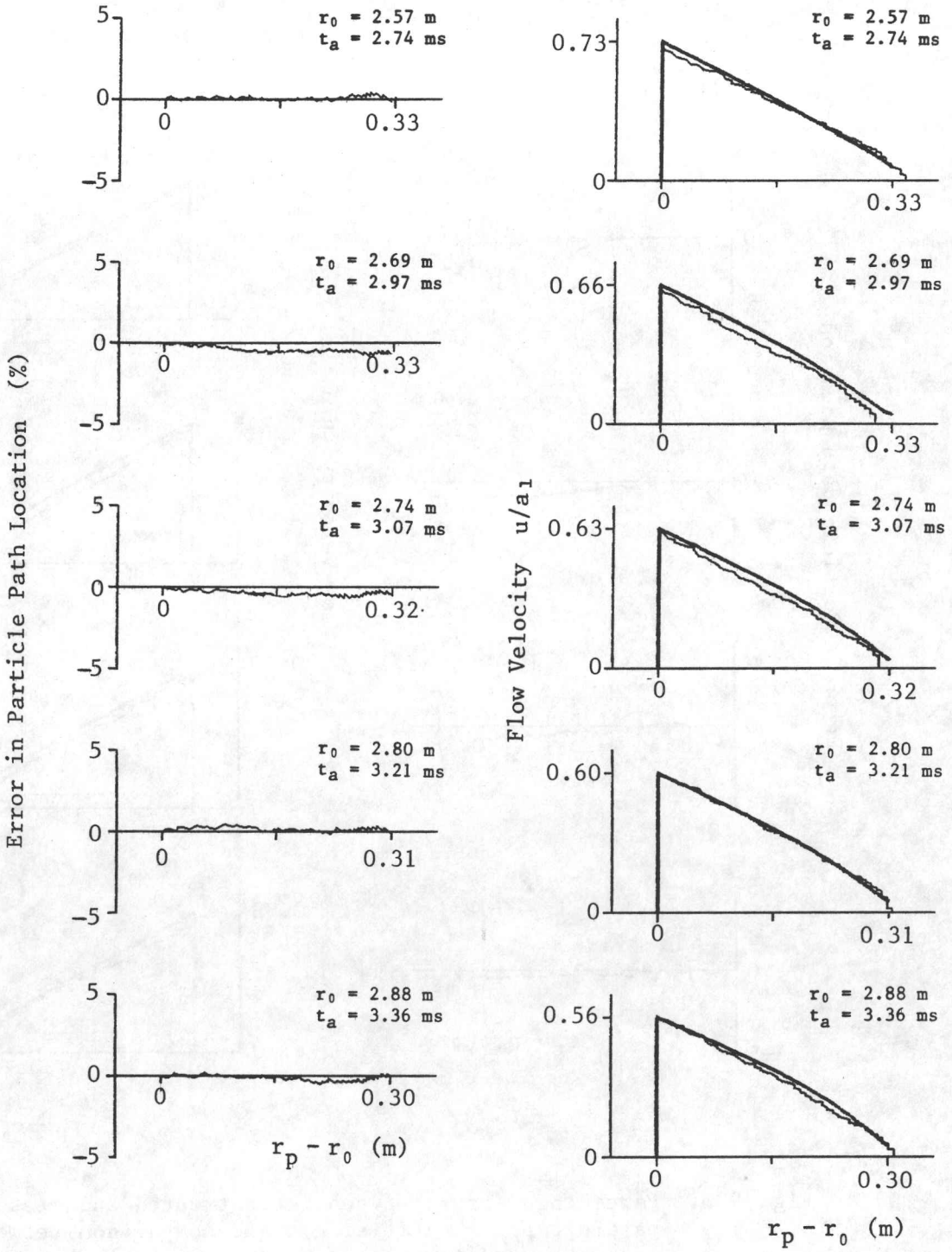

Fig. 23d. Percentage error between reconstructed and measured particle paths (left side), and comparison between reconstructed (wwww) and measured (——) flow velocities of a particle path (right side). The measured results are from particle paths from the 500-ton TNT explosion trial called SNOWBALL.

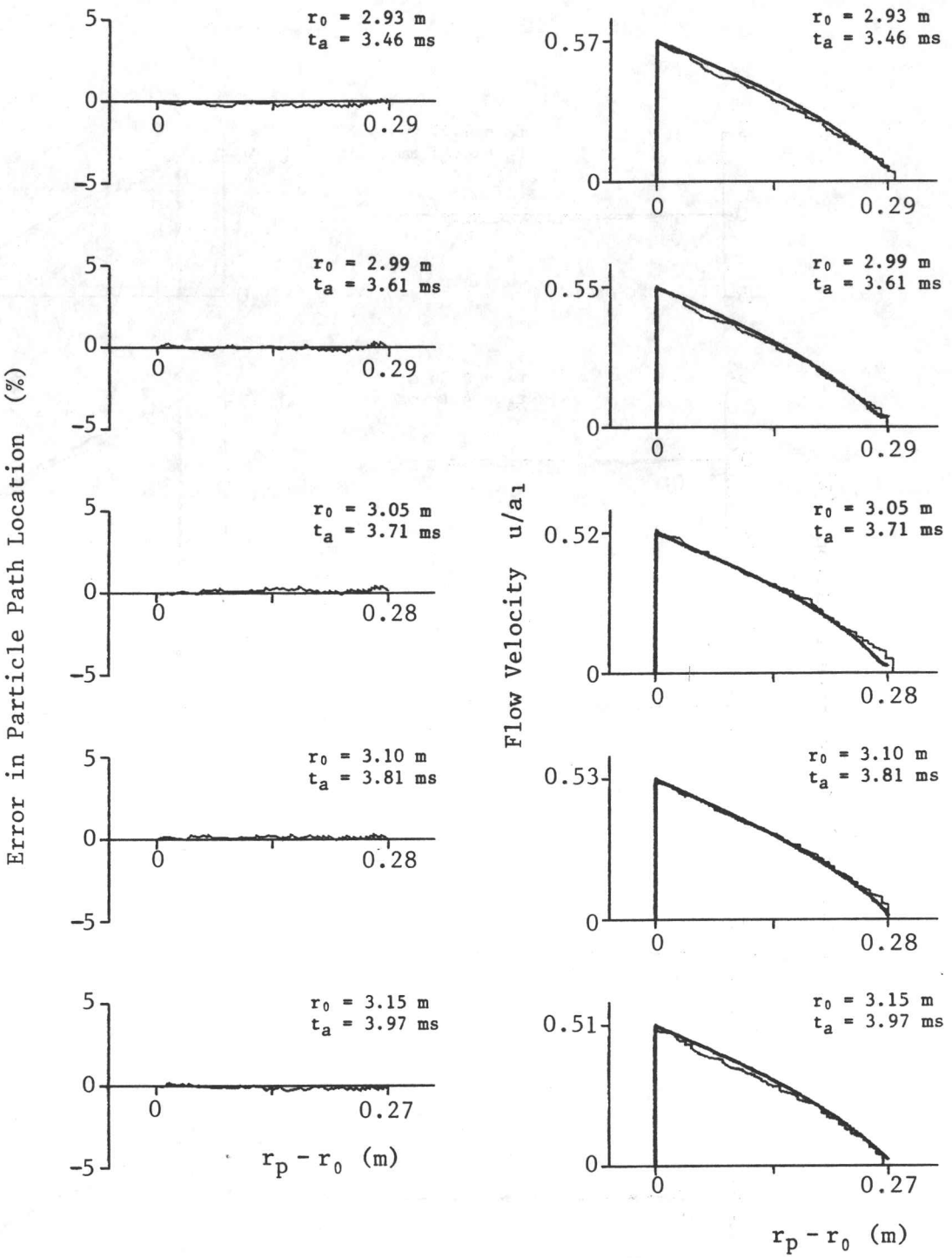

Fig. 23e. Percentage error between reconstructed and measured particle paths (left side), and comparison between reconstructed (wwwww) and measured (——) flow velocities of a particle path (right side). The measured results are from particle paths from the 500-ton TNT explosion trial called SNOWBALL.

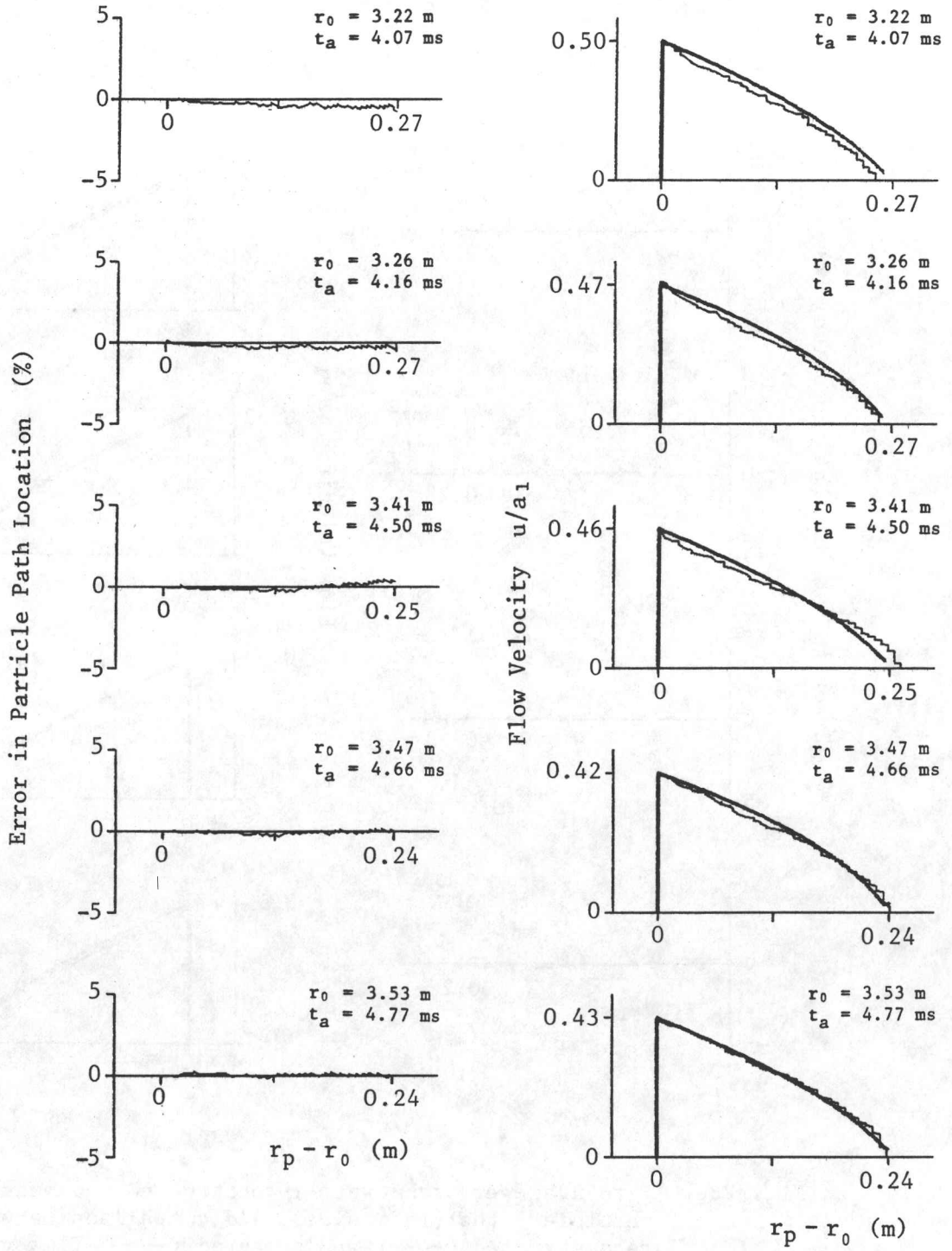

Fig. 23f. Percentage error between reconstructed and measured particle paths (left side), and comparison between reconstructed (wwwww) and measured (——) flow velocities of a particle path (right side). The measured results are from particle paths from the 500-ton TNT explosion trial called SNOWBALL.

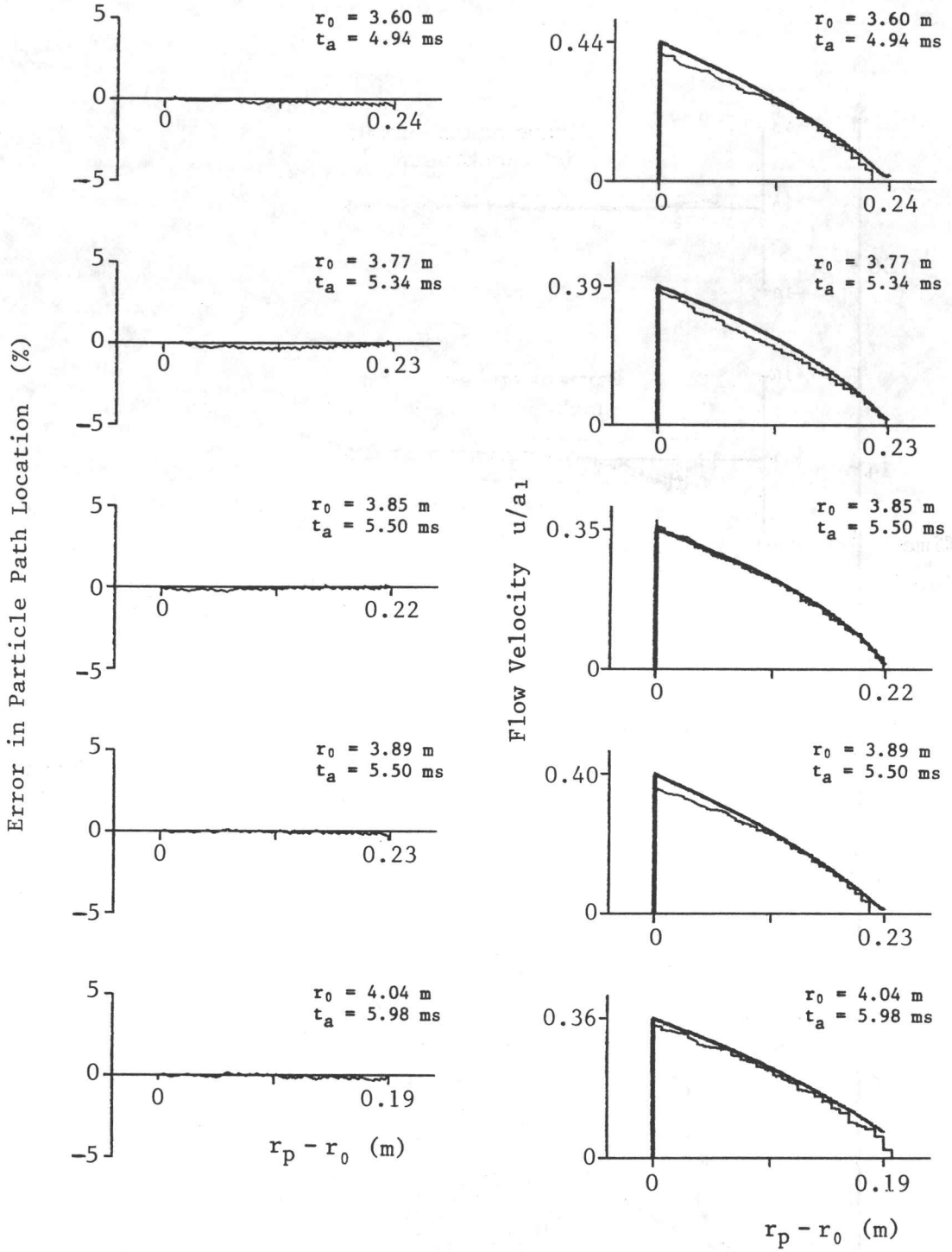

Fig. 23g. Percentage error between reconstructed and measured particle paths (left side), and comparison between reconstructed (wwww) and measured (——) flow velocities of a particle path (right side). The measured results are from particle paths from the 500-ton TNT explosion trial called SNOWBALL.

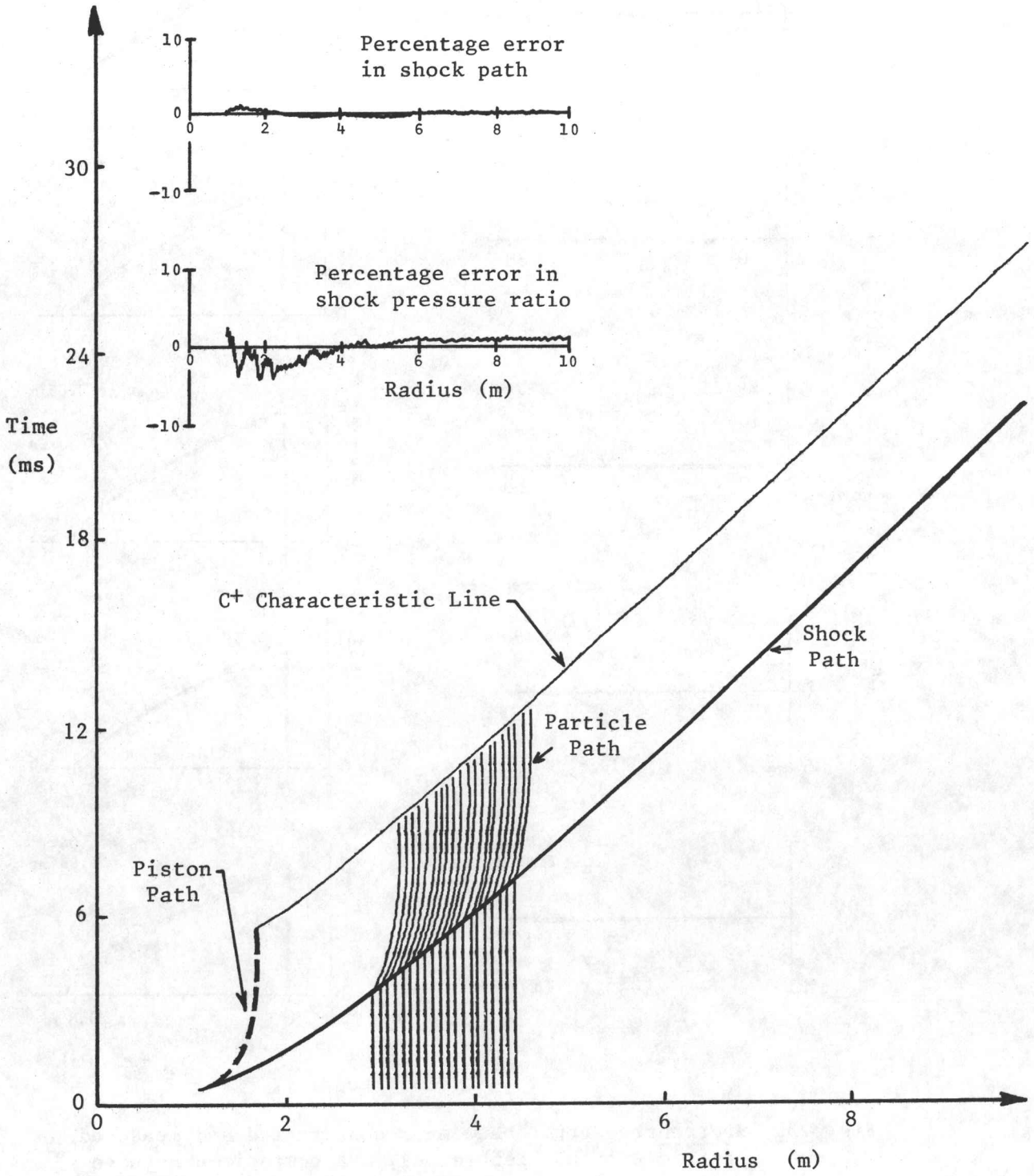

Fig. 24. The reconstructed blast-wave flow field for a 1-kg TNT surface exploaion in a standard atmosphere, showing in the physical plane the piston path and many particle paths between the shock trajectory and a C^+ characteristic line. These particle paths have the same initial positions as those measured in a 500-ton TNT explosion called SAILOR HAT.

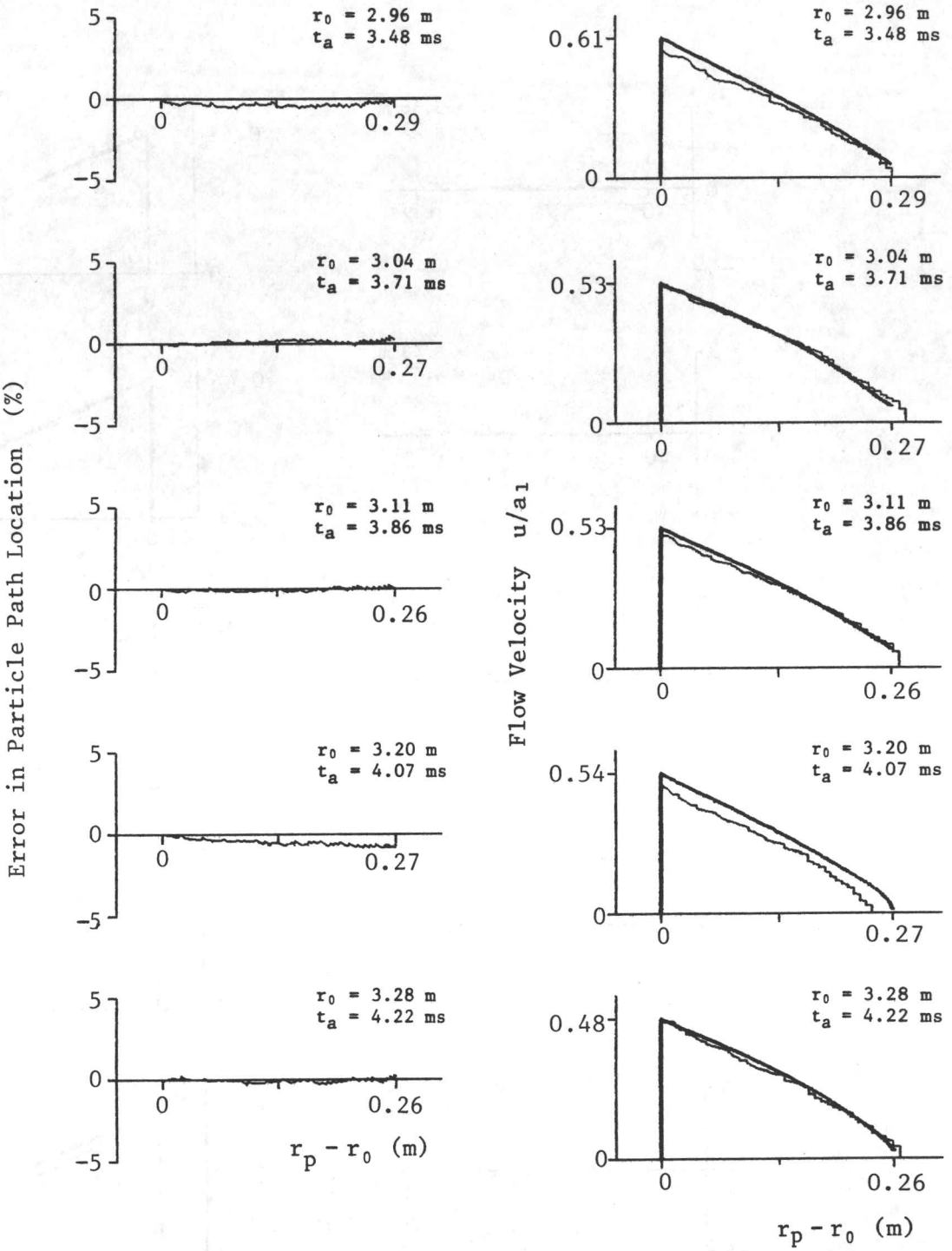

Fig. 25a. Percentage error between reconstructed and measured particle paths (left side), and comparison between reconstructed (wwwww) and measured (——) flow velocities of a particle path (right side). The measured results are from particle paths from the 500-ton TNT explosion trial called SAILOR HAT.

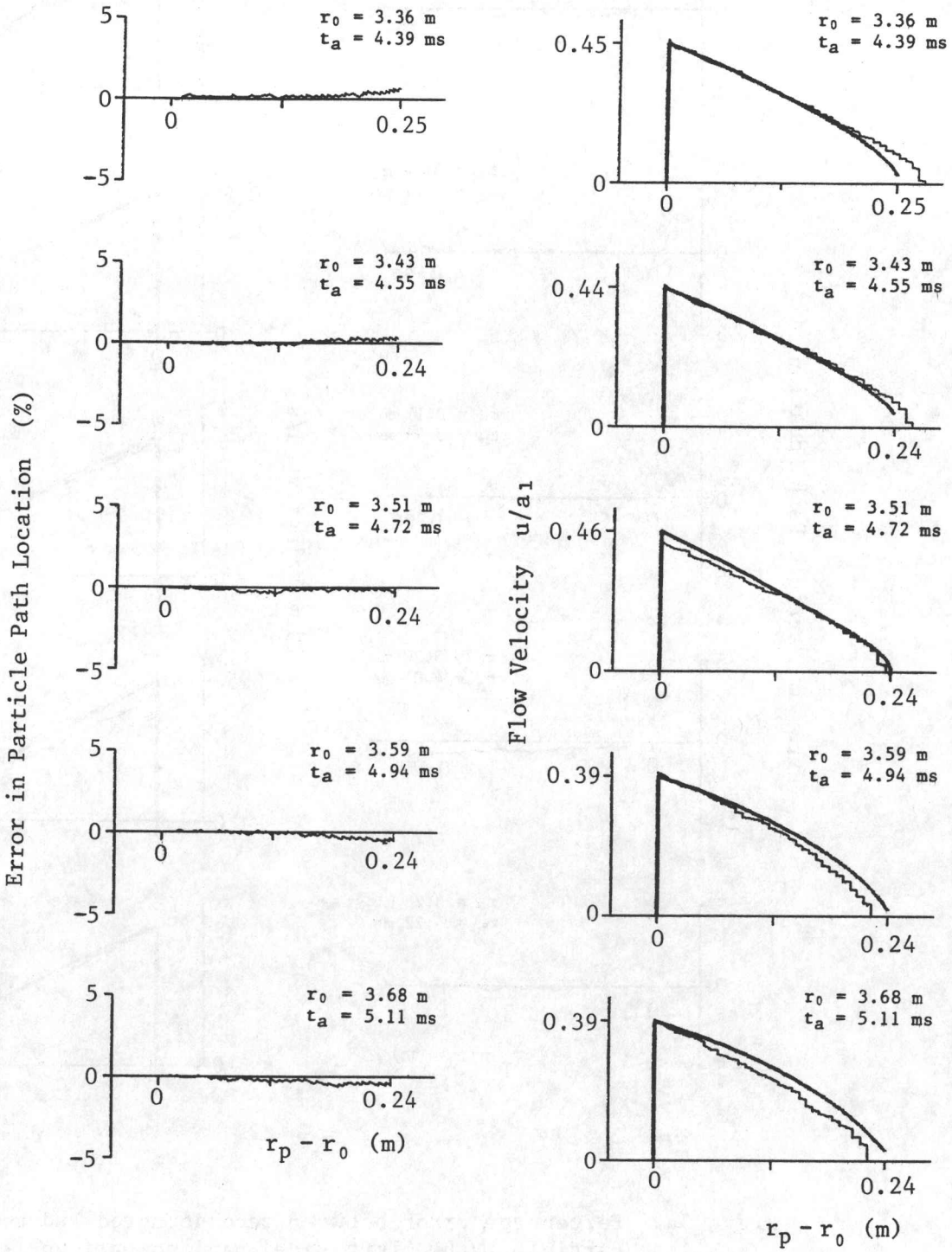

Fig. 25b. Percentage error between reconstructed and measured particle paths (left side), and comparison between reconstructed (wwwww) and measured (——) flow velocities of a particle path (right side). The measured results are from particle paths from the 500-ton TNT explosion trial called SAILOR HAT.

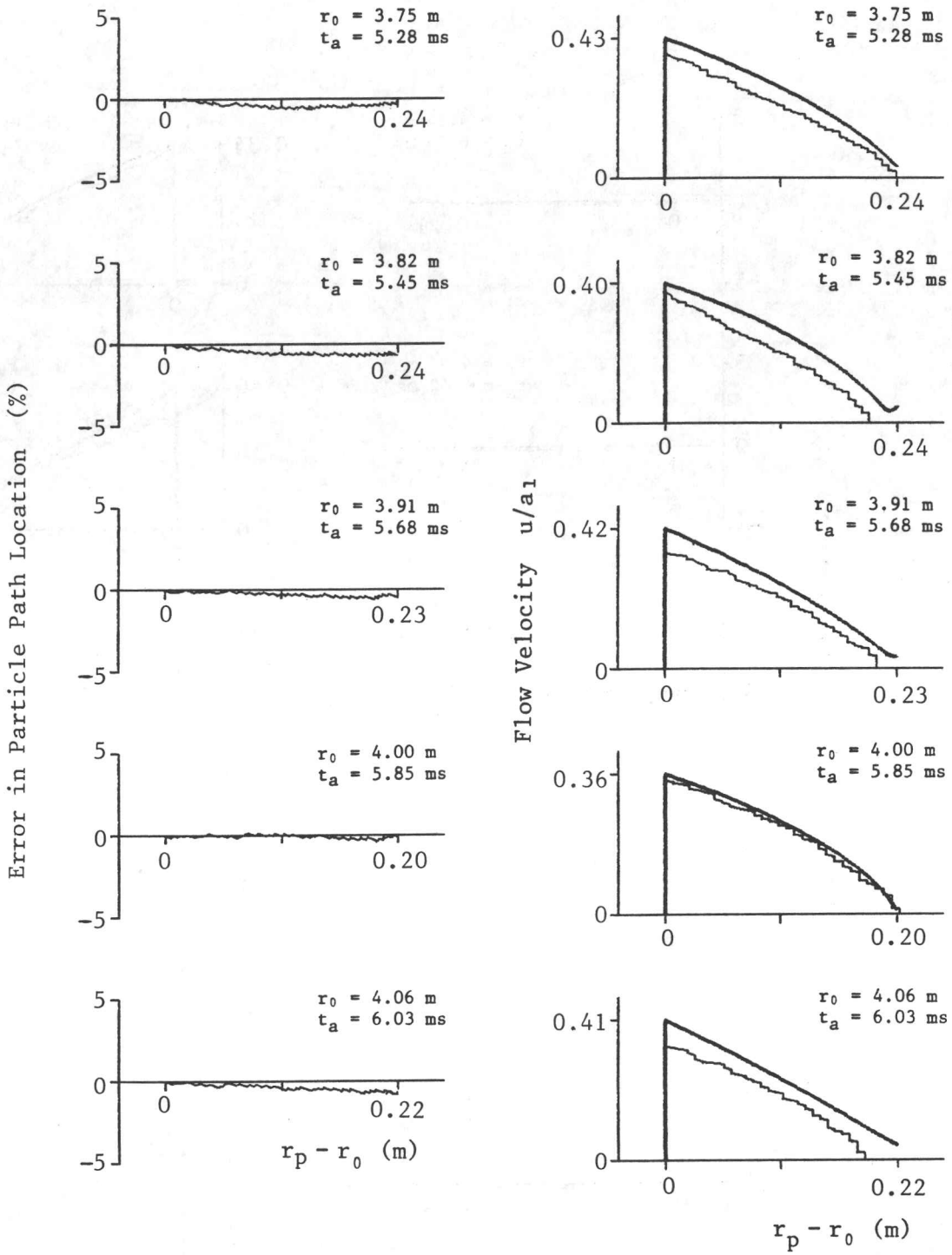

Fig. 25c. Percentage error between reconstructed and measured particle paths (left side), and comparison between reconstructed (wwww) and measured (——) flow velocities of a particle path (right side). The measured results are from particle paths from the 500-ton TNT explosion trial called SAILOR HAT.

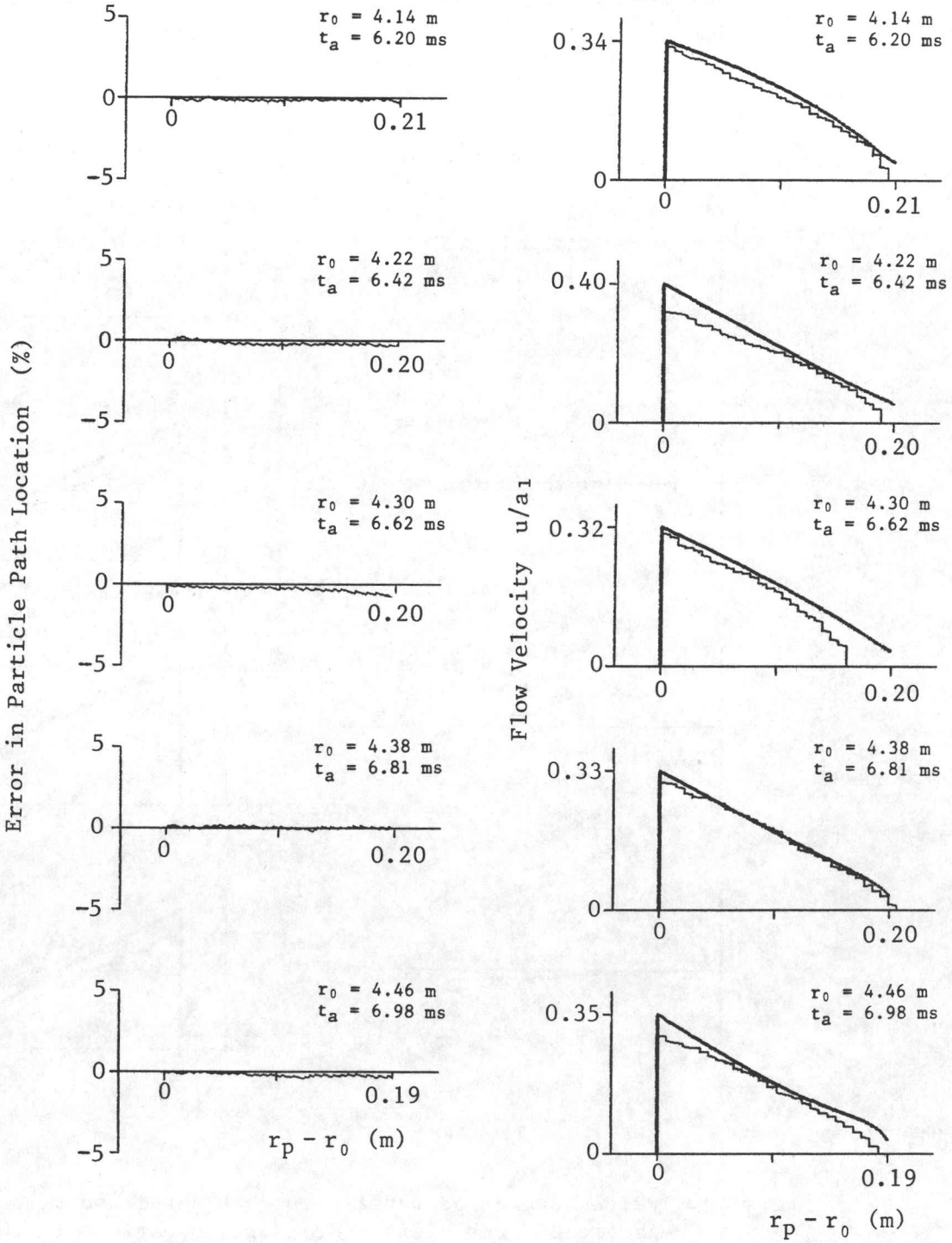

Fig. 25d. Percentage error between reconstructed and measured particle paths (left side), and comparison between reconstructed (wwww) and measured (——) flow velocities of a particle path (right side). The measured results are from particle paths from the 500-ton TNT explosion trial called SAILOR HAT.

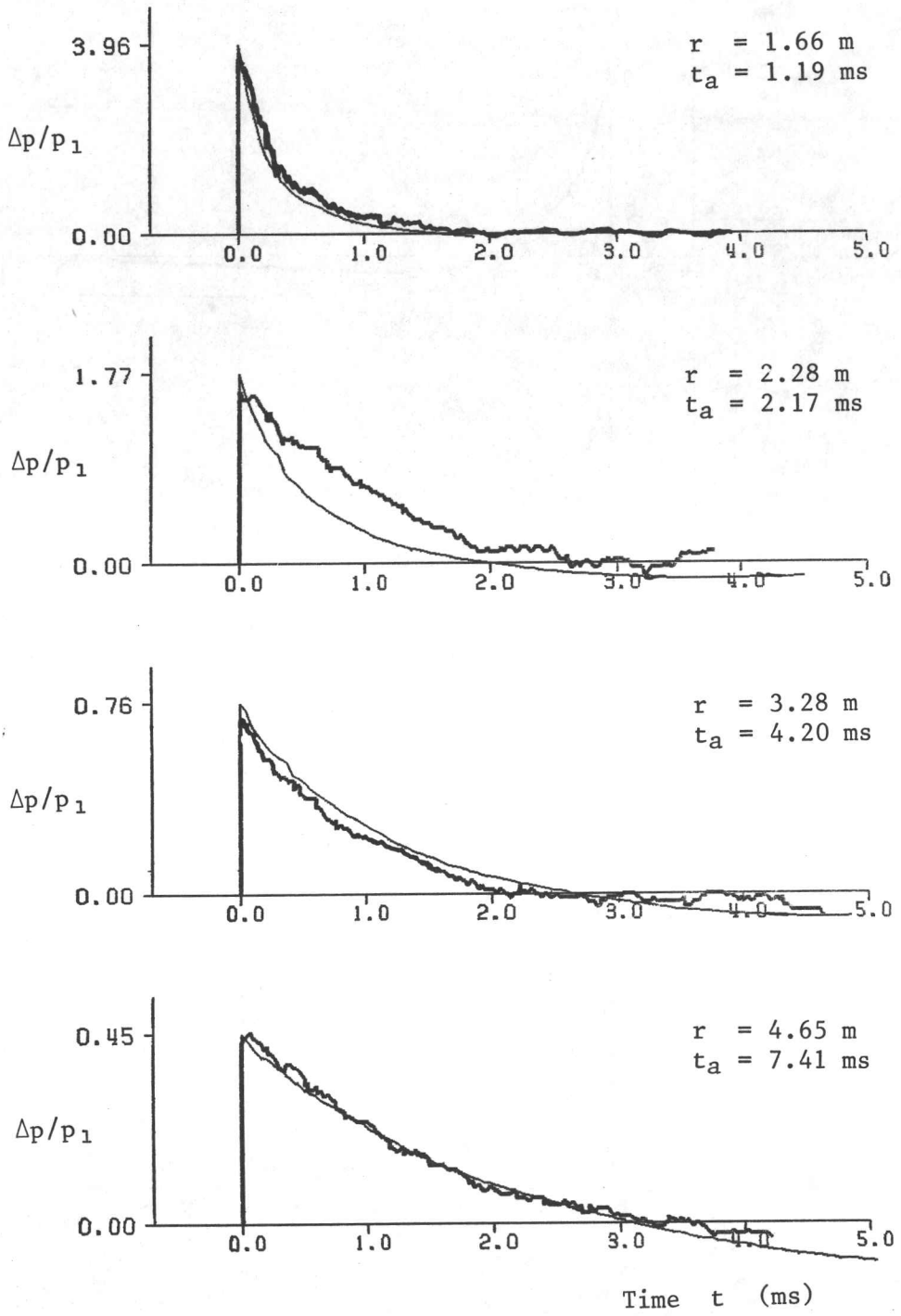

Fig. 26. Comparison of overpressure signatures from 20-ton TNT explosion measurements (~~~) and the RCM reconstructed flow field (~~~).

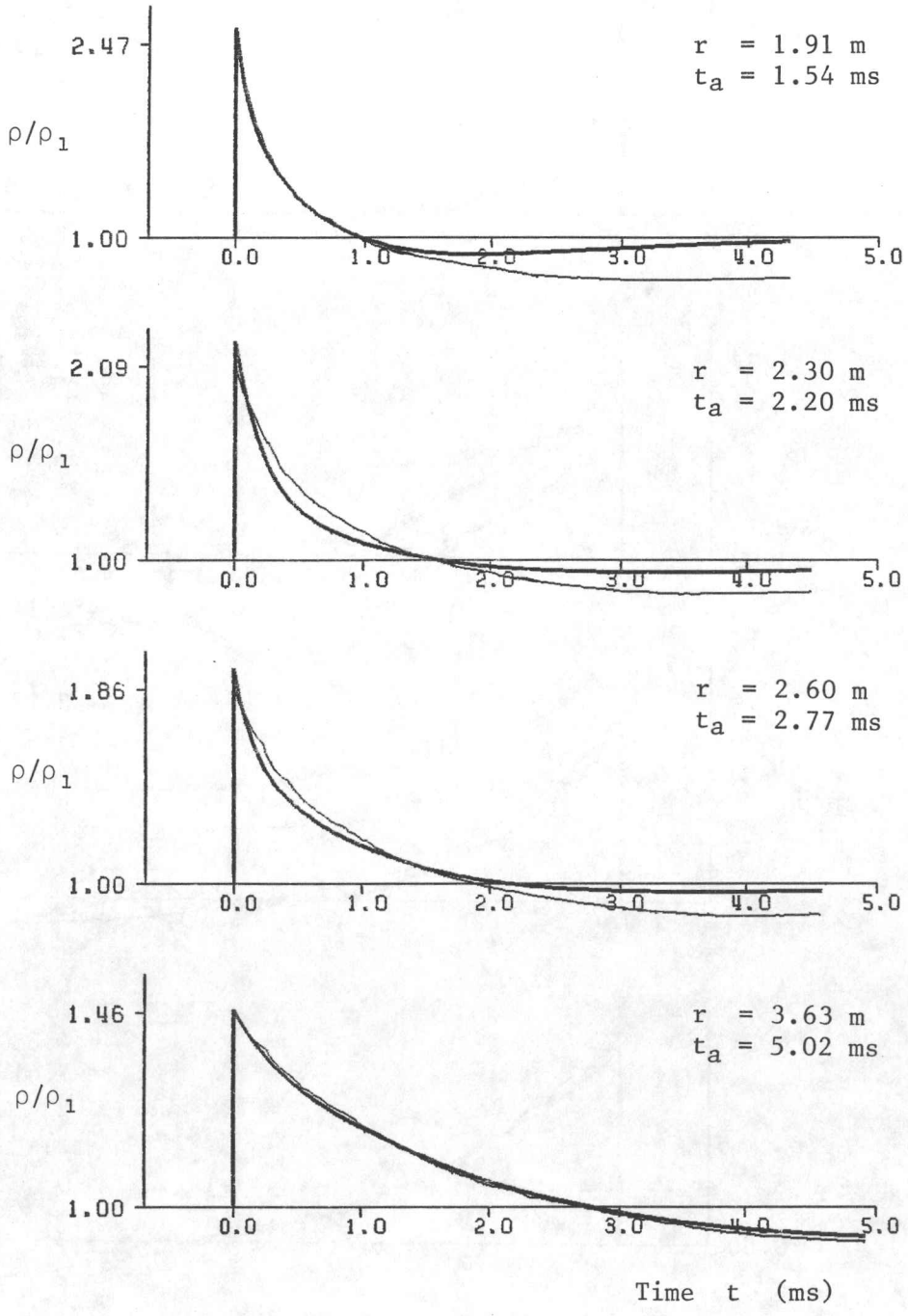

Fig. 27. Comparison of density signatures from 100-ton TNT explosion measurements (——) and the RCM reconstructed flow field (~~~~).

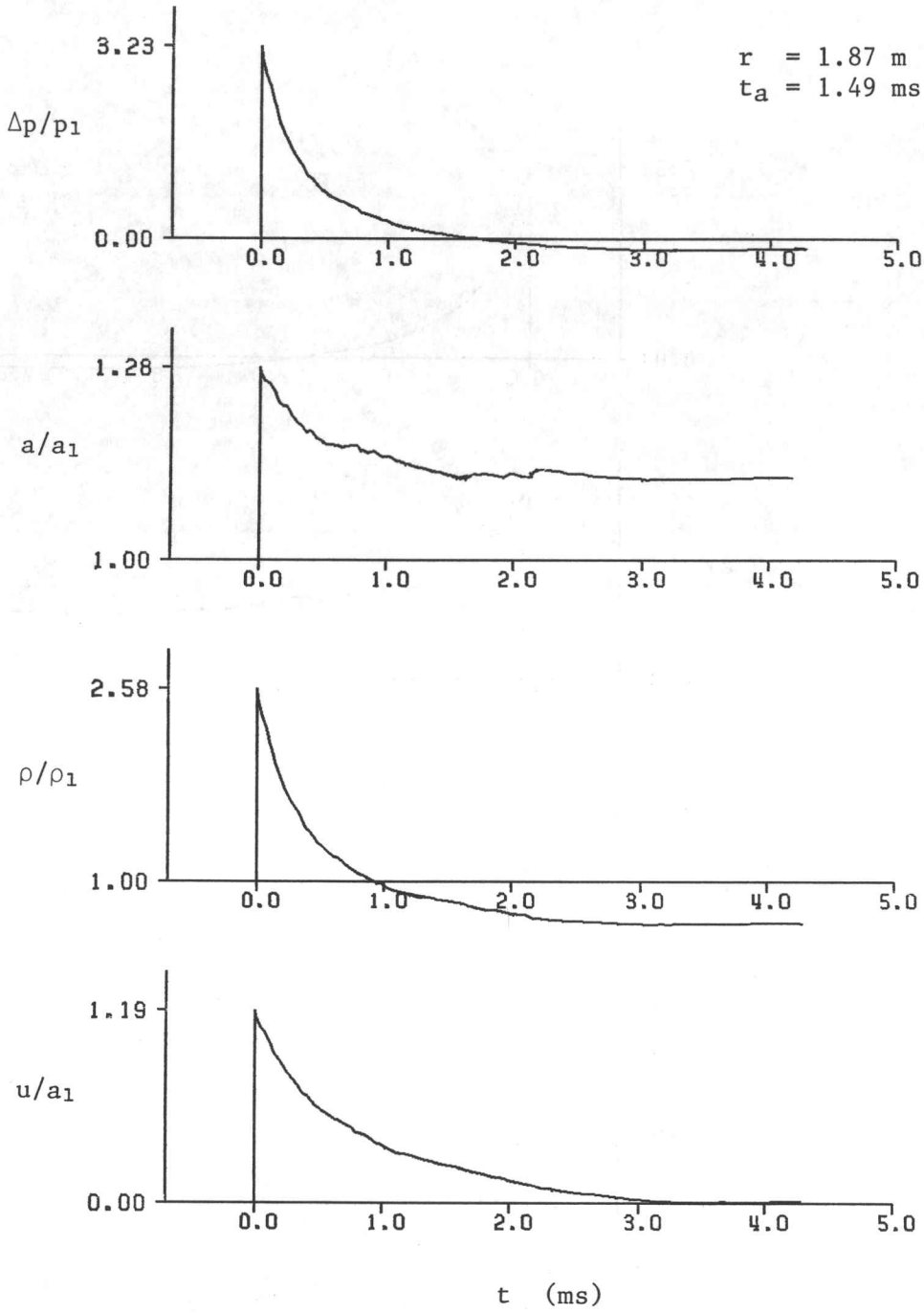

Fig. 28a. Overpressure, sound-speed, density and flow-velocity signatures from the reconstructed blast-wave flow field by the RCM for a 1-kg TNT explosion in a standard atmosphere.

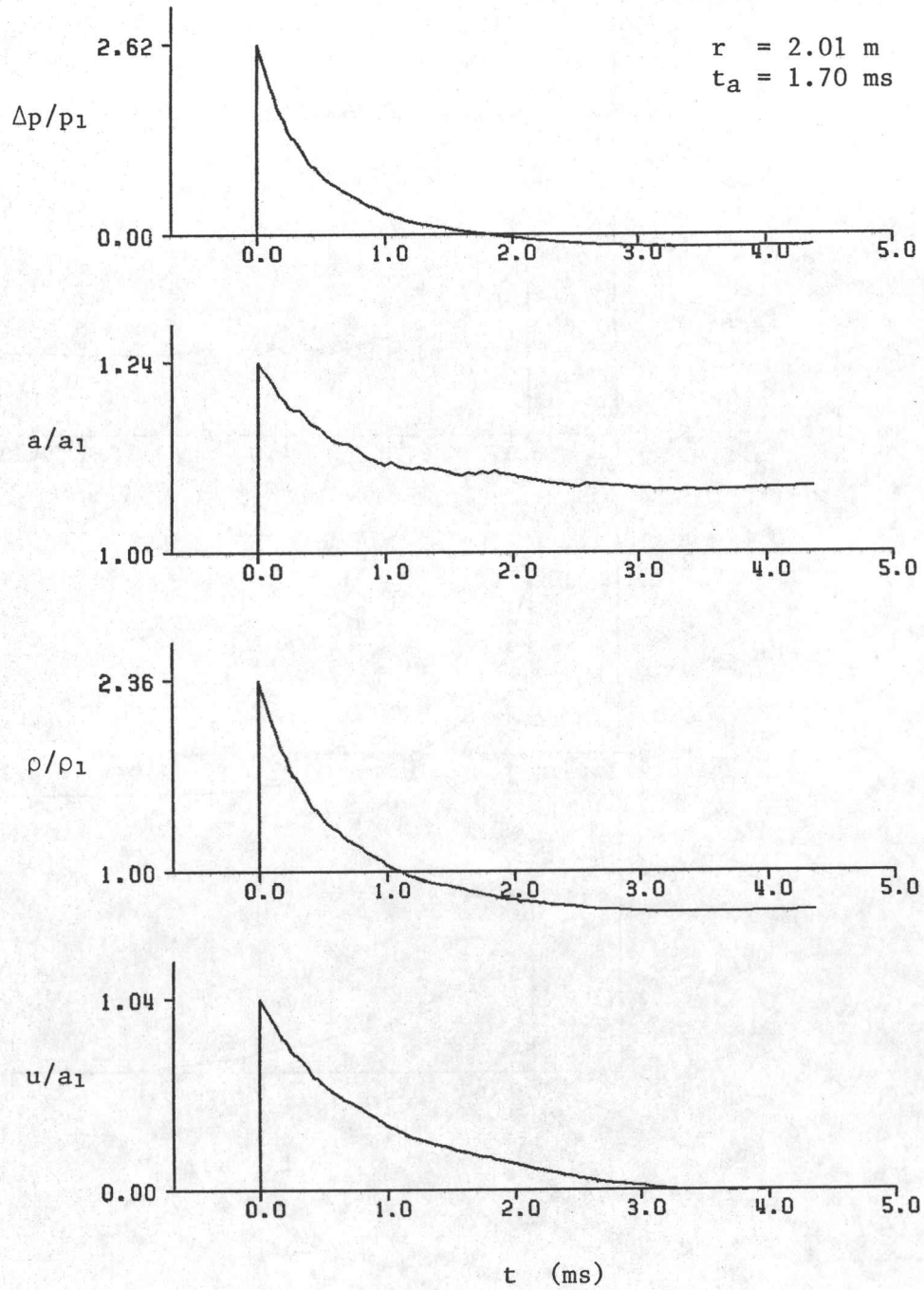

Fig. 28b. Overpressure, sound-speed, density and flow-velocity signatures from the reconstructed blast-wave flow field by the RCM for a 1-kg TNT explosion in a standard atmosphere.

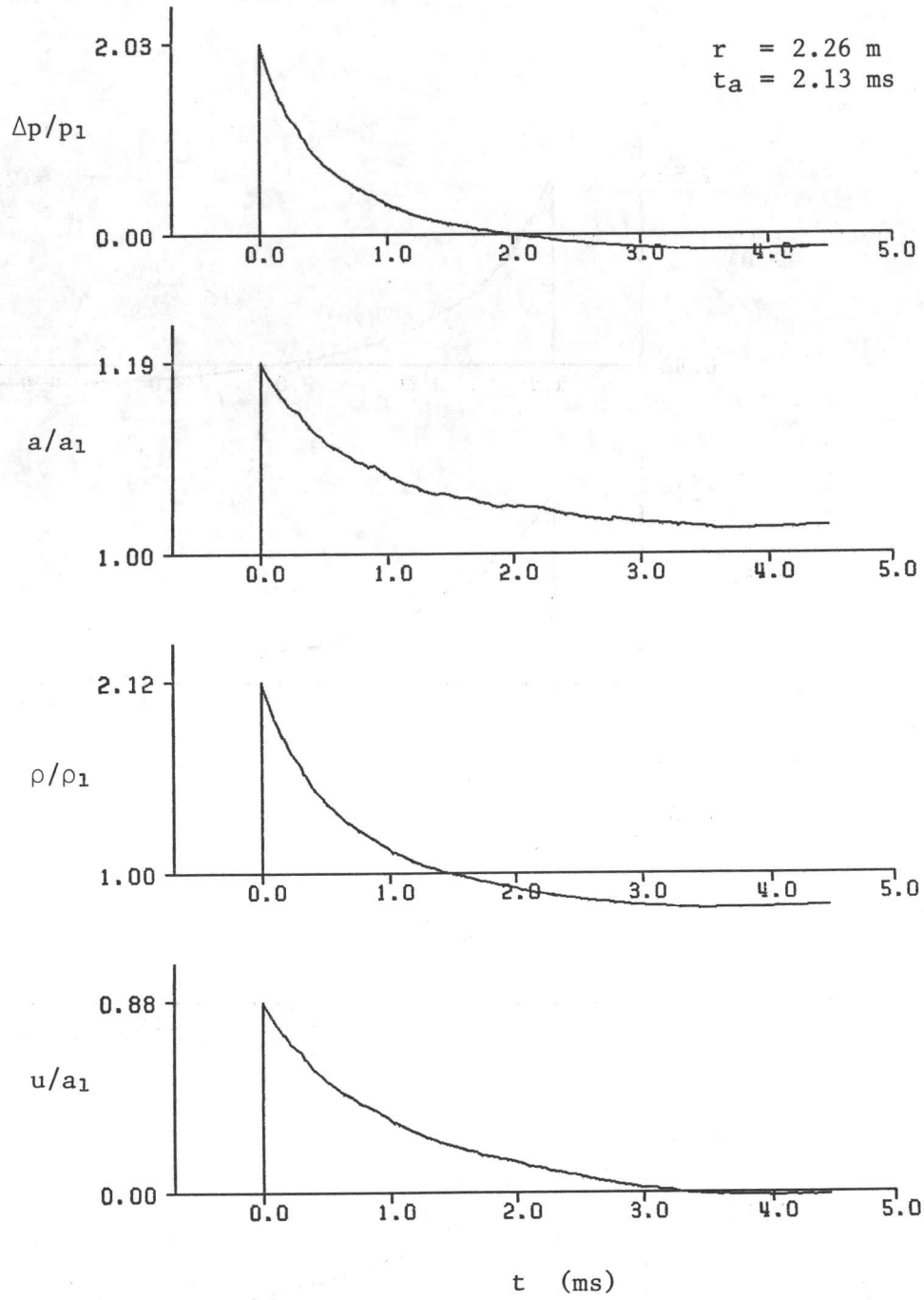

Fig. 28c. Overpressure, sound-speed, density and flow-velocity signatures from the reconstructed blast-wave flow field by the RCM for a 1-kg TNT explosion in a standard atmosphere.

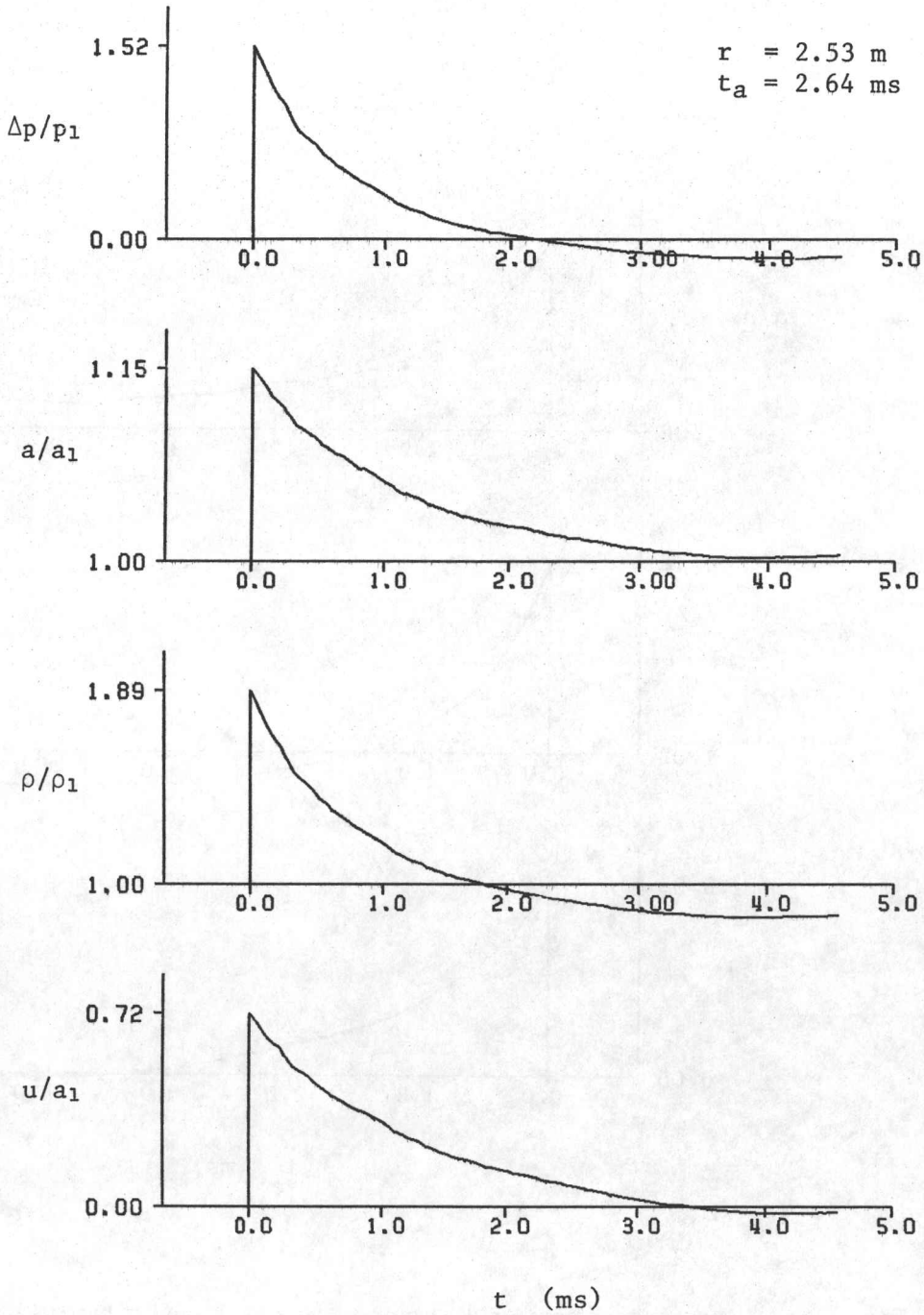

Fig. 28d. Overpressure, sound-speed, density and flow-velocity signatures from the reconstructed blast-wave flow field by the RCM for a 1-kg TNT explosion in a standard atmosphere.

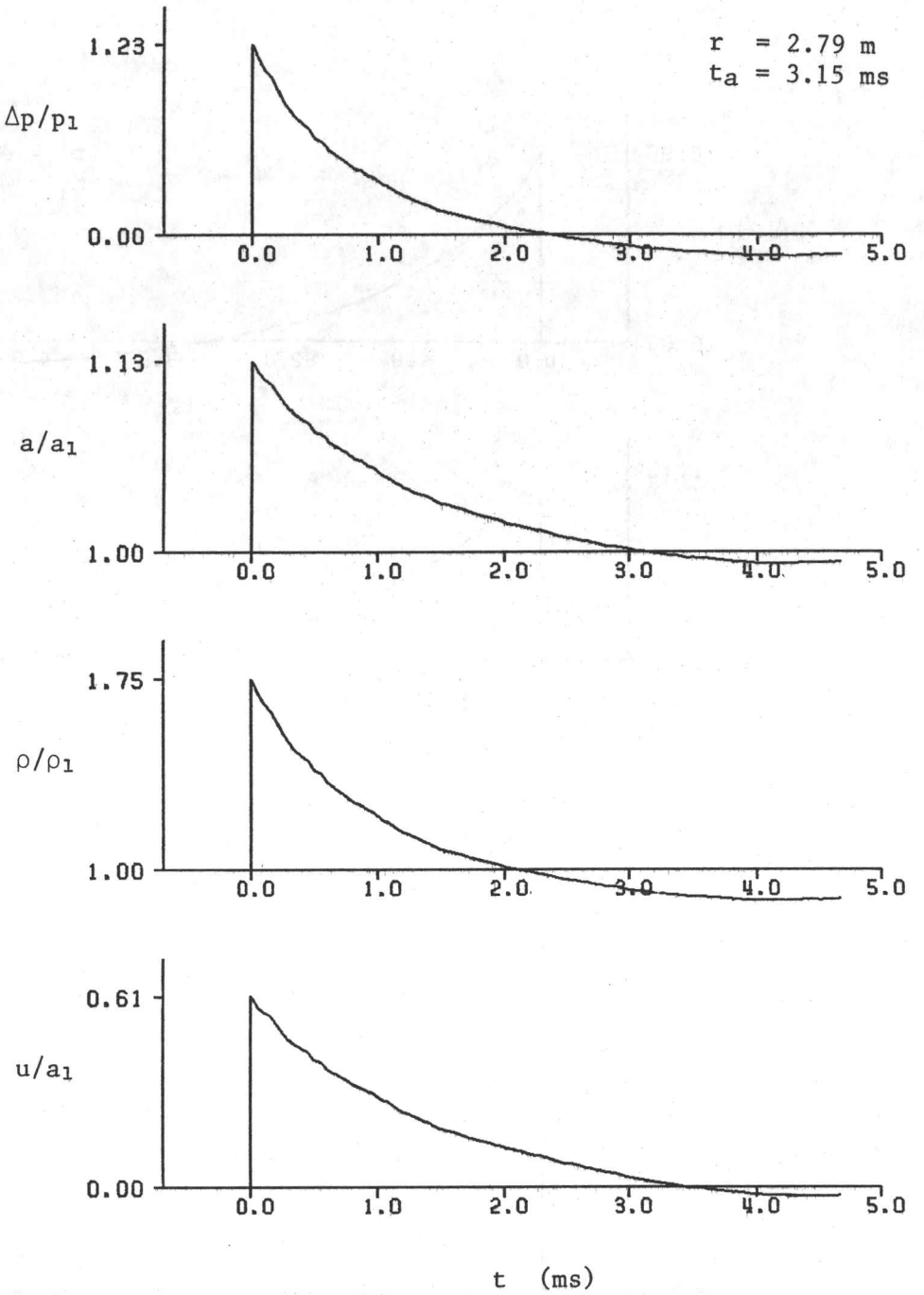

Fig. 28e. Overpressure, sound-speed, density and flow-velocity signatures from the reconstructed blast-wave flow field by the RCM for a 1-kg TNT explosion in a standard atmosphere.

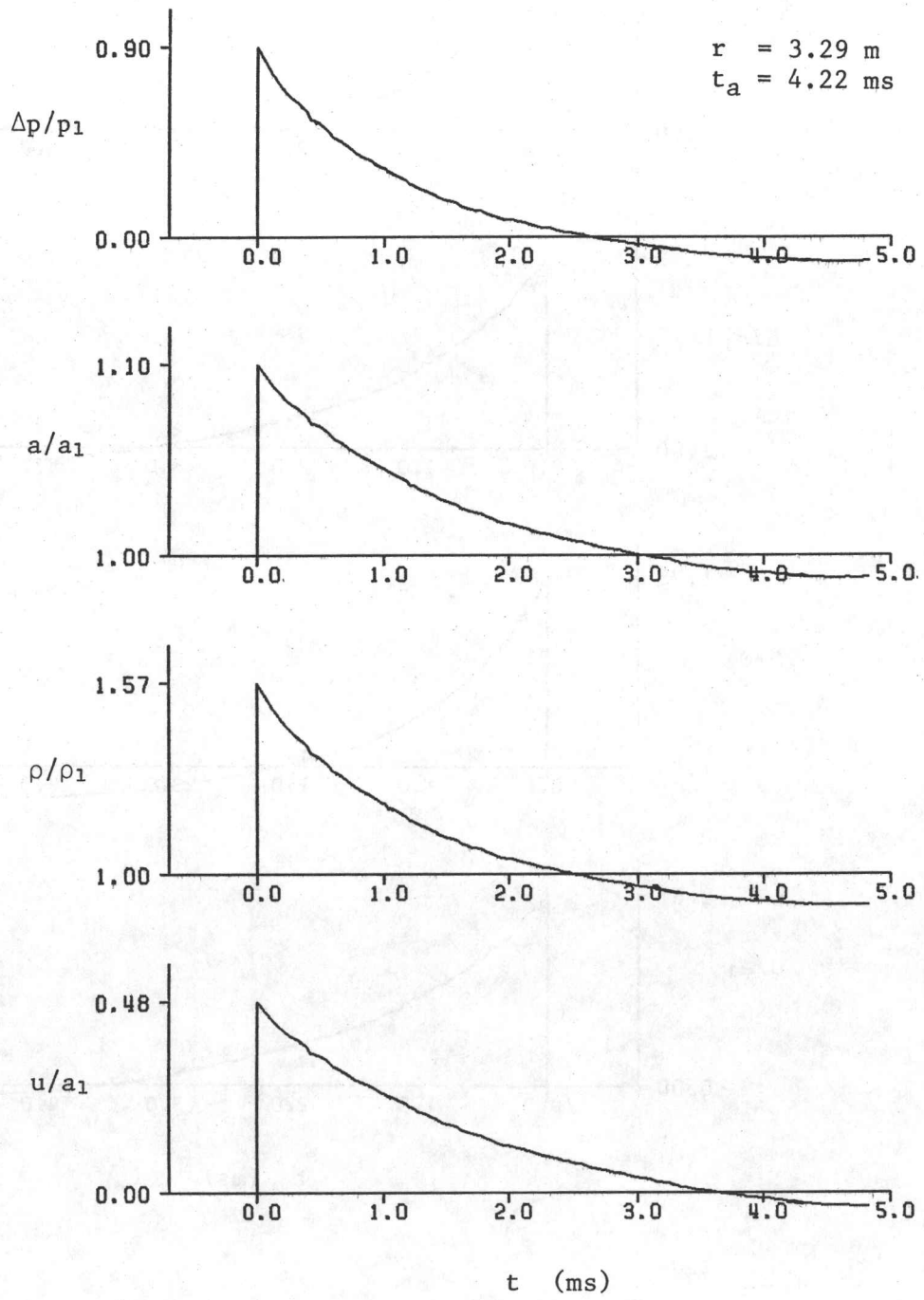

Fig. 28f. Overpressure, sound-speed, density and flow-velocity signatures from the reconstructed blast-wave flow field by the RCM for a 1-kg TNT explosion in a standard atmosphere.

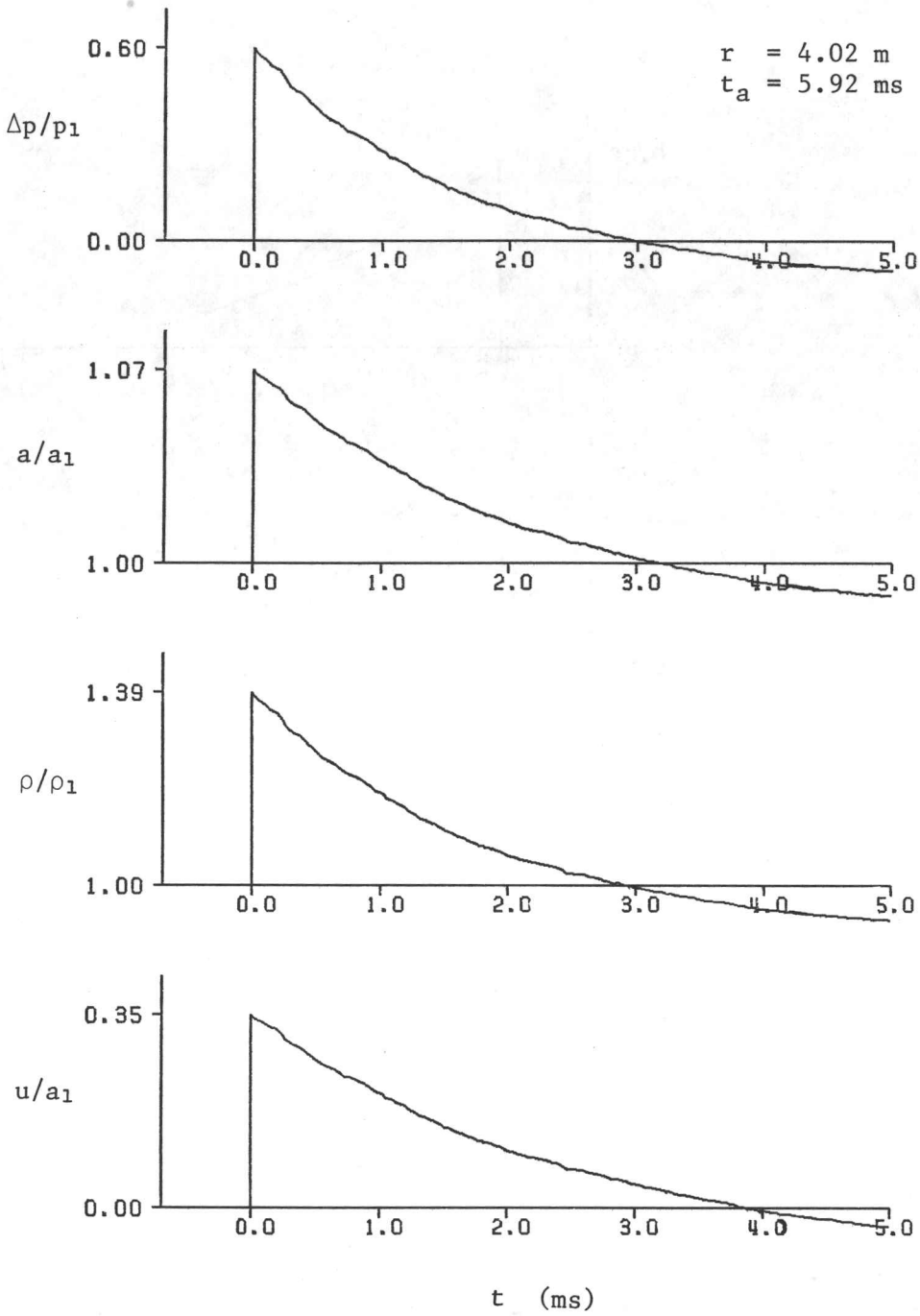

Fig. 28g. Overpressure, sound-speed, density and flow-velocity signatures from the reconstructed blast-wave flow field by the RCM for a 1-kg TNT explosion in a standard atmosphere.

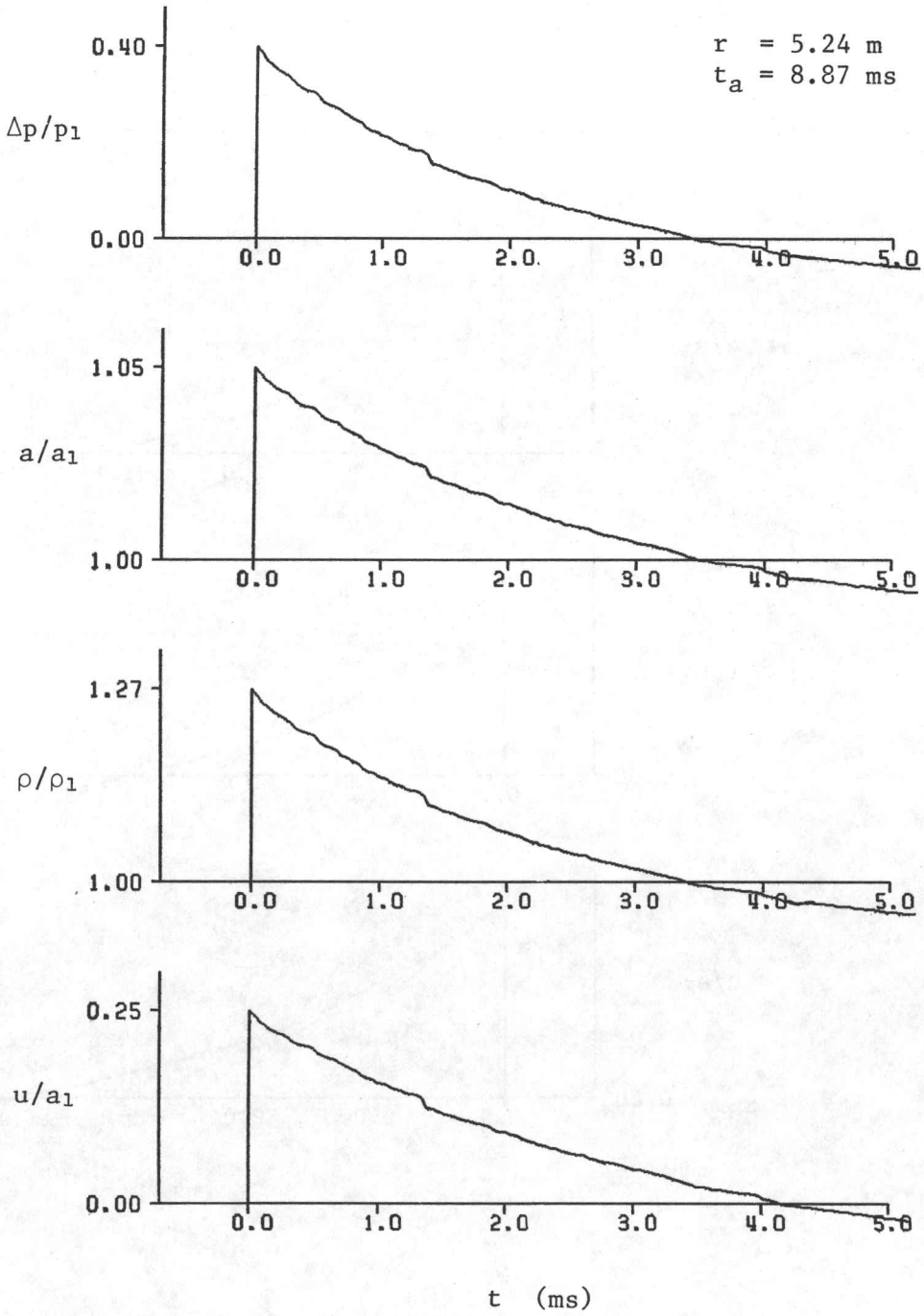

Fig. 28h. Overpressure, sound-speed, density and flow-velocity signatures from the reconstructed blast-wave flow field by the RCM for a 1-kg TNT explosion in a standard atmosphere.

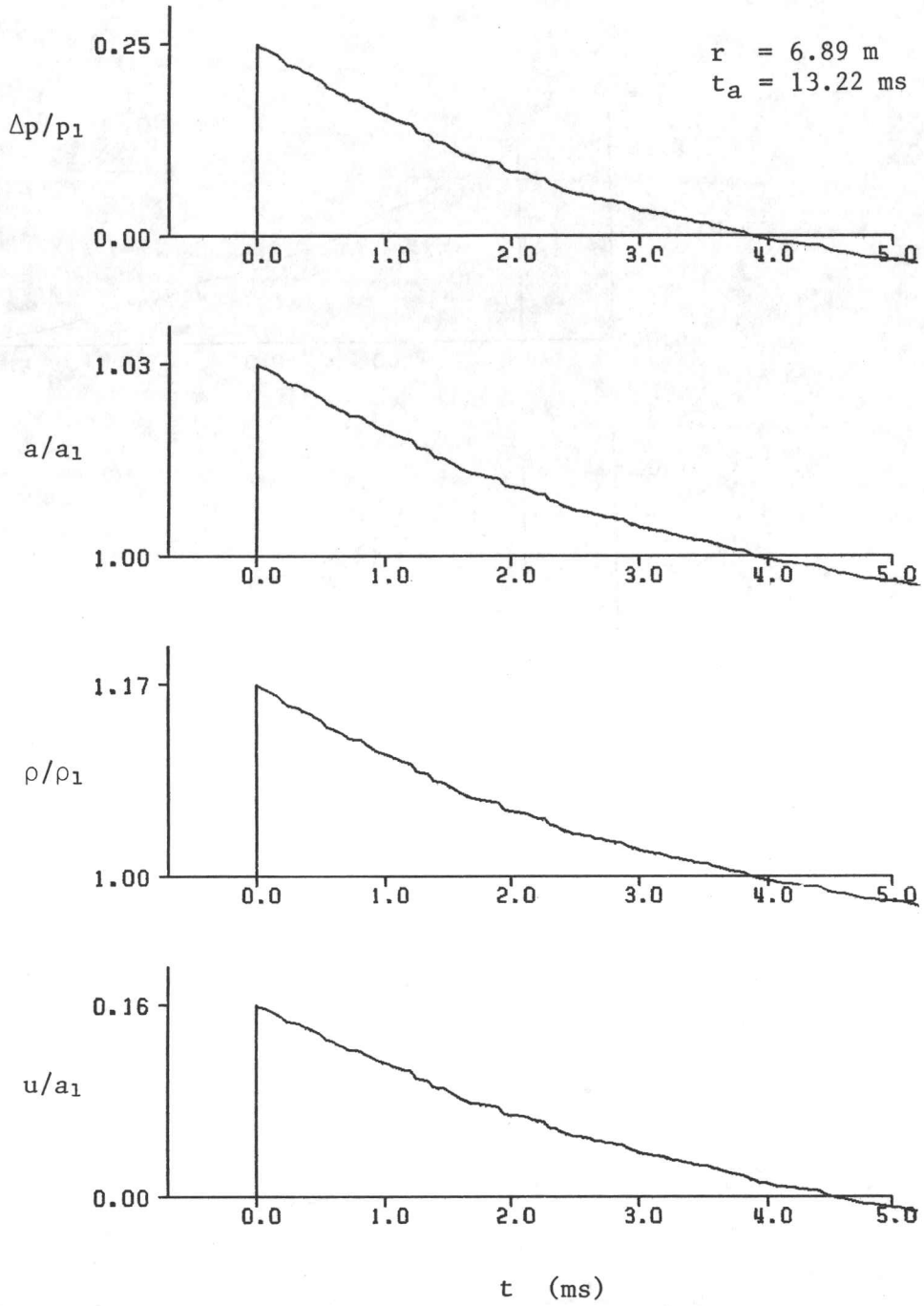

Fig. 28i. Overpressure, sound-speed, density and flow-velocity signatures from the reconstructed blast-wave flow field by the RCM for a 1-kg TNT explosion in a standard atmosphere.

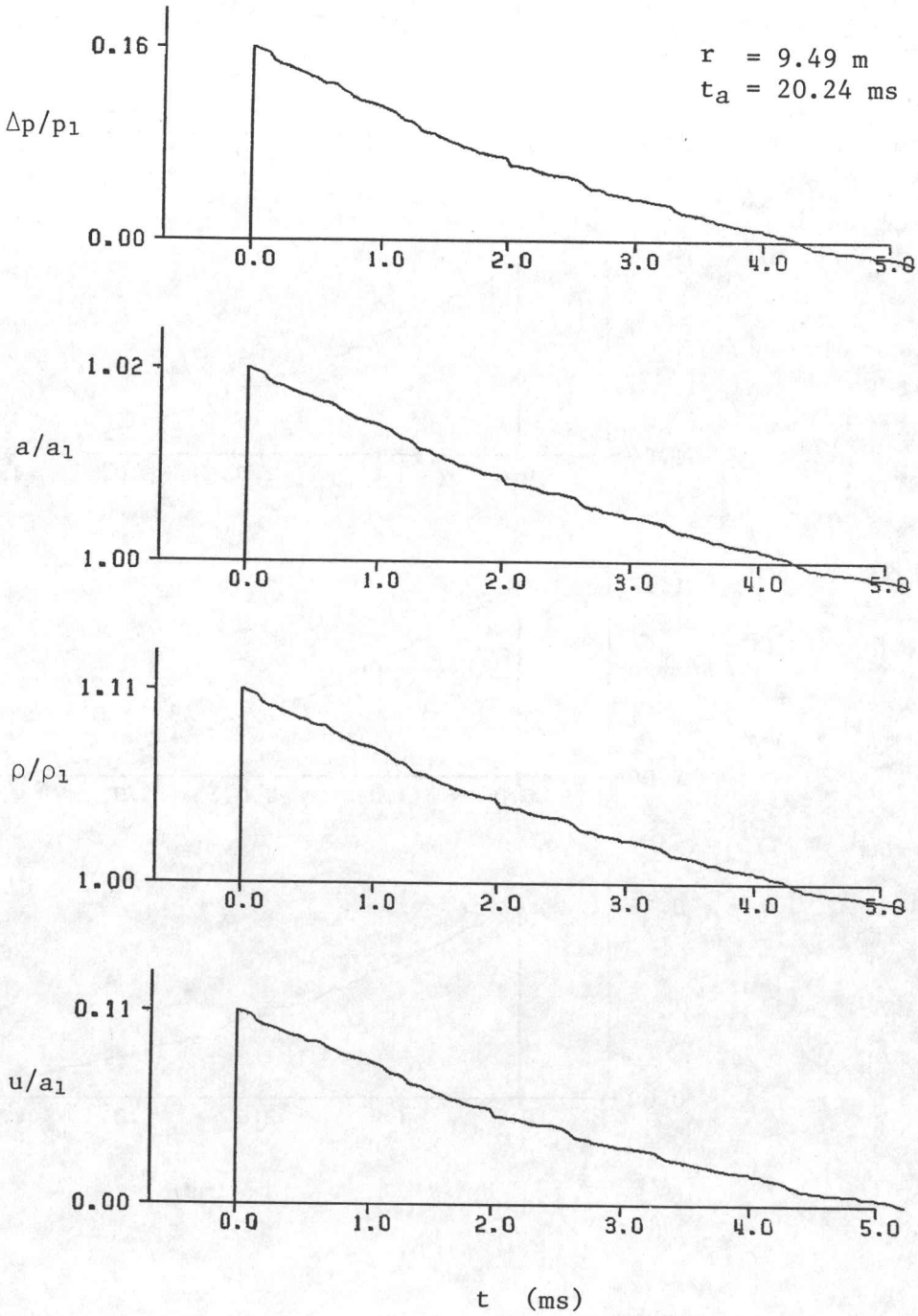

Fig. 28j. Overpressure, sound-speed, density and flow-velocity signatures from the reconstructed blast-wave flow field by the RCM for a 1-kg TNT explosion in a standard atmosphere.

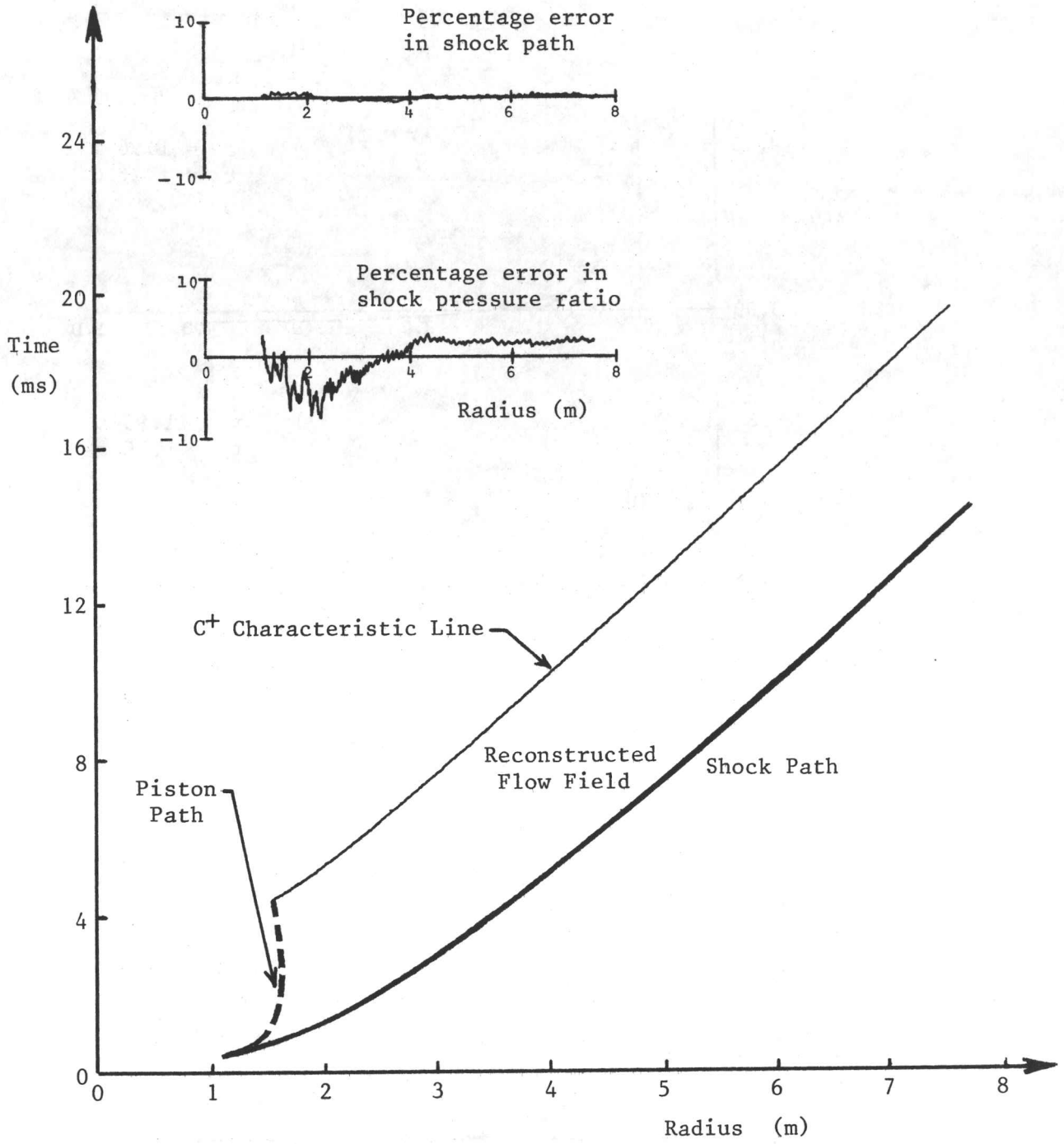

Fig. 29. The reconstructed blast-wave flow field for a 1-kg TNT equivalent ANFO surface explosion, showing the reconstructed flow field bounded by the specified piston path, shock trajectory and C^+ characteristic.

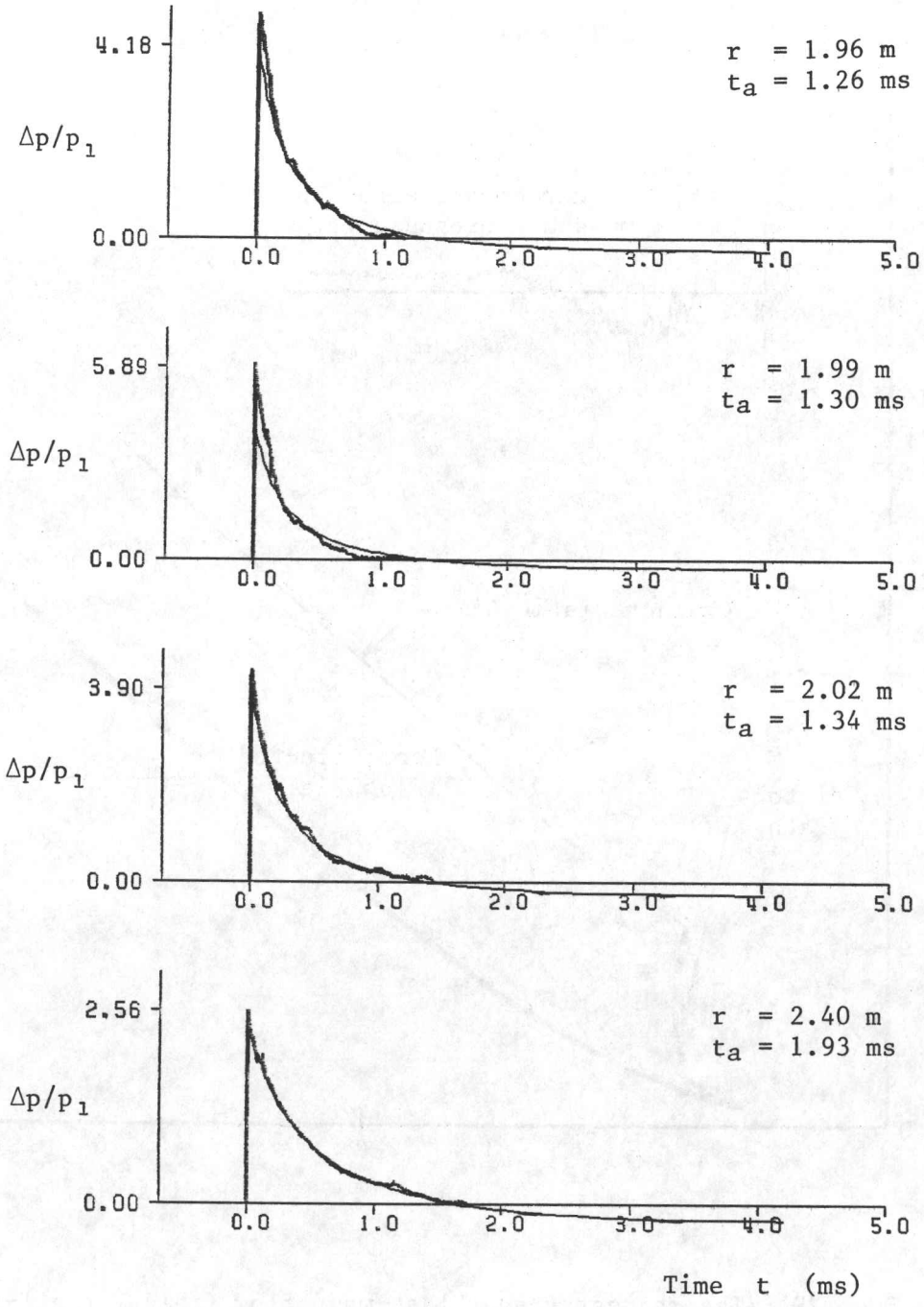

Fig. 30a. Comparison of measured overpressure signatures (〰) from the 628-ton ANFO explosion trial to those from the reconstructed flow field by the RCM (~~).

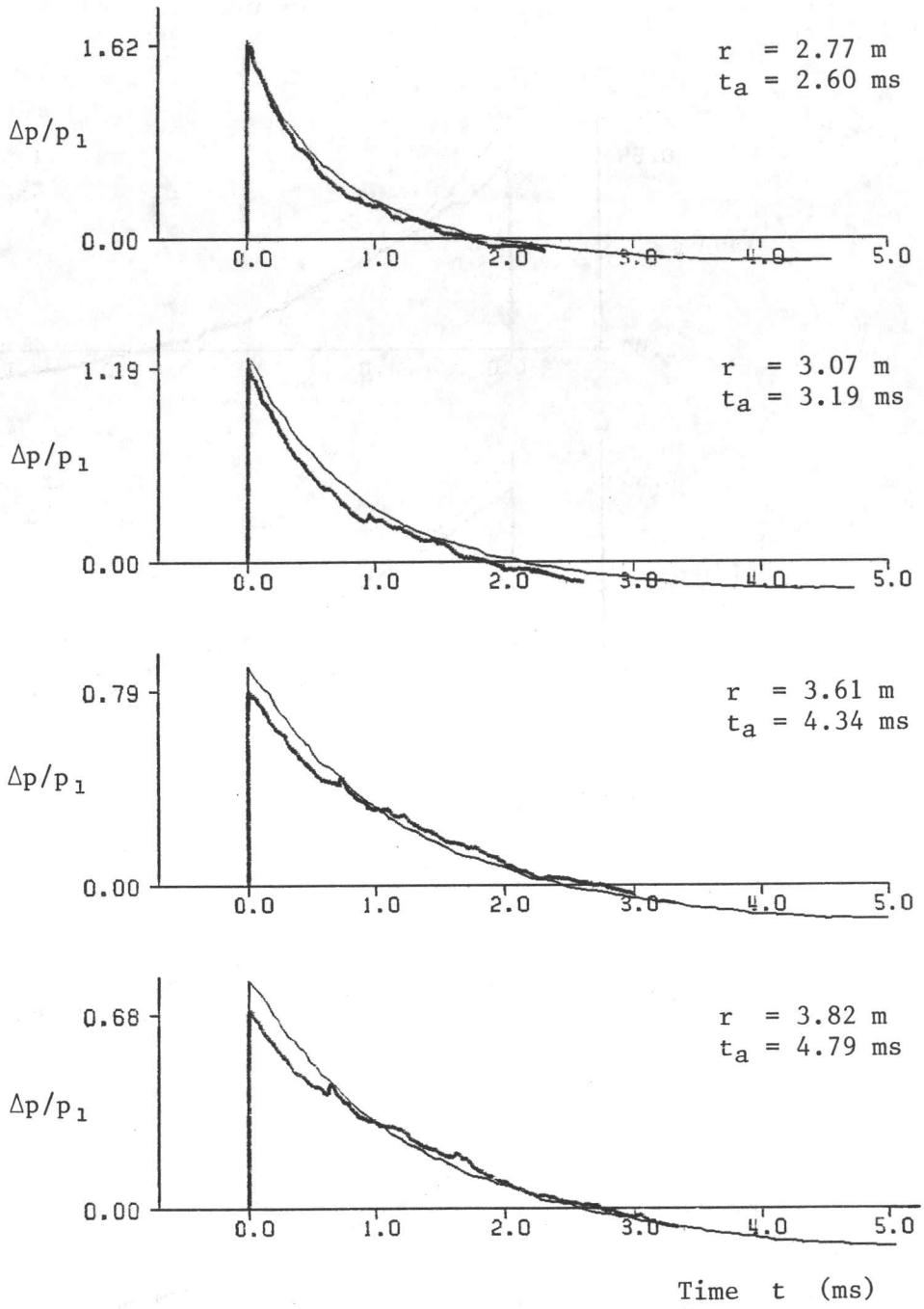

Fig. 30b. Comparison of measured overpressure signatures (〰) from the 628-ton ANFO explosion trial to those from the reconstructed flow field by the RCM (〰).

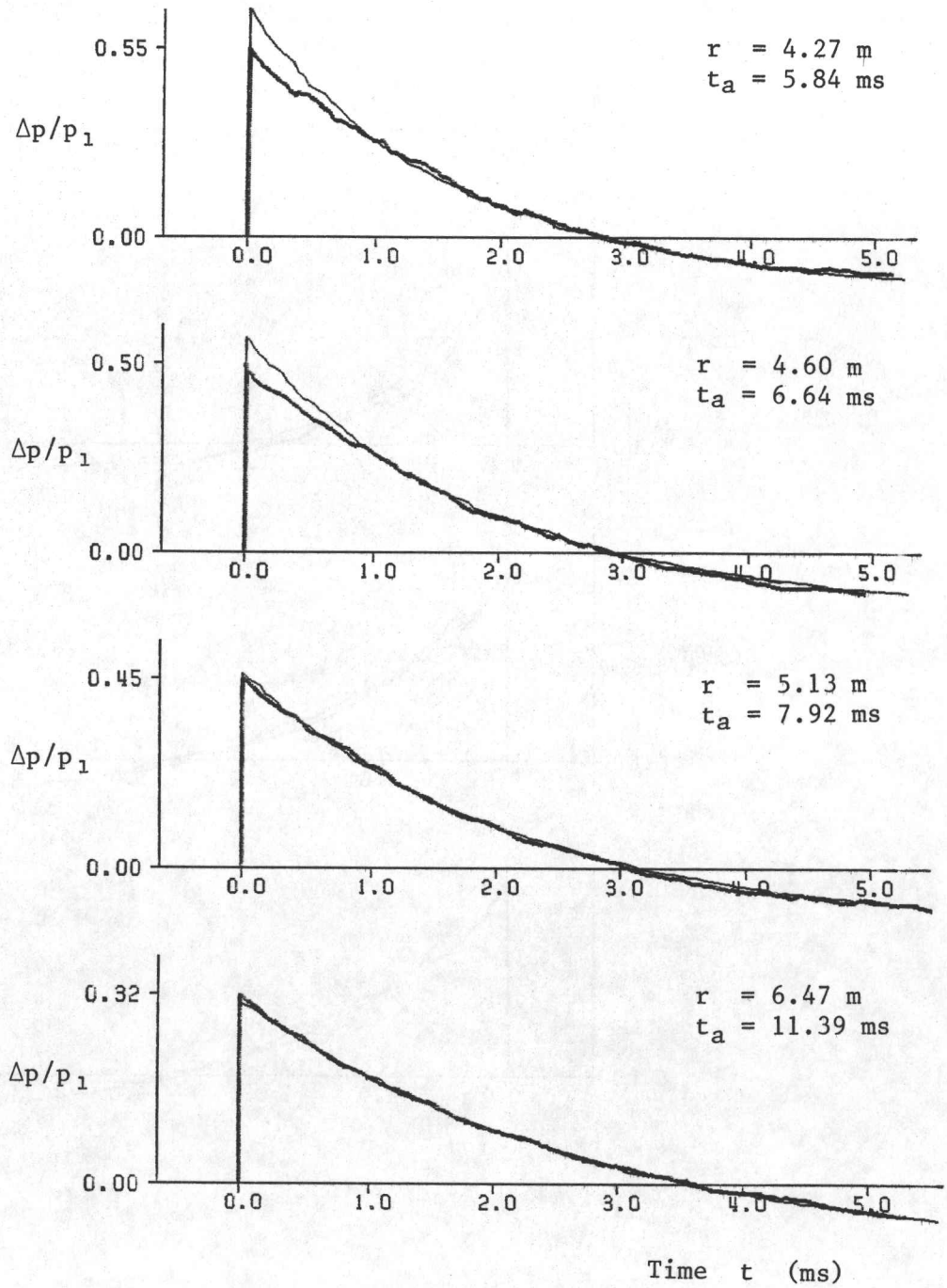

Fig. 30c. Comparison of measured overpressure signatures (~~~) from the 628-ton ANFO explosion trial to those from the reconstructed flow field by the RCM (~~~).

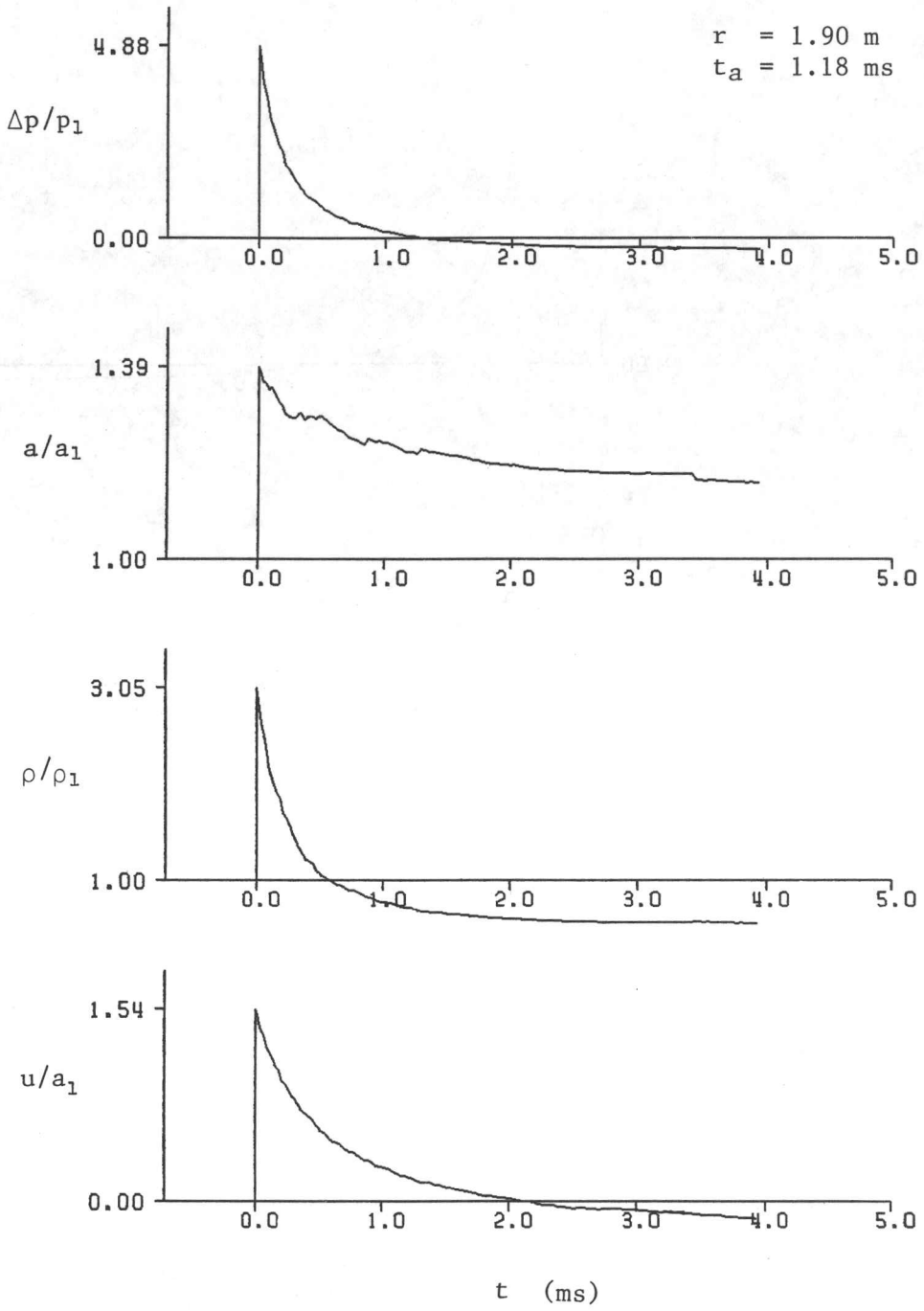

Fig. 31b. Overpressure, sound-speed, density and flow-velocity signatures from the reconstructed blast-wave flow field by the RCM for a 1-kg TNT equivalent ANFO surface explosion in a standard atmosphere.

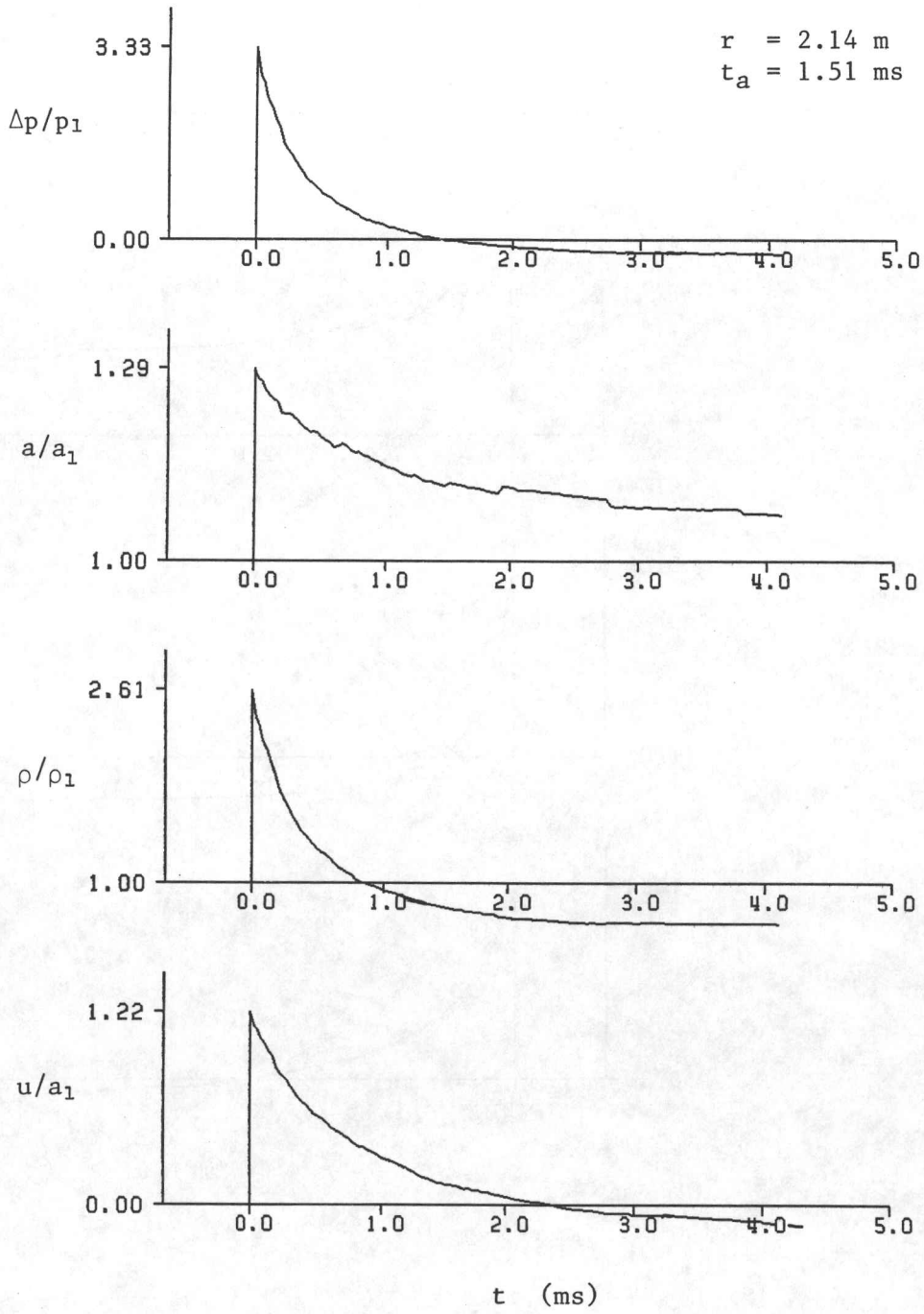

Fig. 31c. Overpressure, sound-speed, density and flow-velocity signatures from the reconstructed blast-wave flow field by the RCM for a 1-kg TNT equivalent ANFO surface explosion in a standard atmosphere.

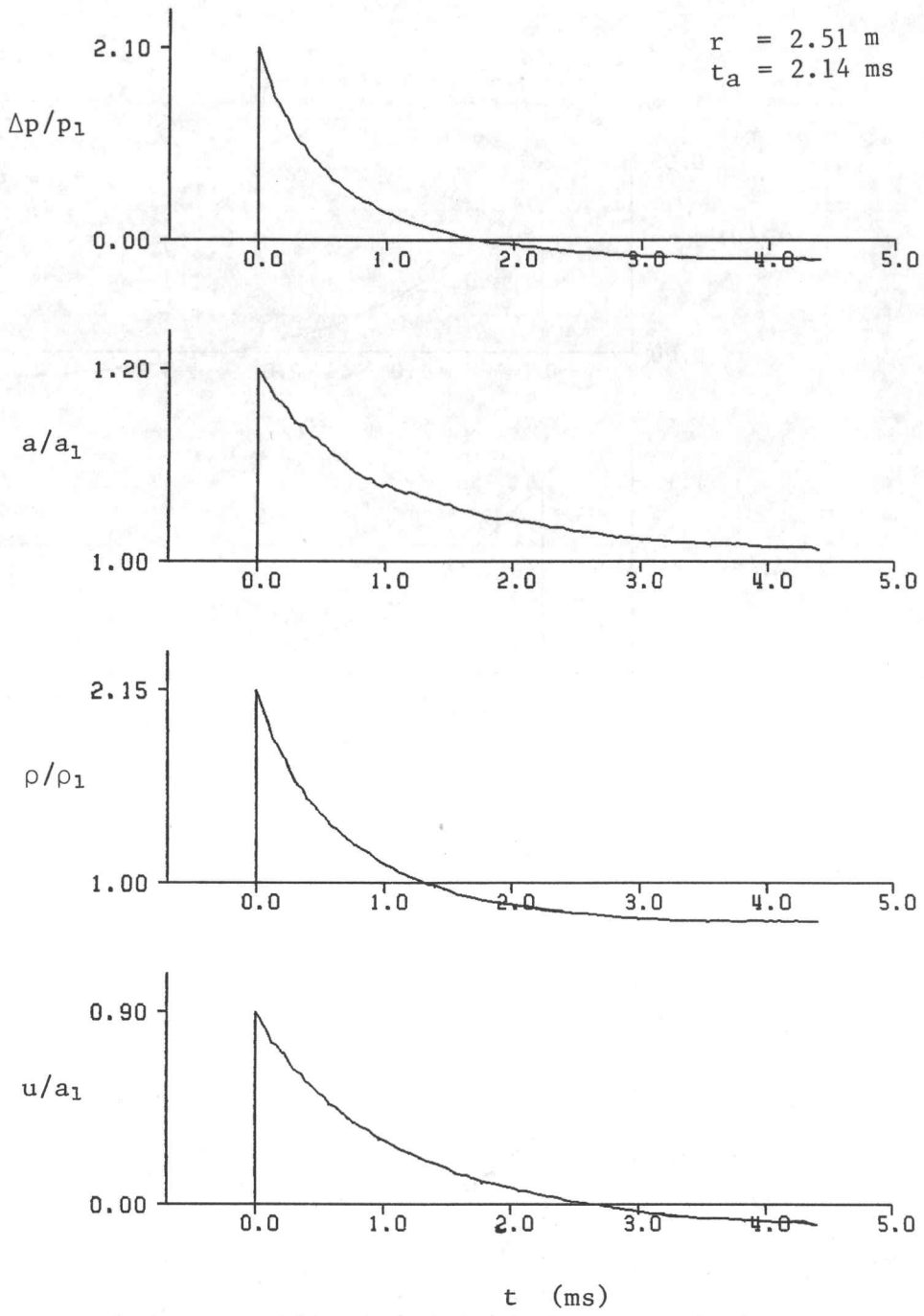

Fig. 31d. Overpressure, sound-speed, density and flow-velocity signatures from the reconstructed blast-wave flow field by the RCM for a 1-kg TNT equivalent ANFO surface explosion in a standard atmosphere.

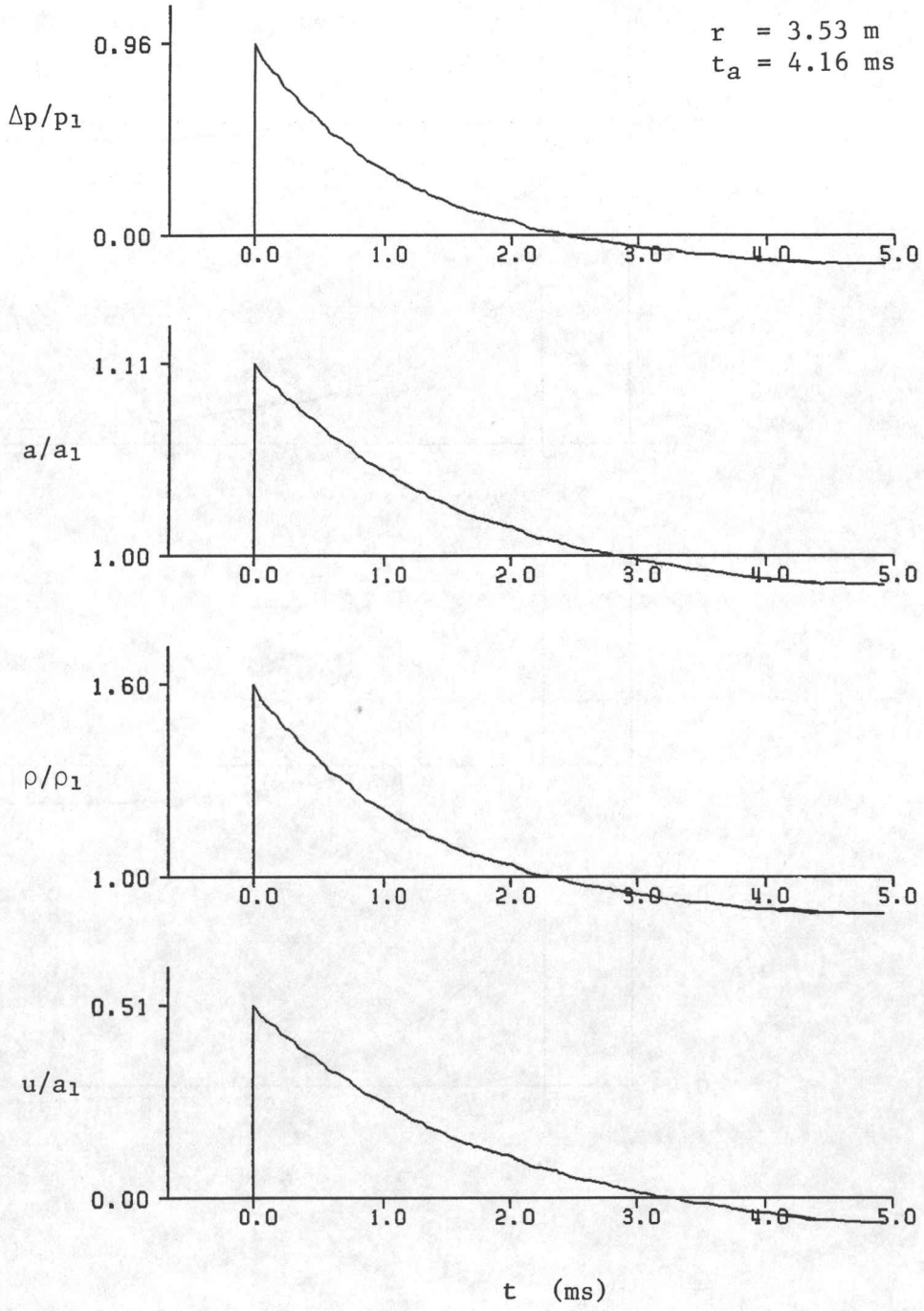

Fig. 3le. Overpressure, sound-speed, density and flow-velocity signatures from the reconstructed blast-wave flow field by the RCM for a 1-kg TNT equivalent ANFO surface explosion in a standard atmosphere.

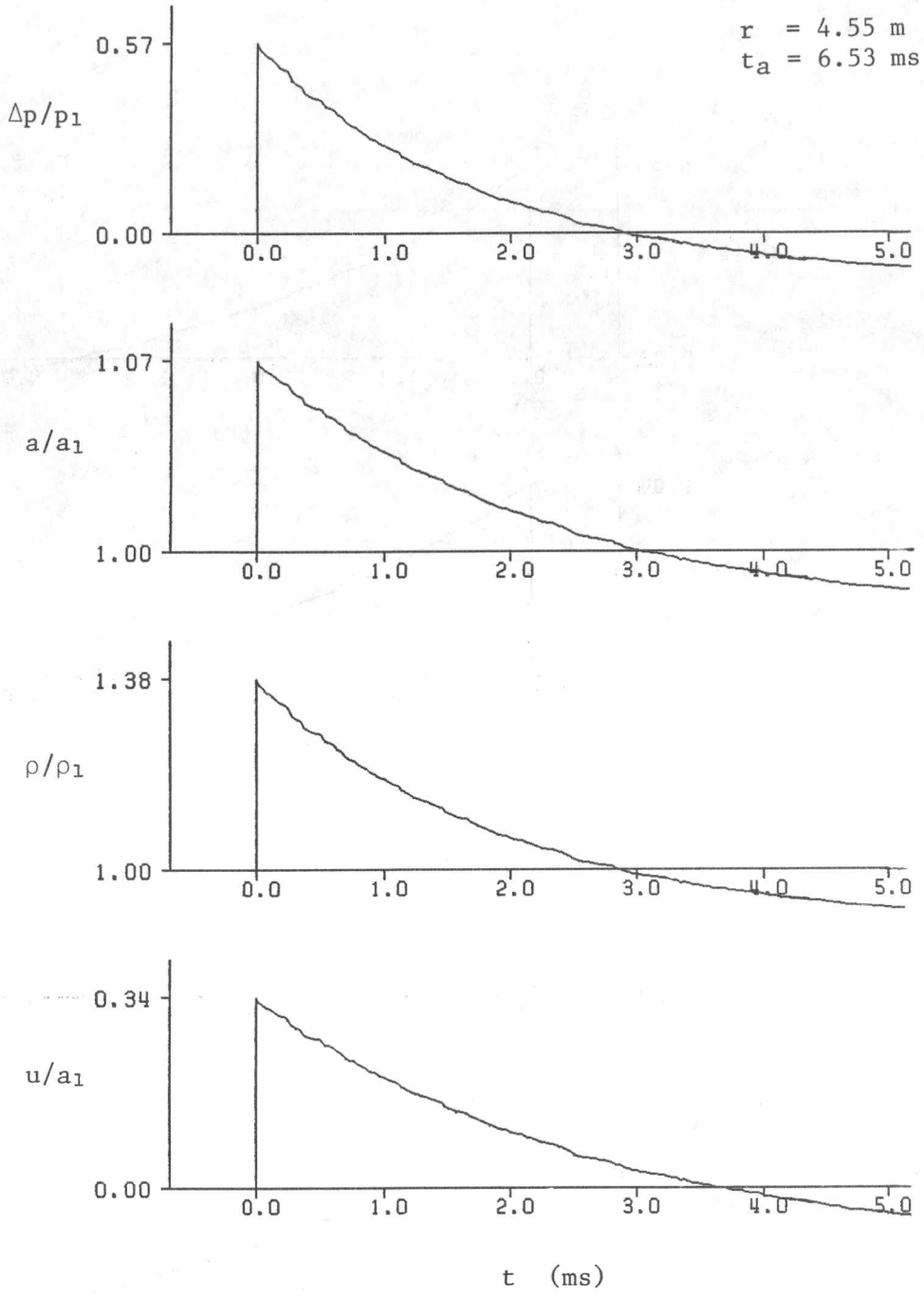

Fig. 31f. Overpressure, sound-speed, density and flow-velocity signatures from the reconstructed blast-wave flow field by the RCM for a 1-kg TNT equivalent ANFO surface explosion in a standard atmosphere.

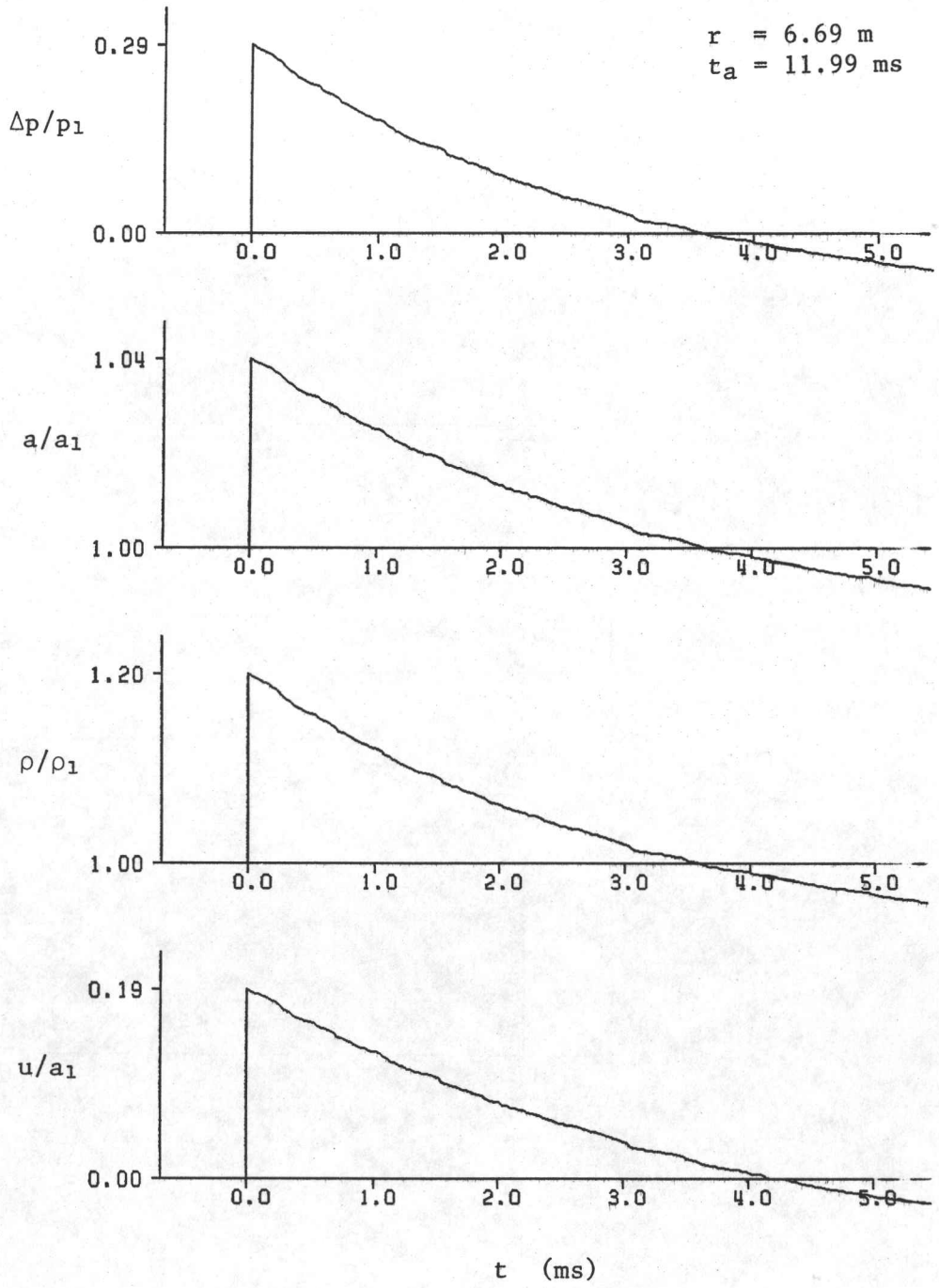

Fig. 31g. Overpressure, sound-speed, density and flow-velocity signatures from the reconstructed blast-wave flow field by the RCM for a 1-kg TNT equivalent ANFO surface explosion in a standard atmosphere.

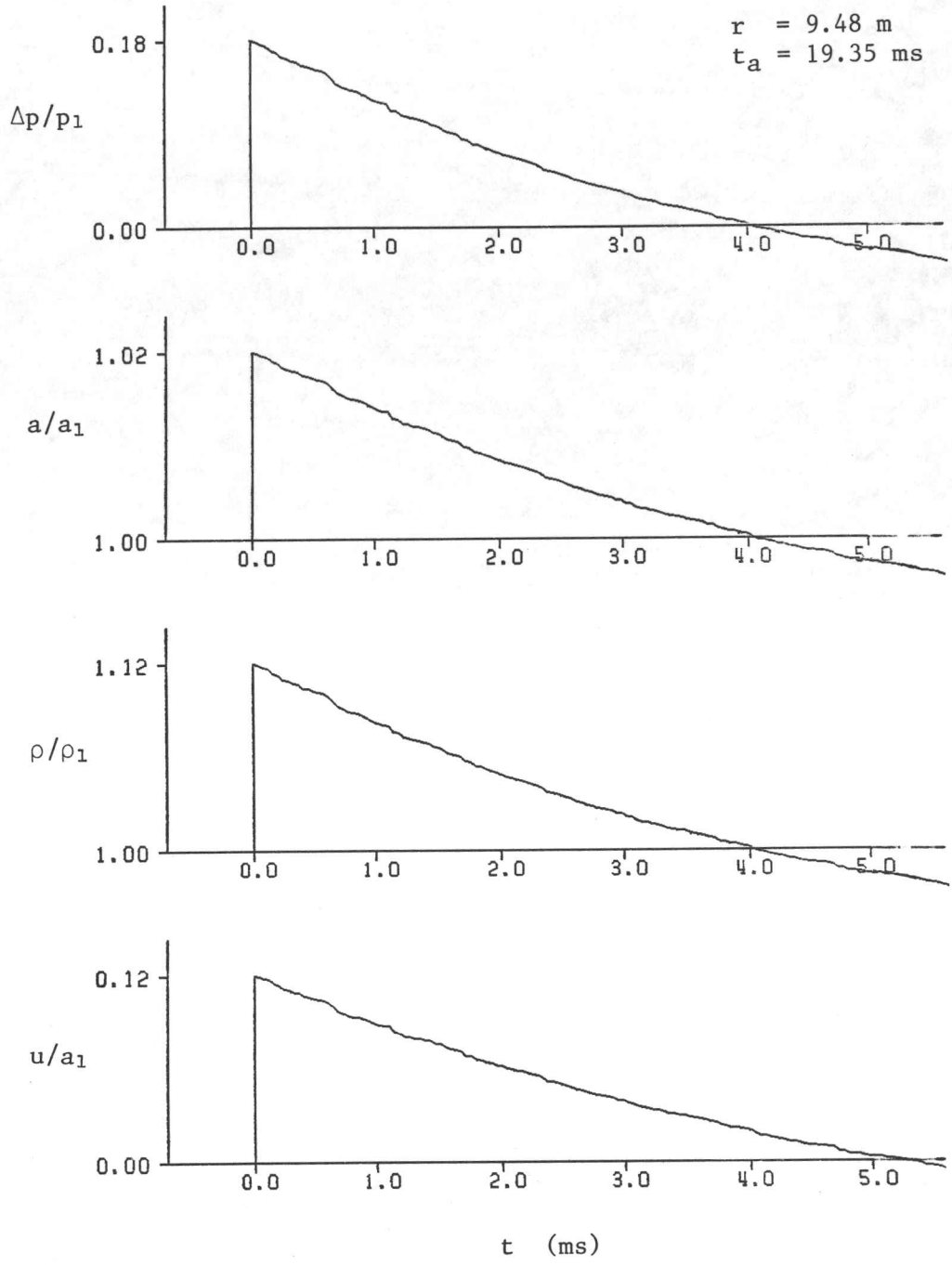

Fig. 31h. Overpressure, sound-speed, density and flow-velocity signatures from the reconstructed blast-wave flow field by the RCM for a 1-kg TNT equivalent ANFO surface explosion in a standard atmosphere.

APPENDIX A

COMPUTER-PROGRAM LISTING FOR THE RANDOM-CHOICE METHOD WITH THE MOVING PISTON BOUNDARY CONDITION

The computer program developed for the present nonstationary flow computations in front of a moving piston with a specified path is a modified version of a fairly general computer program developed originally by G. A. Sod and subsequently adopted and suitably modified and extended for use at UTIAS by Saito and Glass [A1]. The major modification to Satio and Glass's program to enable the present numerical study is the addition of the moving piston boundary condition, which is described in chapter 2. This modification includes the use of cubic splines with suitable interpolation and differentiation. A cubic-spline routine called SPLINE and its associated interpolation and differentiation routine called SEVAL were adopted from Ref. A2. These routines had to be modified slightly in terms of the end boundary conditions for suitable incorporation in the present work. Furthermore, the previous random-number generator has been replaced by the more suitable van der Corput random-number algorithm, as pointed out in Ref. A3. Note that the original program of Saito and Glass [A1] had the capability of following the motion or path of any fluid particle, as well as the contact surface (or surfaces), and this useful capability is retained in the present version. The computer-program listing for the current version of the RCM with the moving piston boundary condition is presented in the following pages of this appendix.

All dependent thermodynamic and dynamic variables used in the computer program are in nondimensional form. They are designated here by using an overhead bar and given as follows:

$$\bar{p} = p/p_1 , \qquad \bar{\rho} = \rho/\rho_1 , \qquad \bar{u} = \sqrt{\gamma}\, u/a_1 , \tag{A1}$$

where p, ρ, a, u, and γ denote the static pressure, density, sound speed, flow velocity, and ratio of the specific heats for a perfect gas, respectively, and the subscript 1 denotes reference or atmospheric conditions. The independent variables time and distance are also given in nondimensional form, by using an overhead bar, and given as follows:

$$\bar{t} = a_1 t / \sqrt{\gamma}\, \bar{R} , \qquad \bar{x} = x / \bar{R} , \tag{A2}$$

where t, x, and $\bar{R}$ denote time, distance, and a certain characteristic radial distance, respectively.

References

A1. T. Saito and I. I. Glass, "Application of Random-Choice Method to Problems in Shock and Detonation-Wave Dynamics", UTIAS Report No. 270, University of Toronto Institute for Aerospace Studies, October 1979.

A2. G. E. Gorsythe, M. A. Malcolm, and C. B. Moler, "Computer Methods for Math-

ematical Computations", Prentice-Hall, Englewood Cliffs, New Jersey, U.S.A., 1977.

A3. O. Igra, J. J. Gottlieb, and T. Saito, "An Analytical and Numerical Study of the Interaction of Rarefaction Waves with Area Changes - Part 2: Area Enlargements", UTIAS Report No. 273, to be printed in 1984.

```
C     ############################################################
C     #                                                          #
C     #              RANDOM-CHOICE METHOD WITH A                 #
C     #            MOVING PISTON BOUNDARY CONDITION              #
C     #                                                          #
C     #                    BY S. C. M. LAU                       #
C     #                                                          #
C     ############################################################
C
C     ------------------------------------------------------------
C                     VARIABLES IN THE MAIN PROGRAM
C                     -----------------------------
C
C      --- INPUT VARIABLES
C
C            N = NUMBER OF GRID POINTS
C           NP = NUMBER OF SPLINED POINTS
C        NSTOP = NUMBER OF TIME STEPS
C       NPRINT = NUMBER OF CYCLES FOR EACH PRINT OUT
C
C           I1 = INPUT CONTROL FOR THE RADIUS OF THE DESIRED
C                TEST SITE TO OBTAIN TIME-VARYING FLOW PROPERTIES
C                0 - IN METER
C                1 - IN GRID NUMBER
C
C         XP(2) = RADIAL COORDINATE OF THE SPLINED POINT
C         TP(2) = TIME COORDINATE OF THE SPLINED POINT
C           GMA = GAMMA--RATIO OF SPECIFIC HEATS (1.400 FOR AIR)
C
C           ETA = GEOMETRIC PARAMETER
C                 1 - PLANAR
C                 2 - CYLINDRICAL
C                 3 - SPHERICAL
C
C           DTB = STARTING TIME FOR A DISTURBANCE CREATED BY THE
C                 SUDDEN ACCELERATION OF THE PISTON
C
C            XL = CHARACTERISTIC DISTANCE IN METER
C            V1 = STARTING VELOCITY OF THE PISTON
C            XO = STARTING POSITION OF THE CREATED DISTURBANCE
C           NOP = NUMBER OF PARTICLE PATHS
C           NOD = NUMBER OF DENSITY-TIME HISTORIES
C           NOV = NUMBER OF FLOW VELOCITY-TIME HISTORIES
C           NOF = NUMBER OF PRESSURE-TIME HISTORIES
C
C       NPT(1) = POSITION OF PARTICLE NO. 1 IN EACH TIME STEP
C       NVS(1) = GRID NUMBER FOR OBTAINING THE VELOCITY-TIME
C                HISTORY AT TEST SITE NO. 1
C
C       NDS(1) = GRID NUMBER FOR OBTAINING THE DENSITY-TIME
C                HISTORY AT TEST SITE NO. 1
C
C       NFS(1) = GRID NUMBER FOR OBTAINING THE PRESSURE-TIME
C                HISTORY AT TEST SITE NO. 1
C
C      --- OUTPUT VARIABLES
C
C         P1(1) = PRESSURE AT GRID POINT NO. 1
C         R1(1) = DENSITY AT GRID POINT NO. 1
C         U1(1) = VELOCITY AT GRID POINT NO. 1
C
C           TIME = TIME LEVEL
C            CNT = EXACT PISTON POSITION AS A REAL NUMBER
C           NPIS = PISTON POSITION AS A GRID NUMBER
C            NSS = SHOCK POSITION IN EACH FULL TIME STEP
C            NBR = POSITION OF THE CREATED DISTURBANCE
C                  IN EACH FULL TIME STEP
C
C       TK(1,I) = STARTING TIME OF THE FLUID-PARTICLE MOTION
C       TK(2,I) = TIME ARRIVAL OF CREATED DISTURBANCE AT
C                 THE PARTICLE PATH
C
C      DSM(1,I) = TIME OF ARRVIAL FOR DENSITY-TIME HISTORY
C      VSM(1,I) = TIME OF ARRVIAL FOR VELOCITY-TIME HISTORY
C      FSM(1,I) = TIME OF ARRVIAL FOR PRESSURE-TIME HISTORY
C      DSM(2,I) = DENSITY AT THE TIME WHEN THE CREATED DISTURBANCE
C                 ARRIVES
C
C      VSM(2,I) = VELOCITY AT THE TIME WHEN THE CREATED DISTURBANCE
C                 ARRIVES
C
C      FSM(2,I) = PRESSURE AT THE TIME WHEN THE CREATED DISTURBANCE
C                 ARRIVES
C
C      --- OTHER VARIABLES
C
C            DT = TIME INTERVAL FOR EACH HALF TIME STEP
C            DX = DISTANCE BETWEEN TWO ADJACENT GRID POINTS
C            XI = RANDOM NUMBER BETWEEN -DX/2 AND DX/2
C     ------------------------------------------------------------
C
C     ------------------------------------------------------------
C                          MAIN PROGRAM
C                          ------------
C
      IMPLICIT REAL*8 (A-H,O-Z)
      COMMON/AO/R1(1002),P1(1002),U1(1002)
      COMMON/BO/DT,RL,UL,PL,RR,UR,PR,R,U,P,XI,Y,GMA
      COMMON/CO/TP(18),XP(18),B(18),C(18),D(18),XO,DTB,NP,N
      INTEGER NPT(40),ND(40),NDD(40),NDS(35),NVS(35),NFS(35)
      REAL*8 TK(2,35),DSM(2,35),VSM(2,35),FSM(2,35)
C
C     --- INPUT DATA
C
      READ(2,1) N,NSTOP,NP,NPRINT,NOP,NOD,NOV,NOF,I1
      READ(2,2) XL,TIME,GMA,V1,ETA,DTB
      READ(2,3) (XP(I),TP(I),I=1,NP)
C
      IF(NOP.EQ.0) GO TO 73
      DO 12 I=1,NOP
      READ(2,33) VA
   12 NPT(I)=INT(VA/XL*N)+1
C
   73 IF(I1.EQ.1) GO TO 208
      READ(2,48) (NVS(I),I=1,NOV)
      READ(2,48) (NDS(I),I=1,NOD)
      READ(2,48) (NFS(I),I=1,NOF)
      GO TO 205
C
  208 IF(NOV.EQ.0) GO TO 201
      DO 202 I=1,NOV
      READ(2,37) VA
  202 NVS(I)=INT(VA/XL*N)+1
C
  201 IF(NOD.EQ.0) GO TO 203
```

```
      DO 204 I=1,NOD
      READ(2,37) VA
  204 NDS(I)=INT(VA/XL*N)+1
C
  203 IF(NOF.EQ.0) GO TO 205
      DO 206 I=1,NOF
      READ(2,37) VA
  206 NFS(I)=INT(VA/XL*N)+1
C
  205 DO 15 I=1,NP
      XP(I)=XP(I)*5./XL*N
   15 TP(I)=TP(I)*5./XL
C
      TIME=TIME*5./XL
      DTB=DTB*5./XL
C
      DO 39 I=1,NOP
   39 ND(I)=0
C
C     --- CALCULATE PISTON PATH AND THE STARTING POSITION
C         OF THE PISTON
C
      CALL SPLINE(V1,GMA)
      CALL SEVAL(DTB,NPIS,CNT,UL)
      NBR=NPIS+1
      NBS=NPIS+1
      ID=0
      M=N+1
      DX=1./DFLOAT(N)
C
C     --- SET INITIAL CONDITIONS
C
      CALL SEVAL(TIME,NPIS,CNT,UL)
      RR=1.
      PR=1.
      UR=0.
      CALL BOUND
      R1(NPIS)=RL
      P1(NPIS)=PL
      U1(NPIS)=UL
      IC=NPIS+1
      DO 16 I=IC,M
      R1(I)=RR
      P1(I)=PR
   16 U1(I)=UR
C
      M1=1
      M2=1
      M3=1
      M4=1
      M5=1
      M6=1
      NY=1
      NW2=1
C
      DO 207 I=1,NOP
      TK(2,I)=0.
  207 TK(1,I)=0.
C
C     --- BEGIN CALCULATIONS
C
      NW=1
      NSS=NPIS
      NRT=NPIS+3
      DO 100 NSTEP=1,NSTOP
C
C     --- FIND MAXIMUM VELOCITY FOR
C         COURANT-FRIEDRICHS-LEWY STABILITY CRITERION
C
      VB=0.
      DO 8 I=NPIS,NRT
      VA=ABS(U1(I))+DSQRT(GMA*P1(I)/R1(I))
    8 IF(VA .GT. VB)  VB=VA
C
C     --- SET TIME INTERVAL
C
      DT=.5*DX/VB
      TIME=TIME+2.*DT
C
C     --- GENERATE RANDOM NUMBER (VAN DER CORPUT ALGORITHM)
C
      NCE=2*NSTEP-1
      M=0
      XI=0
   10 M=M+1
      MD=MOD(NCE,2**M)
      IF(MD.EQ.0) GO TO 10
      XI=XI+1./2.**M
      NCE=NCE-MD
      IF(NCE.EQ.0) GO TO 20
      GO TO 10
   20 CONTINUE
C
C     --- XI LIES BETWEEN -DX/2 AND DX/2
C
      XI=XI*DX-0.5*DX
      IC=NPIS+1
      NW1=2
C     --- COMPUTE THE FIRST HALF STEP
C
      DO 40 I=IC,NRT
      RR=R1(I)
      UR=U1(I)
      PR=P1(I)
      IF(I.EQ.IC) GO TO 43
      RL=VA
      PL=VB
      UL=VC
      GO TO 44
   43 CALL BOUND
   44 CALL GLIMM
C
C     --- DETECT PARTICLE MOTION
C
      IF(NW1.GT.NW) GO TO 90
      MD=NW1-1
      IF(I.NE.NPT(MD)) GO TO 90
      ND(MD)=1
      IF(XI.GE.Y) ND(MD)=0
      NW1=NW1+1
C
```

```
   90 VA=R1(I)
      R1(I)=R
      VB=P1(I)
      P1(I)=P
      VC=U1(I)
      U1(I)=U
   40 CONTINUE
      IF(NW.LT.2) GO TO 80
      MD=NW-1
      DO 81 I=1,MD
   81 NPT(I)=NPT(I)+ND(I)
   80 IC=1
C
C     --- USE OPERATOR SPLITTING METHOD
C
      CALL INH (DX,DT,ETA,GMA,NPIS,NRT,IC,NSS)
C
C     --- END OF FIRST HALF TIME STEP
C
C     --- GENERATE RANDOM NUMBER (VAN DER CORPUT ALGORITHM)
C
      NCE=2*NSTEP
      M=0
      XI=0.
   11 M=M+1
      MD=MOD(NCE,2**M)
      IF(MD.EQ.0) GO TO 11
      XI=XI+1./2.**M
      NCE=NCE-MD
      IF(NCE.EQ.0) GO TO 22
      GO TO 11
   22 CONTINUE
C     --- XI LIES BETWEEN -DX/2 AND DX/2
C
      XI=XI*DX-0.5*DX
      DO 82 I=1,NOP
   82 NDD(I)=NPT(I)-1
      NW1=2
      K=NRT-1
C
C     --- COMPUTE SECOND HALF TIME STEP
C
      VA=TIME-DT
      CALL SEVAL(VA,NNN,CNT,UL)
      NDDD=NPIS
      IF( CNT.GT.(FLOAT(NPIS-1)/N+DX/2.)) NDDD=NDDD+1
C
      DO 60 I=NDDD,K
      RL=R1(I)
      PL=P1(I)
      UL=U1(I)
      RR=R1(I+1)
      PR=P1(I+1)
      UR=U1(I+1)
      IF(I.NE.NPIS) GO TO 64
      VA=TIME-DT
C
C     --- PISTON BOUNDARY CONDITIONS
C
      CALL SEVAL(VA,NNN,CNT,UL)
      CALL BOUND
   64 CALL GLIMM
C
```



```
C     --- DETECT PARTICLE MOTION
C
      IF(NW1.GT.NW) GO TO 120
      MD=NW1-1
      IF(I.NE.NDD(MD)) GO TO 120
      ND(MD)=-1
      IF(XI.LT.Y) ND(MD)=0
      NW1=NW1+1
C
  120 R1(I)=R
      P1(I)=P
      U1(I)=U
   60 CONTINUE
      IF(NW.LT.2) GO TO 62
      MD=NW-1
      DO 61 I=1,MD
   61 NPT(I)=NPT(I)+ND(I)
C
C     --- END OF SECOND HALF TIME STEP
C
C     --- DETERMINE THE SHOCK POSITION
C
   62 IF(NSS+4.GE.N) GO TO 130
      VD=TIME
      M=NSS-2
      MD=NSS+2
      IF(M.LT.0) M=1
      DO 4 I=M,MD
    4 IF(ABS(U1(I)).GE.0.0001) NSS=I
      IF(NW.GT.NOP) GO TO 9
      IF(NSS+1.NE.NPT(NW)) GO TO 9
      TK(1,NW)=TIME
      NW=NW+1
      ID=1
C
C     --- DETECT TIME OF ARRIVAL OF SHOCK WAVE
C
    9 IF(M4.GT.NOD) GO TO 131
      IF(NSS.NE.NDS(M4)) GO TO 131
      DSM(1,M4)=TIME
      M4=M4+1
      ID=1
C
  131 IF(M5.GT.NOV) GO TO 132
      IF(NSS.NE.NVS(M5)) GO TO 132
      VSM(1,M5)=TIME
      M5=M5+1
      ID=1
C
  132 IF(M6.GT.NOF) GO TO 133
      IF(NSS.NF.NFS(M6)) GO TO 133
      FSM(1,M6)=TIME
      M6=M6+1
      ID=1
C
  133 NRT=NSS+2
      GO TO 150
  130 NRT=N+1
  150 IC=2
C
C     --- USE OPERATOR SPLITTING METHOD
C
      CALL INH (DX,DT,ETA,GMA,NPIS,NRT,IC,NSS)
C
```

```
C     --- PISTON BOUNDARY CONDITIONS
C
      CALL SEVAL(TIME,NPIS,CNT,UL)
      RR=R1(NPIS+1)
      UR=U1(NPIS+1)
      PR=P1(NPIS+1)
      CALL BOUND
      R1(NPIS)=RL
      P1(NPIS)=PL
      U1(NPIS)=UL
      NNN=NPIS
C
C     --- DETERMINE THE LOCATION OF THE CREATED DISTURBANCE
C
      IF(TIME.GE.DTB) NY=NY+1
      IF(NY.GE.3) GO TO 135
      NBR=NPIS
      GO TO 134
C
  135 VB=0.
      M=NBR-2
      MD=NBR+1
      DO 211 I=M,MD
      VA=P1(I)-P1(I+1)
      IF(VA.GE.VB) NBR=I
  211 VB=VA
C
      IF(NBR.NE.NPT(NW2)) GO TO 231
      TK(2,NW2)=TIME
      NW2=NW2+1
C
  231 CNT=DFLOAT(NBR-1)
      NNN=NBR+1
  134 IF(M1.GT.NOD) GO TO 118
      IF(NBR.NE.NDS(M1)) GO TO 118
      DSM(2,M1)=TIME
C
      M1=M1+1
  118 IF(M2.GT.NOV) GO TO 119
      IF(NBR.NE.NVS(M2)) GO TO 119
      VSM(2,M2)=TIME
C
      M2=M2+1
  119 IF(M3.GT.NOF) GO TO 136
      IF(NBR.NE.NFS(M3)) GO TO 136
      FSM(2,M3)=TIME
      M3=M3+1
C
  136 IF(NNN.GE.N) GO TO 34
C
C     --- OUTPUT DATA
C
      IF(ID.EQ.1) GO TO 170
      MD=NPRINT
      IF(MOD(NSTEP,MD).NE.0) GO TO 100
  170 ID=0
C
      WRITE(5,99) VD,TIME,CNT,P1(NSS),NSS
C
      IF(NOP.EQ.0) GO TO 117
C
      WRITE(9,111) (NPT(I),I=1,NOP)
      WRITE(10,112) (U1(NPT(I)),I=1,NOP)
C
  117 IF(NOD.NE.0) WRITE(11,114) TIME,(R1(NDS(I)),I=1,NOD)
      IF(NOV.NE.0) WRITE(12,114) TIME,(U1(NVS(I)),I=1,NOV)
      IF(NOF.NE.0) WRITE(13,114) TIME,(P1(NFS(I)),I=1,NOF)
C
  100 CONTINUE
C
   34 VA=9999.90
      VB=99.99
      WRITE(5,33) VA
      IF(NOP.NE.0) WRITE(10,112) VB
      IF(NOP.NE.0) WRITE(5,113) (TK(1,I),TK(2,I),I=1,NOP)
      IF(NOD.EQ.0) GO TO 401
      WRITE(11,114) VB
      WRITE(11,113) (DSM(1,I),DSM(2,I),I=1,NOD)
  401 IF(NOV.EQ.0) GO TO 402
      WRITE(12,114) VB
      WRITE(12,113) (VSM(1,I),VSM(2,I),I=1,NOV)
  402 IF(NOF.EQ.0) GO TO 403
      WRITE(13,114) VB
      WRITE(13,113) (FSM(1,I),FSM(2,I),I=1,NOF)
  403 CONTINUE
C
    1 FORMAT(9I4)
    2 FORMAT(6F10.5)
    3 FORMAT(2F10.5)
   33 FORMAT(F10.5)
   37 FORMAT(2X,F10.5)
   48 FORMAT(I4)
   99 FORMAT(4F10.5,3I4)
  111 FORMAT(10I4)
  112 FORMAT(10F7.4)
  113 FORMAT(2F10.5)
  114 FORMAT(10F10.5)
C
      STOP
      END
C  ------------------------------------------------------------------
C
C  ------------------------------------------------------------------
C                          SUBROUTINE GLIMM
C                          ----------------
C
C     SUBROUTINE FOR SOLVING THE RIEMANN PROBLEM BETWEEN TWO GRID
C     POINTS (THIS SUBROUTINE SOLVES THE RIEMANN PROBLEM BETWEEN TWO
C      ADJACENT GRID POINTS IN THE FLOW FIELD FOR A GIVEN TIME
C      INCREMENT [A1].)
C
C  ------------------------------------------------------------------
C
      IMPLICIT REAL*8 (A-H,O-Z)
      COMMON/BO/DT,RL,UL,PL,RR,UR,PR,R,U,P,XI,Y,GMA
      REAL*8 MR,ML,MRP1,MLP1
      EPS=1.0E-6
      IT=0
      ITSTOP=20
C
C     --- CONSTRUCTION OF RIEMANN PROBLEM
C
C     --- ALFA IS THE CONVERGENCE FACTOR
C     --- INITIALIZE ML AND MR
C
      ALFA=1.
      ALFAM=1.-ALFA
      ML=100.
```

```
      MR=100.
      COEFL=DSQRT(PL*RL)
      COEFR=DSQRT(PR*RR)
      PSTAR=0.5*(PL+PR)
C
C     --- SOLVE RIEMANN PROBLEM USING GODUNOV'S ITERATIVE METHOD
C
   10 IT=IT+1
C
C     --- IF PSTAR IS LESS THAN EPS THEN PSTAR IS SET EQUAL
C         TO 1.0E-6 TO PREVENT PSTAR FROM BECOMING NEGATIVE.
C
      IF(PSTAR.LT.EPS) PSTAR=EPS
C
      MLP1=COEFL*PHI(PSTAR/PL,GMA)
      MRP1=COEFR*PHI(PSTAR/PR,GMA)
      DIFML=ABS(MLP1-ML)
      DIFMR=ABS(MRP1-MR)
      ML=MLP1
      MR=MRP1
C
C     --- COMPUTE NEW PRESSURE PSTAR
C
      PSTARP=PSTAR
      PSTAR=(UL-UR+PR/MR+PL/ML)/(1./ML+1./MR)
      PSTAR=ALFA*PSTAR+ALFAM*PSTARP
      IF(IT .LE. ITSTOP) GO TO 30
      IF(ABS(PSTAR-PSTARP) .LT. EPS) GO TO 40
      IF(DIFML*DIFMR .LT. EPS) GO TO 40
      ALFA=ALFA/2.
      ALFAM=1.-ALFA
      IF(ALFAM .LT. EPS) GO TO 40
      IT=0
   30 IF(DIFML .GT. EPS) GO TO 10
      IF(DIFMR .GT. EPS) GO TO 10
C
C     --- COMPUTE USTAR AT END OF GODUNOV'S ITERATION
C
   40 USTAR=(PL-PR+MR*UR+ML*UL)/(ML+MR)
C
C     --- BEGIN GLIMM'S METHOD
C
      IREGL=1
      IF(PSTAR .LT. PL) IREGL=2
      IREGR=1
      IF(PSTAR .LT. PR) IREGR=2
      X=USTAR*DT
      Y=X
      IF(XI .GE. X) GO TO 200
C
C     --- COMPUTE LEFT SIDE OF THE RIEMANN PROBLEM
C
      IF(IREGL .EQ. 2) GO TO 110
C
C     --- COMPUTE SHOCK SPEED TO THE LEFT
C
      U=UL-ML/RL
      X=U*DT
      IF(XI .GE. X) GO TO 100
C
C     --- STATE ON LEFT SIDE OF LEFT MOVING SHOCK
C
      R=RL
      U=UL
      P=PL
      GO TO 500
C
C     --- STATE ON RIGHT SIDE OF LEFT MOVING SHOCK
C
  100 R=ML/(USTAR-U)
      U=USTAR
      P=PSTAR
      GO TO 500
C
C     --- COMPUTE SOUND SPEED ON LEFT SIDE OF SHOCK FRONT
C
  110 CL=DSQRT(GMA*PL/RL)
      X=(UL-CL)*DT
      IF(XI .GE. X) GO TO 120
C
C     --- STATE ON LEFT SIDE OF LEFT RAREFACTION WAVE
C
      R=RL
      U=UL
      P=PL
      GO TO 500
C
C     --- COMPUTE CONSTANT A FOR ISENTROPIC LAW
C
  120 A=PL/(RL**GMA)
C
C     --- COMPUTE DENSITY AND SOUND SPEED IN STATE STAR
C
      RSTAR=(PSTAR/A)**(1./GMA)
      CSTAR=DSQRT(GMA*PSTAR/RSTAR)
      X=(USTAR-CSTAR)*DT
      IF(XI .GE. X) GO TO 130
C
C     --- STATE INSIDE OF RAREFACTION WAVE MOVING TO THE LEFT
C
      U=(2./(GMA+1.))*(XI/DT+CL+0.5*(GMA-1.)*UL)
      RINT=CL+0.5*(GMA-1.)*(UL-U)
      R=(RINT*RINT/(A*GMA))**(1./(GMA-1.))
      P=A*(R**GMA)
      GO TO 500
C
C     --- STATE ON RIGHT SIDE OF LEFT MOVING RAREFACTION WAVE
C
  130 R=RSTAR
      U=USTAR
      P=PSTAR
      GO TO 500
C
C     --- COMPUTE RIGHT SIDE OF THE RIEMANN PROBLEM
C
  200 IF(IREGR .EQ. 2) GO TO 220
C
C     --- COMPUTE SHOCK SPEED ON THE RIGHT SIDE
C
      U=UR+MR/RR
      X=U*DT
      IF(XI .GE. X) GO TO 210
C
C     --- STATE ON LEFT SIDE OF RIGHT MOVING SHOCK
C
```

```
      R=-MR/(USTAR-U)
      U=USTAR
      P=PSTAR
      GO TO 500
C
C     --- STATE ON RIGHT SIDE OF RIGHT MOVING SHOCK
C
  210 R=RR
      U=UR
      P=PR
      GO TO 500
C
C     --- COMPUTE CONSTANT A FOR ISENTROPIC LAW
C
  220 A=PR/(RR**GMA)
C
C     --- COMPUTE DENSITY AND SOUND SPEED IN STATE STAR
C
      RSTAR=(PSTAR/A)**(1./GMA)
      CSTAR=DSQRT(GMA*PSTAR/RSTAR)
      X=(USTAR+CSTAR)*DT
      IF(XI .GE. X) GO TO 230
C
C     --- STATE ON LEFT SIDE OF RIGHT MOVING RAREFACTION WAVE
C
      R=RSTAR
      U=USTAR
      P=PSTAR
      GO TO 500
C
C     --- COMPUTE SOUND SPEED ON RIGHT SIDE OF SHOCK FRONT
C
  230 CR=DSQRT(GMA*PR/RR)
      X=(UR+CR)*DT
      IF(XI .GE. X) GO TO 240
C
C     --- STATE INSIDE OF RAREFACTION WAVE MOVING TO THE RIGHT
C
      U=(2./(GMA+1.))*(XI/DT-CR+0.5*(GMA-1.)*UR)
      RINT=CR+0.5*(GMA-1.)*(U-UR)
      R=(RINT*RINT/(A*GMA))**(1./(GMA-1.))
      P=A*(R**GMA)
      GO TO 500

C
C     --- STATE ON RIGHT SIDE OF RIGHT MOVING RAREFACTION WAVE
C
  240 R=RR
      U=UR
      P=PR
  500 CONTINUE
      RETURN
      END
C     ------------------------------------------------------------
C                          FUNCTION PHI(X,GMA)
C                          -------------------
C
C     FUNCTION USED IN SUBROUTINE GLIMM
C
C     ------------------------------------------------------------
C
      IMPLICIT REAL*8 (A-H,O-Z)
      EPS=1.0E-6
      IF(ABS(1.-X) .GT. EPS) GO TO 100
      PHI=DSQRT(GMA)
      RETURN
  100 C1=0.5*(GMA+1.)
      C2=0.5*(GMA-1.)
      C3=C2/GMA
      IF(X .GE. 1.) GO TO 200
      PHI=C2*(1.-X)/(DSQRT(GMA)*(1.-(X**C3)))
      RETURN
  200 PHI=DSQRT(C1*X+C2)
      RETURN
      END
C     ------------------------------------------------------------
C
C     ------------------------------------------------------------
C
C                          SUBROUTINE BOUND
C                          ----------------
C
C     SUBROUTINE TO CALCULATE THE PISTON BOUNDARY CONDITIONS
C     (THIS SUBROUTINE IS USED TO CALCULATE THE FLOW AT THE
C      PISTON SURFACE.)
C
C     ------------------------------------------------------------
C
      IMPLICIT REAL*8 (A-H,O-Z)
      COMMON/BO/DT,RL,UL,PL,RR,UR,PR,R,U,P,XI,Y,GMA
C
      IF (UL.GE.UR) GO TO 10
C
C     --- CASE OF A PISTON MOTION PULLING THE GAS
C
      C1=(GMA-1.)/2./DSQRT(GMA)
      C2=2.*GMA/(GMA-1.)
      PL=PR*(1-C1*DSQRT(RR/PR)*(UR-UL))**C2




      RL=RR*(PL/PR)**(1./GMA)
      GO TO 20
C
C     --- CASE OF A PISTON MOTION PUSHING A GAS
C
   10 C1=(1.+GMA)/(GMA-1.)
      C2=(C1+1.)/(C1-1.)**2
      C3=(UL-UR)**2/GMA/(PR/RR)
      PL=1.+C3*C1*C2/2
      RL=1.-C3*C2
      PL=PR*(PL+DSQRT(PL**2-RL))
      RL=(C1*PL/PR+1.)/(C1+PL/PR)*RR
C
   20 CONTINUE
      RETURN
      END
C     ------------------------------------------------------------
C
```

```
C     ------------------------------------------------------------
C
C                       SUBROUTINE SPLINE (V1,GMA)
C                       --------------------------
C
C     SUBROUTINE FOR SPLINING NUMEROUS POINTS WITH A
C     SMOOTH CURVE.  (THIS PROGRAM WAS OBTAINED FROM
C     REF. A1.  THE MAJOR MODIFICATION INVOLVES THE
C     BOUNDARY CONDITIONS AT BOTH ENDS OF THE SPLINE.)
C
C     ------------------------------------------------------------
C
      IMPLICIT REAL*8 (A-H,O-Z)
      COMMON/CO/TP(18),XP(18),B(18),C(18),D(18),XO,DTB,NP,N
      NM1=NP-1
      NM2=NM1-1
      IF(NP.LT.2) RETURN
      IF(NP.LT.3) GO TO 50
      D(1)=TP(2)-TP(1)
      C(2)=(XP(2)-XP(1))/D(1)
C
C     --- SET UP THE TRIDIAGONAL MATRIX FOR CALCULATING
C         THE SPLINE COEFFICIENTS
C
      DO 10 I=2,NM1
         D(I)=TP(I+1)-TP(I)
         B(I)=2.D0*(D(I-1)+D(I))
         C(I+1)=(XP(I+1)-XP(I))/D(I)
         C(I)=C(I+1)-C(I)
   10 CONTINUE
C
C     --- BOUNDARY CONDITIONS (CONSTANT SLOPE AT ONE END
C         AND ZERO SECOND DERIVATIVE AT THE OTHER END OF
C         THE SPLINE FUNCTION)
C
      B(1)=2.D0*D(1)
      B(NP)=1.
      C(1)=0
      C(NP)=0
      IF(NP.EQ.3) GO TO 15
      C(1)=(XP(2)-XP(1))/D(1)-V1*N
      C(NP)=0.
C
C     --- FORWARD ELIMINATION FOR SOLVING MATRIX
C
   15 DO 20 I=2,NM1
         B(I)=-D(I-1)**2/B(I-1)+B(I)
         C(I)=-D(I-1)*C(I-1)/B(I-1)+C(I)
   20 CONTINUE
C
C     --- BACK SUBSTITUTION FOR SOLVING MATRIX
C
         C(NM1)=C(NM1)/B(NM1)
         DO 30 IB=1,NM2
           I=NM1-IB
           C(I)=(C(I)-D(I)*C(I+1))/B(I)
   30 CONTINUE
C
C     --- COMPUTE POLYNOMIAL COEFFICIENTS
C
      B(NP)=(XP(NP)-XP(NM1))/D(NM1)+D(NM1)*(C(NM1)+2.*C(NP))
      DO 40 I=1,NM1
         B(I)=(XP(I+1)-XP(I))/D(I)-D(I)*(C(I+1)+2.D0*C(I))
         D(I)=(C(I+1)-C(I))/D(I)
         C(I)=3.D0*C(I)
   40 CONTINUE
      C(NP)=0.
      D(NP)=0.
      RETURN
C
   50 B(1)=(XP(2)-XP(1))/(TP(2)-TP(1))
      C(1)=0.
      D(1)=0.
      B(2)=B(1)
      C(2)=0.
      D(2)=0.
      RETURN
      END
C     ------------------------------------------------------------
C
C     ------------------------------------------------------------
C
C                  SUBROUTINE SEVAL(TIME,NPIS,CNT,UL)
C                  ----------------------------------
C
C     SUBROUTINE THAT USES THE CUBIC SPLINE
C     FROM A KNOWLEDGE OF THE SPLINE COEFFICIENTS
C     (THIS SUBROUTINE WAS OBTAINED FROM REF. A2.)
C
C     ------------------------------------------------------------
C
      IMPLICIT REAL*8 (A-H,O-Z)
      COMMON/CO/TP(18),XP(18),B(18),C(18),D(18),XO,DTB,NP,N
      IF(TIME.GT.DTB) GO TO 42
      I=1
      IF(I.GE.NP) I=1
      IF(TIME.LT.TP(I)) GO TO 10
      IF(TIME.LE.TP(I+1)) GO TO 30
C
C     --- BINARY SEARCH
C
   10 I=1
      J=NP+1
   20 K=(I+J)/2
      IF(TIME.LT.TP(K)) J=K
      IF(TIME.GE.TP(K)) I=K
      IF(J.GT.I+1) GO TO 20
C
C     --- INTERPOLATION PART OF SPLINE PROGRAM
C
   30 DX=TIME-TP(I)
      CNT=XP(I)+DX*(B(I)+DX*(C(I)+DX*D(I)))
      NPIS=INT(CNT)+1
      UL=(B(I)+2.*C(I)*DX+3.*D(I)*DX**2)/N
      XO=CNT
      GO TO 50
   42 UL=.7
      CNT=UL*(TIME-DTB)*N+XO
      NPIS=INT(CNT)+1
   50 RETURN
      END
C     ------------------------------------------------------------
C
```

```
C     ------------------------------------------------------------
C
C              SUBROUTINE INH(DX,DT,ETA,GMA,NPIS,NRT,IC,NSS)
C              ---------------------------------------------
C
C     SUBROUTINE WHICH APPLIES THE OPERATING-SPLITTING TECHNIQUE
C     (THIS SUBROUTINE APPLIES THE OPERATOR-SPLITTING TECHNIQUE
C      TO OBTAIN THE REQUIRED CYLINDRICAL OR SPHERICAL SOLUTION
C      FROM THE INITIAL PLANAR SOLUTION.)
C
C     ------------------------------------------------------------
C
      IMPLICIT REAL*8 (A-H,O-Z)
      COMMON/AO/R1(1002),P1(1002),U1(1002)
      M=NPIS+1
      DO 100 I=M,NRT
      X=DX*(I-1)
      K=NSS
      IF(IC.NE.1) GO TO 10
      X=X-.5*DX
      K=NSS+1
   10 F=1.
      IF(I.EQ.K) F=.75
      R=R1(I)
      P=P1(I)
      U=U1(I)
      A=DT*U*(ETA-1.)/X*F
      D=R-A*R
      C=R*U-A*U*R
      E=P/(GMA-1.)+.5*R*U*U
      E=E-A*(E+P)
      R1(I)=D
      U1(I)=C/D
      A=C*C*.5/D
      P1(I)=(GMA-1.)*(E-A)
  100 CONTINUE
      RETURN
      END
```

APPENDIX B

RECONSTRUCTED BLAST-WAVE FLOW-FIELD PROPERTIES FOR TNT

Reconstructed blast-wave flow properties are presented in tabular form in this appendix for a 1-kg TNT surface explosion in a standard atmosphere for which p_0 = 101.33 kPa, T_0 = 288.15 K, and a_0 = 340.3 m/s. These reconstructed flow properties consist of thirty-three sets of time histories for the overpressure $(p - p_0)/p_0$, sound speed a/a_0, density ρ/ρ_0 and flow velocity u/a_0, each one at a different fixed radial distance from the explosion center. The particular radius r for each set of results is noted in the caption, along with the time of arrival t_a of the blast-wave front at this specific radius. These results cover in small steps the distance range from approximately 1 to 10 m, for which the peak blast-wave overpressure decays from about 1 to 0.01 MPa.

If the time histories are required for the flow properties of a TNT explosion of a charge size other than 1.0 kg of TNT in an atmosphere with a different pressure and temperature, then these tabulated results have to be scaled to apply to this new case. The procedure is demonstrated here by means of a simple example. Assume that the flow properties are required at a radius r of 31.3 m from a surface explosion of 1000 kg of TNT in an atmosphere in which p_1 = 95 kPa, T_1 = 310 kPa and a_1 = 353 m/s. The scaling factors for radius S_r and time S_t are (see page 17 of this report)

$$S_r = [(W/W_o)\ (p_0/p_1)]^{1/3}$$

$$= [(1000.0\ \text{kg}/1.000\ \text{kg})\ (101.33\ \text{kPa}/95.0\ \text{kPa})]^{1/3} = 10.2,$$

and

$$S_t = (a_0/a_1)\ S_r = (340.3\ \text{m/s}/353.0\ \text{m/s})\ 10.2 = 9.85.$$

The radius r of 31.3 m of interest for the example is now scaled for the case of a 1 kg TNT explosion. Hence, 31.3 m/S_r = 31.3 m/10.2 = 3.07 m. The scaled flow properties of interest are now given for this scaled radius of 3.07 m in table B-20. In order to get the required unscaled flow-field properties for the explosion of 1000 kg of TNT, the times listed in table B-20 are multiplied by S_t or 9.85. The nondimensional amplitudes of the various flow properties remain unchanged, of course, but the dimensional amplitudes depend on the new atmospheric conditions, as indicated by the subscript 1 in the table.

Table B-1. Time histories of overpressure, sound speed, density and flow velocity from the reconstructed blast-wave flow field by the RGM for a 1-kg TNT surface explosion in a standard atmosphere. These signatures are for the specific radius r = 1.486 m, at which the blast-wave front arrives at time t = 0.965 ms.

t (ms)	$\Delta p/p_1$	a/a_1	ρ/ρ_1	u/a_1	t (ms)	$\Delta p/p_1$	a/a_1	ρ/ρ_1	u/a_1
0.0000	5.5768	1.4308	3.2125	1.6631	0.3627	1.1390	1.3622	1.1528	0.7941
0.0070	5.3785	1.4290	3.1236	1.6392	0.3866	1.0597	1.3548	1.1221	0.7692
0.0275	4.9302	1.4214	2.9351	1.5865	0.4110	0.9803	1.3472	1.0910	0.7298
0.0480	4.3855	1.4137	2.6948	1.5099	0.4190	0.9590	1.3452	1.0826	0.7230
0.0553	4.1945	1.4064	2.6262	1.4802	0.4353	0.9414	1.3434	1.0757	0.7202
0.0692	4.0142	1.4004	2.5567	1.4579	0.4604	0.8749	1.3604	1.0131	0.6992
0.0904	3.6015	1.4043	2.3333	1.3914	0.4854	0.7992	1.3547	0.9804	0.6698
0.1116	3.2027	1.3862	2.1870	1.3193	0.5104	0.7564	1.3500	0.9637	0.6616
0.1332	2.8887	1.3994	1.9857	1.2599	0.5188	0.7427	1.3485	0.9584	0.6576
0.1401	2.7933	1.3945	1.9508	1.2409	0.5362	0.7274	1.3468	0.9523	0.6506
0.1547	2.6507	1.3947	1.8768	1.2141	0.5619	0.6908	1.3427	0.9379	0.6209
0.1770	2.3204	1.3901	1.7184	1.1307	0.5883	0.6697	1.3403	0.9295	0.6189
0.1992	2.0916	1.3759	1.6330	1.0759	0.6147	0.6243	1.3350	0.9114	0.6035
0.2218	1.8680	1.3769	1.5127	1.0171					
0.2448	1.7532	1.3689	1.4692	0.9771					
0.2601	1.6617	1.3623	1.4342	0.9533					
0.2677	1.5757	1.3559	1.4009	0.9299					
0.2910	1.5053	1.3597	1.3551	0.9165					
0.3147	1.3705	1.3590	1.2834	0.8730					
0.3387	1.2354	1.3477	1.2308	0.8287					

Table B-2. Time histories of overpressure, sound speed, density and flow velocity from the reconstructed blast-wave flow field by the RCM for a 1-kg TNT surface explosion in a standard atmosphere. These signatures are for the specific radius r = 1.529 m, at which the blast-wave front arrives at time t = 1.020 ms.

t (ms)	$\Delta p/p_1$	a/a_1	ρ/ρ_1	u/a_1	t (ms)	$\Delta p/p_1$	a/a_1	ρ/ρ_1	u/a_1
0.0000	5.1582	1.4055	3.1173	1.5882	0.3800	1.0857	1.3157	1.2049	0.7713
0.0139	4.8730	1.4018	2.9890	1.5544	0.4051	0.9802	1.3245	1.1287	0.7306
0.0351	4.4243	1.3963	2.7823	1.5020	0.4301	0.9173	1.3184	1.1030	0.7106
0.0563	3.9543	1.3853	2.5815	1.4313	0.4551	0.8640	1.3131	1.0810	0.6951
0.0779	3.5497	1.3800	2.3890	1.3657	0.4635	0.8461	1.3113	1.0736	0.6895
0.0848	3.3805	1.3726	2.3252	1.3343	0.4809	0.8093	1.3076	1.0582	0.6753
0.0994	3.1573	1.3634	2.2364	1.2948	0.5066	0.7543	1.3241	1.0006	0.6541
0.1217	2.8580	1.3590	2.0890	1.2337	0.5330	0.7176	1.3201	0.9856	0.6442
0.1440	2.6593	1.3591	1.9811	1.1989	0.5595	0.6624	1.3140	0.9628	0.6240
0.1666	2.3740	1.3509	1.8487	1.1364	0.5772	0.6510	1.3127	0.9581	0.6205
0.1895	2.1490	1.3377	1.7598	1.0861	0.5859	0.6453	1.3120	0.9558	0.6205
0.2048	1.9481	1.3451	1.6294	1.0326	0.6130	0.6138	1.3316	0.9102	0.5980
0.2124	1.8960	1.3493	1.5907	1.0202	0.6401	0.5713	1.3287	0.8900	0.5802
0.2357	1.7314	1.3381	1.5256	0.9780	0.6676	0.5335	1.3241	0.8747	0.5632
0.2594	1.6290	1.3444	1.4545	0.9483	0.6770	0.5212	1.3226	0.8697	0.5586
0.2834	1.4972	1.3346	1.4020	0.9123	0.6954	0.4925	1.3190	0.8579	0.5493
0.3074	1.3579	1.3253	1.3425	0.8531	0.7232	0.4627	1.3152	0.8457	0.5244
0.3314	1.2443	1.3295	1.2697	0.8182	0.7510	0.4265	1.3105	0.8306	0.5094
0.3557	1.1661	1.3228	1.2379	0.7933	0.7792	0.4069	1.3079	0.8225	0.4892
0.3637	1.1277	1.3194	1.2222	0.7802					

Table B-3. Time histories of overpressure, sound speed, density and flow velocity from the reconstructed blast-wave flow field by the RCM for a 1-kg TNT surface explosion in a standard atmosphere. These signatures are for the specific radius r = 1.600 m, at which the blast-wave front arrives at time t = 1.105 ms.

t (ms)	$\Delta p/p_1$	a/a_1	ρ/ρ_1	u/a_1	t (ms)	$\Delta p/p_1$	a/a_1	ρ/ρ_1	u/a_1
0.0000	4.7542	1.3806	3.0189	1.5128	0.6106	0.6402	1.2798	1.0014	0.5860
0.0146	4.4091	1.3748	2.8617	1.4645	0.6384	0.6077	1.2857	0.9726	0.5650
0.0369	4.0104	1.3647	2.6903	1.4081	0.6662	0.5646	1.2807	0.9539	0.5486
0.0591	3.6746	1.3512	2.5603	1.3586	0.6944	0.5257	1.2761	0.9369	0.5335
0.0817	3.2859	1.3459	2.3661	1.2922	0.7229	0.4978	1.2727	0.9247	0.5217
0.1047	2.9612	1.3349	2.2228	1.2331	0.7514	0.4674	1.2690	0.9112	0.4989
0.1200	2.8662	1.3371	2.1625	1.2206	0.7705	0.4322	1.2863	0.8656	0.4868
0.1276	2.7492	1.3312	2.1156	1.1966	0.7799	0.4203	1.2848	0.8605	0.4817
0.1509	2.5215	1.3243	2.0078	1.1526	0.8088	0.3899	1.2808	0.8473	0.4695
0.1745	2.2948	1.3178	1.8973	1.0989	0.8380	0.3555	1.2762	0.8323	0.4520
0.1985	1.9894	1.2996	1.7699	1.0219	0.8574	0.3373	1.2737	0.8243	0.4414
0.2225	1.8108	1.2893	1.6910	0.9781	0.8672	0.3346	1.2734	0.8231	0.4318
0.2465	1.6747	1.2897	1.6081	0.9451	0.8964	0.3100	1.2700	0.8122	0.4217
0.2709	1.5468	1.2905	1.5293	0.9122	0.9263	0.2785	1.2880	0.7707	0.4076
0.2789	1.4709	1.2849	1.4966	0.8883	0.9558	0.2614	1.2855	0.7634	0.3998
0.2952	1.4574	1.2839	1.4908	0.8779	0.9861	0.2290	1.2829	0.7468	0.3848
0.3202	1.3007	1.2983	1.3650	0.8290	1.0163	0.2124	1.2804	0.7395	0.3769
0.3453	1.1721	1.2950	1.2953	0.7868	1.0469	0.1960	1.2779	0.7324	0.3690
0.3703	1.1163	1.2902	1.2714	0.7708	1.0779	0.1736	1.2744	0.7226	0.3548
0.3787	1.0791	1.2869	1.2554	0.7580	1.1088	0.1559	1.2717	0.7148	0.3516
0.3960	1.0456	1.2839	1.2409	0.7463	1.1401	0.1447	1.2699	0.7098	0.3386
0.4218	0.9529	1.2885	1.1763	0.7021	1.1714	0.1370	1.2687	0.7064	0.3335
0.4482	0.8957	1.2831	1.1515	0.6847	1.1926	0.1343	1.2683	0.7052	0.3261
0.4746	0.8424	1.2794	1.1256	0.6656	1.2031	0.1320	1.2679	0.7042	0.3261
0.4924	0.7969	1.2748	1.1057	0.6456	1.2351	0.1178	1.2656	0.6979	0.3197
0.5010	0.7908	1.2742	1.1030	0.6456	1.2670	0.1184	1.2657	0.6982	0.3131
0.5282	0.7444	1.2825	1.0606	0.6209					
0.5553	0.7086	1.2787	1.0450	0.6111					
0.5828	0.6800	1.2842	1.0187	0.6021					
0.5921	0.6519	1.2811	1.0065	0.5896					

Table B-4. Time histories of overpressure, sound speed, density and flow velocity from the reconstructed blast-wave flow field by the RCM for a 1-kg TNT surface explosion in a standard atmosphere. These signatures are for the specific radius r = 1.629 m, at which the blast-wave front arrives at time t = 1.142 ms.

t (ms)	$\Delta p/p_1$	a/a_1	ρ/ρ_1	u/a_1	t (ms)	$\Delta p/p_1$	a/a_1	ρ/ρ_1	u/a_1
0.0000	4.5289	1.3668	2.9595	1.4692	0.7430	0.4752	1.2700	0.9147	0.5009
0.0223	4.1556	1.3591	2.7911	1.4188	0.7719	0.4414	1.2658	0.8997	0.4898
0.0449	3.7725	1.3512	2.6139	1.3616	0.8011	0.4086	1.2616	0.8850	0.4744
0.0678	3.4237	1.3406	2.4614	1.3057	0.8206	0.3841	1.2585	0.8740	0.4613
0.0831	3.1667	1.3292	2.3583	1.2594	0.8303	0.3763	1.2574	0.8704	0.4563
0.0908	3.0478	1.3291	2.2913	1.2373	0.8595	0.3400	1.2526	0.8540	0.4393
0.1140	2.8458	1.3252	2.1899	1.2045	0.8894	0.3112	1.2702	0.8127	0.4286
0.1377	2.6455	1.3192	2.0948	1.1561	0.9190	0.2870	1.2668	0.8020	0.4164
0.1617	2.3617	1.3106	1.9570	1.0947	0.9492	0.2579	1.2627	0.7890	0.4029
0.1857	2.0949	1.3001	1.8309	1.0316	0.9795	0.2393	1.2600	0.7807	0.3961
0.2097	1.9192	1.2952	1.7402	0.9905	1.0101	0.2202	1.2572	0.7721	0.3787
0.2340	1.7512	1.2843	1.6680	0.9485	1.0410	0.2011	1.2544	0.7634	0.3686
0.2420	1.6776	1.2793	1.6360	0.9277	1.0720	0.1812	1.2514	0.7543	0.3477
0.2583	1.6309	1.2761	1.6156	0.9157	1.1033	0.1691	1.2716	0.7230	0.3421
0.2834	1.4687	1.2750	1.5187	0.8696	1.1346	0.1581	1.2699	0.7182	0.3383
0.3084	1.3409	1.2750	1.4400	0.8325	1.1558	0.1497	1.2686	0.7144	0.3253
0.3335	1.2344	1.2666	1.3928	0.7968	1.1662	0.1474	1.2682	0.7134	0.3253
0.3418	1.1893	1.2629	1.3727	0.7819	1.1982	0.1337	1.2682	0.7049	0.3208
0.3592	1.1650	1.2609	1.3618	0.7685	1.2302	0.1252	1.2668	0.7012	0.3209
0.3849	1.0805	1.2608	1.3089	0.7399	1.2625	0.1075	1.2639	0.6933	0.3152
0.4113	1.0117	1.2736	1.2402	0.7197	1.2952	0.0973	1.2623	0.6887	0.3097
0.4378	0.9126	1.2716	1.1828	0.6799	1.3168	0.0919	1.2614	0.6863	0.3001
0.4555	0.8928	1.2697	1.1740	0.6657	1.3279	0.0837	1.2600	0.6826	0.2936
0.4642	0.8863	1.2691	1.1711	0.6657	1.3606	0.0742	1.2584	0.6783	0.2882
0.4913	0.8239	1.2760	1.1202	0.6450	1.3936	0.0666	1.2571	0.6749	0.2769
0.5184	0.7602	1.2695	1.0921	0.6218	1.4266	0.0596	1.2560	0.6717	0.2761
0.5459	0.7273	1.2676	1.0750	0.6118	1.4604	0.0432	1.2532	0.6643	0.2654
0.5553	0.7108	1.2659	1.0676	0.6060	1.4937	0.0420	1.2530	0.6637	0.2563
0.5737	0.6873	1.2634	1.0571	0.5962	1.5049	0.0374	1.2522	0.6617	0.2538
0.6015	0.6469	1.2590	1.0390	0.5711	1.5275	0.0231	1.2497	0.6551	0.2488
0.6293	0.6271	1.2698	1.0091	0.5686					
0.6575	0.5900	1.2656	0.9926	0.5582					
0.6860	0.5506	1.2611	0.9750	0.5403					
0.7145	0.5129	1.2651	0.9452	0.5160					
0.7337	0.4872	1.2714	0.9200	0.5057					

Table B-5. Time histories of overpressure, sound speed, density and flow velocity from the reconstructed blast-wave flow field by the RCM for a 1-kg TNT surface explosion in a standard atmosphere. These signatures are for the specific radius r = 1.686 m, at which the blast-wave front arrives at time t = 1.225 ms.

t (ms)	$\Delta p/p_1$	a/a_1	ρ/ρ_1	u/a_1	t (ms)	$\Delta p/p_1$	a/a_1	ρ/ρ_1	u/a_1
0.0000	4.1067	1.3395	2.8461	1.3845	1.1794	0.1481	1.2253	0.7647	0.3209
0.0076	3.9226	1.3368	2.7548	1.3551	1.2121	0.1324	1.2229	0.7572	0.3118
0.0309	3.5972	1.3266	2.6121	1.3067	1.2337	0.1311	1.2227	0.7566	0.3039
0.0546	3.3683	1.3216	2.5011	1.2684	1.2448	0.1253	1.2218	0.7538	0.3050
0.0786	3.0011	1.3107	2.3289	1.2014	1.2775	0.1139	1.2200	0.7484	0.3011
0.1026	2.8036	1.3081	2.2228	1.1690	1.3105	0.0985	1.2384	0.7162	0.2936
0.1266	2.5250	1.2978	2.0929	1.1126	1.3435	0.0867	1.2365	0.7107	0.2879
0.1509	2.2579	1.2885	1.9622	1.0536	1.3773	0.0725	1.2342	0.7041	0.2752
0.1589	2.1571	1.2828	1.9186	1.0291	1.4106	0.0632	1.2327	0.6997	0.2705
0.1752	2.0708	1.2777	1.8811	0.9997	1.4218	0.0594	1.2320	0.6979	0.2674
0.2003	1.8982	1.2766	1.7783	0.9594	1.4444	0.0588	1.2319	0.6976	0.2680
0.2253	1.7333	1.2725	1.6881	0.9180	1.4784	0.0427	1.2293	0.6900	0.2573
0.2503	1.6068	1.2639	1.6319	0.8888	1.5125	0.0322	1.2275	0.6851	0.2515
0.2587	1.5530	1.2601	1.6078	0.8738	1.5466	0.0174	1.2250	0.6780	0.2410
0.2761	1.4531	1.2577	1.5509	0.8418	1.5807	0.0110	1.2238	0.6750	0.2285
0.3018	1.3731	1.2517	1.5147	0.8186	1.6151	0.0067	1.2231	0.6729	0.2176
0.3282	1.2669	1.2492	1.4526	0.7884	1.6502	-0.0067	1.2423	0.6435	0.2067
0.3547	1.1411	1.2391	1.3946	0.7477	1.6850	-0.0209	1.2398	0.6370	0.1981
0.3724	1.1037	1.2360	1.3771	0.7282	1.7201	-0.0281	1.2406	0.6316	0.1927
0.3811	1.0960	1.2353	1.3735	0.7282	1.7552	-0.0334	1.2396	0.6291	0.1897
0.4082	0.9983	1.2279	1.3253	0.6966	1.7907	-0.0371	1.2389	0.6273	0.1801
0.4353	0.9188	1.2299	1.2685	0.6702	1.8262	-0.0498	1.2365	0.6214	0.1700
0.4628	0.8661	1.2344	1.2247	0.6521	1.8620	-0.0592	1.2348	0.6170	0.1639
0.4722	0.8551	1.2333	1.2196	0.6499	1.8978	-0.0690	1.2330	0.6124	0.1594
0.4906	0.8142	1.2294	1.2003	0.6334	1.9339	-0.0796	1.2310	0.6075	0.1479
0.5184	0.7433	1.2224	1.1666	0.6042	1.9705	-0.0882	1.2293	0.6034	0.1433
0.5462	0.7093	1.2258	1.1375	0.5953	2.0066	-0.0939	1.2282	0.6007	0.1315
0.5744	0.6744	1.2407	1.0878	0.5860	2.0435	-0.1044	1.2261	0.5957	0.1240
0.6029	0.6472	1.2378	1.0751	0.5772	2.0800	-0.1112	1.2248	0.5925	0.1221
0.6314	0.6093	1.2406	1.0455	0.5611	2.1168	-0.1219	1.2227	0.5874	0.1168
0.6506	0.5776	1.2371	1.0308	0.5488	2.1540	-0.1277	1.2215	0.5846	0.1130
0.6599	0.5683	1.2361	1.0265	0.5462	2.1909	-0.1342	1.2202	0.5815	0.1042
0.6888	0.5246	1.2437	0.9856	0.5318	2.2284	-0.1424	1.2186	0.5776	0.0970
0.7180	0.4953	1.2403	0.9720	0.5126	2.2660	-0.1451	1.2180	0.5762	0.0933
0.7375	0.4724	1.2376	0.9614	0.5014	2.3036	-0.1473	1.2176	0.5752	0.0902
0.7472	0.4635	1.2365	0.9572	0.4951	2.3411	-0.1513	1.2168	0.5732	0.0887
0.7764	0.4325	1.2342	0.9405	0.4834	2.3794	-0.1634	1.2143	0.5674	0.0851
0.8063	0.3999	1.2301	0.9251	0.4588	2.4173	-0.1673	1.2134	0.5655	0.0753
0.8359	0.3700	1.2263	0.9110	0.4474	2.4555	-0.1670	1.2135	0.5657	0.0739
0.8661	0.3308	1.2338	0.8742	0.4256	2.4934	-0.1651	1.2139	0.5666	0.0693
0.8964	0.3173	1.2320	0.8679	0.4132	2.5191	-0.1680	1.2133	0.5652	0.0665
0.9270	0.2900	1.2284	0.8550	0.4033	2.5320	-0.1703	1.2128	0.5640	0.0651
0.9579	0.2619	1.2245	0.8416	0.3878	2.5706	-0.1736	1.2121	0.5625	0.0608
0.9889	0.2372	1.2293	0.8187	0.3793	2.6095	-0.1766	1.2115	0.5610	0.0565
1.0202	0.2116	1.2347	0.7947	0.3674	2.6485	-0.1780	1.2112	0.5603	0.0521
1.0515	0.2019	1.2333	0.7902	0.3552	2.6878	-0.1838	1.2100	0.5575	0.0477
1.0727	0.1887	1.2314	0.7840	0.3475	2.7271	-0.1850	1.2097	0.5569	0.0433
1.0831	0.1863	1.2310	0.7828	0.3475	2.7664	-0.1891	1.2089	0.5549	0.0394
1.1151	0.1710	1.2287	0.7756	0.3289	2.8056	-0.1940	1.2078	0.5525	0.0358
1.1471	0.1580	1.2268	0.7694	0.3247	2.8453	-0.1985	1.2069	0.5503	0.0327

Table B-6. Time histories of overpressure, sound speed, density and flow velocity from the reconstructed blast-wave flow field by the RCM for a 1-kg TNT surface explosion in a standard atmosphere. These signatures are for the specific radius r = 1.714 m, at which the blast-wave front arrives at time t = 1.256 ms.

t (ms)	$\Delta p/p_1$	a/a_1	ρ/ρ_1	u/a_1	t (ms)	$\Delta p/p_1$	a/a_1	ρ/ρ_1	u/a_1
0.0000	3.9118	1.3268	2.7900	1.3438	1.2027	0.1350	1.2142	0.7698	0.3107
0.0236	3.6755	1.3270	2.6553	1.3137	1.2138	0.1308	1.2136	0.7678	0.3081
0.0476	3.3378	1.3128	2.5169	1.2591	1.2465	0.1208	1.2211	0.7517	0.3053
0.0716	2.9745	1.3038	2.3379	1.1926	1.2796	0.1121	1.2197	0.7475	0.2976
0.0956	2.7790	1.3001	2.2358	1.1604	1.3126	0.1005	1.2179	0.7419	0.2914
0.1200	2.5034	1.2928	2.0961	1.1043	1.3463	0.0877	1.2159	0.7358	0.2825
0.1280	2.4492	1.2900	2.0729	1.0945	1.3797	0.0715	1.2133	0.7279	0.2724
0.1443	2.2992	1.2818	2.0081	1.0572	1.3908	0.0687	1.2126	0.7265	0.2723
0.1693	2.0414	1.2707	1.8835	0.9958	1.4134	0.0635	1.2120	0.7241	0.2690
0.1944	1.8709	1.2654	1.7928	0.9558	1.4475	0.0565	1.2108	0.7206	0.2655
0.2194	1.7593	1.2638	1.7277	0.9210	1.4816	0.0461	1.2091	0.7156	0.2502
0.2277	1.7121	1.2607	1.7065	0.9094	1.5157	0.0333	1.2277	0.6856	0.2411
0.2451	1.6011	1.2571	1.6461	0.8794	1.5497	0.0294	1.2270	0.6838	0.2317
0.2709	1.4481	1.2526	1.5604	0.8326	1.5841	0.0167	1.2248	0.6777	0.2239
0.2973	1.3841	1.2478	1.5311	0.8198	1.6193	0.0053	1.2229	0.6722	0.2152
0.3237	1.2575	1.2428	1.4616	0.7817	1.6540	-0.0088	1.2204	0.6655	0.2050
0.3414	1.1643	1.2353	1.4182	0.7479	1.7243	-0.0238	1.2177	0.6583	0.1889
0.3501	1.1563	1.2347	1.4144	0.7479	1.7952	-0.0371	1.2154	0.6519	0.1820
0.3773	1.0831	1.2342	1.3675	0.7240	1.8668	-0.0588	1.2114	0.6414	0.1667
0.4044	1.0107	1.2280	1.3333	0.7023	1.9395	-0.0756	1.2083	0.6332	0.1469
0.4319	0.9482	1.2225	1.3036	0.6865	2.0125	-0.0978	1.2254	0.6008	0.1329
0.4412	0.8990	1.2180	1.2800	0.6672	2.0859	-0.1136	1.2243	0.5913	0.1261
0.4597	0.8536	1.2138	1.2581	0.6491	2.1600	-0.1245	1.2222	0.5861	0.1116
0.4875	0.8022	1.2099	1.2311	0.6306	2.2351	-0.1409	1.2189	0.5783	0.0967
0.5153	0.7493	1.2137	1.1874	0.6132	2.3102	-0.1517	1.2167	0.5731	0.0955
0.5435	0.7052	1.2186	1.1483	0.5980	2.3863	-0.1539	1.2162	0.5720	0.0792
0.5720	0.6793	1.2159	1.1359	0.5832	2.4625	-0.1638	1.2142	0.5672	0.0707
0.6005	0.6448	1.2123	1.1192	0.5704	2.5011	-0.1647	1.2140	0.5667	0.0677
0.6196	0.6066	1.2150	1.0883	0.5552	2.5786	-0.1728	1.2123	0.5629	0.0566
0.6290	0.6038	1.2147	1.0869	0.5562	2.6568	-0.1770	1.2114	0.5608	0.0500
0.6579	0.5706	1.2294	1.0392	0.5423	2.7354	-0.1870	1.2093	0.5559	0.0425
0.6871	0.5535	1.2274	1.0311	0.5314	2.8143	-0.1925	1.2081	0.5532	0.0335
0.7065	0.5192	1.2305	1.0034	0.5142	2.8936	-0.1960	1.2074	0.5515	0.0257
0.7163	0.4969	1.2279	0.9929	0.5043	2.9736	-0.1950	1.2076	0.5520	0.0237
0.7455	0.4680	1.2245	0.9791	0.4944	3.0536	-0.1966	1.2073	0.5512	0.0233
0.7754	0.4401	1.2336	0.9463	0.4718	3.1342	-0.1945	1.2077	0.5522	0.0225
0.8049	0.4050	1.2293	0.9298	0.4588	3.2152	-0.1963	1.2073	0.5514	0.0229
0.8352	0.3699	1.2249	0.9131	0.4410	3.2970	-0.1983	1.2069	0.5504	0.0237
0.8654	0.3350	1.2203	0.8964	0.4256	3.3794	-0.1975	1.2071	0.5508	0.0190
0.8960	0.3107	1.2186	0.8826	0.4176	3.4207	-0.1977	1.2070	0.5507	0.0189
0.9270	0.2802	1.2145	0.8679	0.4038	3.5038	-0.1918	1.2083	0.5536	0.0235
0.9579	0.2588	1.2116	0.8575	0.3841	3.5876	-0.1913	1.2084	0.5538	0.0193
0.9892	0.2423	1.2218	0.8323	0.3767	3.6718	-0.1870	1.2093	0.5559	0.0216
1.0205	0.2337	1.2205	0.8281	0.3638	3.7566	-0.1844	1.2099	0.5572	0.0191
1.0417	0.2127	1.2176	0.8180	0.3527	3.8418	-0.1783	1.2111	0.5602	0.0217
1.0522	0.2101	1.2172	0.8168	0.3527	3.9273	-0.1751	1.2118	0.5617	0.0224
1.0841	0.1884	1.2141	0.8063	0.3406	3.9701	-0.1743	1.2120	0.5621	0.0219
1.1161	0.1693	1.2112	0.7970	0.3296	4.0563	-0.1698	1.2129	0.5643	0.0230
1.1485	0.1605	1.2181	0.7821	0.3219	4.1426	-0.1717	1.2125	0.5634	0.0201
1.1812	0.1507	1.2166	0.7774	0.3175					

Table B-7. Time histories of overpressure, sound speed, density and flow velocity from the reconstructed blast-wave flow field by the RCM for a 1-kg TNT surface explosion in a standard atmosphere. These signatures are for the specific radius r = 1.807 m, at which the blast-wave front arrives at time t = 1.384 ms.

t (ms)	$\Delta p/p_1$	a/a_1	ρ/ρ_1	u/a_1	t (ms)	$\Delta p/p_1$	a/a_1	ρ/ρ_1	u/a_1
0.0000	3.5698	1.3042	2.6867	1.2696	1.2517	0.1332	1.1734	0.8231	0.2876
0.0163	3.3786	1.2984	2.5973	1.2399	1.2629	0.1301	1.1729	0.8215	0.2842
0.0414	3.0008	1.2847	2.4241	1.1711	1.2855	0.1300	1.1795	0.8122	0.2799
0.0664	2.7414	1.2729	2.3090	1.1236	1.3195	0.1214	1.1782	0.8078	0.2760
0.0914	2.5759	1.2730	2.2067	1.0960	1.3536	0.1048	1.1757	0.7992	0.2663
0.0998	2.4922	1.2687	2.1696	1.0789	1.3877	0.0939	1.1741	0.7936	0.2621
0.1172	2.3666	1.2661	2.1001	1.0544	1.4218	0.0776	1.1715	0.7851	0.2543
0.1429	2.1323	1.2531	1.9947	0.9971	1.4562	0.0706	1.1704	0.7815	0.2477
0.1693	1.9606	1.2458	1.9076	0.9589	1.4913	0.0579	1.1685	0.7749	0.2415
0.1958	1.7969	1.2400	1.8190	0.9201	1.5261	0.0473	1.1668	0.7693	0.2345
0.2135	1.7011	1.2338	1.7744	0.8865	1.5612	0.0386	1.1773	0.7492	0.2228
0.2222	1.6899	1.2331	1.7691	0.8865	1.5963	0.0326	1.1764	0.7462	0.2242
0.2493	1.5377	1.2282	1.6824	0.8462	1.6318	0.0111	1.1729	0.7351	0.2111
0.2764	1.3863	1.2231	1.5951	0.8027	1.6673	0.0017	1.1713	0.7301	0.2068
0.3039	1.3294	1.2196	1.5661	0.7884	1.7031	-0.0048	1.1702	0.7268	0.1999
0.3133	1.2998	1.2174	1.5518	0.7806	1.7389	-0.0163	1.1683	0.7208	0.1920
0.3317	1.2077	1.2139	1.4983	0.7515	1.8115	-0.0339	1.1652	0.7115	0.1763
0.3595	1.0924	1.2046	1.4420	0.7107	1.8846	-0.0496	1.1639	0.7016	0.1705
0.3873	1.0376	1.2049	1.4034	0.6968	1.9579	-0.0723	1.1599	0.6896	0.1519
0.4155	0.9876	1.2059	1.3668	0.6755	2.0320	-0.0838	1.1578	0.6835	0.1347
0.4440	0.9391	1.2017	1.3429	0.6599	2.1071	-0.1023	1.1664	0.6599	0.1189
0.4725	0.8466	1.1970	1.2888	0.6229	2.1822	-0.1104	1.1648	0.6556	0.1109
0.4917	0.8171	1.2003	1.2611	0.6144	2.2584	-0.1258	1.1619	0.6475	0.0973
0.5010	0.7993	1.1987	1.2523	0.6086	2.3345	-0.1375	1.1597	0.6413	0.0841
0.5299	0.7640	1.1953	1.2347	0.5896	2.3731	-0.1435	1.1586	0.6381	0.0809
0.5591	0.7077	1.1897	1.2064	0.5669	2.4506	-0.1493	1.1574	0.6350	0.0707
0.5786	0.6804	1.1915	1.1837	0.5581	2.5289	-0.1567	1.1560	0.6311	0.0602
0.5883	0.6677	1.1902	1.1773	0.5511	2.6075	-0.1596	1.1554	0.6295	0.0558
0.6175	0.6380	1.1871	1.1623	0.5432	2.6864	-0.1685	1.1614	0.6164	0.0487
0.6474	0.5992	1.1885	1.1322	0.5201	2.7657	-0.1751	1.1601	0.6129	0.0403
0.6770	0.5787	1.1863	1.1218	0.5186	2.8456	-0.1841	1.1583	0.6081	0.0328
0.7072	0.5415	1.1823	1.1028	0.5025	2.9256	-0.1918	1.1567	0.6040	0.0275
0.7375	0.5010	1.1778	1.0821	0.4877	3.0063	-0.1949	1.1561	0.6024	0.0195
0.7681	0.4662	1.1738	1.0641	0.4726	3.0873	-0.1919	1.1567	0.6040	0.0181
0.7990	0.4307	1.1697	1.0456	0.4583	3.1690	-0.1932	1.1564	0.6033	0.0163
0.8300	0.3938	1.1663	1.0247	0.4340	3.2514	-0.1904	1.1570	0.6048	0.0148
0.8613	0.3650	1.1628	1.0095	0.4224	3.2928	-0.1911	1.1569	0.6044	0.0150
0.8926	0.3455	1.1604	0.9992	0.4121	3.3759	-0.1902	1.1571	0.6048	0.0125
0.9138	0.3160	1.1568	0.9835	0.3954	3.4597	-0.1893	1.1572	0.6054	0.0093
0.9242	0.3131	1.1564	0.9819	0.3954	3.5438	-0.1849	1.1581	0.6077	0.0104
0.9562	0.2868	1.1531	0.9678	0.3844	3.6287	-0.1807	1.1590	0.6100	0.0100
0.9882	0.2645	1.1676	0.9275	0.3728	3.7139	-0.1801	1.1591	0.6103	0.0111
1.0205	0.2501	1.1657	0.9200	0.3573	3.7994	-0.1781	1.1595	0.6113	0.0118
1.0532	0.2345	1.1636	0.9118	0.3500	3.8422	-0.1786	1.1594	0.6111	0.0112
1.0748	0.2220	1.1619	0.9051	0.3421	3.9284	-0.1766	1.1598	0.6121	0.0158
1.0859	0.2132	1.1607	0.9005	0.3298	4.0146	-0.1712	1.1609	0.6150	0.0165
1.1186	0.1967	1.1584	0.8917	0.3231	4.1015	-0.1705	1.1610	0.6153	0.0162
1.1516	0.1793	1.1625	0.8726	0.3123	4.1669	-0.1660	1.1619	0.6177	0.0167
1.1846	0.1600	1.1598	0.8624	0.3030	4.2326	-0.1657	1.1620	0.6179	0.0123
1.2184	0.1481	1.1755	0.8308	0.2959					

Table B-8. Time histories of overpressure, sound speed, density and flow velocity from the reconstructed blast-wave flow field by the RCM for a 1-kg TNT surface explosion in a standard atmosphere. These signatures are for the specific radius r = 1.871 m, at which the blast-wave front arrives at time t = 1.483 ms.

t (ms)	$\Delta p/p_1$	a/a_1	ρ/ρ_1	u/a_1	t (ms)	$\Delta p/p_1$	a/a_1	ρ/ρ_1	u/a_1
0.0000	3.1953	1.2788	2.5654	1.1842	1.2879	0.1285	1.1316	0.8812	0.2748
0.0174	2.9560	1.2720	2.4452	1.1398	1.3220	0.1185	1.1302	0.8756	0.2722
0.0431	2.7124	1.2626	2.3287	1.0905	1.3564	0.1089	1.1288	0.8703	0.2693
0.0695	2.5993	1.2604	2.2655	1.0758	1.3915	0.0954	1.1268	0.8627	0.2578
0.0960	2.3789	1.2535	2.1503	1.0318	1.4263	0.0821	1.1249	0.8552	0.2501
0.1137	2.2128	1.2450	2.0726	0.9843	1.4614	0.0682	1.1228	0.8473	0.2397
0.1224	2.1502	1.2415	2.0437	0.9707	1.4965	0.0612	1.1217	0.8433	0.2361
0.1495	1.9552	1.2339	1.9410	0.9258	1.5320	0.0540	1.1207	0.8393	0.2329
0.1766	1.7941	1.2289	1.8502	0.8875	1.5675	0.0414	1.1357	0.8074	0.2254
0.2041	1.6879	1.2260	1.7882	0.8649	1.6033	0.0257	1.1332	0.7987	0.2197
0.2135	1.6613	1.2243	1.7755	0.8598	1.6391	0.0208	1.1324	0.7960	0.2201
0.2319	1.5504	1.2169	1.7224	0.8296	1.6752	0.0057	1.1300	0.7876	0.2027
0.2597	1.4386	1.2091	1.6681	0.7973	1.7118	0.0019	1.1294	0.7855	0.1942
0.2876	1.3416	1.2047	1.6134	0.7720	1.7479	-0.0054	1.1282	0.7813	0.1884
0.3157	1.2384	1.1970	1.5623	0.7398	1.7848	-0.0184	1.1261	0.7741	0.1806
0.3442	1.1807	1.1925	1.5334	0.7252	1.8581	-0.0356	1.1296	0.7558	0.1672
0.3727	1.0641	1.1873	1.4642	0.6872	1.9322	-0.0461	1.1278	0.7499	0.1571
0.3919	1.0177	1.1886	1.4283	0.6735	2.0073	-0.0676	1.1411	0.7161	0.1385
0.4013	0.9840	1.1857	1.4112	0.6620	2.0824	-0.0843	1.1382	0.7069	0.1268
0.4301	0.9512	1.1884	1.3815	0.6493	2.1586	-0.1008	1.1416	0.6899	0.1101
0.4593	0.8590	1.1802	1.3346	0.6135	2.2347	-0.1076	1.1404	0.6862	0.1014
0.4788	0.8209	1.1774	1.3135	0.6011	2.2733	-0.1165	1.1388	0.6813	0.0919
0.4885	0.8105	1.1765	1.3081	0.5963	2.3508	-0.1277	1.1367	0.6751	0.0805
0.5177	0.7774	1.1768	1.2834	0.5884	2.4291	-0.1376	1.1348	0.6696	0.0703
0.5476	0.7126	1.1706	1.2498	0.5619	2.5077	-0.1466	1.1331	0.6646	0.0637
0.5772	0.6728	1.1667	1.2289	0.5467	2.5866	-0.1568	1.1312	0.6589	0.0565
0.6074	0.6350	1.1676	1.1992	0.5318	2.6659	-0.1615	1.1303	0.6563	0.0540
0.6377	0.6102	1.1702	1.1760	0.5230	2.7458	-0.1687	1.1289	0.6523	0.0426
0.6683	0.5781	1.1704	1.1520	0.5041	2.8258	-0.1729	1.1281	0.6500	0.0354
0.6992	0.5475	1.1672	1.1360	0.4920	2.9065	-0.1802	1.1267	0.6458	0.0268
0.7302	0.5067	1.1627	1.1145	0.4730	2.9875	-0.1859	1.1255	0.6426	0.0199
0.7615	0.4713	1.1647	1.0846	0.4594	3.0692	-0.1913	1.1245	0.6396	0.0148
0.7928	0.4532	1.1626	1.0751	0.4448	3.1516	-0.1873	1.1253	0.6418	0.0124
0.8140	0.4324	1.1602	1.0641	0.4351	3.1930	-0.1869	1.1253	0.6421	0.0122
0.8244	0.4291	1.1598	1.0623	0.4351	3.2761	-0.1848	1.1257	0.6432	0.0098
0.8564	0.3863	1.1592	1.0318	0.4152	3.3599	-0.1835	1.1260	0.6440	0.0066
0.8884	0.3567	1.1556	1.0160	0.4048	3.4440	-0.1845	1.1258	0.6434	0.0061
0.9207	0.3407	1.1589	0.9982	0.3930	3.5289	-0.1849	1.1257	0.6432	0.0044
0.9534	0.3098	1.1551	0.9817	0.3762	3.6141	-0.1827	1.1262	0.6444	0.0076
0.9750	0.2986	1.1536	0.9758	0.3656	3.6996	-0.1810	1.1265	0.6454	0.0096
0.9861	0.2915	1.1527	0.9719	0.3608	3.7424	-0.1806	1.1266	0.6456	0.0063
1.0188	0.2679	1.1497	0.9592	0.3506	3.8286	-0.1778	1.1271	0.6472	0.0081
1.0518	0.2424	1.1464	0.9454	0.3368	3.9148	-0.1752	1.1276	0.6487	0.0071
1.0848	0.2254	1.1441	0.9361	0.3305	4.0018	-0.1684	1.1290	0.6525	0.0090
1.1186	0.2021	1.1410	0.9234	0.3144	4.0671	-0.1673	1.1292	0.6531	0.0118
1.1520	0.1855	1.1387	0.9143	0.3086	4.1328	-0.1675	1.1291	0.6530	0.0121
1.1631	0.1784	1.1377	0.9104	0.3033	4.1982	-0.1632	1.1300	0.6554	0.0115
1.1857	0.1707	1.1367	0.9061	0.3008	4.2639	-0.1632	1.1300	0.6554	0.0113
1.2198	0.1536	1.1343	0.8966	0.2907					
1.2538	0.1457	1.1332	0.8922	0.2810					

Table B-9. Time histories of overpressure, sound speed, density and flow velocity from the reconstructed blast-wave flow field by the RCM for a 1-kg TNT surface explosion in a standard atmosphere. These signatures are for the specific radius r = 1.943 m, at which the blast-wave front arrives at time t = 1.597 ms.

t (ms)	$\Delta p/p_1$	a/a_1	ρ/ρ_1	u/a_1	t (ms)	$\Delta p/p_1$	a/a_1	ρ/ρ_1	u/a_1
0.0000	2.8980	1.2583	2.4619	1.1125	1.3477	0.1182	1.1241	0.8849	0.2592
0.0087	2.7785	1.2527	2.4078	1.0883	1.3828	0.1104	1.1230	0.8805	0.2555
0.0358	2.5983	1.2447	2.3227	1.0572	1.4183	0.0989	1.1213	0.8740	0.2491
0.0629	2.4615	1.2402	2.2504	1.0352	1.4538	0.0864	1.1195	0.8669	0.2452
0.0904	2.2815	1.2308	2.1662	0.9904	1.4896	0.0781	1.1183	0.8621	0.2358
0.0998	2.1552	1.2239	2.1063	0.9597	1.5254	0.0635	1.1161	0.8538	0.2265
0.1182	2.0768	1.2234	2.0558	0.9453	1.5615	0.0559	1.1200	0.8417	0.2205
0.1460	1.8954	1.2165	1.9566	0.8995	1.5981	0.0511	1.1193	0.8390	0.2188
0.1739	1.7599	1.2102	1.8843	0.8684	1.6342	0.0391	1.1175	0.8321	0.2114
0.2020	1.6449	1.2082	1.8120	0.8376	1.6711	0.0261	1.1155	0.8247	0.1997
0.2305	1.5796	1.2039	1.7800	0.8173	1.7076	0.0152	1.1138	0.8184	0.1926
0.2590	1.4306	1.1964	1.6982	0.7757	1.7444	0.0069	1.1125	0.8136	0.1876
0.2782	1.3360	1.1901	1.6494	0.7480	1.7816	0.0017	1.1116	0.8106	0.1807
0.2876	1.3172	1.1887	1.6399	0.7441	1.8185	-0.0088	1.1100	0.8045	0.1733
0.3164	1.2546	1.1871	1.5999	0.7264	1.8561	-0.0218	1.1079	0.7970	0.1641
0.3456	1.1631	1.1801	1.5533	0.6973	1.9312	-0.0326	1.1061	0.7907	0.1529
0.3651	1.0750	1.1731	1.5078	0.6678	2.0070	-0.0523	1.1029	0.7792	0.1369
0.3748	1.0515	1.1712	1.4956	0.6594	2.0831	-0.0643	1.1009	0.7721	0.1258
0.4040	0.9998	1.1716	1.4570	0.6460	2.1467	-0.0812	1.0980	0.7621	0.1157
0.4339	0.9324	1.1696	1.4128	0.6261	2.1982	-0.0929	1.0960	0.7552	0.1056
0.4635	0.8855	1.1654	1.3881	0.6073	2.2761	-0.1063	1.0937	0.7472	0.0966
0.4937	0.8065	1.1583	1.3463	0.5762	2.3547	-0.1194	1.0914	0.7394	0.0875
0.5240	0.7820	1.1561	1.3333	0.5687	2.4332	-0.1270	1.0900	0.7347	0.0768
0.5546	0.7448	1.1551	1.3076	0.5512	2.5125	-0.1369	1.0882	0.7288	0.0667
0.5855	0.6806	1.1490	1.2731	0.5245	2.5921	-0.1445	1.0869	0.7242	0.0570
0.6165	0.6415	1.1451	1.2519	0.5097	2.6721	-0.1527	1.0854	0.7193	0.0486
0.6478	0.6134	1.1462	1.2280	0.5019	2.7524	-0.1565	1.0847	0.7169	0.0455
0.6791	0.5795	1.1428	1.2095	0.4847	2.8331	-0.1615	1.0838	0.7139	0.0340
0.7003	0.5661	1.1414	1.2022	0.4822	2.9145	-0.1674	1.0827	0.7103	0.0277
0.7107	0.5622	1.1410	1.2000	0.4822	2.9965	-0.1733	1.0816	0.7067	0.0183
0.7427	0.5264	1.1421	1.1702	0.4670	3.0654	-0.1772	1.0808	0.7044	0.0104
0.7747	0.4844	1.1429	1.1364	0.4474	3.1207	-0.1815	1.0800	0.7017	0.0085
0.8070	0.4630	1.1412	1.1234	0.4347	3.2041	-0.1822	1.0799	0.7013	0.0055
0.8397	0.4387	1.1384	1.1100	0.4244	3.2883	-0.1825	1.0798	0.7011	0.0073
0.8613	0.4157	1.1358	1.0974	0.4165	3.3727	-0.1845	1.0795	0.6999	0.0056
0.8724	0.4004	1.1341	1.0889	0.4107	3.4579	-0.1812	1.0801	0.7019	0.0045
0.9051	0.3697	1.1338	1.0655	0.3980	3.5431	-0.1801	1.0803	0.7026	0.0015
0.9381	0.3370	1.1299	1.0472	0.3817	3.6144	-0.1796	1.0804	0.7029	-0.0009
0.9711	0.3100	1.1266	1.0321	0.3647	3.6718	-0.1771	1.0808	0.7044	0.0004
1.0049	0.2858	1.1282	1.0101	0.3526	3.7580	-0.1758	1.0811	0.7052	0.0033
1.0383	0.2643	1.1255	0.9980	0.3416	3.8446	-0.1755	1.0812	0.7054	0.0011
1.0494	0.2577	1.1247	0.9943	0.3370	3.9207	-0.1721	1.0818	0.7074	0.0028
1.0720	0.2486	1.1284	0.9806	0.3342	3.9861	-0.1707	1.0820	0.7083	0.0025
1.1061	0.2285	1.1258	0.9693	0.3235	4.0518	-0.1686	1.0824	0.7096	0.0045
1.1401	0.2088	1.1267	0.9523	0.3132	4.1172	-0.1638	1.0833	0.7125	0.0040
1.1742	0.1885	1.1240	0.9408	0.3024	4.1829	-0.1612	1.0847	0.7129	0.0053
1.2083	0.1716	1.1217	0.9312	0.2973	4.2483	-0.1607	1.0848	0.7132	0.0053
1.2427	0.1555	1.1194	0.9221	0.2911	4.3140	-0.1557	1.0857	0.7163	0.0054
1.2778	0.1390	1.1228	0.9034	0.2769					
1.3126	0.1276	1.1212	0.8969	0.2708					

Table B-10. Time histories of overpressure, sound speed, density and flow velocity from the reconstructed blast-wave flow field by the RCM for a 1-kg TNT surface explosion in a standard atmosphere. These signatures are for the specific radius r = 2.007 m, at which the blast-wave front arrives at time t = 1.697 ms.

t (ms)	$\Delta p/p_1$	a/a_1	ρ/ρ_1	u/a_1	t (ms)	$\Delta p/p_1$	a/a_1	ρ/ρ_1	u/a_1
0.0000	2.6080	1.2375	2.3561	1.0389	1.4256	0.1044	1.0995	0.9136	0.2441
0.0184	2.5249	1.2348	2.3119	1.0263	1.4618	0.0891	1.1018	0.8972	0.2348
0.0462	2.3633	1.2290	2.2266	0.9923	1.4983	0.0849	1.1012	0.8947	0.2296
0.0741	2.1235	1.2191	2.1017	0.9388	1.5344	0.0702	1.1038	0.8784	0.2190
0.1022	2.0090	1.2129	2.0453	0.9172	1.5713	0.0582	1.1020	0.8713	0.2128
0.1307	1.8650	1.2044	1.9749	0.8774	1.6078	0.0545	1.1015	0.8691	0.2073
0.1592	1.7325	1.1990	1.9007	0.8468	1.6447	0.0430	1.1032	0.8570	0.1998
0.1784	1.6328	1.1927	1.8509	0.8215	1.6819	0.0323	1.1016	0.8507	0.1912
0.1878	1.6136	1.1914	1.8412	0.8185	1.7187	0.0295	1.1011	0.8491	0.1900
0.2166	1.4887	1.1868	1.7668	0.7828	1.7563	0.0129	1.0986	0.8393	0.1791
0.2458	1.3820	1.1830	1.7020	0.7520	1.7938	0.0047	1.0973	0.8344	0.1752
0.2653	1.3089	1.1798	1.6589	0.7315	1.8314	-0.0020	1.0963	0.8305	0.1684
0.2750	1.2927	1.1786	1.6505	0.7268	1.8689	-0.0159	1.0940	0.8221	0.1604
0.3042	1.2274	1.1769	1.6081	0.7110	1.9072	-0.0266	1.0923	0.8158	0.1513
0.3341	1.1421	1.1745	1.5528	0.6808	1.9833	-0.0389	1.0959	0.8002	0.1448
0.3637	1.0533	1.1674	1.5066	0.6503	2.0469	-0.0568	1.0930	0.7896	0.1335
0.3940	0.9883	1.1625	1.4712	0.6279	2.0984	-0.0641	1.0918	0.7852	0.1247
0.4242	0.9328	1.1583	1.4406	0.6119	2.1763	-0.0791	1.0893	0.7762	0.1130
0.4548	0.8924	1.1578	1.4118	0.5951	2.2549	-0.0958	1.0864	0.7661	0.0980
0.4857	0.8111	1.1505	1.3682	0.5631	2.3335	-0.1033	1.0851	0.7616	0.0885
0.5167	0.7718	1.1469	1.3469	0.5528	2.4127	-0.1143	1.0873	0.7492	0.0782
0.5480	0.7281	1.1428	1.3231	0.5390	2.4924	-0.1266	1.0851	0.7417	0.0693
0.5793	0.6826	1.1430	1.2879	0.5226	2.5723	-0.1337	1.0838	0.7374	0.0577
0.6005	0.6475	1.1395	1.2687	0.5088	2.6527	-0.1418	1.0824	0.7325	0.0489
0.6109	0.6433	1.1391	1.2663	0.5088	2.7333	-0.1470	1.0815	0.7293	0.0407
0.6429	0.6100	1.1394	1.2401	0.4929	2.8147	-0.1489	1.0861	0.7216	0.0360
0.6749	0.5656	1.1349	1.2155	0.4739	2.8967	-0.1593	1.0841	0.7152	0.0289
0.7072	0.5512	1.1334	1.2075	0.4700	2.9656	-0.1660	1.0829	0.7112	0.0213
0.7399	0.5210	1.1302	1.1907	0.4576	3.0209	-0.1699	1.0822	0.7088	0.0184
0.7615	0.5043	1.1284	1.1813	0.4501	3.1043	-0.1773	1.0808	0.7043	0.0119
0.7726	0.4837	1.1262	1.1698	0.4386	3.1885	-0.1793	1.0804	0.7030	0.0060
0.8053	0.4539	1.1230	1.1529	0.4277	3.2730	-0.1796	1.0804	0.7029	0.0027
0.8383	0.4256	1.1223	1.1319	0.4156	3.3581	-0.1772	1.0808	0.7044	0.0013
0.8714	0.4006	1.1194	1.1177	0.4075	3.4433	-0.1766	1.0809	0.7047	0.0011
0.9051	0.3591	1.1146	1.0939	0.3891	3.5146	-0.1774	1.0808	0.7042	0.0007
0.9385	0.3322	1.1153	1.0710	0.3786	3.5720	-0.1782	1.0806	0.7037	0.0016
0.9496	0.3278	1.1148	1.0685	0.3710	3.6582	-0.1777	1.0807	0.7040	-0.0025
0.9722	0.3167	1.1134	1.0621	0.3675	3.7448	-0.1739	1.0814	0.7064	-0.0011
1.0063	0.2807	1.1090	1.0413	0.3480	3.8209	-0.1712	1.0820	0.7080	-0.0011
1.0403	0.2602	1.1113	1.0205	0.3309	3.8863	-0.1714	1.0819	0.7079	-0.0025
1.0744	0.2472	1.1148	1.0036	0.3251	3.9520	-0.1682	1.0825	0.7098	-0.0013
1.1085	0.2296	1.1125	0.9934	0.3161	4.0174	-0.1650	1.0831	0.7118	-0.0028
1.1429	0.2129	1.1104	0.9838	0.3107	4.0831	-0.1629	1.0835	0.7131	-0.0007
1.1780	0.1895	1.1079	0.9690	0.2944	4.1485	-0.1598	1.0841	0.7150	0.0002
1.2128	0.1726	1.1089	0.9535	0.2850	4.2142	-0.1588	1.0842	0.7155	0.0030
1.2479	0.1601	1.1072	0.9462	0.2766	4.2469	-0.1590	1.0842	0.7154	0.0024
1.2830	0.1436	1.1050	0.9366	0.2671					
1.3185	0.1316	1.1033	0.9296	0.2609					
1.3540	0.1177	1.1014	0.9214	0.2533					
1.3898	0.1121	1.1006	0.9182	0.2479					

Table B-11. Time histories of overpressure, sound speed, density and flow velocity from the reconstructed blast-wave flow field by the RCM for a 1-kg TNT surface explosion in a standard atmosphere. These signatures are for the specific radius r = 2.114 m, at which the blast-wave front arrives at time t = 1.875 ms.

t (ms)	$\Delta p/p_1$	a/a_1	ρ/ρ_1	u/a_1	t (ms)	$\Delta p/p_1$	a/a_1	ρ/ρ_1	u/a_1
0.0000	2.3695	1.2202	2.2632	0.9751	1.5035	0.0913	1.0779	0.9393	0.2230
0.0094	2.3122	1.2172	2.2356	0.9638	1.5403	0.0817	1.0765	0.9334	0.2178
0.0382	2.1679	1.2112	2.1594	0.9321	1.5779	0.0663	1.0743	0.9239	0.2050
0.0675	1.9777	1.2007	2.0656	0.8889	1.6154	0.0584	1.0732	0.9190	0.2004
0.0869	1.8802	1.1959	2.0139	0.8670	1.6530	0.0509	1.0721	0.9144	0.1960
0.0967	1.8074	1.1915	1.9774	0.8455	1.6905	0.0483	1.0717	0.9128	0.1930
0.1259	1.6984	1.1860	1.9183	0.8213	1.7288	0.0342	1.0696	0.9040	0.1839
0.1558	1.5753	1.1806	1.8477	0.7910	1.7667	0.0221	1.0702	0.8925	0.1771
0.1853	1.4935	1.1752	1.8055	0.7723	1.8049	0.0173	1.0694	0.8895	0.1706
0.2156	1.4013	1.1713	1.7504	0.7423	1.8428	0.0092	1.0682	0.8844	0.1655
0.2458	1.2942	1.1636	1.6943	0.7125	1.8686	0.0024	1.0672	0.8802	0.1617
0.2764	1.2385	1.1596	1.6648	0.6972	1.8814	0.0009	1.0670	0.8792	0.1577
0.3074	1.1458	1.1554	1.6074	0.6667	1.9200	-0.0095	1.0654	0.8727	0.1514
0.3383	1.0619	1.1491	1.5614	0.6348	1.9590	-0.0181	1.0677	0.8613	0.1459
0.3696	0.9946	1.1437	1.5249	0.6149	2.0372	-0.0320	1.0655	0.8525	0.1323
0.4009	0.9493	1.1403	1.4992	0.6005	2.1158	-0.0421	1.0640	0.8462	0.1236
0.4221	0.9043	1.1365	1.4744	0.5839	2.1947	-0.0587	1.0613	0.8357	0.1088
0.4325	0.8990	1.1360	1.4715	0.5839	2.2740	-0.0730	1.0590	0.8266	0.0977
0.4645	0.8403	1.1332	1.4332	0.5640	2.3540	-0.0886	1.0564	0.8166	0.0830
0.4965	0.7632	1.1263	1.3900	0.5358	2.4339	-0.1010	1.0589	0.8017	0.0759
0.5289	0.7363	1.1273	1.3662	0.5303	2.5146	-0.1111	1.0572	0.7953	0.0652
0.5615	0.7109	1.1250	1.3519	0.5195	2.5956	-0.1218	1.0603	0.7811	0.0589
0.5831	0.6835	1.1258	1.3283	0.5081	2.6773	-0.1295	1.0590	0.7762	0.0487
0.5942	0.6600	1.1235	1.3151	0.4965	2.7597	-0.1380	1.0575	0.7709	0.0410
0.6269	0.6215	1.1217	1.2888	0.4836	2.8011	-0.1423	1.0567	0.7681	0.0339
0.6599	0.5865	1.1212	1.2620	0.4695	2.8842	-0.1453	1.0562	0.7662	0.0290
0.6930	0.5639	1.1189	1.2491	0.4612	2.9680	-0.1519	1.0550	0.7619	0.0227
0.7267	0.5302	1.1173	1.2258	0.4471	3.0522	-0.1562	1.0549	0.7583	0.0194
0.7601	0.4962	1.1158	1.2017	0.4327	3.1370	-0.1634	1.0536	0.7537	0.0119
0.7712	0.4868	1.1148	1.1964	0.4287	3.2222	-0.1695	1.0525	0.7497	0.0040
0.7938	0.4618	1.1125	1.1810	0.4187	3.3077	-0.1731	1.0519	0.7474	-0.0001
0.8279	0.4377	1.1099	1.1671	0.4057	3.3505	-0.1720	1.0520	0.7481	-0.0025
0.8620	0.4123	1.1075	1.1515	0.3928	3.4367	-0.1723	1.0520	0.7479	-0.0028
0.8960	0.3891	1.1077	1.1321	0.3844	3.5230	-0.1708	1.0523	0.7489	-0.0065
0.9301	0.3682	1.1053	1.1198	0.3709	3.6099	-0.1697	1.0525	0.7496	-0.0064
0.9645	0.3416	1.1022	1.1043	0.3579	3.6753	-0.1671	1.0529	0.7512	-0.0058
0.9997	0.3124	1.0988	1.0870	0.3434	3.7410	-0.1700	1.0524	0.7494	-0.0066
1.0344	0.2765	1.0944	1.0657	0.3252	3.8063	-0.1696	1.0525	0.7496	-0.0093
1.0695	0.2643	1.0929	1.0585	0.3157	3.8721	-0.1671	1.0523	0.7521	-0.0081
1.1047	0.2445	1.0905	1.0465	0.3054	3.9374	-0.1644	1.0528	0.7539	-0.0069
1.1401	0.2270	1.0883	1.0360	0.2944	4.0031	-0.1634	1.0530	0.7545	-0.0092
1.1756	0.2133	1.0865	1.0278	0.2875	4.0466	-0.1625	1.0531	0.7551	-0.0102
1.2114	0.1994	1.0847	1.0193	0.2808	4.1012	-0.1610	1.0534	0.7560	-0.0074
1.2472	0.1797	1.0822	1.0074	0.2710	4.1669	-0.1601	1.0536	0.7567	-0.0068
1.2834	0.1624	1.0842	0.9890	0.2591	4.2323	-0.1579	1.0540	0.7581	-0.0040
1.3199	0.1462	1.0820	0.9790	0.2496	4.2980	-0.1543	1.0546	0.7604	-0.0044
1.3561	0.1362	1.0841	0.9668	0.2447					
1.3929	0.1245	1.0825	0.9596	0.2394					
1.4294	0.1105	1.0805	0.9511	0.2303					
1.4663	0.1013	1.0793	0.9455	0.2277					

Table B-12. Time histories of overpressure, sound speed, density and flow velocity from the reconstructed blast-wave flow field by the RCM for a 1-kg TNT surface explosion in a standard atmosphere. These signatures are for the specific radius r = 2.164 m, at which the blast-wave front arrives at time t = 1.962 ms.

t (ms)	$\Delta p/p_1$	a/a_1	ρ/ρ_1	u/a_1	t (ms)	$\Delta p/p_1$	a/a_1	ρ/ρ_1	u/a_1
0.0000	2.2464	1.2109	2.2140	0.9409	1.5661	0.0830	1.0690	0.9477	0.2086
0.0097	2.1847	1.2076	2.1838	0.9246	1.6036	0.0722	1.0675	0.9409	0.2023
0.0389	1.9974	1.1983	2.0875	0.8826	1.6419	0.0590	1.0656	0.9326	0.1924
0.0688	1.8571	1.1918	2.0117	0.8513	1.6798	0.0516	1.0645	0.9280	0.1881
0.0984	1.7018	1.1823	1.9330	0.8113	1.7180	0.0474	1.0639	0.9253	0.1863
0.1287	1.6304	1.1795	1.8908	0.7920	1.7559	0.0357	1.0622	0.9179	0.1800
0.1589	1.5232	1.1726	1.8351	0.7657	1.7816	0.0271	1.0652	0.9053	0.1717
0.1895	1.4586	1.1692	1.7986	0.7495	1.7945	0.0241	1.0647	0.9034	0.1688
0.2204	1.3347	1.1617	1.7299	0.7147	1.8331	0.0181	1.0638	0.8996	0.1634
0.2514	1.2439	1.1563	1.6784	0.6870	1.8721	0.0114	1.0662	0.8897	0.1575
0.2827	1.1900	1.1536	1.6457	0.6747	1.9110	0.0045	1.0652	0.8853	0.1532
0.3140	1.0986	1.1466	1.5964	0.6443	1.9503	-0.0064	1.0635	0.8785	0.1431
0.3352	1.0412	1.1420	1.5651	0.6238	1.9896	-0.0144	1.0623	0.8734	0.1374
0.3456	1.0353	1.1416	1.5618	0.6238	2.0682	-0.0264	1.0604	0.8658	0.1258
0.3776	0.9570	1.1375	1.5124	0.5962	2.1474	-0.0379	1.0586	0.8585	0.1198
0.4096	0.9008	1.1328	1.4813	0.5794	2.2271	-0.0551	1.0559	0.8475	0.1067
0.4419	0.8672	1.1299	1.4625	0.5693	2.3070	-0.0730	1.0530	0.8360	0.0939
0.4746	0.8193	1.1257	1.4356	0.5538	2.3874	-0.0881	1.0506	0.8263	0.0830
0.4962	0.7644	1.1235	1.3977	0.5284	2.4680	-0.0973	1.0490	0.8203	0.0724
0.5073	0.7519	1.1224	1.3906	0.5224	2.5494	-0.1029	1.0481	0.8167	0.0659
0.5400	0.7262	1.1203	1.3753	0.5166	2.6314	-0.1181	1.0455	0.8067	0.0534
0.5730	0.6872	1.1170	1.3523	0.5022	2.7003	-0.1241	1.0445	0.8028	0.0447
0.6061	0.6447	1.1129	1.3279	0.4866	2.7556	-0.1277	1.0439	0.8004	0.0414
0.6398	0.6044	1.1112	1.2994	0.4670	2.8390	-0.1407	1.0417	0.7919	0.0312
0.6732	0.5708	1.1078	1.2799	0.4533	2.9232	-0.1425	1.0414	0.7907	0.0277
0.6843	0.5626	1.1070	1.2751	0.4492	3.0077	-0.1460	1.0408	0.7884	0.0243
0.7069	0.5361	1.1078	1.2517	0.4392	3.0928	-0.1542	1.0393	0.7830	0.0168
0.7410	0.5148	1.1056	1.2393	0.4325	3.1780	-0.1598	1.0383	0.7793	0.0082
0.7750	0.4857	1.1059	1.2149	0.4158	3.2493	-0.1641	1.0376	0.7765	0.0028
0.8091	0.4513	1.1040	1.1907	0.4021	3.3067	-0.1668	1.0371	0.7746	-0.0028
0.8432	0.4340	1.1021	1.1805	0.3933	3.3929	-0.1687	1.0368	0.7734	-0.0052
0.8776	0.4163	1.1002	1.1701	0.3860	3.4795	-0.1685	1.0368	0.7735	-0.0060
0.9127	0.3868	1.0969	1.1526	0.3720	3.5556	-0.1688	1.0367	0.7733	-0.0059
0.9475	0.3493	1.0956	1.1242	0.3534	3.6210	-0.1679	1.0369	0.7739	-0.0091
0.9826	0.3286	1.0950	1.1081	0.3407	3.6867	-0.1669	1.0371	0.7746	-0.0086
1.0177	0.3089	1.0926	1.0964	0.3331	3.7521	-0.1649	1.0374	0.7759	-0.0074
1.0532	0.2761	1.0887	1.0767	0.3137	3.8178	-0.1644	1.0375	0.7763	-0.0114
1.0887	0.2594	1.0887	1.0626	0.3073	3.8832	-0.1665	1.0371	0.7748	-0.0118
1.1245	0.2421	1.0865	1.0521	0.2958	3.9489	-0.1636	1.0377	0.7768	-0.0095
1.1603	0.2308	1.0851	1.0453	0.2936	3.9816	-0.1630	1.0378	0.7771	-0.0077
1.1965	0.2071	1.0825	1.0301	0.2809	4.0473	-0.1620	1.0380	0.7778	-0.0100
1.2330	0.1917	1.0805	1.0207	0.2754	4.1127	-0.1591	1.0385	0.7797	-0.0088
1.2691	0.1732	1.0785	1.0086	0.2653	4.1780	-0.1577	1.0387	0.7807	-0.0078
1.3060	0.1537	1.0760	0.9965	0.2552	4.2438	-0.1544	1.0393	0.7829	-0.0078
1.3425	0.1378	1.0766	0.9816	0.2417	4.3091	-0.1514	1.0398	0.7849	-0.0069
1.3793	0.1283	1.0753	0.9758	0.2370					
1.4166	0.1223	1.0745	0.9721	0.2319					
1.4534	0.1095	1.0727	0.9641	0.2242					
1.4910	0.0996	1.0714	0.9580	0.2204					
1.5285	0.0896	1.0700	0.9518	0.2159					

Table B-13. Time histories of overpressure, sound speed, density and flow velocity from the reconstructed blast-wave flow field by the RCM for a 1-kg TNT surface explosion in a standard atmosphere. These signatures are for the specific radius r = 2.257 m, at which the blast-wave front arrives at time t = 2.121 ms.

t (ms)	$\Delta p/p_1$	a/a_1	ρ/ρ_1	u/a_1	t (ms)	$\Delta p/p_1$	a/a_1	ρ/ρ_1	u/a_1
0.0000	1.9735	1.1902	2.0990	0.8617	1.6227	0.0851	1.0591	0.9673	0.1929
0.0306	1.8709	1.1867	2.0388	0.8385	1.6356	0.0823	1.0587	0.9656	0.1907
0.0615	1.7416	1.1801	1.9686	0.8086	1.6742	0.0669	1.0566	0.9558	0.1825
0.0925	1.6296	1.1733	1.9102	0.7805	1.7132	0.0582	1.0553	0.9502	0.1789
0.1238	1.5133	1.1657	1.8495	0.7511	1.7521	0.0525	1.0545	0.9465	0.1738
0.1551	1.4421	1.1625	1.8069	0.7306	1.7914	0.0453	1.0535	0.9419	0.1699
0.1763	1.3810	1.1583	1.7745	0.7121	1.8307	0.0349	1.0520	0.9352	0.1634
0.1867	1.3735	1.1578	1.7705	0.7121	1.8700	0.0235	1.0503	0.9278	0.1569
0.2187	1.2773	1.1522	1.7155	0.6830	1.9093	0.0158	1.0492	0.9228	0.1531
0.2507	1.1943	1.1474	1.6666	0.6599	1.9489	0.0065	1.0506	0.9119	0.1458
0.2830	1.1560	1.1448	1.6452	0.6502	1.9885	-0.0008	1.0495	0.9071	0.1417
0.3157	1.0678	1.1379	1.5969	0.6206	2.0282	-0.0081	1.0485	0.9024	0.1337
0.3373	1.0125	1.1338	1.5656	0.6005	2.0682	-0.0159	1.0473	0.8973	0.1283
0.3484	0.9797	1.1311	1.5474	0.5873	2.1081	-0.0256	1.0458	0.8910	0.1183
0.3811	0.9310	1.1285	1.5163	0.5738	2.1881	-0.0344	1.0462	0.8823	0.1138
0.4141	0.8782	1.1241	1.4863	0.5566	2.2688	-0.0494	1.0438	0.8725	0.0995
0.4471	0.8488	1.1216	1.4696	0.5456	2.3498	-0.0636	1.0435	0.8599	0.0908
0.4809	0.8040	1.1186	1.4418	0.5296	2.4315	-0.0781	1.0412	0.8503	0.0807
0.5143	0.7333	1.1133	1.3984	0.5015	2.5139	-0.0890	1.0394	0.8431	0.0689
0.5254	0.7230	1.1124	1.3925	0.4975	2.5553	-0.0957	1.0384	0.8388	0.0656
0.5480	0.7098	1.1122	1.3822	0.4952	2.6384	-0.1047	1.0369	0.8328	0.0555
0.5821	0.6744	1.1089	1.3617	0.4800	2.7222	-0.1136	1.0354	0.8268	0.0457
0.6161	0.6144	1.1044	1.3236	0.4570	2.8063	-0.1215	1.0345	0.8210	0.0388
0.6502	0.5875	1.1018	1.3078	0.4490	2.8912	-0.1277	1.0334	0.8168	0.0301
0.6843	0.5620	1.0992	1.2928	0.4395	2.9764	-0.1341	1.0323	0.8125	0.0221
0.7187	0.5402	1.0970	1.2799	0.4317	3.0619	-0.1382	1.0316	0.8098	0.0202
0.7538	0.5070	1.0958	1.2550	0.4186	3.1047	-0.1453	1.0304	0.8050	0.0146
0.7886	0.4772	1.0927	1.2372	0.4034	3.1909	-0.1470	1.0301	0.8039	0.0096
0.8237	0.4459	1.0894	1.2184	0.3892	3.2771	-0.1547	1.0288	0.7986	0.0034
0.8588	0.4206	1.0866	1.2031	0.3782	3.3641	-0.1575	1.0283	0.7967	-0.0029
0.8943	0.4055	1.0876	1.1881	0.3697	3.4294	-0.1618	1.0276	0.7939	-0.0068
0.9298	0.3822	1.0853	1.1734	0.3610	3.4951	-0.1639	1.0272	0.7924	-0.0089
0.9656	0.3530	1.0820	1.1557	0.3453	3.5605	-0.1655	1.0269	0.7914	-0.0091
1.0014	0.3254	1.0788	1.1388	0.3342	3.6262	-0.1625	1.0270	0.7940	-0.0105
1.0376	0.3001	1.0762	1.1226	0.3188	3.6916	-0.1636	1.0268	0.7933	-0.0117
1.0741	0.2794	1.0737	1.1098	0.3083	3.7573	-0.1621	1.0271	0.7942	-0.0108
1.1102	0.2621	1.0737	1.0947	0.3001	3.8008	-0.1625	1.0270	0.7940	-0.0116
1.1471	0.2374	1.0707	1.0794	0.2879	3.8554	-0.1590	1.0276	0.7964	-0.0118
1.1836	0.2244	1.0691	1.0713	0.2802	3.9211	-0.1591	1.0276	0.7963	-0.0147
1.2204	0.2065	1.0668	1.0601	0.2705	3.9865	-0.1612	1.0273	0.7948	-0.0154
1.2577	0.1935	1.0652	1.0519	0.2637	4.0522	-0.1570	1.0280	0.7977	-0.0144
1.2945	0.1761	1.0629	1.0409	0.2522	4.1175	-0.1545	1.0284	0.7994	-0.0134
1.3321	0.1617	1.0611	1.0318	0.2425	4.1829	-0.1561	1.0282	0.7983	-0.0142
1.3696	0.1492	1.0595	1.0239	0.2355	4.2486	-0.1534	1.0286	0.8002	-0.0124
1.4072	0.1355	1.0610	1.0087	0.2260	4.3140	-0.1501	1.0292	0.8024	-0.0134
1.4447	0.1264	1.0597	1.0029	0.2213	4.3797	-0.1469	1.0297	0.8045	-0.0134
1.4830	0.1139	1.0581	0.9950	0.2115					
1.5209	0.1070	1.0603	0.9846	0.2079					
1.5591	0.1002	1.0594	0.9803	0.2041					
1.5970	0.0928	1.0584	0.9756	0.1982					

Table B-14. Time histories of overpressure, sound speed, density and flow velocity from the reconstructed blast-wave flow field by the RCM for a 1-kg TNT surface explosion in a standard atmosphere. These signatures are for the specific radius r = 2.350 m, at which the blast-wave front arrives at time t = 2.297 ms.

t (ms)	$\Delta p/p_1$	a/a_1	ρ/ρ_1	u/a_1	t (ms)	$\Delta p/p_1$	a/a_1	ρ/ρ_1	u/a_1
0.0000	1.8209	1.1783	2.0318	0.8139	1.6544	0.0888	1.0461	0.9950	0.1869
0.0104	1.7622	1.1748	2.0015	0.7988	1.6937	0.0794	1.0448	0.9888	0.1825
0.0424	1.6796	1.1705	1.9557	0.7769	1.7330	0.0720	1.0438	0.9839	0.1747
0.0744	1.5645	1.1643	1.8918	0.7485	1.7726	0.0584	1.0419	0.9750	0.1662
0.1067	1.4739	1.1585	1.8433	0.7239	1.8122	0.0481	1.0404	0.9682	0.1606
0.1394	1.4018	1.1536	1.8048	0.7049	1.8519	0.0436	1.0398	0.9653	0.1590
0.1610	1.3391	1.1494	1.7705	0.6881	1.8919	0.0346	1.0385	0.9593	0.1531
0.1721	1.3103	1.1474	1.7550	0.6790	1.9319	0.0228	1.0362	0.9515	0.1463
0.2048	1.2394	1.1423	1.7163	0.6608	1.9718	0.0174	1.0385	0.9433	0.1412
0.2378	1.1737	1.1381	1.6782	0.6393	2.0118	0.0109	1.0376	0.9390	0.1358
0.2709	1.1269	1.1346	1.6523	0.6260	2.0522	0.0041	1.0366	0.9344	0.1321
0.3046	1.0412	1.1314	1.5946	0.5973	2.0925	-0.0072	1.0349	0.9269	0.1235
0.3380	0.9508	1.1243	1.5433	0.5672	2.1328	-0.0147	1.0338	0.9219	0.1183
0.3491	0.9287	1.1224	1.5309	0.5604	2.1735	-0.0212	1.0331	0.9171	0.1137
0.3717	0.9038	1.1204	1.5167	0.5540	2.2142	-0.0265	1.0323	0.9135	0.1081
0.4058	0.8528	1.1160	1.4876	0.5372	2.2963	-0.0361	1.0308	0.9071	0.1015
0.4398	0.8240	1.1137	1.4706	0.5264	2.3651	-0.0509	1.0286	0.8971	0.0888
0.4739	0.7895	1.1120	1.4471	0.5170	2.4204	-0.0592	1.0273	0.8915	0.0808
0.5080	0.7223	1.1061	1.4078	0.4883	2.5038	-0.0719	1.0253	0.8829	0.0712
0.5424	0.6946	1.1035	1.3916	0.4797	2.5880	-0.0834	1.0235	0.8751	0.0626
0.5775	0.6656	1.1018	1.3720	0.4676	2.6725	-0.0914	1.0225	0.8691	0.0544
0.6123	0.6144	1.0969	1.3418	0.4482	2.7577	-0.1017	1.0208	0.8621	0.0457
0.6474	0.5859	1.0954	1.3217	0.4371	2.8428	-0.1106	1.0193	0.8560	0.0375
0.6825	0.5559	1.0924	1.3037	0.4254	2.9141	-0.1166	1.0184	0.8518	0.0297
0.7180	0.5304	1.0901	1.2880	0.4127	2.9715	-0.1238	1.0172	0.8469	0.0247
0.7535	0.4971	1.0868	1.2674	0.4001	3.0577	-0.1311	1.0160	0.8418	0.0188
0.7893	0.4730	1.0857	1.2497	0.3880	3.1443	-0.1341	1.0155	0.8398	0.0147
0.8251	0.4565	1.0839	1.2396	0.3817	3.2205	-0.1356	1.0152	0.8387	0.0124
0.8613	0.4269	1.0809	1.2214	0.3662	3.2858	-0.1418	1.0142	0.8344	0.0079
0.8978	0.4088	1.0789	1.2103	0.3589	3.3515	-0.1459	1.0135	0.8316	0.0033
0.9339	0.3913	1.0770	1.1995	0.3526	3.4169	-0.1482	1.0131	0.8300	-0.0023
0.9708	0.3653	1.0741	1.1835	0.3383	3.4826	-0.1524	1.0124	0.8270	-0.0069
1.0073	0.3320	1.0711	1.1609	0.3198	3.5480	-0.1564	1.0117	0.8242	-0.0107
1.0442	0.3094	1.0696	1.1446	0.3097	3.6137	-0.1569	1.0116	0.8239	-0.0140
1.0814	0.2955	1.0680	1.1358	0.2999	3.6464	-0.1568	1.0116	0.8240	-0.0140
1.1182	0.2753	1.0656	1.1231	0.2899	3.7121	-0.1573	1.0115	0.8236	-0.0140
1.1558	0.2532	1.0639	1.1071	0.2797	3.7775	-0.1568	1.0116	0.8240	-0.0146
1.1933	0.2281	1.0609	1.0912	0.2675	3.8428	-0.1547	1.0120	0.8254	-0.0160
1.2309	0.2225	1.0614	1.0852	0.2623	3.9086	-0.1538	1.0121	0.8260	-0.0179
1.2684	0.2081	1.0596	1.0761	0.2565	3.9739	-0.1538	1.0121	0.8260	-0.0172
1.3067	0.1910	1.0574	1.0651	0.2473	4.0393	-0.1544	1.0120	0.8256	-0.0176
1.3446	0.1720	1.0550	1.0530	0.2375	4.1050	-0.1538	1.0121	0.8260	-0.0202
1.3828	0.1561	1.0529	1.0428	0.2295	4.1704	-0.1519	1.0124	0.8274	-0.0178
1.4207	0.1474	1.0518	1.0372	0.2249	4.2361	-0.1503	1.0127	0.8285	-0.0156
1.4465	0.1337	1.0500	1.0283	0.2165	4.3015	-0.1513	1.0125	0.8278	-0.0170
1.4593	0.1297	1.0495	1.0257	0.2141	4.3672	-0.1474	1.0132	0.8305	-0.0166
1.4979	0.1224	1.0485	1.0210	0.2087	4.4326	-0.1463	1.0134	0.8313	-0.0161
1.5369	0.1161	1.0498	1.0127	0.2043					
1.5758	0.1033	1.0481	1.0044	0.1977					
1.6151	0.0974	1.0473	1.0006	0.1916					

Table B-15. Time histories of overpressure, sound speed, density and flow velocity from the reconstructed blast-wave flow field by the RCM for a 1-kg TNT surface explosion in a standard atmosphere. These signatures are for the specific radius r = 2.429 m, at which the blast-wave front arrives at time t = 2.458 ms.

t (ms)	$\Delta p/p_1$	a/a_1	ρ/ρ_1	u/a_1	t (ms)	$\Delta p/p_1$	a/a_1	ρ/ρ_1	u/a_1
0.0000	1.6453	1.1644	1.9511	0.7591	1.7309	0.0752	1.0380	0.9978	0.1717
0.0111	1.5817	1.1603	1.9176	0.7391	1.7709	0.0593	1.0358	0.9873	0.1593
0.0438	1.5265	1.1573	1.8865	0.7291	1.8109	0.0539	1.0359	0.9821	0.1560
0.0768	1.4347	1.1521	1.8344	0.7062	1.8508	0.0471	1.0349	0.9776	0.1521
0.1099	1.3639	1.1472	1.7961	0.6879	1.8912	0.0428	1.0343	0.9748	0.1505
0.1436	1.2790	1.1429	1.7447	0.6611	1.9315	0.0342	1.0331	0.9690	0.1436
0.1770	1.2057	1.1377	1.7042	0.6414	1.9718	0.0243	1.0317	0.9624	0.1368
0.1881	1.1812	1.1358	1.6907	0.6322	2.0125	0.0198	1.0310	0.9594	0.1313
0.2107	1.1349	1.1331	1.6627	0.6192	2.0532	0.0127	1.0300	0.9546	0.1267
0.2448	1.0991	1.1315	1.6397	0.6097	2.0942	0.0032	1.0286	0.9482	0.1212
0.2789	1.0165	1.1251	1.5929	0.5815	2.1353	-0.0046	1.0275	0.9429	0.1145
0.3129	0.9425	1.1191	1.5510	0.5576	2.1766	-0.0132	1.0262	0.9371	0.1104
0.3470	0.8889	1.1148	1.5198	0.5366	2.2041	-0.0190	1.0253	0.9331	0.1059
0.3814	0.8630	1.1126	1.5050	0.5295	2.2180	-0.0196	1.0252	0.9327	0.1059
0.4166	0.8139	1.1090	1.4749	0.5127	2.3011	-0.0297	1.0248	0.9240	0.0960
0.4513	0.7752	1.1056	1.4522	0.5011	2.3849	-0.0446	1.0225	0.9138	0.0857
0.4864	0.7235	1.1032	1.4161	0.4792	2.4691	-0.0558	1.0218	0.9044	0.0776
0.5216	0.6840	1.0996	1.3928	0.4640	2.5539	-0.0671	1.0200	0.8967	0.0668
0.5570	0.6547	1.0980	1.3726	0.4524	2.6391	-0.0808	1.0179	0.8873	0.0569
0.5925	0.6245	1.0953	1.3542	0.4429	2.7246	-0.0906	1.0163	0.8805	0.0506
0.6283	0.5807	1.0910	1.3280	0.4208	2.7674	-0.0929	1.0159	0.8789	0.0457
0.6641	0.5608	1.0890	1.3161	0.4139	2.8536	-0.1063	1.0138	0.8696	0.0366
0.7003	0.5292	1.0858	1.2970	0.4015	2.9399	-0.1134	1.0126	0.8647	0.0292
0.7368	0.4999	1.0828	1.2792	0.3874	3.0268	-0.1160	1.0122	0.8629	0.0239
0.7730	0.4876	1.0816	1.2717	0.3836	3.0922	-0.1236	1.0109	0.8575	0.0168
0.8098	0.4571	1.0784	1.2530	0.3703	3.1579	-0.1274	1.0103	0.8549	0.0137
0.8463	0.4271	1.0753	1.2341	0.3571	3.2232	-0.1291	1.0100	0.8537	0.0097
0.8832	0.4019	1.0739	1.2156	0.3473	3.2890	-0.1313	1.0108	0.8502	0.0081
0.9204	0.3847	1.0721	1.2047	0.3407	3.3543	-0.1387	1.0096	0.8451	0.0028
0.9572	0.3647	1.0699	1.1922	0.3315	3.4200	-0.1430	1.0089	0.8420	-0.0022
0.9948	0.3427	1.0684	1.1763	0.3214	3.4635	-0.1438	1.0087	0.8415	-0.0058
1.0323	0.3111	1.0648	1.1564	0.3060	3.5181	-0.1457	1.0084	0.8401	-0.0082
1.0699	0.2933	1.0627	1.1452	0.2942	3.5838	-0.1489	1.0079	0.8378	-0.0126
1.1074	0.2774	1.0608	1.1352	0.2867	3.6492	-0.1523	1.0073	0.8354	-0.0147
1.1457	0.2538	1.0580	1.1202	0.2721	3.7149	-0.1528	1.0072	0.8351	-0.0181
1.1836	0.2401	1.0576	1.1087	0.2653	3.7803	-0.1513	1.0075	0.8361	-0.0172
1.2218	0.2202	1.0553	1.0956	0.2548	3.8456	-0.1528	1.0072	0.8351	-0.0168
1.2597	0.2084	1.0539	1.0880	0.2499	3.9113	-0.1541	1.0070	0.8342	-0.0177
1.2855	0.1997	1.0530	1.0820	0.2430	3.9767	-0.1513	1.0075	0.8362	-0.0187
1.2983	0.1950	1.0524	1.0790	0.2393	4.0424	-0.1507	1.0076	0.8366	-0.0187
1.3369	0.1828	1.0508	1.0711	0.2331	4.1078	-0.1503	1.0076	0.8369	-0.0199
1.3759	0.1655	1.0500	1.0573	0.2242	4.1732	-0.1516	1.0074	0.8360	-0.0208
1.4148	0.1541	1.0485	1.0498	0.2179	4.2389	-0.1469	1.0082	0.8392	-0.0204
1.4541	0.1417	1.0469	1.0418	0.2117	4.2935	-0.1450	1.0085	0.8406	-0.0191
1.4934	0.1275	1.0451	1.0323	0.2035	4.3373	-0.1459	1.0084	0.8400	-0.0202
1.5327	0.1176	1.0438	1.0258	0.2000	4.4027	-0.1421	1.0090	0.8427	-0.0200
1.5720	0.1130	1.0432	1.0228	0.1948					
1.6116	0.1001	1.0414	1.0143	0.1868					
1.6513	0.0891	1.0399	1.0070	0.1823					
1.6909	0.0810	1.0388	1.0017	0.1747					

Table B-16. Time histories of overpressure, sound speed, density and flow velocity from the reconstructed blast-wave flow field by the RCM for a 1-kg TNT surface explosion in a standard atmosphere. These signatures are for the specific radius r = 2.529 m, at which the blast-wave front arrives at time t = 2.646 ms.

t (ms)	$\Delta p/p_1$	a/a_1	ρ/ρ_1	u/a_1	t (ms)	$\Delta p/p_1$	a/a_1	ρ/ρ_1	u/a_1
0.0000	1.5122	1.1535	1.8881	0.7138	1.8244	0.0624	1.0322	0.9971	0.1522
0.0226	1.4661	1.1505	1.8631	0.7032	1.8651	0.0557	1.0313	0.9927	0.1480
0.0567	1.3869	1.1456	1.8186	0.6797	1.9061	0.0465	1.0300	0.9865	0.1423
0.0908	1.3173	1.1418	1.7775	0.6601	1.9472	0.0428	1.0295	0.9838	0.1405
0.1248	1.2099	1.1342	1.7180	0.6282	1.9885	0.0355	1.0285	0.9789	0.1340
0.1589	1.1549	1.1302	1.6870	0.6113	2.0160	0.0294	1.0276	0.9747	0.1285
0.1933	1.1065	1.1265	1.6599	0.5979	2.0299	0.0287	1.0275	0.9743	0.1285
0.2284	1.0717	1.1244	1.6386	0.5885	2.0713	0.0186	1.0270	0.9657	0.1233
0.2632	0.9893	1.1184	1.5904	0.5621	2.1130	0.0120	1.0261	0.9612	0.1187
0.2983	0.9177	1.1125	1.5493	0.5388	2.1547	0.0056	1.0252	0.9569	0.1151
0.3334	0.8632	1.1080	1.5177	0.5194	2.1968	-0.0023	1.0240	0.9515	0.1114
0.3689	0.8174	1.1049	1.4888	0.5023	2.2389	-0.0119	1.0226	0.9449	0.1020
0.4044	0.7908	1.1026	1.4731	0.4959	2.2810	-0.0180	1.0217	0.9408	0.0976
0.4402	0.7617	1.1006	1.4544	0.4828	2.3234	-0.0242	1.0208	0.9365	0.0932
0.4760	0.7391	1.0986	1.4410	0.4760	2.4086	-0.0335	1.0194	0.9301	0.0871
0.5122	0.6747	1.0937	1.4001	0.4504	2.4937	-0.0461	1.0175	0.9214	0.0753
0.5487	0.6457	1.0910	1.3826	0.4382	2.5650	-0.0549	1.0161	0.9153	0.0670
0.5848	0.6220	1.0895	1.3664	0.4297	2.6224	-0.0650	1.0146	0.9084	0.0606
0.6217	0.5711	1.0846	1.3356	0.4078	2.7086	-0.0724	1.0134	0.9032	0.0535
0.6582	0.5575	1.0842	1.3249	0.4010	2.7952	-0.0841	1.0128	0.8930	0.0444
0.6951	0.5321	1.0818	1.3091	0.3926	2.8714	-0.0880	1.0122	0.8902	0.0414
0.7323	0.5073	1.0793	1.2939	0.3808	2.9367	-0.0960	1.0109	0.8847	0.0351
0.7691	0.4767	1.0761	1.2751	0.3686	3.0024	-0.1020	1.0099	0.8804	0.0277
0.8067	0.4512	1.0736	1.2590	0.3584	3.0678	-0.1069	1.0091	0.8770	0.0218
0.8442	0.4344	1.0718	1.2486	0.3516	3.1335	-0.1114	1.0084	0.8739	0.0184
0.8818	0.4057	1.0693	1.2294	0.3387	3.1989	-0.1186	1.0072	0.8688	0.0116
0.9193	0.3888	1.0675	1.2188	0.3317	3.2646	-0.1216	1.0067	0.8666	0.0081
0.9576	0.3641	1.0647	1.2033	0.3215	3.2973	-0.1242	1.0063	0.8648	0.0071
0.9955	0.3444	1.0626	1.1907	0.3139	3.3630	-0.1269	1.0059	0.8629	0.0058
1.0337	0.3260	1.0627	1.1743	0.3022	3.4284	-0.1326	1.0049	0.8589	0.0008
1.0716	0.3031	1.0600	1.1597	0.2909	3.4938	-0.1360	1.0044	0.8565	-0.0047
1.0974	0.2844	1.0589	1.1454	0.2814	3.5595	-0.1400	1.0037	0.8536	-0.0084
1.1102	0.2769	1.0581	1.1406	0.2785	3.6248	-0.1425	1.0033	0.8519	-0.0119
1.1488	0.2593	1.0560	1.1294	0.2682	3.6902	-0.1456	1.0028	0.8497	-0.0143
1.1878	0.2450	1.0542	1.1202	0.2597	3.7559	-0.1464	1.0026	0.8491	-0.0183
1.2267	0.2234	1.0516	1.1063	0.2489	3.8213	-0.1476	1.0024	0.8483	-0.0194
1.2660	0.2145	1.0505	1.1005	0.2417	3.8870	-0.1474	1.0025	0.8485	-0.0200
1.3053	0.2037	1.0493	1.0932	0.2365	3.9524	-0.1459	1.0027	0.8495	-0.0221
1.3446	0.1919	1.0479	1.0855	0.2310	4.0181	-0.1448	1.0029	0.8503	-0.0217
1.3839	0.1812	1.0465	1.0786	0.2241	4.0835	-0.1450	1.0029	0.8501	-0.0224
1.4235	0.1612	1.0440	1.0655	0.2121	4.1161	-0.1450	1.0029	0.8501	-0.0220
1.4631	0.1458	1.0420	1.0554	0.2017	4.1819	-0.1436	1.0031	0.8511	-0.0242
1.5028	0.1407	1.0413	1.0520	0.1983	4.2472	-0.1439	1.0030	0.8509	-0.0251
1.5428	0.1262	1.0394	1.0424	0.1910	4.3130	-0.1419	1.0034	0.8523	-0.0239
1.5828	0.1175	1.0383	1.0367	0.1845	4.3783	-0.1404	1.0036	0.8534	-0.0242
1.6227	0.1056	1.0367	1.0288	0.1784	4.4440	-0.1386	1.0039	0.8546	-0.0224
1.6627	0.0982	1.0357	1.0239	0.1757					
1.7031	0.0918	1.0348	1.0196	0.1724					
1.7434	0.0803	1.0334	1.0116	0.1636					
1.7837	0.0757	1.0328	1.0085	0.1600					

Table B-17. Time histories of overpressure, sound speed, density and flow velocity from the reconstructed blast-wave flow field by the RCM for a 1-kg TNT surface explosion in a standard atmosphere. These signatures are for the specific radius r = 2.671 m, at which the blast-wave front arrives at time t = 2.910 ms.

t (ms)	$\Delta p/p_1$	a/a_1	ρ/ρ_1	u/a_1	t (ms)	$\Delta p/p_1$	a/a_1	ρ/ρ_1	u/a_1
0.0000	1.3536	1.1403	1.8100	0.6596	1.8498	0.0725	1.0270	1.0169	0.1484
0.0351	1.2841	1.1355	1.7714	0.6398	1.8915	0.0665	1.0262	1.0128	0.1441
0.0702	1.2243	1.1313	1.7379	0.6234	1.9336	0.0548	1.0246	1.0049	0.1374
0.1057	1.1446	1.1263	1.6906	0.5968	1.9757	0.0480	1.0236	1.0002	0.1327
0.1412	1.0807	1.1215	1.6543	0.5785	2.0177	0.0456	1.0242	0.9967	0.1304
0.1770	1.0494	1.1198	1.6344	0.5702	2.0602	0.0352	1.0228	0.9897	0.1226
0.2128	1.0101	1.1167	1.6119	0.5586	2.1026	0.0272	1.0216	0.9842	0.1183
0.2490	0.9396	1.1110	1.5713	0.5347	2.1453	0.0182	1.0205	0.9777	0.1129
0.2855	0.8722	1.1055	1.5318	0.5087	2.1878	0.0112	1.0195	0.9729	0.1090
0.3216	0.8469	1.1034	1.5170	0.5013	2.2305	0.0085	1.0191	0.9711	0.1063
0.3585	0.8092	1.1002	1.4946	0.4885	2.2733	0.0022	1.0182	0.9668	0.1027
0.3950	0.7640	1.0967	1.4667	0.4725	2.3018	-0.0037	1.0173	0.9627	0.0960
0.4319	0.7304	1.0937	1.4465	0.4622	2.3161	-0.0084	1.0166	0.9594	0.0921
0.4691	0.6821	1.0898	1.4164	0.4399	2.3592	-0.0113	1.0162	0.9574	0.0907
0.5059	0.6520	1.0870	1.3983	0.4288	2.4023	-0.0201	1.0149	0.9513	0.0832
0.5435	0.6254	1.0854	1.3798	0.4200	2.4885	-0.0293	1.0137	0.9447	0.0782
0.5810	0.5981	1.0827	1.3632	0.4103	2.5755	-0.0409	1.0119	0.9366	0.0672
0.6186	0.5656	1.0796	1.3433	0.3953	2.6408	-0.0481	1.0108	0.9316	0.0636
0.6561	0.5398	1.0770	1.3275	0.3851	2.7065	-0.0582	1.0093	0.9245	0.0574
0.6944	0.5151	1.0746	1.3120	0.3728	2.7719	-0.0656	1.0082	0.9193	0.0516
0.7323	0.4941	1.0726	1.2987	0.3659	2.8376	-0.0695	1.0076	0.9166	0.0462
0.7705	0.4614	1.0692	1.2784	0.3498	2.9030	-0.0781	1.0062	0.9105	0.0386
0.8084	0.4492	1.0679	1.2708	0.3463	2.9687	-0.0826	1.0055	0.9073	0.0363
0.8341	0.4350	1.0669	1.2607	0.3385	3.0122	-0.0863	1.0049	0.9047	0.0331
0.8470	0.4287	1.0662	1.2568	0.3359	3.0668	-0.0926	1.0040	0.9003	0.0260
0.8856	0.3998	1.0631	1.2386	0.3240	3.1325	-0.0989	1.0030	0.8958	0.0209
0.9246	0.3785	1.0608	1.2250	0.3138	3.1979	-0.1057	1.0019	0.8910	0.0153
0.9635	0.3623	1.0590	1.2147	0.3075	3.2636	-0.1064	1.0018	0.8905	0.0125
1.0028	0.3462	1.0572	1.2044	0.2975	3.3289	-0.1131	1.0007	0.8857	0.0061
1.0421	0.3300	1.0559	1.1930	0.2902	3.3943	-0.1164	1.0001	0.8834	0.0032
1.0814	0.3146	1.0541	1.1831	0.2835	3.4600	-0.1193	0.9997	0.8813	0.0007
1.1207	0.2930	1.0516	1.1692	0.2725	3.5254	-0.1193	0.9997	0.8813	-0.0023
1.1603	0.2691	1.0488	1.1537	0.2599	3.5911	-0.1254	0.9987	0.8769	-0.0076
1.1999	0.2452	1.0468	1.1365	0.2473	3.6565	-0.1299	0.9979	0.8737	-0.0118
1.2396	0.2337	1.0454	1.1288	0.2397	3.7218	-0.1317	0.9976	0.8724	-0.0147
1.2796	0.2181	1.0435	1.1186	0.2314	3.7876	-0.1352	0.9971	0.8699	-0.0171
1.3195	0.2068	1.0421	1.1112	0.2261	3.8422	-0.1385	0.9965	0.8675	-0.0198
1.3595	0.1959	1.0408	1.1040	0.2214	3.8860	-0.1398	0.9963	0.8666	-0.0217
1.3995	0.1812	1.0389	1.0943	0.2130	3.9513	-0.1414	0.9960	0.8654	-0.0238
1.4399	0.1694	1.0375	1.0865	0.2075	4.0171	-0.1383	0.9966	0.8677	-0.0244
1.4802	0.1481	1.0353	1.0712	0.1961	4.0824	-0.1384	0.9966	0.8676	-0.0250
1.5205	0.1407	1.0343	1.0663	0.1921	4.1481	-0.1390	0.9964	0.8671	-0.0261
1.5612	0.1371	1.0349	1.0618	0.1880	4.2135	-0.1374	0.9967	0.8683	-0.0262
1.6019	0.1209	1.0327	1.0510	0.1783	4.2789	-0.1366	0.9968	0.8689	-0.0262
1.6429	0.1110	1.0314	1.0444	0.1730	4.3446	-0.1376	0.9967	0.8682	-0.0261
1.6839	0.0989	1.0299	1.0361	0.1677	4.4100	-0.1383	0.9966	0.8677	-0.0273
1.7253	0.0939	1.0292	1.0327	0.1637	4.4757	-0.1362	0.9969	0.8692	-0.0250
1.7528	0.0889	1.0285	1.0293	0.1604	4.5410	-0.1336	0.9973	0.8710	-0.0243
1.7667	0.0880	1.0284	1.0287	0.1604					
1.8081	0.0775	1.0277	1.0202	0.1515					

Table B-18. Time histories of overpressure, sound speed, density and flow velocity from the reconstructed blast-wave flow field by the RCM for a 1-kg TNT surface explosion in a standard atmosphere. These signatures are for the specific radius r = 2.786 m, at which the blast-wave front arrives at time t = 3.159 ms.

t (ms)	$\Delta p/p_1$	a/a_1	ρ/ρ_1	u/a_1	t (ms)	$\Delta p/p_1$	a/a_1	ρ/ρ_1	u/a_1
0.0000	1.2316	1.1299	1.7480	0.6144	1.8964	0.0715	1.0226	1.0246	0.1383
0.0365	1.1652	1.1251	1.7105	0.5927	1.9388	0.0659	1.0219	1.0207	0.1340
0.0727	1.1067	1.1210	1.6765	0.5756	1.9816	0.0548	1.0204	1.0130	0.1274
0.1095	1.0472	1.1165	1.6424	0.5571	2.0243	0.0488	1.0196	1.0089	0.1252
0.1460	1.0167	1.1141	1.6247	0.5490	2.0529	0.0430	1.0188	1.0049	0.1221
0.1829	0.9768	1.1110	1.6015	0.5386	2.0671	0.0431	1.0188	1.0050	0.1225
0.2201	0.9129	1.1063	1.5630	0.5137	2.1102	0.0342	1.0176	0.9988	0.1172
0.2570	0.8592	1.1018	1.5315	0.4945	2.1533	0.0304	1.0170	0.9962	0.1147
0.2945	0.8222	1.0987	1.5096	0.4820	2.1965	0.0230	1.0160	0.9911	0.1077
0.3321	0.7850	1.0958	1.4865	0.4698	2.2396	0.0148	1.0149	0.9852	0.1022
0.3696	0.7415	1.0923	1.4597	0.4542	2.2830	0.0106	1.0143	0.9823	0.0985
0.4072	0.7112	1.0895	1.4415	0.4433	2.3265	0.0057	1.0136	0.9789	0.0963
0.4454	0.6923	1.0878	1.4301	0.4359	2.3592	0.0026	1.0132	0.9768	0.0941
0.4833	0.6414	1.0832	1.3990	0.4165	2.3919	-0.0037	1.0122	0.9723	0.0881
0.5216	0.6162	1.0808	1.3834	0.4050	2.4246	-0.0097	1.0114	0.9681	0.0835
0.5595	0.5996	1.0793	1.3733	0.3994	2.4576	-0.0151	1.0106	0.9644	0.0796
0.5852	0.5806	1.0782	1.3595	0.3914	2.4903	-0.0201	1.0098	0.9609	0.0764
0.5981	0.5697	1.0772	1.3528	0.3869	2.5556	-0.0238	1.0093	0.9583	0.0740
0.6367	0.5287	1.0732	1.3274	0.3695	2.6214	-0.0322	1.0081	0.9524	0.0680
0.6756	0.5162	1.0722	1.3189	0.3656	2.6867	-0.0409	1.0068	0.9463	0.0591
0.7145	0.4873	1.0692	1.3009	0.3540	2.7524	-0.0453	1.0061	0.9432	0.0560
0.7538	0.4527	1.0660	1.2782	0.3390	2.7851	-0.0539	1.0048	0.9371	0.0498
0.7931	0.4417	1.0649	1.2712	0.3354	2.8508	-0.0613	1.0037	0.9318	0.0444
0.8324	0.4240	1.0631	1.2601	0.3260	2.9162	-0.0650	1.0031	0.9293	0.0391
0.8717	0.4116	1.0617	1.2522	0.3212	2.9816	-0.0738	1.0022	0.9222	0.0323
0.9113	0.3853	1.0590	1.2353	0.3089	3.0473	-0.0773	1.0017	0.9197	0.0295
0.9510	0.3631	1.0565	1.2212	0.2994	3.1127	-0.0841	1.0006	0.9148	0.0232
0.9906	0.3478	1.0549	1.2112	0.2938	3.1780	-0.0915	0.9994	0.9096	0.0176
1.0306	0.3300	1.0529	1.1997	0.2853	3.2438	-0.0969	0.9986	0.9057	0.0128
1.0706	0.3117	1.0508	1.1879	0.2753	3.3091	-0.1015	0.9979	0.9024	0.0098
1.1106	0.2900	1.0487	1.1729	0.2650	3.3748	-0.1052	0.9973	0.8997	0.0047
1.1506	0.2675	1.0461	1.1582	0.2509	3.4402	-0.1108	0.9964	0.8957	-0.0007
1.1909	0.2535	1.0444	1.1491	0.2440	3.5059	-0.1121	0.9962	0.8947	-0.0021
1.2312	0.2375	1.0426	1.1385	0.2342	3.5713	-0.1132	0.9960	0.8940	-0.0036
1.2716	0.2243	1.0410	1.1298	0.2283	3.6040	-0.1134	0.9960	0.8938	-0.0052
1.3122	0.2096	1.0396	1.1192	0.2201	3.6697	-0.1189	0.9951	0.8899	-0.0094
1.3529	0.1984	1.0382	1.1118	0.2150	3.7351	-0.1215	0.9947	0.8880	-0.0110
1.3940	0.1868	1.0368	1.1041	0.2066	3.8008	-0.1262	0.9939	0.8846	-0.0152
1.4350	0.1760	1.0354	1.0969	0.2010	3.8661	-0.1300	0.9933	0.8818	-0.0175
1.4764	0.1650	1.0340	1.0896	0.1954	3.9319	-0.1306	0.9932	0.8814	-0.0201
1.5038	0.1509	1.0323	1.0801	0.1873	3.9972	-0.1338	0.9922	0.8798	-0.0233
1.5177	0.1499	1.0321	1.0794	0.1873	4.0629	-0.1353	0.9920	0.8788	-0.0250
1.5591	0.1385	1.0315	1.0700	0.1797	4.1283	-0.1356	0.9919	0.8785	-0.0258
1.6008	0.1326	1.0308	1.0660	0.1774	4.1940	-0.1339	0.9922	0.8798	-0.0259
1.6426	0.1217	1.0293	1.0586	0.1687	4.2594	-0.1345	0.9921	0.8793	-0.0271
1.6846	0.1140	1.0283	1.0535	0.1645	4.3248	-0.1327	0.9924	0.8807	-0.0274
1.7267	0.1064	1.0273	1.0483	0.1586	4.3905	-0.1299	0.9929	0.8827	-0.0276
1.7688	0.0956	1.0259	1.0410	0.1527	4.4559	-0.1308	0.9927	0.8820	-0.0290
1.8112	0.0883	1.0249	1.0360	0.1486	4.5216	-0.1314	0.9926	0.8816	-0.0301
1.8536	0.0800	1.0238	1.0304	0.1450	4.5762	-0.1291	0.9930	0.8832	-0.0283

Table B-19. Time histories of overpressure, sound speed, density and flow velocity from the reconstructed blast-wave flow field by the RCM for a 1-kg TNT surface explosion in a standard atmosphere. These signatures are for the specific radius r = 2.950 m, at which the blast-wave front arrives at time t = 3.491 ms.

t (ms)	$\Delta p/p_1$	a/a_1	ρ/ρ_1	u/a_1	t (ms)	$\Delta p/p_1$	a/a_1	ρ/ρ_1	u/a_1
0.0000	1.0844	1.1170	1.6705	0.5590	1.9075	0.0842	1.0208	1.0405	0.1365
0.0376	1.0499	1.1144	1.6506	0.5495	1.9510	0.0731	1.0193	1.0329	0.1293
0.0751	0.9899	1.1097	1.6160	0.5300	1.9944	0.0680	1.0186	1.0293	0.1268
0.1134	0.9654	1.1078	1.6016	0.5208	2.0271	0.0632	1.0179	1.0260	0.1227
0.1513	0.9357	1.1058	1.5829	0.5138	2.0598	0.0574	1.0172	1.0221	0.1180
0.1895	0.8738	1.1008	1.5464	0.4904	2.0925	0.0519	1.0164	1.0182	0.1150
0.2274	0.8239	1.0966	1.5168	0.4714	2.1255	0.0469	1.0157	1.0148	0.1114
0.2531	0.8010	1.0946	1.5031	0.4646	2.1582	0.0433	1.0152	1.0123	0.1097
0.2660	0.7880	1.0935	1.4953	0.4596	2.1909	0.0420	1.0150	1.0114	0.1086
0.3046	0.7530	1.0908	1.4733	0.4477	2.2236	0.0398	1.0147	1.0098	0.1076
0.3435	0.7162	1.0875	1.4511	0.4341	2.2566	0.0333	1.0139	1.0052	0.1023
0.3825	0.6862	1.0848	1.4329	0.4237	2.2893	0.0266	1.0129	1.0006	0.0983
0.4218	0.6687	1.0832	1.4221	0.4157	2.3220	0.0245	1.0126	0.9991	0.0976
0.4611	0.6307	1.0797	1.3988	0.4006	2.3547	0.0155	1.0114	0.9928	0.0913
0.5003	0.5972	1.0765	1.3782	0.3871	2.3877	0.0106	1.0107	0.9894	0.0887
0.5396	0.5860	1.0754	1.3713	0.3841	2.4204	0.0097	1.0105	0.9887	0.0872
0.5793	0.5633	1.0734	1.3568	0.3769	2.4312	0.0071	1.0102	0.9870	0.0858
0.6189	0.5234	1.0695	1.3320	0.3593	2.4531	0.0015	1.0093	0.9830	0.0821
0.6586	0.5006	1.0672	1.3177	0.3492	2.5188	-0.0088	1.0079	0.9758	0.0748
0.6985	0.4771	1.0647	1.3029	0.3381	2.5842	-0.0132	1.0072	0.9727	0.0695
0.7385	0.4551	1.0629	1.2879	0.3274	2.6495	-0.0204	1.0062	0.9675	0.0645
0.7785	0.4343	1.0608	1.2747	0.3190	2.7152	-0.0261	1.0054	0.9635	0.0605
0.8185	0.4199	1.0592	1.2655	0.3117	2.7806	-0.0363	1.0039	0.9563	0.0522
0.8588	0.4064	1.0578	1.2569	0.3069	2.8460	-0.0409	1.0032	0.9530	0.0487
0.8992	0.3896	1.0563	1.2454	0.2997	2.9117	-0.0477	1.0022	0.9481	0.0450
0.9395	0.3633	1.0534	1.2285	0.2875	2.9771	-0.0578	1.0014	0.9395	0.0373
0.9802	0.3509	1.0521	1.2205	0.2800	3.0428	-0.0634	1.0006	0.9355	0.0340
1.0209	0.3303	1.0498	1.2072	0.2701	3.1081	-0.0690	0.9997	0.9315	0.0289
1.0619	0.3201	1.0487	1.2004	0.2660	3.1739	-0.0742	0.9989	0.9278	0.0242
1.1029	0.3043	1.0469	1.1900	0.2599	3.2392	-0.0778	0.9984	0.9252	0.0213
1.1443	0.2798	1.0441	1.1740	0.2478	3.2719	-0.0814	0.9978	0.9227	0.0186
1.1718	0.2629	1.0421	1.1629	0.2392	3.3376	-0.0894	0.9966	0.9169	0.0122
1.1857	0.2616	1.0420	1.1621	0.2392	3.4030	-0.0928	0.9960	0.9144	0.0084
1.2271	0.2430	1.0397	1.1497	0.2289	3.4687	-0.0951	0.9957	0.9128	0.0049
1.2688	0.2311	1.0383	1.1419	0.2235	3.5341	-0.0967	0.9954	0.9116	0.0033
1.3105	0.2198	1.0374	1.1334	0.2157	3.5998	-0.1021	0.9946	0.9078	-0.0030
1.3526	0.2082	1.0360	1.1257	0.2099	3.6652	-0.1057	0.9940	0.9051	-0.0068
1.3946	0.1944	1.0343	1.1165	0.2010	3.7309	-0.1075	0.9937	0.9039	-0.0075
1.4367	0.1872	1.0334	1.1116	0.1981	3.7963	-0.1118	0.9930	0.9008	-0.0128
1.4791	0.1726	1.0316	1.1018	0.1903	3.8620	-0.1142	0.9926	0.8990	-0.0144
1.5216	0.1619	1.0303	1.0946	0.1849	3.9273	-0.1182	0.9920	0.8961	-0.0181
1.5643	0.1458	1.0285	1.0830	0.1734	3.9927	-0.1204	0.9916	0.8945	-0.0204
1.6068	0.1389	1.0277	1.0784	0.1698	4.0584	-0.1221	0.9914	0.8932	-0.0236
1.6495	0.1322	1.0271	1.0733	0.1660	4.1238	-0.1240	0.9911	0.8919	-0.0256
1.6923	0.1236	1.0260	1.0674	0.1618	4.1895	-0.1262	0.9907	0.8902	-0.0275
1.7208	0.1128	1.0246	1.0601	0.1546	4.2441	-0.1278	0.9904	0.8891	-0.0293
1.7351	0.1096	1.0241	1.0579	0.1526	4.2876	-0.1272	0.9905	0.8895	-0.0294
1.7782	0.1043	1.0234	1.0543	0.1488	4.3533	-0.1254	0.9901	0.8923	-0.0296
1.8213	0.0953	1.0222	1.0482	0.1425	4.4187	-0.1265	0.9899	0.8915	-0.0303
1.8644	0.0910	1.0217	1.0452	0.1405	4.4844	-0.1254	0.9901	0.8923	-0.0300

Table B-20. Time histories of overpressure, sound speed, density and flow velocity from the reconstructed blast-wave flow field by the RCM for a 1-kg TNT surface explosion in a standard atmosphere. These signatures are for the specific radius r = 3.071 m, at which the blast-wave front arrives at time t = 3.744 ms.

t (ms)	$\Delta p/p_1$	a/a_1	ρ/ρ_1	u/a_1	t (ms)	$\Delta p/p_1$	a/a_1	ρ/ρ_1	u/a_1
0.0000	1.0016	1.1096	1.6258	0.5260	2.0362	0.0668	1.0169	1.0317	0.1193
0.0129	0.9777	1.1077	1.6119	0.5167	2.1015	0.0550	1.0152	1.0236	0.1118
0.0515	0.9491	1.1057	1.5943	0.5091	2.1673	0.0479	1.0143	1.0187	0.1060
0.0904	0.9183	1.1032	1.5762	0.4989	2.1999	0.0434	1.0136	1.0155	0.1032
0.1293	0.8620	1.0985	1.5430	0.4793	2.2657	0.0344	1.0124	1.0092	0.0983
0.1686	0.8172	1.0947	1.5163	0.4624	2.3310	0.0255	1.0111	1.0031	0.0926
0.2079	0.7845	1.0919	1.4967	0.4516	2.3964	0.0146	1.0096	0.9954	0.0860
0.2472	0.7528	1.0893	1.4773	0.4380	2.4621	0.0083	1.0087	0.9910	0.0825
0.2865	0.7321	1.0874	1.4648	0.4315	2.5275	0.0012	1.0077	0.9860	0.0764
0.3261	0.6923	1.0841	1.4400	0.4169	2.5928	-0.0094	1.0061	0.9785	0.0690
0.3658	0.6637	1.0815	1.4225	0.4068	2.6586	-0.0182	1.0049	0.9723	0.0628
0.4054	0.6475	1.0801	1.4123	0.4018	2.7239	-0.0238	1.0043	0.9678	0.0589
0.4454	0.5982	1.0754	1.3819	0.3824	2.7896	-0.0286	1.0036	0.9644	0.0547
0.4854	0.5747	1.0732	1.3673	0.3732	2.8550	-0.0372	1.0023	0.9583	0.0470
0.5254	0.5598	1.0717	1.3580	0.3695	2.9207	-0.0412	1.0018	0.9555	0.0442
0.5654	0.5371	1.0695	1.3437	0.3598	2.9861	-0.0480	1.0007	0.9506	0.0373
0.6057	0.5083	1.0667	1.3257	0.3465	3.0188	-0.0501	1.0004	0.9491	0.0354
0.6460	0.4868	1.0649	1.3110	0.3364	3.0845	-0.0552	0.9996	0.9454	0.0315
0.6864	0.4625	1.0624	1.2957	0.3264	3.1499	-0.0616	0.9987	0.9409	0.0275
0.7271	0.4466	1.0608	1.2856	0.3188	3.2156	-0.0671	0.9978	0.9369	0.0219
0.7677	0.4212	1.0581	1.2695	0.3078	3.2810	-0.0707	0.9973	0.9344	0.0197
0.8088	0.4058	1.0565	1.2595	0.3014	3.3467	-0.0774	0.9963	0.9295	0.0144
0.8498	0.3928	1.0551	1.2511	0.2966	3.4120	-0.0848	0.9951	0.9242	0.0079
0.8912	0.3787	1.0536	1.2421	0.2885	3.4778	-0.0881	0.9946	0.9218	0.0043
0.9186	0.3609	1.0516	1.2306	0.2795	3.5431	-0.0912	0.9941	0.9196	0.0016
0.9325	0.3593	1.0514	1.2295	0.2795	3.6088	-0.0926	0.9939	0.9185	0.0000
0.9739	0.3395	1.0493	1.2166	0.2702	3.6742	-0.0989	0.9929	0.9140	-0.0052
1.0156	0.3195	1.0470	1.2036	0.2605	3.7396	-0.1011	0.9926	0.9124	-0.0082
1.0574	0.3116	1.0465	1.1976	0.2576	3.8053	-0.1036	0.9922	0.9106	-0.0104
1.0994	0.3003	1.0452	1.1902	0.2526	3.8707	-0.1049	0.9920	0.9096	-0.0118
1.1415	0.2846	1.0434	1.1799	0.2423	3.9364	-0.1091	0.9913	0.9066	-0.0156
1.1836	0.2655	1.0412	1.1673	0.2325	3.9910	-0.1122	0.9908	0.9044	-0.0192
1.2260	0.2440	1.0387	1.1530	0.2212	4.0344	-0.1142	0.9905	0.9029	-0.0214
1.2684	0.2333	1.0374	1.1459	0.2161	4.1002	-0.1169	0.9900	0.9009	-0.0240
1.3112	0.2198	1.0358	1.1370	0.2093	4.1655	-0.1182	0.9898	0.9000	-0.0257
1.3536	0.2040	1.0339	1.1264	0.2002	4.2312	-0.1197	0.9896	0.8989	-0.0280
1.3964	0.1957	1.0329	1.1207	0.1941	4.2966	-0.1217	0.9893	0.8974	-0.0298
1.4392	0.1846	1.0315	1.1133	0.1882	4.3623	-0.1218	0.9893	0.8974	-0.0303
1.4677	0.1757	1.0304	1.1073	0.1836	4.4277	-0.1209	0.9894	0.8980	-0.0312
1.4819	0.1742	1.0302	1.1063	0.1829	4.4934	-0.1213	0.9893	0.8977	-0.0315
1.5250	0.1643	1.0291	1.0993	0.1776	4.5588	-0.1206	0.9895	0.8982	-0.0309
1.5682	0.1543	1.0279	1.0926	0.1724	4.6245	-0.1207	0.9895	0.8981	-0.0312
1.6113	0.1413	1.0262	1.0837	0.1645	4.6899	-0.1204	0.9895	0.8984	-0.0321
1.6544	0.1326	1.0251	1.0778	0.1588					
1.6978	0.1250	1.0241	1.0726	0.1552					
1.7413	0.1131	1.0226	1.0645	0.1485					
1.7740	0.1064	1.0217	1.0599	0.1448					
1.8394	0.0922	1.0203	1.0493	0.1359					
1.9051	0.0863	1.0195	1.0452	0.1326					
1.9705	0.0795	1.0186	1.0406	0.1265					

Table B-21. Time histories of overpressure, sound speed, density and flow velocity from the reconstructed blast-wave flow field by the RCM for a 1-kg TNT surface explosion in a standard atmosphere. These signatures are for the specific radius r = 3.286 m, at which the blast-wave front arrives at time t = 4.229 ms.

t (ms)	$\Delta p/p_1$	a/a_1	ρ/ρ_1	u/a_1	t (ms)	$\Delta p/p_1$	a/a_1	ρ/ρ_1	u/a_1
0.0000	0.8870	1.0990	1.5623	0.4781	1.8783	0.0970	1.0185	1.0575	0.1277
0.0400	0.8602	1.0968	1.5464	0.4710	1.9440	0.0867	1.0172	1.0503	0.1214
0.0800	0.8063	1.0922	1.5141	0.4485	2.0094	0.0798	1.0162	1.0455	0.1178
0.1203	0.7610	1.0883	1.4869	0.4315	2.0748	0.0681	1.0147	1.0374	0.1098
0.1606	0.7383	1.0863	1.4731	0.4238	2.1405	0.0607	1.0137	1.0322	0.1056
0.2010	0.7021	1.0830	1.4511	0.4101	2.2058	0.0521	1.0125	1.0263	0.1002
0.2417	0.6726	1.0804	1.4328	0.3997	2.2716	0.0436	1.0113	1.0204	0.0949
0.2823	0.6504	1.0784	1.4192	0.3922	2.3369	0.0388	1.0107	1.0170	0.0913
0.3234	0.6277	1.0762	1.4052	0.3832	2.4023	0.0306	1.0096	1.0112	0.0859
0.3644	0.6132	1.0749	1.3962	0.3780	2.4680	0.0220	1.0084	1.0052	0.0801
0.4058	0.5687	1.0706	1.3685	0.3587	2.5226	0.0150	1.0074	1.0002	0.0751
0.4332	0.5514	1.0689	1.3577	0.3513	2.5664	0.0114	1.0070	0.9974	0.0719
0.4472	0.5492	1.0687	1.3563	0.3513	2.6318	0.0028	1.0058	0.9914	0.0662
0.4885	0.5351	1.0675	1.3472	0.3450	2.6975	-0.0064	1.0044	0.9848	0.0596
0.5303	0.5149	1.0655	1.3345	0.3376	2.7629	-0.0117	1.0037	0.9811	0.0559
0.5720	0.5002	1.0641	1.3249	0.3316	2.8286	-0.0175	1.0028	0.9770	0.0510
0.6140	0.4652	1.0605	1.3028	0.3160	2.8940	-0.0218	1.0022	0.9740	0.0480
0.6561	0.4504	1.0590	1.2934	0.3080	2.9593	-0.0325	1.0006	0.9663	0.0400
0.6982	0.4336	1.0572	1.2826	0.3010	3.0250	-0.0359	1.0001	0.9639	0.0373
0.7406	0.4172	1.0556	1.2718	0.2941	3.0904	-0.0393	0.9996	0.9614	0.0342
0.7830	0.3940	1.0531	1.2569	0.2834	3.1561	-0.0469	0.9985	0.9559	0.0288
0.8258	0.3792	1.0515	1.2473	0.2770	3.2215	-0.0511	0.9979	0.9530	0.0255
0.8682	0.3659	1.0501	1.2387	0.2713	3.2872	-0.0565	0.9970	0.9491	0.0205
0.9110	0.3575	1.0492	1.2332	0.2669	3.3526	-0.0626	0.9961	0.9447	0.0160
0.9538	0.3350	1.0467	1.2185	0.2564	3.4183	-0.0658	0.9956	0.9424	0.0138
0.9823	0.3229	1.0454	1.2106	0.2506	3.4837	-0.0723	0.9946	0.9377	0.0090
0.9965	0.3189	1.0449	1.2080	0.2483	3.5164	-0.0738	0.9944	0.9366	0.0080
1.0396	0.3027	1.0432	1.1970	0.2416	3.5821	-0.0781	0.9938	0.9335	0.0039
1.0828	0.2934	1.0421	1.1909	0.2376	3.6474	-0.0831	0.9930	0.9299	0.0001
1.1259	0.2849	1.0412	1.1853	0.2338	3.7132	-0.0854	0.9926	0.9282	-0.0028
1.1690	0.2675	1.0392	1.1738	0.2255	3.7785	-0.0870	0.9924	0.9271	-0.0041
1.2125	0.2422	1.0362	1.1570	0.2117	3.8442	-0.0920	0.9916	0.9235	-0.0080
1.2559	0.2353	1.0354	1.1524	0.2074	3.9096	-0.0968	0.9909	0.9200	-0.0120
1.2886	0.2243	1.0340	1.1451	0.2013	3.9753	-0.0965	0.9909	0.9202	-0.0127
1.3213	0.2154	1.0329	1.1391	0.1962	4.0407	-0.0974	0.9908	0.9195	-0.0145
1.3540	0.2079	1.0323	1.1334	0.1931	4.1064	-0.1015	0.9901	0.9166	-0.0185
1.3870	0.1982	1.0311	1.1269	0.1872	4.1718	-0.1035	0.9898	0.9151	-0.0199
1.4197	0.1917	1.0303	1.1226	0.1844	4.2375	-0.1075	0.9892	0.9122	-0.0235
1.4524	0.1791	1.0288	1.1141	0.1767	4.3029	-0.1094	0.9888	0.9108	-0.0263
1.4851	0.1755	1.0283	1.1117	0.1753	4.3686	-0.1106	0.9887	0.9099	-0.0279
1.5181	0.1684	1.0274	1.1068	0.1705	4.4343	-0.1123	0.9884	0.9087	-0.0298
1.5508	0.1633	1.0268	1.1033	0.1683	4.4997	-0.1135	0.9882	0.9078	-0.0319
1.5835	0.1587	1.0262	1.1002	0.1655	4.5654	-0.1136	0.9882	0.9078	-0.0324
1.6161	0.1497	1.0254	1.0935	0.1606	4.6311	-0.1130	0.9883	0.9082	-0.0329
1.6492	0.1376	1.0238	1.0853	0.1523	4.6968	-0.1131	0.9883	0.9081	-0.0333
1.6819	0.1335	1.0233	1.0825	0.1503	4.7625	-0.1123	0.9884	0.9087	-0.0329
1.6926	0.1324	1.0232	1.0817	0.1500					
1.7145	0.1252	1.0222	1.0768	0.1453					
1.7472	0.1220	1.0218	1.0746	0.1439					
1.8129	0.1087	1.0201	1.0655	0.1341					

Table B-22. Time histories of overpressure, sound speed, density and flow velocity from the reconstructed blast-wave flow field by the RCM for a 1-kg TNT surface explosion in a standard atmosphere. These signatures are for the specific radius r = 3.479 m, at which the blast-wave front arrives at time t = 4.662 ms.

t (ms)	$\Delta p/p_1$	a/a_1	ρ/ρ_1	u/a_1	t (ms)	$\Delta p/p_1$	a/a_1	ρ/ρ_1	u/a_1
0.0000	0.7838	1.0893	1.5034	0.4335	1.7726	0.1228	1.0205	1.0782	0.1360
0.0139	0.7708	1.0881	1.4956	0.4289	1.8383	0.1130	1.0192	1.0714	0.1309
0.0553	0.7337	1.0848	1.4731	0.4142	1.9037	0.0974	1.0172	1.0607	0.1212
0.0970	0.7105	1.0828	1.4590	0.4062	1.9691	0.0847	1.0155	1.0518	0.1133
0.1387	0.6806	1.0801	1.4407	0.3944	2.0348	0.0816	1.0151	1.0497	0.1106
0.1808	0.6454	1.0768	1.4191	0.3808	2.0894	0.0754	1.0143	1.0454	0.1070
0.2229	0.6254	1.0749	1.4067	0.3732	2.1332	0.0693	1.0134	1.0412	0.1037
0.2650	0.6164	1.0743	1.4006	0.3722	2.1985	0.0592	1.0121	1.0341	0.0965
0.3074	0.5943	1.0722	1.3869	0.3632	2.2643	0.0514	1.0110	1.0287	0.0912
0.3498	0.5791	1.0707	1.3774	0.3584	2.3296	0.0430	1.0098	1.0228	0.0863
0.3926	0.5335	1.0663	1.3488	0.3369	2.3953	0.0389	1.0093	1.0199	0.0843
0.4350	0.5178	1.0647	1.3389	0.3315	2.4607	0.0314	1.0082	1.0147	0.0796
0.4777	0.5049	1.0637	1.3301	0.3263	2.5261	0.0240	1.0072	1.0094	0.0743
0.5205	0.4904	1.0622	1.3209	0.3202	2.5918	0.0163	1.0061	1.0040	0.0700
0.5490	0.4773	1.0609	1.3126	0.3149	2.6572	0.0104	1.0053	0.9999	0.0654
0.5633	0.4617	1.0593	1.3027	0.3072	2.7229	0.0027	1.0042	0.9944	0.0596
0.6064	0.4415	1.0572	1.2896	0.2984	2.7883	-0.0051	1.0030	0.9889	0.0539
0.6495	0.4288	1.0559	1.2815	0.2921	2.8540	-0.0114	1.0022	0.9842	0.0500
0.6926	0.4139	1.0543	1.2720	0.2848	2.9193	-0.0170	1.0014	0.9802	0.0455
0.7357	0.3985	1.0527	1.2620	0.2781	2.9851	-0.0209	1.0009	0.9775	0.0426
0.7792	0.3766	1.0504	1.2477	0.2678	3.0504	-0.0298	0.9995	0.9711	0.0360
0.8227	0.3654	1.0492	1.2404	0.2631	3.0831	-0.0309	0.9994	0.9703	0.0347
0.8554	0.3568	1.0482	1.2348	0.2602	3.1488	-0.0345	0.9988	0.9677	0.0324
0.8880	0.3482	1.0473	1.2292	0.2559	3.2142	-0.0402	0.9980	0.9636	0.0282
0.9207	0.3394	1.0463	1.2235	0.2527	3.2799	-0.0446	0.9974	0.9604	0.0240
0.9538	0.3256	1.0448	1.2144	0.2447	3.3453	-0.0486	0.9968	0.9576	0.0211
0.9864	0.3180	1.0439	1.2094	0.2416	3.4110	-0.0523	0.9962	0.9549	0.0175
1.0191	0.3036	1.0423	1.2000	0.2339	3.4764	-0.0572	0.9955	0.9514	0.0133
1.0518	0.2960	1.0414	1.1950	0.2306	3.5421	-0.0617	0.9948	0.9481	0.0095
1.0848	0.2852	1.0402	1.1878	0.2251	3.6075	-0.0648	0.9943	0.9459	0.0070
1.1175	0.2796	1.0396	1.1841	0.2230	3.6732	-0.0704	0.9935	0.9419	0.0021
1.1502	0.2683	1.0382	1.1766	0.2167	3.7385	-0.0747	0.9928	0.9387	-0.0007
1.1829	0.2568	1.0369	1.1690	0.2114	3.8043	-0.0776	0.9924	0.9366	-0.0039
1.2159	0.2417	1.0351	1.1589	0.2020	3.8696	-0.0802	0.9919	0.9348	-0.0062
1.2486	0.2325	1.0340	1.1528	0.1976	3.9353	-0.0845	0.9913	0.9316	-0.0100
1.2594	0.2311	1.0340	1.1515	0.1972	4.0011	-0.0877	0.9908	0.9293	-0.0117
1.2813	0.2212	1.0328	1.1449	0.1916	4.0664	-0.0897	0.9905	0.9279	-0.0143
1.3140	0.2149	1.0320	1.1407	0.1884	4.1321	-0.0918	0.9902	0.9263	-0.0161
1.3470	0.2062	1.0310	1.1349	0.1837	4.1979	-0.0926	0.9900	0.9258	-0.0176
1.3797	0.1998	1.0302	1.1305	0.1803	4.2636	-0.0961	0.9895	0.9232	-0.0211
1.4124	0.1902	1.0290	1.1241	0.1749	4.3293	-0.0990	0.9890	0.9211	-0.0240
1.4451	0.1781	1.0275	1.1159	0.1686	4.3950	-0.1008	0.9888	0.9198	-0.0258
1.4778	0.1750	1.0271	1.1138	0.1667	4.4604	-0.1028	0.9884	0.9183	-0.0283
1.5108	0.1714	1.0267	1.1113	0.1642	4.5261	-0.1040	0.9882	0.9174	-0.0297
1.5435	0.1621	1.0255	1.1050	0.1589	4.5918	-0.1052	0.9881	0.9165	-0.0318
1.5762	0.1585	1.0250	1.1026	0.1570	4.6575	-0.1075	0.9877	0.9149	-0.0328
1.6088	0.1536	1.0245	1.0992	0.1548	4.7229	-0.1075	0.9877	0.9149	-0.0333
1.6415	0.1478	1.0237	1.0952	0.1517	4.7886	-0.1075	0.9877	0.9149	-0.0334
1.6742	0.1399	1.0227	1.0899	0.1468					
1.7072	0.1310	1.0216	1.0838	0.1417					

Table B-23. Time histories of overpressure, sound speed, density and flow velocity from the reconstructed blast-wave flow field by the RCM for a 1-kg TNT surface explosion in a standard atmosphere. These signatures are for the specific radius r = 3.721 m, at which the blast-wave front arrives at time t = 5.211 ms.

t (ms)	$\Delta p/p_1$	a/a_1	ρ/ρ_1	u/a_1	t (ms)	$\Delta p/p_1$	a/a_1	ρ/ρ_1	u/a_1
0.0000	0.6881	1.0799	1.4474	0.3906	1.6168	0.1484	1.0227	1.0980	0.1451
0.0143	0.6749	1.0787	1.4394	0.3847	1.6822	0.1390	1.0215	1.0916	0.1399
0.0574	0.6564	1.0770	1.4279	0.3787	1.7479	0.1275	1.0200	1.0837	0.1326
0.1005	0.6300	1.0746	1.4117	0.3675	1.8133	0.1162	1.0185	1.0759	0.1255
0.1436	0.6008	1.0718	1.3935	0.3560	1.8790	0.1073	1.0174	1.0698	0.1209
0.1867	0.5891	1.0707	1.3862	0.3519	1.9444	0.0944	1.0157	1.0609	0.1131
0.2302	0.5684	1.0687	1.3732	0.3443	2.0101	0.0874	1.0148	1.0560	0.1082
0.2736	0.5554	1.0674	1.3650	0.3394	2.0755	0.0781	1.0135	1.0496	0.1026
0.3063	0.5266	1.0646	1.3469	0.3267	2.1412	0.0727	1.0128	1.0458	0.0988
0.3390	0.5070	1.0626	1.3345	0.3175	2.2065	0.0658	1.0119	1.0410	0.0942
0.3717	0.4950	1.0614	1.3269	0.3135	2.2719	0.0582	1.0108	1.0357	0.0892
0.4047	0.4909	1.0610	1.3244	0.3115	2.3376	0.0484	1.0095	1.0288	0.0829
0.4374	0.4794	1.0598	1.3170	0.3070	2.4030	0.0419	1.0086	1.0242	0.0784
0.4701	0.4668	1.0586	1.3090	0.3012	2.4687	0.0372	1.0080	1.0209	0.0760
0.5028	0.4612	1.0580	1.3054	0.2997	2.5233	0.0346	1.0076	1.0191	0.0737
0.5358	0.4379	1.0556	1.2905	0.2886	2.5668	0.0294	1.0069	1.0154	0.0700
0.5685	0.4216	1.0539	1.2801	0.2814	2.6325	0.0232	1.0061	1.0108	0.0661
0.6012	0.4090	1.0526	1.2717	0.2751	2.6979	0.0145	1.0049	1.0047	0.0602
0.6339	0.3981	1.0514	1.2646	0.2710	2.7636	0.0094	1.0042	1.0010	0.0572
0.6669	0.3912	1.0507	1.2602	0.2671	2.8289	0.0030	1.0032	0.9965	0.0524
0.6996	0.3830	1.0498	1.2549	0.2640	2.8947	-0.0043	1.0022	0.9913	0.0471
0.7104	0.3774	1.0492	1.2512	0.2615	2.9600	-0.0095	1.0015	0.9876	0.0435
0.7323	0.3677	1.0481	1.2449	0.2568	3.0257	-0.0137	1.0008	0.9846	0.0400
0.7650	0.3560	1.0469	1.2373	0.2515	3.0911	-0.0177	1.0003	0.9818	0.0371
0.7980	0.3491	1.0461	1.2328	0.2480	3.1568	-0.0217	0.9997	0.9790	0.0336
0.8307	0.3417	1.0453	1.2279	0.2451	3.2222	-0.0296	0.9985	0.9733	0.0278
0.8634	0.3349	1.0445	1.2235	0.2416	3.2879	-0.0318	0.9982	0.9717	0.0257
0.8960	0.3244	1.0434	1.2165	0.2373	3.3536	-0.0382	0.9973	0.9671	0.0210
0.9287	0.3159	1.0425	1.2109	0.2323	3.4190	-0.0430	0.9966	0.9637	0.0181
0.9618	0.3030	1.0410	1.2024	0.2259	3.4847	-0.0459	0.9961	0.9616	0.0158
0.9944	0.2896	1.0395	1.1935	0.2185	3.5504	-0.0494	0.9956	0.9590	0.0133
1.0271	0.2820	1.0386	1.1885	0.2157	3.6161	-0.0539	0.9949	0.9558	0.0094
1.0598	0.2741	1.0377	1.1833	0.2121	3.6819	-0.0583	0.9943	0.9526	0.0059
1.0925	0.2679	1.0370	1.1791	0.2098	3.7472	-0.0636	0.9935	0.9488	0.0012
1.1252	0.2609	1.0361	1.1745	0.2059	3.8129	-0.0663	0.9930	0.9468	-0.0010
1.1582	0.2541	1.0353	1.1699	0.2022	3.8787	-0.0696	0.9925	0.9444	-0.0043
1.1909	0.2442	1.0342	1.1633	0.1967	3.9444	-0.0727	0.9921	0.9421	-0.0069
1.2236	0.2353	1.0331	1.1574	0.1923	4.0101	-0.0751	0.9917	0.9404	-0.0092
1.2563	0.2199	1.0314	1.1468	0.1844	4.0755	-0.0777	0.9913	0.9386	-0.0112
1.2893	0.2180	1.0311	1.1455	0.1836	4.1412	-0.0806	0.9909	0.9365	-0.0140
1.3220	0.2086	1.0300	1.1392	0.1780	4.2069	-0.0847	0.9902	0.9335	-0.0176
1.3547	0.2001	1.0290	1.1335	0.1737	4.2726	-0.0847	0.9902	0.9334	-0.0180
1.3873	0.1944	1.0283	1.1297	0.1700	4.3380	-0.0860	0.9900	0.9325	-0.0192
1.4200	0.1841	1.0272	1.1223	0.1647	4.4037	-0.0899	0.9894	0.9297	-0.0224
1.4531	0.1755	1.0261	1.1165	0.1597	4.4694	-0.0914	0.9892	0.9286	-0.0239
1.4858	0.1689	1.0253	1.1120	0.1558	4.5351	-0.0944	0.9887	0.9264	-0.0269
1.5184	0.1626	1.0245	1.1077	0.1526	4.6009	-0.0955	0.9886	0.9256	-0.0282
1.5403	0.1601	1.0242	1.1060	0.1513	4.6666	-0.0976	0.9882	0.9240	-0.0301
1.5511	0.1596	1.0241	1.1057	0.1513	4.7323	-0.0989	0.9880	0.9231	-0.0318
1.5842	0.1524	1.0232	1.1008	0.1475	4.7977	-0.1004	0.9878	0.9220	-0.0334

Table B-24. Time histories of overpressure, sound speed, density and flow velocity from the reconstructed blast-wave flow field by the RCM for a 1-kg TNT surface explosion in a standard atmosphere. These signatures are for the specific radius r = 4.021 m, at which the blast-wave front arrives at time t = 5.922 ms.

t (ms)	$\Delta p/p_1$	a/a_1	ρ/ρ_1	u/a_1	t (ms)	$\Delta p/p_1$	a/a_1	ρ/ρ_1	u/a_1
0.0000	0.5961	1.0707	1.3923	0.3469	1.5946	0.1488	1.0218	1.1002	0.1362
0.0219	0.5774	1.0689	1.3807	0.3386	1.6273	0.1441	1.0212	1.0970	0.1338
0.0546	0.5639	1.0676	1.3721	0.3335	1.6926	0.1365	1.0203	1.0918	0.1291
0.0876	0.5545	1.0667	1.3661	0.3304	1.7583	0.1278	1.0192	1.0858	0.1250
0.1203	0.5493	1.0662	1.3629	0.3289	1.8129	0.1169	1.0177	1.0782	0.1181
0.1530	0.5315	1.0645	1.3517	0.3207	1.8564	0.1131	1.0173	1.0756	0.1159
0.1857	0.5218	1.0635	1.3455	0.3177	1.9221	0.1036	1.0160	1.0691	0.1110
0.2184	0.5167	1.0630	1.3423	0.3157	1.9875	0.0919	1.0145	1.0610	0.1033
0.2514	0.4841	1.0597	1.3216	0.3004	2.0532	0.0841	1.0134	1.0556	0.0986
0.2841	0.4692	1.0582	1.3121	0.2939	2.1186	0.0754	1.0123	1.0495	0.0927
0.3168	0.4637	1.0576	1.3086	0.2925	2.1843	0.0725	1.0119	1.0475	0.0912
0.3494	0.4593	1.0572	1.3057	0.2910	2.2497	0.0682	1.0113	1.0445	0.0882
0.3821	0.4485	1.0561	1.2988	0.2868	2.3154	0.0583	1.0100	1.0375	0.0816
0.4148	0.4370	1.0548	1.2914	0.2811	2.3807	0.0526	1.0092	1.0334	0.0779
0.4478	0.4259	1.0537	1.2843	0.2760	2.4465	0.0455	1.0083	1.0284	0.0735
0.4805	0.4013	1.0511	1.2685	0.2635	2.5118	0.0387	1.0073	1.0237	0.0688
0.5132	0.3963	1.0505	1.2652	0.2620	2.5775	0.0352	1.0068	1.0212	0.0665
0.5459	0.3842	1.0492	1.2573	0.2562	2.6433	0.0326	1.0065	1.0194	0.0649
0.5789	0.3782	1.0486	1.2534	0.2541	2.7086	0.0268	1.0057	1.0153	0.0611
0.6116	0.3683	1.0475	1.2470	0.2494	2.7743	0.0195	1.0046	1.0101	0.0566
0.6443	0.3598	1.0466	1.2415	0.2459	2.8401	0.0114	1.0035	1.0043	0.0510
0.6770	0.3528	1.0458	1.2369	0.2420	2.9058	0.0077	1.0030	1.0017	0.0480
0.7097	0.3440	1.0448	1.2311	0.2385	2.9715	0.0031	1.0023	0.9985	0.0450
0.7427	0.3335	1.0437	1.2242	0.2333	3.0369	-0.0043	1.0013	0.9932	0.0394
0.7754	0.3313	1.0434	1.2228	0.2327	3.1026	-0.0087	1.0006	0.9900	0.0363
0.8081	0.3207	1.0422	1.2158	0.2270	3.1683	-0.0126	1.0001	0.9873	0.0336
0.8300	0.3171	1.0418	1.2135	0.2256	3.2340	-0.0160	0.9996	0.9848	0.0308
0.8408	0.3163	1.0417	1.2129	0.2256	3.2997	-0.0199	0.9990	0.9821	0.0277
0.8738	0.3087	1.0409	1.2079	0.2217	3.3651	-0.0271	0.9980	0.9768	0.0222
0.9065	0.3017	1.0401	1.2033	0.2185	3.4308	-0.0294	0.9976	0.9752	0.0205
0.9392	0.2844	1.0381	1.1918	0.2091	3.4965	-0.0341	0.9969	0.9719	0.0174
0.9718	0.2755	1.0372	1.1857	0.2045	3.5623	-0.0386	0.9963	0.9686	0.0144
1.0049	0.2697	1.0365	1.1819	0.2022	3.6276	-0.0417	0.9958	0.9664	0.0115
1.0376	0.2636	1.0358	1.1778	0.1991	3.6933	-0.0435	0.9955	0.9651	0.0099
1.0702	0.2539	1.0346	1.1713	0.1943	3.7591	-0.0482	0.9948	0.9617	0.0061
1.1029	0.2513	1.0343	1.1696	0.1931	3.8248	-0.0527	0.9942	0.9585	0.0027
1.1360	0.2448	1.0336	1.1652	0.1895	3.8905	-0.0547	0.9939	0.9570	0.0006
1.1686	0.2379	1.0328	1.1607	0.1863	3.9562	-0.0589	0.9932	0.9540	-0.0027
1.2013	0.2288	1.0317	1.1545	0.1810	4.0219	-0.0630	0.9926	0.9510	-0.0063
1.2340	0.2192	1.0305	1.1480	0.1762	4.0873	-0.0659	0.9922	0.9489	-0.0086
1.2667	0.2107	1.0295	1.1423	0.1712	4.1530	-0.0691	0.9917	0.9466	-0.0109
1.2997	0.2060	1.0289	1.1392	0.1687	4.2187	-0.0707	0.9915	0.9454	-0.0128
1.3324	0.1966	1.0278	1.1328	0.1631	4.2844	-0.0733	0.9911	0.9435	-0.0150
1.3651	0.1910	1.0271	1.1290	0.1604	4.3502	-0.0753	0.9907	0.9421	-0.0170
1.3978	0.1852	1.0264	1.1251	0.1570	4.4159	-0.0786	0.9902	0.9396	-0.0193
1.4308	0.1817	1.0259	1.1227	0.1556	4.4816	-0.0784	0.9903	0.9398	-0.0198
1.4635	0.1729	1.0248	1.1167	0.1502	4.5473	-0.0797	0.9901	0.9388	-0.0208
1.4962	0.1651	1.0239	1.1114	0.1455	4.6130	-0.0833	0.9895	0.9362	-0.0238
1.5289	0.1581	1.0230	1.1067	0.1412	4.6784	-0.0844	0.9893	0.9354	-0.0253
1.5615	0.1558	1.0227	1.1051	0.1404	4.7441	-0.0873	0.9889	0.9333	-0.0280

Table B-25. Time histories of overpressure, sound speed, density and flow velocity from the reconstructed blast-wave flow field by the RCM for a 1-kg TNT surface explosion in a standard atmosphere. These signatures are for the specific radius r = 4.364 m, at which the blast-wave front arrives at time t = 6.752 ms.

t (ms)	$\Delta p/p_1$	a/a_1	ρ/ρ_1	u/a_1	t (ms)	$\Delta p/p_1$	a/a_1	ρ/ρ_1	u/a_1
0.0000	0.5162	1.0624	1.3434	0.3072	1.5838	0.1466	1.0209	1.1001	0.1287
0.0108	0.5152	1.0623	1.3428	0.3072	1.6165	0.1421	1.0204	1.0970	0.1264
0.0438	0.4996	1.0607	1.3329	0.3002	1.6819	0.1318	1.0190	1.0899	0.1203
0.0765	0.4907	1.0598	1.3272	0.2970	1.7476	0.1266	1.0184	1.0863	0.1175
0.1092	0.4845	1.0592	1.3232	0.2941	1.8133	0.1205	1.0176	1.0821	0.1139
0.1419	0.4540	1.0560	1.3037	0.2799	1.8787	0.1116	1.0164	1.0759	0.1085
0.1749	0.4464	1.0553	1.2989	0.2767	1.9444	0.1016	1.0151	1.0691	0.1025
0.2076	0.4430	1.0549	1.2967	0.2757	2.0101	0.0944	1.0142	1.0640	0.0978
0.2403	0.4333	1.0539	1.2905	0.2719	2.0758	0.0838	1.0128	1.0566	0.0911
0.2729	0.4292	1.0535	1.2878	0.2704	2.1415	0.0790	1.0121	1.0533	0.0879
0.3060	0.4202	1.0525	1.2820	0.2660	2.2069	0.0706	1.0110	1.0474	0.0827
0.3387	0.4109	1.0515	1.2760	0.2620	2.2726	0.0678	1.0106	1.0454	0.0814
0.3713	0.4047	1.0509	1.2720	0.2594	2.3383	0.0622	1.0099	1.0415	0.0780
0.4040	0.3932	1.0496	1.2645	0.2546	2.4040	0.0544	1.0088	1.0361	0.0726
0.4367	0.3736	1.0475	1.2518	0.2444	2.4698	0.0510	1.0084	1.0337	0.0706
0.4698	0.3677	1.0469	1.2480	0.2418	2.5351	0.0425	1.0072	1.0277	0.0651
0.5024	0.3571	1.0457	1.2410	0.2370	2.6008	0.0369	1.0064	1.0237	0.0613
0.5351	0.3530	1.0453	1.2383	0.2352	2.6666	0.0339	1.0060	1.0216	0.0593
0.5678	0.3437	1.0442	1.2323	0.2309	2.7323	0.0313	1.0056	1.0198	0.0579
0.6008	0.3361	1.0434	1.2272	0.2275	2.7976	0.0258	1.0049	1.0159	0.0540
0.6335	0.3293	1.0426	1.2228	0.2240	2.8634	0.0188	1.0039	1.0109	0.0492
0.6662	0.3215	1.0418	1.2176	0.2205	2.9291	0.0149	1.0033	1.0082	0.0466
0.6989	0.3138	1.0409	1.2126	0.2165	2.9948	0.0101	1.0027	1.0048	0.0430
0.7316	0.3105	1.0405	1.2104	0.2151	3.0605	0.0056	1.0020	1.0015	0.0399
0.7646	0.3020	1.0396	1.2047	0.2113	3.1262	0.0018	1.0015	0.9988	0.0369
0.7973	0.2956	1.0388	1.2005	0.2085	3.1919	-0.0029	1.0008	0.9955	0.0336
0.8300	0.2885	1.0380	1.1958	0.2050	3.2573	-0.0074	1.0002	0.9922	0.0301
0.8627	0.2822	1.0373	1.1916	0.2018	3.3230	-0.0109	0.9997	0.9898	0.0275
0.8957	0.2759	1.0366	1.1874	0.1984	3.3887	-0.0142	0.9992	0.9874	0.0250
0.9284	0.2647	1.0353	1.1799	0.1929	3.4545	-0.0179	0.9986	0.9847	0.0223
0.9611	0.2567	1.0343	1.1746	0.1883	3.5202	-0.0241	0.9977	0.9803	0.0178
0.9830	0.2550	1.0341	1.1735	0.1877	3.5859	-0.0269	0.9973	0.9783	0.0157
0.9937	0.2545	1.0341	1.1732	0.1877	3.6516	-0.0309	0.9967	0.9754	0.0127
1.0264	0.2455	1.0330	1.1672	0.1828	3.7173	-0.0349	0.9962	0.9726	0.0097
1.0595	0.2397	1.0323	1.1633	0.1798	3.7830	-0.0365	0.9959	0.9714	0.0084
1.0921	0.2347	1.0318	1.1599	0.1775	3.8484	-0.0390	0.9956	0.9696	0.0065
1.1248	0.2285	1.0310	1.1557	0.1742	3.9141	-0.0425	0.9950	0.9671	0.0036
1.1575	0.2228	1.0303	1.1519	0.1709	3.9798	-0.0470	0.9944	0.9639	0.0001
1.1905	0.2141	1.0293	1.1460	0.1661	4.0456	-0.0493	0.9940	0.9622	-0.0015
1.2232	0.2069	1.0284	1.1411	0.1621	4.1113	-0.0539	0.9933	0.9589	-0.0054
1.2559	0.2046	1.0281	1.1396	0.1611	4.1770	-0.0558	0.9931	0.9575	-0.0069
1.2886	0.1929	1.0267	1.1316	0.1546	4.2427	-0.0583	0.9927	0.9557	-0.0091
1.3216	0.1913	1.0265	1.1306	0.1539	4.3084	-0.0605	0.9923	0.9540	-0.0110
1.3543	0.1833	1.0255	1.1251	0.1490	4.3741	-0.0633	0.9919	0.9520	-0.0132
1.3870	0.1784	1.0249	1.1218	0.1464	4.4399	-0.0648	0.9917	0.9510	-0.0149
1.4197	0.1729	1.0242	1.1180	0.1433	4.5056	-0.0673	0.9913	0.9492	-0.0169
1.4527	0.1696	1.0238	1.1158	0.1420	4.5713	-0.0694	0.9910	0.9477	-0.0185
1.4854	0.1653	1.0233	1.1128	0.1394	4.6377	-0.0712	0.9907	0.9463	-0.0204
1.5181	0.1607	1.0227	1.1097	0.1367	4.7041	-0.0729	0.9904	0.9451	-0.0217
1.5508	0.1482	1.0211	1.1011	0.1295	4.7705	-0.0739	0.9903	0.9444	-0.0226

Table B-26. Time histories of overpressure, sound speed, density and flow velocity from the reconstructed blast-wave flow field by the RCM for a 1-kg TNT surface explosion in a standard atmosphere. These signatures are for the specific radius r = 4.764 m, at which the blast-wave front arrives at time t = 7.735 ms.

t (ms)	$\Delta p/p_1$	a/a_1	ρ/ρ_1	u/a_1	t (ms)	$\Delta p/p_1$	a/a_1	ρ/ρ_1	u/a_1
0.0000	0.4496	1.0553	1.3018	0.2730	1.6179	0.1362	1.0192	1.0937	0.1164
0.0108	0.4489	1.0552	1.3013	0.2730	1.6506	0.1343	1.0190	1.0924	0.1156
0.0435	0.4218	1.0524	1.2838	0.2592	1.7163	0.1247	1.0178	1.0858	0.1097
0.0765	0.4191	1.0521	1.2821	0.2584	1.7820	0.1188	1.0170	1.0817	0.1063
0.1092	0.4115	1.0513	1.2772	0.2554	1.8477	0.1133	1.0163	1.0779	0.1034
0.1419	0.4043	1.0505	1.2725	0.2522	1.9134	0.1074	1.0155	1.0738	0.0997
0.1745	0.3994	1.0500	1.2694	0.2500	1.9791	0.0985	1.0143	1.0676	0.0942
0.2076	0.3904	1.0490	1.2635	0.2464	2.0449	0.0919	1.0135	1.0631	0.0904
0.2403	0.3851	1.0484	1.2601	0.2439	2.1102	0.0872	1.0128	1.0598	0.0873
0.2729	0.3805	1.0479	1.2571	0.2421	2.1759	0.0793	1.0118	1.0543	0.0824
0.3056	0.3690	1.0467	1.2496	0.2367	2.2417	0.0729	1.0109	1.0498	0.0785
0.3387	0.3644	1.0462	1.2466	0.2351	2.3074	0.0690	1.0104	1.0471	0.0759
0.3713	0.3465	1.0442	1.2349	0.2256	2.3731	0.0632	1.0096	1.0430	0.0724
0.4040	0.3412	1.0436	1.2314	0.2232	2.4388	0.0590	1.0091	1.0400	0.0698
0.4367	0.3328	1.0427	1.2259	0.2188	2.5045	0.0534	1.0083	1.0361	0.0663
0.4698	0.3277	1.0421	1.2225	0.2170	2.5699	0.0474	1.0075	1.0319	0.0623
0.5024	0.3195	1.0412	1.2171	0.2128	2.6356	0.0420	1.0067	1.0281	0.0588
0.5351	0.3168	1.0409	1.2154	0.2120	2.7013	0.0371	1.0061	1.0246	0.0553
0.5678	0.3074	1.0398	1.2092	0.2070	2.7670	0.0333	1.0055	1.0220	0.0529
0.6008	0.3048	1.0395	1.2075	0.2060	2.8328	0.0305	1.0051	1.0200	0.0509
0.6335	0,2977	1.0387	1.2028	0.2028	2.8985	0.0290	1.0049	1.0190	0.0503
0.6662	0,2906	1.0379	1.1980	0.1991	2.9642	0.0233	1.0041	1.0149	0.0464
0.6989	0,2872	1.0375	1.1958	0.1975	3.0299	0.0176	1.0033	1.0108	0.0422
0.7319	0,2800	1.0367	1.1910	0.1940	3.0956	0.0140	1.0028	1.0083	0.0399
0.7646	0,2747	1.0361	1.1874	0.1912	3.1613	0.0096	1.0022	1.0052	0.0365
0.7973	0,2712	1.0357	1.1851	0.1896	3.2271	0.0054	1.0016	1.0022	0.0337
0.8303	0,2622	1.0346	1.1791	0.1850	3.2924	0.0009	1.0010	0.9989	0.0302
0.8630	0,2562	1.0339	1.1751	0.1819	3.3581	-0.0031	1.0004	0.9962	0.0275
0.8957	0,2495	1.0332	1.1706	0.1782	3.4239	-0.0062	1.0000	0.9939	0.0250
0.9287	0.2442	1.0325	1.1670	0.1757	3.4896	-0.0093	0.9995	0.9917	0.0228
0.9614	0.2370	1.0317	1.1622	0.1717	3.5553	-0.0114	0.9992	0.9902	0.0214
0.9941	0.2330	1.0312	1.1595	0.1701	3.6214	-0.0164	0.9985	0.9866	0.0177
1.0271	0.2275	1.0305	1.1559	0.1670	3.6878	-0.0217	0.9977	0.9828	0.0139
1.0598	0.2223	1.0299	1.1524	0.1642	3.7542	-0.0232	0.9975	0.9817	0.0125
1.0928	0.2165	1.0292	1.1484	0.1609	3.8209	-0.0267	0.9970	0.9792	0.0100
1.1255	0.2136	1.0289	1.1465	0.1598	3.8874	-0.0297	0.9965	0.9770	0.0079
1.1586	0.2101	1.0284	1.1441	0.1579	3.9538	-0.0322	0.9962	0.9752	0.0061
1.1912	0.2028	1.0276	1.1392	0.1541	4.0202	-0.0352	0.9957	0.9731	0.0035
1.2239	0.1972	1.0269	1.1353	0.1508	4.0869	-0.0373	0.9954	0.9715	0.0021
1.2570	0.1901	1.0260	1.1306	0.1467	4.1534	-0.0406	0.9949	0.9692	-0.0004
1.2896	0.1826	1.0251	1.1254	0.1426	4.2198	-0.0442	0.9944	0.9666	-0.0034
1.3227	0.1785	1.0246	1.1227	0.1405	4.2865	-0.0462	0.9941	0.9652	-0.0049
1.3554	0.1704	1.0236	1.1172	0.1356	4.3529	-0.0503	0.9935	0.9622	-0.0084
1.3880	0.1686	1.0233	1.1159	0.1350	4.4193	-0.0533	0.9930	0.9600	-0.0106
1.4211	0.1632	1.0227	1.1122	0.1317	4.4858	-0.0551	0.9928	0.9587	-0.0120
1.4538	0.1598	1.0222	1.1099	0.1303	4.5525	-0.0575	0.9924	0.9570	-0.0142
1.4868	0.1574	1.0219	1.1083	0.1287	4.6189	-0.0588	0.9922	0.9560	-0.0153
1.5195	0.1530	1.0214	1.1052	0.1265	4.6853	-0.0596	0.9921	0.9555	-0.0162
1.5522	0.1460	1.0205	1.1004	0.1223	4.7521	-0.0622	0.9917	0.9536	-0.0186
1.5852	0.1421	1.0200	1.0978	0.1201	4.8185	-0.0650	0.9913	0.9515	-0.0209

Table B-27. Time histories of overpressure, sound speed, density and flow velocity from the reconstructed blast-wave flow field by the RCM for a 1-kg TNT surface explosion in a standard atmosphere. These signatures are for the specific radius r = 5.250 m, at which the blast-wave front arrives at time t = 8.992 ms.

t (ms)	$\Delta p/p_1$	a/a_1	ρ/ρ_1	u/a_1	t (ms)	$\Delta p/p_1$	a/a_1	ρ/ρ_1	u/a_1
0.0000	0.3707	1.0466	1.2515	0.2309	1.6415	0.1254	1.0175	1.0870	0.1048
0.0327	0.3671	1.0462	1.2491	0.2294	1.6742	0.1210	1.0170	1.0840	0.1023
0.0657	0.3619	1.0456	1.2457	0.2272	1.7399	0.1186	1.0166	1.0823	0.1009
0.0984	0.3541	1.0447	1.2406	0.2237	1.8056	0.1108	1.0156	1.0769	0.0961
0.1311	0.3501	1.0443	1.2380	0.2220	1.8714	0.1041	1.0148	1.0723	0.0921
0.1641	0.3452	1.0438	1.2348	0.2196	1.9371	0.1014	1.0144	1.0704	0.0907
0.1968	0.3386	1.0430	1.2304	0.2165	2.0028	0.0949	1.0135	1.0658	0.0865
0.2298	0.3328	1.0424	1.2266	0.2137	2.0685	0.0870	1.0125	1.0604	0.0816
0.2625	0.3181	1.0407	1.2169	0.2064	2.1342	0.0828	1.0119	1.0574	0.0788
0.2952	0.3134	1.0402	1.2138	0.2040	2.1999	0.0734	1.0107	1.0509	0.0729
0.3282	0.3056	1.0393	1.2087	0.2001	2.2657	0.0711	1.0104	1.0492	0.0714
0.3609	0.2985	1.0385	1.2040	0.1963	2.3314	0.0669	1.0098	1.0463	0.0689
0.3936	0.2960	1.0382	1.2023	0.1956	2.3978	0.0617	1.0091	1.0427	0.0658
0.4266	0.2916	1.0377	1.1994	0.1935	2.4642	0.0576	1.0085	1.0398	0.0633
0.4593	0.2859	1.0371	1.1956	0.1909	2.5306	0.0542	1.0081	1.0374	0.0610
0.4924	0.2815	1.0366	1.1927	0.1886	2.5970	0.0491	1.0074	1.0338	0.0577
0.5250	0.2763	1.0360	1.1893	0.1860	2.6634	0.0441	1.0067	1.0302	0.0542
0.5577	0.2700	1.0352	1.1850	0.1825	2.7302	0.0388	1.0060	1.0266	0.0508
0.5908	0.2669	1.0349	1.1830	0.1812	2.7966	0.0349	1.0054	1.0238	0.0481
0.6234	0.2636	1.0345	1.1807	0.1798	2.8630	0.0316	1.0050	1.0214	0.0460
0.6565	0.2588	1.0339	1.1776	0.1777	2.9298	0.0281	1.0045	1.0189	0.0438
0.6892	0.2541	1.0334	1.1744	0.1751	2.9962	0.0268	1.0043	1.0181	0.0432
0.7222	0.2491	1.0328	1.1711	0.1725	3.0626	0.0222	1.0036	1.0148	0.0399
0.7549	0.2424	1.0320	1.1666	0.1687	3.1294	0.0175	1.0030	1.0115	0.0367
0.7879	0.2395	1.0316	1.1646	0.1676	3.1958	0.0132	1.0024	1.0084	0.0339
0.8206	0.2303	1.0305	1.1585	0.1625	3.2622	0.0097	1.0019	1.0059	0.0314
0.8533	0.2283	1.0303	1.1571	0.1619	3.3286	0.0065	1.0014	1.0037	0.0293
0.8863	0.2237	1.0298	1.1540	0.1593	3.3954	0.0031	1.0009	1.0012	0.0270
0.9190	0.2179	1.0291	1.1501	0.1562	3.4618	-0.0021	1.0002	0.9975	0.0231
0.9520	0.2160	1.0288	1.1488	0.1555	3.5282	-0.0041	0.9999	0.9960	0.0217
0.9847	0.2092	1.0280	1.1442	0.1517	3.5949	-0.0062	0.9996	0.9946	0.0201
1.0174	0.2040	1.0274	1.1407	0.1487	3.6613	-0.0091	0.9992	0.9925	0.0180
1.0504	0.1999	1.0269	1.1379	0.1467	3.7278	-0.0118	0.9988	0.9906	0.0159
1.0831	0.1962	1.0264	1.1354	0.1446	3.7942	-0.0158	0.9982	0.9876	0.0128
1.1161	0.1940	1.0262	1.1340	0.1436	3.8609	-0.0200	0.9976	0.9847	0.0098
1.1488	0.1864	1.0252	1.1287	0.1393	3.9273	-0.0220	0.9974	0.9833	0.0085
1.1819	0.1818	1.0246	1.1257	0.1368	3.9941	-0.0242	0.9970	0.9816	0.0066
1.2145	0.1803	1.0245	1.1246	0.1360	4.0605	-0.0269	0.9966	0.9797	0.0047
1.2476	0.1739	1.0237	1.1203	0.1325	4.1269	-0.0292	0.9963	0.9780	0.0030
1.2803	0.1672	1.0228	1.1157	0.1286	4.1933	-0.0320	0.9959	0.9760	0.0007
1.3129	0.1642	1.0224	1.1136	0.1272	4.2601	-0.0338	0.9956	0.9747	-0.0007
1.3460	0.1623	1.0222	1.1123	0.1261	4.3265	-0.0368	0.9952	0.9726	-0.0029
1.3787	0.1583	1.0217	1.1096	0.1241	4.3933	-0.0390	0.9949	0.9710	-0.0048
1.4117	0.1515	1.0209	1.1049	0.1197	4.4597	-0.0407	0.9946	0.9697	-0.0063
1.4444	0.1489	1.0205	1.1032	0.1184	4.5261	-0.0450	0.9940	0.9666	-0.0095
1.4774	0.1451	1.0200	1.1005	0.1161	4.5929	-0.0464	0.9938	0.9656	-0.0106
1.5101	0.1417	1.0196	1.0982	0.1143	4.6593	-0.0484	0.9934	0.9642	-0.0124
1.5431	0.1369	1.0190	1.0949	0.1113	4.7257	-0.0503	0.9932	0.9628	-0.0139
1.5758	0.1338	1.0186	1.0928	0.1095	4.7924	-0.0526	0.9928	0.9611	-0.0157
1.6085	0.1274	1.0178	1.0884	0.1058	4.8588	-0.0535	0.9927	0.9605	-0.0165

Table B-28. Time histories of overpressure, sound speed, density and flow velocity from the reconstructed blast-wave flow field by the RCM for a 1-kg TNT surface explosion in a standard atmosphere. These signatures are for the specific radius r = 5.925 m, at which the blast-wave front arrives at time t = 10.732 ms.

t (ms)	$\Delta p/p_1$	a/a_1	ρ/ρ_1	u/a_1	t (ms)	$\Delta p/p_1$	a/a_1	ρ/ρ_1	u/a_1
0.0000	0.3094	1.0396	1.2116	0.1966	1.6554	0.1126	1.0157	1.0786	0.0917
0.0330	0.3047	1.0390	1.2086	0.1945	1.6885	0.1106	1.0154	1.0772	0.0906
0.0657	0.3004	1.0385	1.2057	0.1925	1.7552	0.1075	1.0150	1.0750	0.0889
0.0987	0.2935	1.0377	1.2011	0.1892	1.8216	0.1020	1.0143	1.0712	0.0854
0.1314	0.2858	1.0369	1.1959	0.1850	1.8880	0.0965	1.0136	1.0674	0.0821
0.1645	0.2830	1.0365	1.1941	0.1838	1.9548	0.0929	1.0131	1.0648	0.0798
0.1971	0.2748	1.0356	1.1887	0.1793	2.0212	0.0904	1.0127	1.0631	0.0785
0.2302	0.2730	1.0354	1.1875	0.1787	2.0876	0.0827	1.0117	1.0577	0.0737
0.2629	0.2672	1.0347	1.1836	0.1758	2.1540	0.0775	1.0110	1.0541	0.0703
0.2955	0.2631	1.0342	1.1808	0.1739	2.2208	0.0719	1.0103	1.0502	0.0668
0.3286	0.2578	1.0336	1.1773	0.1710	2.2872	0.0659	1.0095	1.0460	0.0628
0.3613	0.2536	1.0331	1.1745	0.1689	2.3536	0.0641	1.0092	1.0447	0.0618
0.3943	0.2517	1.0329	1.1732	0.1680	2.4204	0.0598	1.0086	1.0417	0.0593
0.4270	0.2479	1.0324	1.1707	0.1663	2.4868	0.0565	1.0082	1.0394	0.0573
0.4600	0.2421	1.0318	1.1668	0.1631	2.5536	0.0525	1.0076	1.0365	0.0545
0.4927	0.2396	1.0315	1.1651	0.1618	2.6200	0.0499	1.0073	1.0348	0.0531
0.5257	0.2373	1.0312	1.1636	0.1607	2.6864	0.0456	1.0067	1.0317	0.0503
0.5584	0.2359	1.0310	1.1626	0.1603	2.7531	0.0405	1.0060	1.0281	0.0468
0.5914	0.2305	1.0304	1.1590	0.1572	2.8195	0.0373	1.0056	1.0259	0.0448
0.6245	0.2259	1.0298	1.1559	0.1550	2.8860	0.0330	1.0050	1.0229	0.0418
0.6579	0.2206	1.0292	1.1524	0.1522	2.9527	0.0306	1.0046	1.0211	0.0401
0.6909	0.2171	1.0288	1.1500	0.1503	3.0191	0.0276	1.0042	1.0190	0.0381
0.7243	0.2113	1.0281	1.1461	0.1470	3.0855	0.0259	1.0040	1.0178	0.0371
0.7573	0.2066	1.0275	1.1429	0.1446	3.1523	0.0240	1.0037	1.0165	0.0360
0.7907	0.2038	1.0272	1.1410	0.1432	3.2187	0.0197	1.0031	1.0134	0.0332
0.8241	0.2009	1.0268	1.1390	0.1418	3.2851	0.0160	1.0026	1.0108	0.0305
0.8571	0.1957	1.0262	1.1355	0.1388	3.3519	0.0151	1.0025	1.0101	0.0298
0.8905	0.1941	1.0260	1.1344	0.1380	3.4183	0.0104	1.0018	1.0068	0.0265
0.9235	0.1881	1.0252	1.1304	0.1345	3.4847	0.0080	1.0015	1.0051	0.0248
0.9569	0.1868	1.0251	1.1295	0.1342	3.5515	0.0047	1.0010	1.0027	0.0224
0.9903	0.1809	1.0243	1.1254	0.1307	3.6179	0.0019	1.0006	1.0007	0.0203
1.0233	0.1790	1.0241	1.1241	0.1300	3.6843	-0.0021	1.0000	0.9979	0.0174
1.0567	0.1756	1.0237	1.1218	0.1281	3.7511	-0.0042	0.9997	0.9964	0.0159
1.0901	0.1725	1.0233	1.1197	0.1266	3.8175	-0.0073	0.9993	0.9942	0.0137
1.1231	0.1670	1.0226	1.1159	0.1233	3.8839	-0.0090	0.9990	0.9930	0.0125
1.1565	0.1624	1.0220	1.1128	0.1206	3.9506	-0.0110	0.9987	0.9915	0.0109
1.1899	0.1577	1.0215	1.1096	0.1178	4.0171	-0.0130	0.9984	0.9901	0.0095
1.2229	0.1560	1.0212	1.1084	0.1171	4.0838	-0.0172	0.9978	0.9870	0.0064
1.2563	0.1501	1.0205	1.1044	0.1135	4.1502	-0.0186	0.9976	0.9861	0.0054
1.2896	0.1492	1.0204	1.1038	0.1131	4.2166	-0.0214	0.9972	0.9840	0.0034
1.3227	0.1463	1.0200	1.1018	0.1116	4.2834	-0.0236	0.9969	0.9824	0.0016
1.3561	0.1424	1.0195	1.0991	0.1093	4.3498	-0.0255	0.9966	0.9811	0.0002
1.3894	0.1392	1.0191	1.0969	0.1073	4.4166	-0.0266	0.9965	0.9803	-0.0009
1.4225	0.1356	1.0186	1.0944	0.1053	4.4830	-0.0283	0.9962	0.9791	-0.0022
1.4558	0.1316	1.0181	1.0916	0.1029	4.5494	-0.0303	0.9959	0.9776	-0.0034
1.4889	0.1307	1.0180	1.0910	0.1025	4.6161	-0.0333	0.9955	0.9755	-0.0058
1.5223	0.1272	1.0176	1.0886	0.1003	4.6826	-0.0355	0.9952	0.9739	-0.0074
1.5556	0.1256	1.0174	1.0875	0.0996	4.7490	-0.0370	0.9949	0.9728	-0.0086
1.5887	0.1201	1.0166	1.0837	0.0961	4.8157	-0.0398	0.9945	0.9708	-0.0108
1.6220	0.1168	1.0162	1.0815	0.0943	4.8821	-0.0412	0.9943	0.9698	-0.0121

Table B-29. Time histories of overpressure, sound speed, density and flow velocity from the reconstructed blast-wave flow field by the RCM for a 1-kg TNT surface explosion in a standard atmosphere. These signatures are for the specific radius r = 6.900 m, at which the blast-wave front arrives at time t = 13.318 ms.

t (ms)	$\Delta p/p_1$	a/a_1	ρ/ρ_1	u/a_1	t (ms)	$\Delta p/p_1$	a/a_1	ρ/ρ_1	u/a_1
0.0000	0.2392	1.0313	1.1652	0.1557	1.6634	0.0993	1.0138	1.0696	0.0784
0.0334	0.2379	1.0311	1.1643	0.1552	1.6968	0.0978	1.0136	1.0686	0.0775
0.0668	0.2358	1.0309	1.1629	0.1541	1.7632	0.0941	1.0131	1.0660	0.0753
0.0998	0.2317	1.0304	1.1602	0.1521	1.8300	0.0910	1.0127	1.0639	0.0736
0.1332	0.2285	1.0300	1.1580	0.1503	1.8964	0.0864	1.0121	1.0606	0.0706
0.1666	0.2241	1.0295	1.1550	0.1482	1.9628	0.0821	1.0115	1.0577	0.0680
0.1996	0.2207	1.0291	1.1528	0.1463	2.0296	0.0806	1.0113	1.0566	0.0671
0.2330	0.2193	1.0289	1.1518	0.1457	2.0960	0.0784	1.0110	1.0551	0.0659
0.2663	0.2146	1.0283	1.1487	0.1431	2.1624	0.0717	1.0101	1.0504	0.0617
0.2994	0.2120	1.0280	1.1469	0.1419	2.2291	0.0677	1.0095	1.0476	0.0590
0.3328	0.2091	1.0276	1.1449	0.1401	2.2956	0.0628	1.0089	1.0441	0.0559
0.3661	0.2069	1.0274	1.1434	0.1392	2.3623	0.0607	1.0086	1.0427	0.0548
0.3992	0.2032	1.0269	1.1409	0.1371	2.4287	0.0566	1.0080	1.0398	0.0520
0.4325	0.1994	1.0265	1.1384	0.1351	2.4951	0.0545	1.0078	1.0383	0.0508
0.4659	0.1973	1.0262	1.1370	0.1340	2.5619	0.0508	1.0073	1.0357	0.0483
0.4990	0.1958	1.0260	1.1359	0.1333	2.6283	0.0479	1.0069	1.0337	0.0465
0.5323	0.1922	1.0256	1.1335	0.1314	2.6947	0.0451	1.0065	1.0317	0.0446
0.5657	0.1891	1.0252	1.1314	0.1299	2.7615	0.0442	1.0063	1.0310	0.0440
0.5988	0.1871	1.0250	1.1300	0.1288	2.8279	0.0402	1.0058	1.0282	0.0413
0.6321	0.1801	1.0241	1.1253	0.1247	2.8947	0.0381	1.0055	1.0268	0.0400
0.6655	0.1779	1.0238	1.1237	0.1235	2.9611	0.0342	1.0050	1.0240	0.0373
0.6985	0.1753	1.0235	1.1220	0.1222	3.0275	0.0302	1.0044	1.0212	0.0347
0.7319	0.1744	1.0234	1.1213	0.1218	3.0942	0.0283	1.0041	1.0198	0.0334
0.7653	0.1702	1.0229	1.1185	0.1195	3.1607	0.0258	1.0038	1.0180	0.0319
0.7983	0.1689	1.0227	1.1176	0.1189	3.2274	0.0233	1.0034	1.0163	0.0301
0.8317	0.1666	1.0224	1.1160	0.1176	3.2938	0.0218	1.0032	1.0152	0.0291
0.8651	0.1627	1.0219	1.1133	0.1155	3.3606	0.0208	1.0031	1.0145	0.0284
0.8981	0.1608	1.0217	1.1120	0.1145	3.4270	0.0174	1.0026	1.0121	0.0260
0.9315	0.1571	1.0212	1.1095	0.1122	3.4934	0.0142	1.0022	1.0098	0.0238
0.9649	0.1544	1.0209	1.1077	0.1108	3.5602	0.0133	1.0020	1.0092	0.0232
0.9979	0.1516	1.0205	1.1058	0.1092	3.6266	0.0093	1.0015	1.0063	0.0204
1.0313	0.1502	1.0203	1.1048	0.1085	3.6930	0.0078	1.0013	1.0053	0.0194
1.0647	0.1438	1.0195	1.1004	0.1045	3.7597	0.0055	1.0009	1.0036	0.0177
1.0977	0.1419	1.0193	1.0991	0.1036	3.8262	0.0027	1.0005	1.0016	0.0160
1.1311	0.1411	1.0192	1.0985	0.1030	3.8926	0.0003	1.0002	0.9999	0.0142
1.1645	0.1404	1.0191	1.0980	0.1028	3.9593	-0.0023	0.9998	0.9981	0.0125
1.1975	0.1357	1.0185	1.0948	0.0999	4.0257	-0.0041	0.9996	0.9967	0.0110
1.2309	0.1305	1.0178	1.0913	0.0969	4.0925	-0.0067	0.9992	0.9949	0.0092
1.2643	0.1286	1.0176	1.0899	0.0957	4.1589	-0.0076	0.9991	0.9942	0.0084
1.2973	0.1281	1.0175	1.0896	0.0955	4.2253	-0.0095	0.9988	0.9929	0.0071
1.3307	0.1241	1.0170	1.0868	0.0930	4.2921	-0.0111	0.9986	0.9917	0.0058
1.3641	0.1221	1.0167	1.0854	0.0920	4.3585	-0.0140	0.9981	0.9896	0.0037
1.3971	0.1203	1.0165	1.0842	0.0909	4.4249	-0.0159	0.9979	0.9883	0.0023
1.4305	0.1165	1.0160	1.0815	0.0885	4.4917	-0.0171	0.9977	0.9874	0.0013
1.4638	0.1141	1.0157	1.0799	0.0870	4.5581	-0.0193	0.9974	0.9858	-0.0003
1.4972	0.1130	1.0156	1.0791	0.0866	4.6248	-0.0209	0.9972	0.9847	-0.0014
1.5303	0.1104	1.0152	1.0774	0.0852	4.6913	-0.0225	0.9969	0.9835	-0.0028
1.5636	0.1092	1.0151	1.0765	0.0845	4.7580	-0.0237	0.9967	0.9827	-0.0037
1.5970	0.1044	1.0144	1.0732	0.0815	4.8244	-0.0248	0.9966	0.9819	-0.0046
1.6300	0.1032	1.0143	1.0724	0.0809	4.8912	-0.0266	0.9963	0.9806	-0.0060

Table B-30. Time histories of overpressure, sound speed, density and flow velocity from the reconstructed blast-wave flow field by the RCM for a 1-kg TNT surface explosion in a standard atmosphere. These signatures are for the specific radius r = 7.363 m, at which the blast-wave front arrives at time t = 14.549 ms.

t (ms)	$\Delta p/p_1$	a/a_1	ρ/ρ_1	u/a_1	t (ms)	$\Delta p/p_1$	a/a_1	ρ/ρ_1	u/a_1
0.0000	0.2198	1.0289	1.1522	0.1441	1.6638	0.0935	1.0130	1.0657	0.0732
0.0334	0.2164	1.0285	1.1499	0.1423	1.6968	0.0922	1.0128	1.0648	0.0723
0.0664	0.2150	1.0283	1.1490	0.1417	1.7636	0.0889	1.0124	1.0625	0.0703
0.0998	0.2088	1.0276	1.1448	0.1381	1.8300	0.0859	1.0120	1.0604	0.0685
0.1332	0.2079	1.0275	1.1442	0.1379	1.8964	0.0814	1.0114	1.0573	0.0657
0.1662	0.2043	1.0270	1.1417	0.1358	1.9632	0.0774	1.0108	1.0545	0.0633
0.1996	0.2022	1.0268	1.1403	0.1348	2.0296	0.0759	1.0106	1.0534	0.0625
0.2330	0.1990	1.0264	1.1382	0.1330	2.0963	0.0743	1.0104	1.0523	0.0615
0.2663	0.1967	1.0261	1.1366	0.1319	2.1627	0.0695	1.0098	1.0489	0.0584
0.2994	0.1950	1.0259	1.1355	0.1310	2.2291	0.0656	1.0092	1.0462	0.0559
0.3328	0.1941	1.0258	1.1348	0.1306	2.2959	0.0619	1.0087	1.0436	0.0535
0.3661	0.1879	1.0250	1.1306	0.1272	2.3623	0.0587	1.0083	1.0414	0.0515
0.3992	0.1869	1.0249	1.1300	0.1269	2.4291	0.0570	1.0081	1.0401	0.0504
0.4325	0.1844	1.0246	1.1282	0.1255	2.4955	0.0524	1.0074	1.0369	0.0474
0.4659	0.1819	1.0243	1.1265	0.1242	2.5619	0.0502	1.0071	1.0354	0.0462
0.4993	0.1784	1.0238	1.1242	0.1221	2.6287	0.0467	1.0067	1.0329	0.0438
0.5323	0.1764	1.0236	1.1228	0.1212	2.6951	0.0437	1.0062	1.0308	0.0419
0.5657	0.1700	1.0228	1.1184	0.1173	2.7615	0.0421	1.0060	1.0296	0.0410
0.5991	0.1687	1.0226	1.1176	0.1167	2.8282	0.0407	1.0058	1.0287	0.0402
0.6321	0.1662	1.0223	1.1159	0.1153	2.8947	0.0372	1.0054	1.0262	0.0379
0.6655	0.1650	1.0222	1.1150	0.1148	2.9614	0.0338	1.0049	1.0238	0.0355
0.6989	0.1642	1.0221	1.1144	0.1144	3.0278	0.0306	1.0044	1.0215	0.0334
0.7319	0.1598	1.0215	1.1114	0.1118	3.0942	0.0284	1.0041	1.0199	0.0319
0.7653	0.1575	1.0212	1.1098	0.1104	3.1610	0.0266	1.0039	1.0187	0.0306
0.7987	0.1538	1.0208	1.1073	0.1084	3.2274	0.0232	1.0034	1.0163	0.0283
0.8317	0.1521	1.0205	1.1061	0.1074	3.2942	0.0219	1.0032	1.0154	0.0275
0.8651	0.1500	1.0203	1.1047	0.1062	3.3606	0.0205	1.0030	1.0143	0.0266
0.8985	0.1461	1.0198	1.1021	0.1039	3.4270	0.0195	1.0029	1.0136	0.0259
0.9315	0.1445	1.0196	1.1009	0.1031	3.4938	0.0163	1.0024	1.0113	0.0238
0.9649	0.1430	1.0194	1.0999	0.1023	3.5602	0.0129	1.0020	1.0090	0.0215
0.9983	0.1416	1.0192	1.0990	0.1017	3.6269	0.0117	1.0018	1.0081	0.0206
1.0313	0.1372	1.0187	1.0959	0.0989	3.6933	0.0086	1.0014	1.0059	0.0185
1.0647	0.1338	1.0182	1.0936	0.0971	3.7601	0.0073	1.0012	1.0050	0.0175
1.0981	0.1329	1.0181	1.0930	0.0966	3.8265	0.0061	1.0010	1.0041	0.0166
1.1314	0.1323	1.0180	1.0926	0.0964	3.8929	0.0028	1.0005	1.0018	0.0143
1.1645	0.1278	1.0175	1.0895	0.0937	3.9597	0.0009	1.0002	1.0004	0.0128
1.1979	0.1246	1.0170	1.0872	0.0919	4.0261	-0.0016	0.9999	0.9986	0.0110
1.2312	0.1223	1.0167	1.0856	0.0905	4.0929	-0.0033	0.9997	0.9974	0.0098
1.2643	0.1206	1.0165	1.0845	0.0896	4.1593	-0.0046	0.9995	0.9965	0.0089
1.2976	0.1192	1.0163	1.0835	0.0887	4.2257	-0.0069	0.9991	0.9948	0.0073
1.3310	0.1165	1.0160	1.0816	0.0872	4.2924	-0.0084	0.9989	0.9937	0.0061
1.3641	0.1139	1.0157	1.0799	0.0856	4.3588	-0.0094	0.9988	0.9930	0.0054
1.3974	0.1130	1.0155	1.0792	0.0851	4.4256	-0.0128	0.9983	0.9906	0.0029
1.4308	0.1079	1.0149	1.0757	0.0818	4.4698	-0.0138	0.9981	0.9899	0.0021
1.4638	0.1071	1.0148	1.0751	0.0815	4.5254	-0.0144	0.9980	0.9894	0.0016
1.4972	0.1058	1.0146	1.0742	0.0807	4.5918	-0.0158	0.9978	0.9885	0.0007
1.5306	0.1039	1.0143	1.0729	0.0796	4.6586	-0.0182	0.9975	0.9868	-0.0011
1.5636	0.1006	1.0139	1.0706	0.0775	4.7250	-0.0196	0.9973	0.9858	-0.0021
1.5970	0.0983	1.0136	1.0690	0.0761	4.7914	-0.0211	0.9971	0.9846	-0.0034
1.6304	0.0958	1.0133	1.0673	0.0746	4.8582	-0.0223	0.9969	0.9838	-0.0043

Table B-31. Time histories of overpressure, sound speed, density and flow velocity from the reconstructed blast-wave flow field by the RCM for a 1-kg TNT surface explosion in a standard atmosphere. These signatures are for the specific radius r = 8.200 m, at which the blast-wave front arrives at time t = 16.845 ms.

t (ms)	$\Delta p/p_1$	a/a_1	ρ/ρ_1	u/a_1	t (ms)	$\Delta p/p_1$	a/a_1	ρ/ρ_1	u/a_1
0.0000	0.1865	1.0248	1.1298	0.1238	1.6638	0.0843	1.0117	1.0594	0.0652
0.0334	0.1834	1.0244	1.1276	0.1221	1.6968	0.0831	1.0115	1.0585	0.0645
0.0664	0.1811	1.0241	1.1261	0.1208	1.7636	0.0809	1.0113	1.0570	0.0632
0.0998	0.1798	1.0240	1.1252	0.1202	1.8300	0.0786	1.0109	1.0553	0.0617
0.1332	0.1779	1.0237	1.1239	0.1192	1.8967	0.0740	1.0103	1.0522	0.0588
0.1662	0.1765	1.0236	1.1229	0.1185	1.9632	0.0714	1.0100	1.0503	0.0571
0.1996	0.1731	1.0231	1.1206	0.1166	2.0299	0.0688	1.0096	1.0485	0.0556
0.2330	0.1714	1.0229	1.1194	0.1158	2.0963	0.0676	1.0095	1.0477	0.0550
0.2660	0.1692	1.0227	1.1180	0.1146	2.1627	0.0642	1.0090	1.0453	0.0528
0.2994	0.1669	1.0224	1.1164	0.1133	2.1961	0.0627	1.0088	1.0442	0.0517
0.3328	0.1647	1.0221	1.1149	0.1120	2.2625	0.0592	1.0083	1.0417	0.0495
0.3658	0.1615	1.0217	1.1127	0.1102	2.3293	0.0555	1.0078	1.0392	0.0471
0.3992	0.1599	1.0215	1.1116	0.1093	2.3957	0.0529	1.0075	1.0374	0.0455
0.4325	0.1588	1.0214	1.1109	0.1088	2.4625	0.0513	1.0072	1.0362	0.0445
0.4656	0.1539	1.0207	1.1075	0.1058	2.5289	0.0480	1.0068	1.0339	0.0423
0.4990	0.1532	1.0206	1.1070	0.1056	2.5956	0.0463	1.0066	1.0327	0.0413
0.5323	0.1513	1.0204	1.1057	0.1045	2.6620	0.0432	1.0061	1.0305	0.0392
0.5657	0.1493	1.0202	1.1043	0.1033	2.7285	0.0408	1.0058	1.0288	0.0376
0.5988	0.1484	1.0200	1.1037	0.1030	2.7952	0.0387	1.0055	1.0273	0.0363
0.6321	0.1444	1.0195	1.1010	0.1006	2.8616	0.0377	1.0054	1.0266	0.0356
0.6655	0.1422	1.0193	1.0995	0.0995	2.9284	0.0357	1.0051	1.0252	0.0343
0.6985	0.1403	1.0190	1.0982	0.0984	2.9948	0.0337	1.0048	1.0238	0.0329
0.7319	0.1377	1.0187	1.0964	0.0968	3.0616	0.0299	1.0043	1.0211	0.0304
0.7653	0.1371	1.0186	1.0959	0.0966	3.1280	0.0276	1.0040	1.0195	0.0289
0.7983	0.1339	1.0182	1.0938	0.0947	3.1944	0.0256	1.0037	1.0181	0.0276
0.8317	0.1327	1.0180	1.0929	0.0942	3.2611	0.0230	1.0033	1.0162	0.0257
0.8651	0.1303	1.0177	1.0913	0.0927	3.3275	0.0219	1.0032	1.0155	0.0251
0.8981	0.1289	1.0175	1.0903	0.0921	3.3943	0.0199	1.0029	1.0140	0.0236
0.9315	0.1257	1.0171	1.0881	0.0901	3.4607	0.0186	1.0027	1.0131	0.0228
0.9649	0.1237	1.0169	1.0867	0.0889	3.5271	0.0179	1.0026	1.0126	0.0223
0.9983	0.1206	1.0165	1.0845	0.0869	3.5939	0.0154	1.0023	1.0109	0.0206
1.0313	0.1200	1.0164	1.0842	0.0868	3.6603	0.0141	1.0021	1.0099	0.0196
1.0647	0.1167	1.0160	1.0819	0.0847	3.7267	0.0110	1.0016	1.0077	0.0174
1.0981	0.1155	1.0158	1.0810	0.0840	3.7935	0.0089	1.0013	1.0062	0.0160
1.1311	0.1118	1.0153	1.0785	0.0817	3.8599	0.0073	1.0011	1.0051	0.0149
1.1645	0.1110	1.0152	1.0779	0.0813	3.9266	0.0062	1.0010	1.0042	0.0141
1.1978	0.1094	1.0150	1.0768	0.0803	3.9931	0.0037	1.0006	1.0025	0.0124
1.2312	0.1089	1.0150	1.0765	0.0801	4.0595	0.0026	1.0004	1.0017	0.0115
1.2643	0.1075	1.0148	1.0755	0.0793	4.1262	0.0009	1.0002	1.0005	0.0103
1.2976	0.1052	1.0145	1.0739	0.0780	4.1926	-0.0013	0.9999	0.9989	0.0087
1.3310	0.1029	1.0142	1.0723	0.0765	4.2594	-0.0029	0.9997	0.9978	0.0076
1.3644	0.1021	1.0141	1.0717	0.0761	4.3258	-0.0040	0.9995	0.9970	0.0068
1.3974	0.0989	1.0136	1.0695	0.0740	4.3926	-0.0061	0.9992	0.9955	0.0053
1.4308	0.0968	1.0134	1.0681	0.0728	4.4590	-0.0075	0.9990	0.9945	0.0043
1.4642	0.0956	1.0132	1.0672	0.0721	4.5254	-0.0084	0.9989	0.9938	0.0037
1.4972	0.0940	1.0130	1.0661	0.0711	4.5922	-0.0116	0.9984	0.9916	0.0015
1.5306	0.0922	1.0128	1.0649	0.0700	4.6586	-0.0124	0.9983	0.9910	0.0008
1.5640	0.0907	1.0126	1.0638	0.0691	4.7253	-0.0134	0.9982	0.9903	0.0001
1.5970	0.0886	1.0123	1.0624	0.0679	4.7917	-0.0145	0.9980	0.9895	-0.0007
1.6304	0.0877	1.0122	1.0617	0.0674	4.8582	-0.0163	0.9977	0.9882	-0.0021

Table B-32. Time histories of overpressure, sound speed, density and flow velocity from the reconstructed blast-wave flow field by the RCM for a 1-kg TNT surface explosion in a standard atmosphere. These signatures are for the specific radius r = 9.000 m, at which the blast-wave front arrives at time t = 19.019 ms.

t (ms)	$\Delta p/p_1$	a/a_1	ρ/ρ_1	u/a_1	t (ms)	$\Delta p/p_1$	a/a_1	ρ/ρ_1	u/a_1
0.0000	0.1638	1.0220	1.1143	0.1096	1.6860	0.0772	1.0107	1.0544	0.0590
0.0223	0.1632	1.0219	1.1139	0.1093	1.7528	0.0748	1.0104	1.0527	0.0575
0.0556	0.1619	1.0217	1.1130	0.1087	1.8192	0.0731	1.0102	1.0516	0.0565
0.0887	0.1610	1.0216	1.1124	0.1082	1.8856	0.0708	1.0099	1.0500	0.0551
0.1220	0.1585	1.0213	1.1107	0.1068	1.9524	0.0669	1.0093	1.0472	0.0525
0.1554	0.1553	1.0209	1.1085	0.1050	2.0188	0.0640	1.0090	1.0452	0.0507
0.1888	0.1540	1.0207	1.1076	0.1043	2.0855	0.0628	1.0088	1.0443	0.0500
0.2218	0.1523	1.0205	1.1065	0.1033	2.1520	0.0611	1.0086	1.0432	0.0490
0.2552	0.1502	1.0202	1.1050	0.1022	2.2187	0.0585	1.0082	1.0414	0.0474
0.2886	0.1472	1.0199	1.1030	0.1003	2.2851	0.0558	1.0078	1.0394	0.0456
0.3216	0.1459	1.0197	1.1020	0.0997	2.3515	0.0527	1.0074	1.0372	0.0435
0.3550	0.1424	1.0193	1.0997	0.0975	2.4183	0.0507	1.0072	1.0359	0.0423
0.3884	0.1410	1.0191	1.0987	0.0968	2.4847	0.0478	1.0067	1.0338	0.0403
0.4218	0.1398	1.0189	1.0979	0.0962	2.5515	0.0445	1.0063	1.0315	0.0382
0.4548	0.1387	1.0188	1.0971	0.0956	2.6179	0.0439	1.0062	1.0310	0.0379
0.4882	0.1369	1.0186	1.0959	0.0945	2.6843	0.0415	1.0059	1.0294	0.0364
0.5216	0.1361	1.0184	1.0953	0.0942	2.7511	0.0386	1.0055	1.0273	0.0344
0.5546	0.1325	1.0180	1.0928	0.0920	2.8175	0.0373	1.0053	1.0264	0.0336
0.5880	0.1320	1.0179	1.0925	0.0917	2.8842	0.0360	1.0051	1.0255	0.0327
0.6213	0.1289	1.0175	1.0903	0.0898	2.9506	0.0347	1.0049	1.0246	0.0320
0.6547	0.1278	1.0174	1.0896	0.0893	3.0174	0.0326	1.0046	1.0231	0.0306
0.6878	0.1259	1.0171	1.0883	0.0882	3.0838	0.0308	1.0044	1.0218	0.0293
0.7211	0.1245	1.0170	1.0873	0.0875	3.1502	0.0279	1.0040	1.0197	0.0274
0.7545	0.1227	1.0167	1.0861	0.0864	3.2170	0.0263	1.0038	1.0186	0.0263
0.7876	0.1217	1.0166	1.0854	0.0858	3.2834	0.0244	1.0035	1.0172	0.0250
0.8209	0.1195	1.0163	1.0839	0.0845	3.3501	0.0220	1.0032	1.0156	0.0234
0.8543	0.1183	1.0162	1.0830	0.0839	3.4166	0.0207	1.0030	1.0146	0.0224
0.8877	0.1173	1.0160	1.0823	0.0833	3.4830	0.0192	1.0028	1.0135	0.0214
0.9207	0.1151	1.0157	1.0808	0.0821	3.5497	0.0181	1.0026	1.0128	0.0207
0.9541	0.1109	1.0152	1.0779	0.0794	3.6161	0.0170	1.0025	1.0120	0.0199
0.9875	0.1104	1.0151	1.0775	0.0791	3.6850	0.0163	1.0024	1.0115	0.0195
1.0205	0.1097	1.0150	1.0771	0.0788	3.7542	0.0135	1.0020	1.0095	0.0176
1.0539	0.1068	1.0147	1.0750	0.0770	3.8237	0.0115	1.0017	1.0081	0.0162
1.0873	0.1035	1.0142	1.0728	0.0750	3.8929	0.0104	1.0015	1.0073	0.0154
1.1203	0.1023	1.0141	1.0720	0.0744	3.9621	0.0081	1.0012	1.0057	0.0138
1.1537	0.1013	1.0139	1.0713	0.0737	4.0313	0.0066	1.0010	1.0046	0.0128
1.1871	0.1001	1.0138	1.0704	0.0730	4.1005	0.0051	1.0008	1.0035	0.0117
1.2204	0.0988	1.0136	1.0695	0.0722	4.1700	0.0033	1.0005	1.0022	0.0105
1.2535	0.0984	1.0136	1.0693	0.0721	4.2392	0.0014	1.0002	1.0009	0.0092
1.2869	0.0964	1.0133	1.0679	0.0708	4.3084	0.0003	1.0001	1.0001	0.0084
1.3202	0.0950	1.0131	1.0668	0.0700	4.3776	-0.0016	0.9998	0.9987	0.0070
1.3533	0.0936	1.0129	1.0659	0.0691	4.4468	-0.0033	0.9996	0.9975	0.0058
1.3867	0.0906	1.0125	1.0638	0.0673	4.5164	-0.0051	0.9993	0.9963	0.0046
1.4200	0.0888	1.0123	1.0625	0.0661	4.5856	-0.0057	0.9992	0.9958	0.0041
1.4531	0.0880	1.0122	1.0620	0.0657	4.6547	-0.0073	0.9990	0.9947	0.0030
1.4864	0.0861	1.0119	1.0606	0.0646	4.7239	-0.0085	0.9988	0.9938	0.0020
1.5198	0.0852	1.0118	1.0600	0.0640	4.7935	-0.0107	0.9985	0.9922	0.0003
1.5529	0.0832	1.0115	1.0586	0.0627	4.8627	-0.0118	0.9983	0.9914	-0.0004
1.5862	0.0813	1.0113	1.0573	0.0616					
1.6196	0.0805	1.0112	1.0567	0.0611					

Table B-33. Time histories of overpressure, sound speed, density and flow velocity from the reconstructed blast-wave flow field by the RCM for a 1-kg TNT surface explosion in a standard atmosphere. These signatures are for the specific radius r = 9.486 m, at which the blast-wave front arrives at time t = 20.372 ms.

t (ms)	$\Delta p/p_1$	a/a_1	ρ/ρ_1	u/a_1	t (ms)	$\Delta p/p_1$	a/a_1	ρ/ρ_1	u/a_1
0.0000	0.1534	1.0206	1.1072	0.1031	1.7305	0.0717	1.0100	1.0506	0.0549
0.0334	0.1499	1.0202	1.1048	0.1010	1.7969	0.0697	1.0097	1.0492	0.0536
0.0668	0.1480	1.0200	1.1035	0.0999	1.8637	0.0674	1.0094	1.0476	0.0521
0.0998	0.1468	1.0198	1.1027	0.0993	1.9301	0.0640	1.0089	1.0452	0.0499
0.1332	0.1451	1.0196	1.1016	0.0983	1.9969	0.0609	1.0085	1.0430	0.0479
0.1666	0.1437	1.0194	1.1006	0.0976	2.0633	0.0597	1.0084	1.0422	0.0472
0.1996	0.1410	1.0191	1.0987	0.0960	2.1297	0.0585	1.0082	1.0413	0.0465
0.2330	0.1399	1.0189	1.0979	0.0955	2.1965	0.0560	1.0079	1.0396	0.0449
0.2663	0.1387	1.0188	1.0971	0.0948	2.2629	0.0549	1.0077	1.0388	0.0443
0.2997	0.1354	1.0183	1.0948	0.0928	2.3317	0.0518	1.0073	1.0366	0.0422
0.3328	0.1339	1.0182	1.0938	0.0919	2.4009	0.0485	1.0068	1.0343	0.0401
0.3661	0.1329	1.0180	1.0932	0.0915	2.4705	0.0464	1.0065	1.0328	0.0387
0.3995	0.1304	1.0177	1.0914	0.0899	2.5396	0.0447	1.0063	1.0316	0.0376
0.4325	0.1299	1.0176	1.0911	0.0897	2.6088	0.0419	1.0059	1.0297	0.0357
0.4659	0.1268	1.0172	1.0889	0.0878	2.6780	0.0406	1.0058	1.0288	0.0350
0.4993	0.1260	1.0171	1.0884	0.0874	2.7472	0.0376	1.0053	1.0267	0.0330
0.5323	0.1242	1.0169	1.0871	0.0863	2.8168	0.0360	1.0051	1.0255	0.0319
0.5657	0.1218	1.0166	1.0855	0.0849	2.8860	0.0348	1.0049	1.0247	0.0311
0.5991	0.1203	1.0164	1.0844	0.0840	2.9552	0.0331	1.0047	1.0234	0.0300
0.6325	0.1198	1.0163	1.0841	0.0838	3.0243	0.0319	1.0045	1.0226	0.0294
0.6655	0.1182	1.0161	1.0830	0.0829	3.0935	0.0294	1.0042	1.0208	0.0279
0.6989	0.1168	1.0160	1.0820	0.0821	3.1631	0.0278	1.0040	1.0197	0.0270
0.7323	0.1159	1.0158	1.0814	0.0815	3.2323	0.0247	1.0035	1.0175	0.0251
0.7656	0.1137	1.0155	1.0799	0.0802	3.3015	0.0225	1.0032	1.0159	0.0238
0.7987	0.1127	1.0154	1.0792	0.0796	3.3707	0.0201	1.0029	1.0142	0.0224
0.8321	0.1123	1.0154	1.0789	0.0796	3.4402	0.0188	1.0027	1.0133	0.0218
0.8654	0.1096	1.0150	1.0770	0.0779	3.5094	0.0171	1.0025	1.0121	0.0208
0.8985	0.1079	1.0148	1.0758	0.0769	3.5786	0.0162	1.0023	1.0114	0.0204
0.9319	0.1051	1.0144	1.0739	0.0751	3.6478	0.0147	1.0021	1.0104	0.0196
0.9652	0.1047	1.0144	1.0736	0.0749	3.7173	0.0139	1.0020	1.0098	0.0193
0.9983	0.1018	1.0140	1.0716	0.0731	3.7865	0.0116	1.0017	1.0082	0.0179
1.0316	0.1008	1.0139	1.0709	0.0725	3.8557	0.0091	1.0013	1.0064	0.0163
1.0650	0.0976	1.0134	1.0687	0.0705	3.9249	0.0075	1.0011	1.0053	0.0154
1.0981	0.0965	1.0133	1.0680	0.0699	3.9944	0.0058	1.0009	1.0040	0.0143
1.1314	0.0954	1.0131	1.0672	0.0692	4.0636	0.0041	1.0006	1.0028	0.0133
1.1648	0.0951	1.0131	1.0669	0.0691	4.1328	0.0029	1.0005	1.0020	0.0127
1.1982	0.0940	1.0130	1.0661	0.0684	4.2020	0.0007	1.0001	1.0004	0.0113
1.2312	0.0936	1.0129	1.0659	0.0683	4.2712	-0.0012	0.9999	0.9991	0.0101
1.2646	0.0917	1.0127	1.0646	0.0671	4.3408	-0.0018	0.9998	0.9987	0.0099
1.2980	0.0897	1.0124	1.0632	0.0659	4.4100	-0.0041	0.9995	0.9970	0.0084
1.3310	0.0886	1.0122	1.0624	0.0653	4.4792	-0.0055	0.9993	0.9960	0.0076
1.3644	0.0872	1.0121	1.0615	0.0645	4.5483	-0.0066	0.9991	0.9952	0.0069
1.3978	0.0847	1.0117	1.0597	0.0629	4.6179	-0.0085	0.9988	0.9939	0.0057
1.4312	0.0842	1.0117	1.0594	0.0626	4.6871	-0.0096	0.9987	0.9931	0.0050
1.4642	0.0819	1.0114	1.0578	0.0611	4.7563	-0.0106	0.9985	0.9923	0.0044
1.4976	0.0810	1.0112	1.0571	0.0606	4.8255	-0.0121	0.9983	0.9912	0.0035
1.5310	0.0791	1.0110	1.0558	0.0594					
1.5640	0.0788	1.0109	1.0556	0.0592					
1.5974	0.0766	1.0106	1.0541	0.0579					
1.6641	0.0734	1.0102	1.0518	0.0558					

APPENDIX C

RECONSTRUCTED BLAST-WAVE FLOW-FIELD PROPERTIES FOR ANFO

Reconstructed blast-wave flow properties are given in tabular form in this appendix for a 1-kg TNT equivalent ANFO surface explosion in a standard atmosphere for which p_0 = 101.33 kPa, T_0 = 288.15 K, and a_0 = 340.3 m/s. Note that since 500 tons of TNT are considered equivalent to 628 tons of ANFO, 1 kg of TNT is equivalent to 1.256 kg of ANFO. These reconstructed flow properties consist of thirty-nine sets of time histories for the overpressure $(p - p_0)/p_0$, sound speed a/a_0, density ρ/ρ_0 and flow velocity u/a_0, each one at a different fixed radial distance from the explosion center. The particular radius r for each set of results is noted in the caption, along with the time of arrival t_a of the blast-wave front at this specific radius. These results cover in small steps the distance range from about 1 to 10 m, for which the peak blast-wave overpressure decays from approximately 2 to 0.01 MPa.

If the time histories are required for the flow properties of an ANFO explosion of a charge size other than 1.256 kg of ANFO (1-kg TNT equivalent) in an atmosphere with a different pressure and temperature, then these tabulated results have to be scaled to apply to this new case. The procedure is demonstrated here by means of a simple example. Assume that the flow properties are required at a radius r of 23.8 m from a surface explosion of 1000 kg of ANFO in an atmosphere in which p_1 = 95 kPa, T_1 = 310 kPa and a_1 = 353 m/s. The scaling factors for radius S_r and time S_t are (see page 17 of this report)

$$S_r = [(W/W_o)\ (p_0/p_1)]^{1/3}$$

$$= [(1000.0\ \text{kg}/1.256\ \text{kg})\ (101.33\ \text{kPa}/95.0\ \text{kPa})]^{1/3} = 9.47,$$

and

$$S_t = (a_0/a_1)\ S_r = (340.3\ \text{m/s}/353.0\ \text{m/s})\ 9.47 = 9.13.$$

The radius r of 23.8 m of interest for the example is now scaled for the case of a 1 kg TNT equivalent ANFO explosion (1.256 kg ANFO). Consequently, the result follows as $23.8\ \text{m}/S_r = 23.8\ \text{m}/9.47 = 2.51$ m. The scaled flow properties of interest are now given for this scaled radius of 2.51 m in table C-18. In order to get the required unscaled flow properties for the explosion of 1000 kg of ANFO, the times listed in table C-18 are simply multiplied by S_t or 9.13. The nondimensional amplitudes of the flow-field properties remain unchanged, of course, but the dimensional amplitudes depend on the atmospheric conditions for the example in question, as indicated by the subscript 1 in the table.

Table C-1. Time histories of overpressure, sound speed, density and flow velocity from the reconstructed blast-wave flow field by the RCM for a 1-kg TNT equivalent ANFO surface explosion in a standard atmosphere. These signatures are for the specific radius r = 1.570 m, at which the blast-wave front arrives at time t = 0.791 ms.

t (ms)	$\Delta p/p_1$	a/a_1	ρ/ρ_1	u/a_1	t (ms)	$\Delta p/p_1$	a/a_1	ρ/ρ_1	u/a_1
0.0000	8.5912	1.6004	3.7447	2.1292	1.0734	0.0354	1.4031	0.5259	0.1580
0.0170	7.2710	1.5903	3.2705	1.9927	1.1304	0.0044	1.3970	0.5146	0.1399
0.0518	5.6580	1.5650	2.7185	1.7922	1.1401	-0.0028	1.3956	0.5120	0.1410
0.0581	5.3794	1.5554	2.6368	1.7569	1.1885	-0.0175	1.3926	0.5066	0.1215
0.0883	4.0628	1.5362	2.1453	1.5349	1.2375	-0.0294	1.3902	0.5022	0.1064
0.1252	3.3424	1.5431	1.8237	1.4032	1.2472	-0.0336	1.3894	0.5006	0.1049
0.1314	3.1164	1.5633	1.6843	1.3502	1.3070	-0.0576	1.3844	0.4917	0.0912
0.1631	2.6031	1.5360	1.5271	1.2299	1.3571	-0.0779	1.3801	0.4841	0.0723
0.1888	2.1846	1.5281	1.3639	1.1153	1.3672	-0.0813	1.3793	0.4829	0.0699
0.2017	2.0685	1.5200	1.3282	1.0811	1.4277	-0.0919	1.3771	0.4789	0.0552
0.2420	1.7955	1.5320	1.1911	0.9825	1.4892	-0.1191	1.3711	0.4686	0.0405
0.2830	1.4004	1.4990	1.0682	0.8471	1.5515	-0.1202	1.3709	0.4682	0.0257
0.3248	1.1916	1.4797	1.0010	0.7702	1.5619	-0.1225	1.3703	0.4673	0.0233
0.3672	1.0497	1.4656	0.9543	0.7055	1.6144	-0.1371	1.3671	0.4617	0.0109
0.3891	0.9585	1.4561	0.9237	0.6694	1.6780	-0.1559	1.3628	0.4545	-0.0039
0.4113	0.8986	1.4496	0.9035	0.6463	1.7424	-0.1740	1.3586	0.4475	-0.0189
0.4485	0.7902	1.4735	0.8245	0.5762	1.8741	-0.1915	1.3544	0.4407	-0.0484
0.4562	0.7854	1.4730	0.8229	0.5762	1.9412	-0.2073	1.3506	0.4346	-0.0608
0.4791	0.6918	1.4617	0.7919	0.5359	2.0775	-0.2237	1.3466	0.4281	-0.0800
0.5028	0.6571	1.4573	0.7803	0.5222	2.1467	-0.2370	1.3432	0.4229	-0.0782
0.5421	0.5721	1.4464	0.7514	0.4851	2.2869	-0.2430	1.3417	0.4205	-0.0921
0.5501	0.5684	1.4459	0.7502	0.4851	2.4166	-0.2414	1.3421	0.4211	-0.0901
0.5981	0.4567	1.4308	0.7116	0.4342	2.5004	-0.2416	1.3421	0.4211	-0.0981
0.6471	0.3869	1.4601	0.6505	0.3974	2.6457	-0.2484	1.3403	0.4184	-0.0988
0.6554	0.3696	1.4575	0.6447	0.3970	2.7316	-0.2600	1.3374	0.4137	-0.1063
0.6972	0.3124	1.4487	0.6254	0.3680	2.8679	-0.2691	1.3350	0.4101	-0.1255
0.7312	0.2828	1.4439	0.6152	0.3381	3.0181	-0.2757	1.3333	0.4074	-0.1379
0.7483	0.2699	1.4419	0.6108	0.3318	3.0939	-0.2807	1.3320	0.4054	-0.1443
0.7917	0.2027	1.4335	0.5853	0.2784	3.2479	-0.2831	1.3288	0.4060	-0.1555
0.8004	0.1882	1.4310	0.5803	0.2675	3.3651	-0.2970	1.3250	0.4004	-0.1631
0.8533	0.1642	1.4268	0.5719	0.2388	3.4833	-0.3003	1.3242	0.3990	-0.1749
0.9072	0.1334	1.4214	0.5610	0.2148					
0.9614	0.0890	1.4133	0.5452	0.1965					
1.0167	0.0694	1.4096	0.5382	0.1803					
1.0261	0.0537	1.4066	0.5326	0.1680					

Table C-2. Time histories of overpressure, sound speed, density and flow velocity from the reconstructed blast-wave flow field by the RCM for a 1-kg TNT equivalent ANFO surface explosion in a standard atmosphere. These signatures are for the specific radius r = 1.616 m, at which the blast-wave front arrives at time t = 0.849 ms.

t (ms)	$\Delta p/p_1$	a/a_1	ρ/ρ_1	u/a_1	t (ms)	$\Delta p/p_1$	a/a_1	ρ/ρ_1	u/a_1
0.0000	7.2064	1.5403	3.4589	1.9501	1.1304	0.0168	1.3591	0.5505	0.1581
0.0303	5.9568	1.5514	2.8903	1.8046	1.1794	-0.0024	1.3554	0.5430	0.1377
0.0671	4.4625	1.5213	2.3602	1.5782	1.1892	-0.0081	1.3543	0.5408	0.1374
0.0734	4.2080	1.5110	2.2811	1.5326	1.2490	-0.0302	1.3500	0.5322	0.1097
0.1050	3.4186	1.4759	2.0284	1.3861	1.2990	-0.0456	1.3842	0.4981	0.1104
0.1307	2.9718	1.4839	1.8039	1.2949	1.3091	-0.0497	1.3834	0.4966	0.1068
0.1436	2.7727	1.4730	1.7388	1.2248	1.3696	-0.0748	1.3781	0.4872	0.0905
0.1839	2.2112	1.4501	1.5271	1.0853	1.4312	-0.0945	1.3739	0.4798	0.0629
0.2250	1.8286	1.4817	1.2884	0.9802	1.4934	-0.1016	1.3723	0.4771	0.0517
0.2667	1.5136	1.4590	1.1808	0.8804	1.5038	-0.1141	1.3696	0.4723	0.0464
0.3091	1.2434	1.4535	1.0620	0.7833	1.5563	-0.1301	1.3660	0.4662	0.0307
0.3310	1.1522	1.4449	1.0309	0.7583	1.6200	-0.1272	1.3667	0.4673	0.0265
0.3533	1.0630	1.4669	0.9587	0.7243	1.6843	-0.1438	1.3629	0.4609	0.0056
0.3905	0.9548	1.4557	0.9225	0.6874	1.7497	-0.1622	1.3587	0.4538	-0.0086
0.3981	0.9488	1.4550	0.9205	0.6874	1.8161	-0.1815	1.3542	0.4463	-0.0201
0.4211	0,8480	1.4440	0.8862	0.6472	1.8832	-0.1928	1.3515	0.4420	-0.0309
0.4447	0.7744	1.4357	0.8609	0.6144	2.0195	-0.2154	1.3097	0.4574	-0.0503
0.4840	0.6585	1.4219	0.8203	0.5617	2.0887	-0.2304	1.3061	0.4512	-0.0630
0.4920	0.6542	1.4214	0.8188	0.5617	2.2288	-0.2392	1.3040	0.4474	-0.0770
0.5400	0.5692	1.4107	0.7885	0.5082	2.3585	-0.2400	1.3037	0.4471	-0.0892
0.5890	0.4862	1.3998	0.7585	0.4590	2.4423	-0.2400	1.3038	0.4471	-0.0873
0.5974	0.4638	1.3968	0.7503	0.4467	2.5876	-0.2488	1.3016	0.4434	-0.0865
0.6391	0.4152	1.3900	0.7325	0.4033	2.6735	-0.2476	1.3019	0.4439	-0.0925
0.6732	0.3768	1.3846	0.7182	0.3851	2.8098	-0.2575	1.2994	0.4397	-0.1014
0.6902	0.3590	1.3820	0.7115	0.3829	2.9600	-0.2671	1.2970	0.4357	-0.1276
0.7337	0.3096	1.4092	0.6595	0.3497	3.0358	-0.2637	1.2979	0.4371	-0.1323
0.7424	0.3007	1.4078	0.6563	0.3446	3.1899	-0.2794	1.2939	0.4304	-0.1333
0.7952	0.2320	1.3969	0.6314	0.3057	3.3070	-0.2840	1.2927	0.4285	-0.1447
0.8491	0.1708	1.3868	0.6088	0.2567	3.4253	-0.2962	1.2895	0.4232	-0.1537
0.9033	0.1280	1.3794	0.5928	0.2302	3.5654	-0.2968	1.2894	0.4230	-0.1683
0.9586	0.0950	1.3736	0.5804	0.2209					
0.9680	0.0951	1.3736	0.5804	0.2127					
1.0153	0.0695	1.3690	0.5707	0.1948					
1.0723	0.0347	1.3625	0.5574	0.1613					
1.0821	0.0313	1.3619	0.5561	0.1608					

Table C-3. Time histories of overpressure, sound speed, density and flow velocity from the reconstructed blast-wave flow field by the RCM for a 1-kg TNT equivalent ANFO surface explosion in a standard atmosphere. These signatures are for the specific radius r = 1.691 m, at which the blast-wave front arrives at time t = 0.923 ms.

t (ms)	$\Delta p/p_1$	a/a_1	ρ/ρ_1	u/a_1	t (ms)	$\Delta p/p_1$	a/a_1	ρ/ρ_1	u/a_1
0.0000	6.7143	1.5017	3.4210	1.8512	1.1756	0.0124	1.3251	0.5766	0.1586
0.0316	5.4284	1.4728	2.9636	1.7062	1.2257	-0.0001	1.3227	0.5715	0.1436
0.0574	4.5491	1.4682	2.5744	1.5765	1.2357	-0.0041	1.3220	0.5698	0.1406
0.0702	4.1647	1.4649	2.4067	1.5132	1.2962	-0.0321	1.3166	0.5584	0.1195
0.1106	3.2322	1.4668	1.9670	1.3372	1.3578	-0.0521	1.3127	0.5501	0.1089
0.1516	2.6464	1.4360	1.7684	1.2010	1.4200	-0.0671	1.3097	0.5439	0.0886
0.1933	2.1078	1.4035	1.5776	1.0662	1.4305	-0.0743	1.3082	0.5408	0.0835
0.2357	1.8196	1.3998	1.4389	0.9917	1.4830	-0.0924	1.3046	0.5333	0.0611
0.2577	1.6633	1.4015	1.3560	0.9466	1.5466	-0.1019	1.3026	0.5293	0.0577
0.2799	1.4347	1.3939	1.2531	0.8682	1.6109	-0.1259	1.2976	0.5192	0.0424
0.3171	1.2230	1.3759	1.1743	0.7727	1.6763	-0.1298	1.2967	0.5175	0.0319
0.3248	1.2156	1.3752	1.1715	0.7727	1.7427	-0.1494	1.2925	0.5091	0.0222
0.3477	1.1336	1.3941	1.0979	0.7442	1.7987	-0.1673	1.2886	0.5015	0.0088
0.3714	1.0749	1.3885	1.0762	0.7262	1.8098	-0.1673	1.2886	0.5015	0.0088
0.4106	0.9330	1.4033	0.9816	0.6617	1.8776	-0.1801	1.2858	0.4960	-0.0083
0.4186	0.9272	1.4027	0.9796	0.6617	2.0038	-0.2006	1.2811	0.4871	-0.0264
0.4666	0.7588	1.3864	0.9150	0.5931	2.0852	-0.2139	1.2781	0.4813	-0.0451
0.5156	0.6505	1.3739	0.8744	0.5466	2.2260	-0.2272	1.2749	0.4754	-0.0651
0.5240	0.6343	1.3891	0.8469	0.5403	2.2969	-0.2368	1.2727	0.4712	-0.0669
0.5657	0.5517	1.3789	0.8161	0.4895	2.4412	-0.2425	1.2713	0.4687	-0.0791
0.5998	0.5098	1.3735	0.8003	0.4721	2.5876	-0.2457	1.2705	0.4673	-0.0799
0.6168	0.4874	1.3706	0.7918	0.4617	2.6620	-0.2404	1.2718	0.4696	-0.0853
0.6603	0.4029	1.3883	0.7279	0.4235	2.8116	-0.2400	1.2719	0.4698	-0.0939
0.6690	0.3987	1.3877	0.7263	0.4226	2.8992	-0.2539	1.2685	0.4636	-0.0972
0.7218	0.3414	1.3794	0.7050	0.3840	3.0390	-0.2659	1.2656	0.4583	-0.1099
0.7757	0.2783	1.3700	0.6811	0.3506	3.1944	-0.2745	1.2635	0.4545	-0.1178
0.8300	0.2226	1.3613	0.6598	0.3035	3.2730	-0.2778	1.2627	0.4530	-0.1250
0.8853	0.1557	1.3504	0.6338	0.2619	3.4312	-0.2802	1.2620	0.4519	-0.1446
0.8946	0.1503	1.3495	0.6316	0.2588	3.5525	-0.2829	1.2614	0.4507	-0.1505
0.9419	0.1282	1.3457	0.6230	0.2393	3.6433	-0.2857	1.2607	0.4495	-0.1582
0.9990	0.1003	1.3409	0.6119	0.2157					
1.0087	0.0906	1.3392	0.6080	0.2101					
1.0570	0.0716	1.3359	0.6005	0.2073					
1.1061	0.0401	1.3302	0.5878	0.1883					
1.1158	0.0368	1.3296	0.5865	0.1862					

Table C-4. Time histories of overpressure, sound speed, density and flow velocity from the reconstructed blast-wave flow field by the RCM for a 1-kg TNT equivalent ANFO surface explosion in a standard atmosphere. These signatures are for the specific radius r = 1.737 m, at which the blast-wave front arrives at time t = 0.980 ms.

t (ms)	$\Delta p/p_1$	a/a_1	ρ/ρ_1	u/a_1	t (ms)	$\Delta p/p_1$	a/a_1	ρ/ρ_1	u/a_1
0.0000	6.0764	1.4601	3.3191	1.7475	1.1784	0.0189	1.3263	0.5793	0.1683
0.0129	5.5940	1.4557	3.1116	1.6867	1.2389	0.0040	1.3235	0.5732	0.1503
0.0532	4.3111	1.4321	2.5896	1.4995	1.3004	-0.0178	1.3194	0.5643	0.1291
0.0942	3.4792	1.4126	2.2446	1.3648	1.3627	-0.0448	1.3141	0.5531	0.1094
0.1360	2.8033	1.4232	1.8778	1.2292	1.3731	-0.0514	1.3128	0.5504	0.1042
0.1784	2.3669	1.4197	1.6705	1.1300	1.4256	-0.0672	1.3097	0.5439	0.0972
0.2003	2.0321	1.3986	1.5501	1.0374	1.4892	-0.0781	1.3075	0.5393	0.0823
0.2225	1.8777	1.3882	1.4933	0.9976	1.5536	-0.1056	1.3018	0.5278	0.0659
0.2597	1.6514	1.3720	1.4085	0.9204	1.6189	-0.1166	1.2995	0.5231	0.0601
0.2674	1.6412	1.3713	1.4046	0.9204	1.6853	-0.1401	1.2945	0.5131	0.0415
0.2903	1.4182	1.3541	1.3188	0.8431	1.7413	-0.1417	1.2942	0.5125	0.0378
0.3140	1.2790	1.3427	1.2641	0.7961	1.7524	-0.1419	1.2941	0.5124	0.0378
0.3533	1.1034	1.3550	1.1456	0.7328	1.8202	-0.1591	1.2904	0.5050	0.0204
0.3613	1.0967	1.3544	1.1430	0.7328	1.8887	-0.1690	1.2882	0.5007	0.0059
0.4093	0.9311	1.3485	1.0620	0.6726	1.9465	-0.1791	1.2860	0.4964	-0.0114
0.4583	0.8119	1.3363	1.0147	0.6214	2.0278	-0.1920	1.2831	0.4908	-0.0251
0.4666	0.7951	1.3601	0.9704	0.6152	2.1686	-0.2213	1.2763	0.4780	-0.0452
0.5083	0.6864	1.3480	0.9281	0.5672	2.2396	-0.2278	1.2748	0.4752	-0.0505
0.5424	0.6096	1.3391	0.8977	0.5331	2.3839	-0.2362	1.2728	0.4715	-0.0673
0.5595	0.5941	1.3372	0.8915	0.5131	2.5303	-0.2394	1.2720	0.4700	-0.0773
0.6029	0.5167	1.3555	0.8255	0.4771	2.6047	-0.2348	1.2731	0.4721	-0.0760
0.6116	0.5028	1.3537	0.8201	0.4704	2.7542	-0.2446	1.2708	0.4678	-0.0785
0.6645	0.4197	1.3427	0.7874	0.4288	2.8418	-0.2460	1.2704	0.4671	-0.0807
0.7184	0.3570	1.3360	0.7603	0.3972	2.9816	-0.2558	1.2681	0.4628	-0.0883
0.7726	0.3002	1.3279	0.7374	0.3618	3.1370	-0.2657	1.2656	0.4584	-0.1106
0.8279	0.2471	1.3200	0.7158	0.3218	3.2156	-0.2646	1.2659	0.4589	-0.1123
0.8373	0.2272	1.3169	0.7076	0.3148	3.3738	-0.2686	1.2649	0.4571	-0.1264
0.8846	0.1870	1.3271	0.6740	0.2924	3.4951	-0.2768	1.2629	0.4534	-0.1402
0.9416	0.1433	1.3200	0.6562	0.2484	3.5859	-0.2827	1.2350	0.4703	-0.1466
0.9513	0.1260	1.3171	0.6491	0.2362	3.6770	-0.2819	1.2351	0.4707	-0.1396
0.9997	0.1004	1.3128	0.6385	0.2256					
1.0487	0.0815	1.3376	0.6045	0.2071					
1.0584	0.0780	1.3370	0.6031	0.2051					
1.1182	0.0506	1.3321	0.5921	0.1875					
1.1683	0.0325	1.3288	0.5847	0.1799					

Table C-5. Time histories of overpressure, sound speed, density and flow velocity from the reconstructed blast-wave flow field by the RCM for a 1-kg TNT equivalent ANFO surface explosion in a standard atmosphere. These signatures are for the specific radius r = 1.782 m, at which the blast-wave front arrives at time t = 1.033 ms.

t (ms)	$\Delta p/p_1$	a/a_1	ρ/ρ_1	u/a_1	t (ms)	$\Delta p/p_1$	a/a_1	ρ/ρ_1	u/a_1
0.0000	5.5576	1.4295	3.2090	1.6587	1.2472	0.0012	1.2792	0.6118	0.1544
0.0410	4.4522	1.4240	2.6889	1.5122	1.3095	-0.0189	1.2755	0.6031	0.1412
0.0828	3.4520	1.3882	2.3102	1.3403	1.3199	-0.0208	1.2751	0.6022	0.1319
0.1252	2.8095	1.3667	2.0395	1.2149	1.3724	-0.0494	1.2698	0.5896	0.1150
0.1471	2.5485	1.3773	1.8707	1.1590	1.4360	-0.0583	1.2681	0.5857	0.1092
0.1693	2.3373	1.3763	1.7619	1.1119	1.5004	-0.0833	1.2790	0.5604	0.0960
0.2065	1.9583	1.3922	1.5263	1.0113	1.5657	-0.1009	1.2755	0.5527	0.0735
0.2142	1.8857	1.3873	1.4994	0.9906	1.6321	-0.1132	1.2729	0.5473	0.0591
0.2371	1.7600	1.3799	1.4495	0.9536	1.6881	-0.1311	1.2692	0.5393	0.0438
0.2608	1.6433	1.3714	1.4054	0.9227	1.6992	-0.1313	1.2692	0.5393	0.0438
0.3001	1.2795	1.3427	1.2644	0.7988	1.7670	-0.1395	1.2675	0.5356	0.0306
0.3081	1.2718	1.3421	1.2613	0.7988	1.8355	-0.1516	1.2649	0.5302	0.0201
0.3561	1.1229	1.3291	1.2017	0.7371	1.8933	-0.1643	1.2622	0.5245	0.0093
0.4051	0.9664	1.3147	1.1377	0.6798	1.9047	-0.1666	1.2617	0.5235	0.0073
0.4134	0.9483	1.3129	1.1302	0.6740	1.9746	-0.1836	1.2580	0.5159	-0.0035
0.4551	0.8260	1.3156	1.0551	0.6256	2.1154	-0.2003	1.2543	0.5083	-0.0237
0.4892	0.7404	1.3188	1.0006	0.5882	2.1864	-0.2128	1.2515	0.5026	-0.0418
0.5063	0.7155	1.3161	0.9904	0.5708	2.3307	-0.2247	1.2487	0.4972	-0.0587
0.5497	0.6162	1.3050	0.9491	0.5259	2.4771	-0.2322	1.2470	0.4937	-0.0766
0.5584	0.5952	1.3025	0.9403	0.5160	2.5515	-0.2384	1.2456	0.4909	-0.0744
0.6113	0.5072	1.3016	0.8897	0.4775	2.7010	-0.2398	1.2452	0.4903	-0.0700
0.6652	0.4331	1.2922	0.8582	0.4314	2.7886	-0.2450	1.2440	0.4879	-0.0747
0.7194	0.3680	1.3083	0.7992	0.4088	2.9284	-0.2474	1.2435	0.4868	-0.0759
0.7747	0.3135	1.3007	0.7764	0.3615	3.0838	-0.2547	1.2264	0.4955	-0.0933
0.7841	0.2942	1.2980	0.7682	0.3542	3.1624	-0.2580	1.2256	0.4940	-0.1061
0.8314	0.2588	1.2928	0.7531	0.3355	3.3206	-0.2628	1.2245	0.4917	-0.1184
0.8884	0.1971	1.3104	0.6971	0.2887	3.4419	-0.2677	1.2216	0.4908	-0.1226
0.8981	0.1836	1.3083	0.6915	0.2855	3.5327	-0.2759	1.2196	0.4868	-0.1265
0.9465	0.1410	1.3014	0.6736	0.2512	3.6238	-0.2802	1.2186	0.4848	-0.1309
0.9955	0.1100	1.2964	0.6605	0.2344					
1.0052	0.1056	1.2956	0.6586	0.2319					
1.0650	0.0834	1.2919	0.6492	0.2106					
1.1151	0.0708	1.2897	0.6438	0.1976					
1.1252	0.0656	1.2888	0.6415	0.1940					
1.1857	0.0352	1.2835	0.6284	0.1750					

Table C-6. Time histories of overpressure, sound speed, density and flow velocity from the reconstructed blast-wave flow field by the RCM for a 1-kg TNT equivalent ANFO surface explosion in a standard atmosphere. These signatures are for the specific radius r = 1.857 m, at which the blast-wave front arrives at time t = 1.116 ms.

t (ms)	$\Delta p/p_1$	a/a_1	ρ/ρ_1	u/a_1	t (ms)	$\Delta p/p_1$	a/a_1	ρ/ρ_1	u/a_1
0.0000	5.1968	1.4077	3.1270	1.5942	1.2371	0.0185	1.2307	0.6725	0.1784
0.0424	4.0013	1.3752	2.6445	1.4136	1.2896	-0.0041	1.2268	0.6618	0.1548
0.0643	3.6802	1.3764	2.4705	1.3638	1.3533	-0.0176	1.2244	0.6554	0.1418
0.0866	3.1611	1.3631	2.2397	1.2634	1.4176	-0.0510	1.2183	0.6393	0.1202
0.1238	2.7409	1.3493	2.0546	1.1829	1.4830	-0.0653	1.2157	0.6324	0.1051
0.1314	2.6947	1.3469	2.0365	1.1753	1.5494	-0.0743	1.2373	0.6047	0.0921
0.1544	2.4305	1.3375	1.9178	1.1128	1.6054	-0.0955	1.2332	0.5948	0.0728
0.1780	2.2718	1.3284	1.8540	1.0803	1.6165	-0.0958	1.2331	0.5946	0.0728
0.2173	1.8557	1.3106	1.6626	0.9585	1.6843	-0.1093	1.2305	0.5883	0.0671
0.2253	1.8446	1.3099	1.6579	0.9585	1.7528	-0.1316	1.2260	0.5777	0.0521
0.2733	1.5647	1.3148	1.4835	0.8828	1.8105	-0.1441	1.2235	0.5717	0.0409
0.3223	1.2364	1.3192	1.2851	0.7755	1.8220	-0.1463	1.2231	0.5707	0.0389
0.3307	1.2070	1.3167	1.2730	0.7661	1.8919	-0.1483	1.2227	0.5697	0.0328
0.3724	1.0738	1.3233	1.1842	0.7233	1.9621	-0.1680	1.2186	0.5603	0.0123
0.4065	0.9992	1.3164	1.1537	0.6969	2.0327	-0.1790	1.2163	0.5550	-0.0001
0.4235	0.9865	1.3152	1.1484	0.6790	2.1036	-0.1867	1.2146	0.5512	-0.0142
0.4670	0.8420	1.3025	1.0859	0.6247	2.2479	-0.2002	1.2117	0.5447	-0.0367
0.4757	0.8020	1.2984	1.0689	0.6069	2.3943	-0.2255	1.2062	0.5324	-0.0462
0.5285	0.6940	1.2870	1.0228	0.5539	2.4687	-0.2279	1.2056	0.5311	-0.0521
0.5824	0.5952	1.2760	0.9798	0.5092	2.6182	-0.2411	1.2027	0.5247	-0.0629
0.6367	0.5258	1.2679	0.9492	0.4765	2.7059	-0.2416	1.2026	0.5244	-0.0653
0.6919	0.4358	1.2569	0.9088	0.4340	2.8456	-0.2384	1.2033	0.5260	-0.0688
0.7013	0.4126	1.2540	0.8983	0.4201	3.0011	-0.2379	1.1808	0.5467	-0.0792
0.7486	0.3603	1.2473	0.8744	0.3945	3.0796	-0.2408	1.1801	0.5452	-0.0858
0.8056	0.3069	1.2659	0.8155	0.3567	3.2378	-0.2520	1.1776	0.5394	-0.0982
0.8154	0.2973	1.2646	0.8112	0.3517	3.3592	-0.2616	1.1754	0.5344	-0.1020
0.8637	0.2608	1.2595	0.7948	0.3251	3.4499	-0.2646	1.1747	0.5329	-0.1072
0.9127	0.2108	1.2522	0.7722	0.2957	3.5410	-0.2637	1.1749	0.5334	-0.1155
0.9225	0.2005	1.2507	0.7675	0.2894	3.6624	-0.2679	1.1654	0.5391	-0.1241
0.9823	0.1413	1.2417	0.7403	0.2552					
1.0323	0.1234	1.2480	0.7212	0.2376					
1.0424	0.1211	1.2477	0.7202	0.2369					
1.1029	0.0811	1.2412	0.7017	0.2153					
1.1645	0.0553	1.2369	0.6897	0.1983					
1.2267	0.0307	1.2328	0.6782	0.1885					

Table C-7. Time histories of overpressure, sound speed, density and flow velocity from the reconstructed blast-wave flow field by the RCM for a 1-kg TNT equivalent ANFO surface explosion in a standard atmosphere. These signatures are for the specific radius r = 1.903 m, at which the blast-wave front arrives at time t = 1.181 ms.

t (ms)	$\Delta p/p_1$	a/a_1	ρ/ρ_1	u/a_1	t (ms)	$\Delta p/p_1$	a/a_1	ρ/ρ_1	u/a_1
0.0000	4.6254	1.3727	2.9852	1.4872	1.2889	0.0177	1.1966	0.7107	0.1703
0.0223	4.1116	1.3628	2.7522	1.4087	1.3533	-0.0082	1.2057	0.6822	0.1452
0.0595	3.5156	1.3498	2.4786	1.3131	1.4186	-0.0287	1.2021	0.6721	0.1340
0.0671	3.3361	1.3419	2.4078	1.2787	1.4851	-0.0531	1.2090	0.6478	0.1144
0.0901	3.0445	1.3341	2.2724	1.2153	1.5410	-0.0692	1.2060	0.6400	0.1070
0.1137	2.8035	1.3287	2.1543	1.1702	1.5522	-0.0697	1.2059	0.6397	0.1070
0.1530	2.4053	1.3313	1.9213	1.0863	1.6200	-0.0863	1.2028	0.6316	0.0937
0.1610	2.3200	1.3265	1.8867	1.0662	1.6885	-0.1042	1.1994	0.6226	0.0724
0.2090	1.8931	1.3007	1.7101	0.9599	1.7462	-0.1155	1.1973	0.6170	0.0583
0.2580	1.6046	1.2858	1.5753	0.8806	1.7577	-0.1178	1.1968	0.6159	0.0564
0.2663	1.5841	1.2920	1.5480	0.8767	1.8275	-0.1344	1.1936	0.6076	0.0480
0.3081	1.3369	1.2736	1.4407	0.7974	1.8978	-0.1396	1.1926	0.6050	0.0338
0.3421	1.1824	1.2621	1.3700	0.7497	1.9684	-0.1570	1.1891	0.5962	0.0228
0.3592	1.1308	1.2578	1.3468	0.7233	2.0275	-0.1642	1.1876	0.5926	0.0080
0.4026	1.0137	1.2804	1.2282	0.6860	2.0393	-0.1657	1.1873	0.5918	0.0065
0.4113	0.9908	1.2783	1.2182	0.6782	2.1836	-0.1886	1.1826	0.5802	-0.0073
0.4642	0.8585	1.2847	1.1260	0.6271	2.3300	-0.2088	1.1784	0.5698	-0.0287
0.5181	0.7401	1.2906	1.0448	0.5712	2.4044	-0.2207	1.1758	0.5637	-0.0373
0.5723	0.6359	1.2792	0.9997	0.5254	2.5539	-0.2272	1.1744	0.5604	-0.0524
0.6276	0.5459	1.2702	0.9581	0.4770	2.6415	-0.2364	1.1724	0.5555	-0.0626
0.6370	0.5232	1.2676	0.9480	0.4652	2.7813	-0.2333	1.1731	0.5572	-0.0705
0.6843	0.4713	1.2613	0.9248	0.4427	2.9367	-0.2330	1.1622	0.5678	-0.0755
0.7413	0.3815	1.2500	0.8842	0.3988	3.0153	-0.2352	1.1487	0.5795	-0.0752
0.7510	0.3659	1.2480	0.8770	0.3896	3.1735	-0.2455	1.1465	0.5739	-0.0812
0.7994	0.3373	1.2442	0.8639	0.3693	3.2949	-0.2530	1.1449	0.5699	-0.0923
0.8484	0.2845	1.2371	0.8394	0.3452	3.3856	-0.2548	1.1445	0.5689	-0.1030
0.8581	0.2692	1.2350	0.8322	0.3361	3.4767	-0.2556	1.1443	0.5685	-0.1051
0.9179	0.2242	1.2286	0.8110	0.3162	3.5981	-0.2644	1.1424	0.5637	-0.1089
0.9680	0.1832	1.2226	0.7915	0.2880	3.7194	-0.2690	1.1414	0.5612	-0.1188
0.9781	0.1692	1.2206	0.7848	0.2788					
1.0386	0.1147	1.2123	0.7585	0.2447					
1.1001	0.0857	1.2077	0.7444	0.2228					
1.1624	0.0649	1.2044	0.7342	0.2025					
1.1728	0.0563	1.2030	0.7299	0.1973					
1.2253	0.0308	1.1988	0.7173	0.1835					

Table C-8. Time histories of overpressure, sound speed, density and flow velocity from the reconstructed blast-wave flow field by the RCM for a 1-kg TNT equivalent ANFO surface explosion in a standard atmosphere. These signatures are for the specific radius r = 1.948 m, at which the blast-wave front arrives at time t = 1.240 ms.

t (ms)	$\Delta p/p_1$	a/a_1	ρ/ρ_1	u/a_1	t (ms)	$\Delta p/p_1$	a/a_1	ρ/ρ_1	u/a_1
0.0000	4.2968	1.3519	2.8982	1.4225	1.3592	-0.0110	1.1917	0.6964	0.1505
0.0076	4.0763	1.3437	2.8115	1.3859	1.4256	-0.0287	1.1886	0.6874	0.1397
0.0306	3.7029	1.3380	2.6268	1.3273	1.4816	-0.0430	1.1861	0.6802	0.1231
0.0542	3.4528	1.3362	2.4939	1.2895	1.4927	-0.0437	1.1860	0.6799	0.1231
0.0935	2.8390	1.3181	2.2096	1.1710	1.5605	-0.0624	1.1827	0.6703	0.1033
0.1015	2.7593	1.3142	2.1768	1.1555	1.6290	-0.0788	1.1797	0.6619	0.0946
0.1495	2.2822	1.3010	1.9390	1.0531	1.6867	-0.1011	1.1756	0.6505	0.0734
0.1985	1.9062	1.2949	1.7332	0.9511	1.6982	-0.1024	1.1753	0.6498	0.0725
0.2069	1.8687	1.2991	1.6998	0.9426	1.7681	-0.1128	1.1734	0.6444	0.0593
0.2486	1.6661	1.2856	1.6131	0.8893	1.8383	-0.1273	1.1706	0.6369	0.0436
0.2827	1.5177	1.2751	1.5485	0.8467	1.9089	-0.1357	1.1690	0.6325	0.0292
0.2997	1.4423	1.2696	1.5152	0.8155	1.9680	-0.1426	1.1677	0.6288	0.0313
0.3432	1.1835	1.2538	1.3889	0.7292	1.9798	-0.1462	1.1670	0.6270	0.0280
0.3519	1.1266	1.2491	1.3630	0.7083	2.0518	-0.1644	1.1634	0.6174	0.0191
0.4047	1.0249	1.2478	1.3006	0.6767	2.1241	-0.1758	1.1611	0.6113	0.0058
0.4586	0.8859	1.2361	1.2344	0.6266	2.2705	-0.1989	1.1564	0.5991	-0.0133
0.5129	0.7651	1.2366	1.1542	0.5820	2.3449	-0.2021	1.1557	0.5974	-0.0178
0.5682	0.6511	1.2446	1.0659	0.5329	2.4944	-0.2212	1.1517	0.5871	-0.0444
0.5775	0.6287	1.2422	1.0555	0.5143	2.5821	-0.2236	1.1512	0.5858	-0.0535
0.6248	0.5498	1.2518	0.9890	0.4788	2.7218	-0.2295	1.1500	0.5826	-0.0663
0.6819	0.4667	1.2420	0.9508	0.4432	2.8773	-0.2315	1.1495	0.5816	-0.0678
0.6916	0.4561	1.2407	0.9459	0.4389	2.9559	-0.2361	1.1486	0.5791	-0.0680
0.7399	0.4123	1.2353	0.9255	0.4162	3.1141	-0.2364	1.1485	0.5789	-0.0683
0.7889	0.3400	1.2433	0.8669	0.3798	3.2354	-0.2399	1.1477	0.5770	-0.0833
0.7987	0.3359	1.2427	0.8650	0.3787	3.3262	-0.2465	1.1463	0.5734	-0.0909
0.8585	0.2837	1.2357	0.8408	0.3450	3.4173	-0.2544	1.1446	0.5691	-0.0987
0.9086	0.2478	1.2319	0.8221	0.3286	3.5386	-0.2562	1.1442	0.5681	-0.0994
0.9186	0.2328	1.2298	0.8151	0.3194	3.6600	-0.2582	1.1437	0.5670	-0.1104
0.9791	0.1899	1.2236	0.7947	0.2864	3.7813	-0.2623	1.1428	0.5648	-0.1203
1.0407	0.1251	1.2139	0.7636	0.2476	3.9030	-0.2621	1.1429	0.5649	-0.1251
1.1029	0.1049	1.2107	0.7537	0.2306					
1.1134	0.0881	1.2081	0.7455	0.2188					
1.1659	0.0736	1.2058	0.7384	0.2037					
1.2295	0.0484	1.2017	0.7260	0.1906					
1.2938	0.0285	1.1984	0.7161	0.1753					

Table C-9. Time histories of overpressure, sound speed, density and flow velocity from the reconstructed blast-wave flow field by the RCM for a 1-kg TNT equivalent ANFO surface explosion in a standard atmosphere. These signatures are for the specific radius r = 1.971 m, at which the blast-wave front arrives at time t = 1.271 ms.

t (ms)	$\Delta p/p_1$	a/a_1	ρ/ρ_1	u/a_1	t (ms)	$\Delta p/p_1$	a/a_1	ρ/ρ_1	u/a_1
0.0000	4.0691	1.3372	2.8347	1.3760	1.4510	-0.0300	1.1884	0.6868	0.1335
0.0236	3.6892	1.3286	2.6566	1.3158	1.4621	-0.0307	1.1883	0.6864	0.1335
0.0629	3.0756	1.3194	2.3411	1.2061	1.5299	-0.0564	1.1837	0.6734	0.1120
0.0709	3.0006	1.3159	2.3102	1.1929	1.5984	-0.0712	1.1811	0.6658	0.0987
0.1189	2.5549	1.3037	2.0916	1.1073	1.6561	-0.0793	1.1796	0.6617	0.0866
0.1679	2.1945	1.2899	1.9200	1.0209	1.6676	-0.0820	1.1791	0.6603	0.0846
0.1763	2.0957	1.2902	1.8596	0.9957	1.7375	-0.0998	1.1758	0.6511	0.0681
0.2180	1.7869	1.2781	1.7061	0.9136	1.8077	-0.1116	1.1736	0.6450	0.0511
0.2521	1.6263	1.2763	1.6123	0.8701	1.8783	-0.1288	1.1703	0.6360	0.0401
0.2691	1.5692	1.2723	1.5871	0.8537	1.9374	-0.1440	1.1674	0.6281	0.0364
0.3126	1.3123	1.2597	1.4572	0.7738	1.9492	-0.1460	1.1670	0.6271	0.0346
0.3213	1.2911	1.2580	1.4476	0.7685	2.0212	-0.1562	1.1650	0.6217	0.0244
0.3741	1.0714	1.2401	1.3470	0.6935	2.0935	-0.1700	1.1622	0.6144	0.0130
0.4280	0.9629	1.2349	1.2872	0.6595	2.1666	-0.1825	1.1597	0.6078	0.0034
0.4823	0.8410	1.2309	1.2151	0.6063	2.2399	-0.1918	1.1578	0.6029	-0.0077
0.5376	0.7129	1.2192	1.1524	0.5579	2.3143	-0.1952	1.1571	0.6011	-0.0167
0.5469	0.6821	1.2160	1.1375	0.5419	2.4638	-0.2133	1.1534	0.5914	-0.0427
0.5942	0.5958	1.2189	1.0740	0.5092	2.5515	-0.2202	1.1519	0.5877	-0.0523
0.6513	0.5127	1.2292	1.0012	0.4659	2.6912	-0.2251	1.1509	0.5850	-0.0628
0.6610	0.4933	1.2269	0.9920	0.4584	2.8467	-0.2330	1.1492	0.5807	-0.0664
0.7093	0.4433	1.2209	0.9682	0.4375	2.9253	-0.2333	1.1492	0.5806	-0.0638
0.7583	0.3837	1.2317	0.9121	0.4001	3.0835	-0.2337	1.1491	0.5804	-0.0715
0.7681	0.3647	1.2293	0.9031	0.3895	3.2048	-0.2382	1.1481	0.5780	-0.0792
0.8279	0.3145	1.2227	0.8792	0.3655	3.2956	-0.2416	1.1474	0.5761	-0.0815
0.8780	0.2725	1.2171	0.8591	0.3357	3.3867	-0.2508	1.1454	0.5711	-0.0878
0.8880	0.2586	1.2152	0.8524	0.3276	3.5080	-0.2530	1.1449	0.5699	-0.0987
0.9485	0.2205	1.2268	0.8110	0.3114	3.6294	-0.2532	1.1448	0.5698	-0.1053
1.0101	0.1632	1.2184	0.7836	0.2689	3.7507	-0.2564	1.1441	0.5680	-0.1152
1.0723	0.1158	1.2124	0.7591	0.2313	3.8724	-0.2596	1.1434	0.5663	-0.1229
1.0828	0.1111	1.2117	0.7568	0.2285					
1.1353	0.0831	1.2073	0.7431	0.2133					
1.1989	0.0681	1.2049	0.7357	0.2027					
1.2632	0.0366	1.1998	0.7202	0.1862					
1.3286	0.0091	1.1951	0.7065	0.1684					
1.3950	-0.0159	1.1909	0.6939	0.1437					

Table C-10. Time histories of overpressure, sound speed, density and flow velocity from the reconstructed blast-wave flow field by the RCM for a 1-kg TNT equivalent ANFO surface explosion in a standard atmosphere. These signatures are for the specific radius r = 2.016 m, at which the blast-wave front arrives at time t = 1.334 ms.

t (ms)	$\Delta p/p_1$	a/a_1	ρ/ρ_1	u/a_1	t (ms)	$\Delta p/p_1$	a/a_1	ρ/ρ_1	u/a_1
0.0000	3.8705	1.3243	2.7773	1.3344	1.4670	-0.0183	1.1728	0.7137	0.1365
0.0080	3.7344	1.3189	2.7216	1.3117	1.5355	-0.0332	1.1866	0.6866	0.1233
0.0560	3.0268	1.2940	2.4050	1.1874	1.5932	-0.0521	1.1833	0.6770	0.1016
0.1050	2.6300	1.2866	2.1930	1.1058	1.6047	-0.0575	1.1823	0.6743	0.0972
0.1134	2.5854	1.2872	2.1641	1.0984	1.6746	-0.0726	1.1796	0.6665	0.0891
0.1551	2.2377	1.2767	1.9862	1.0202	1.7448	-0.0968	1.1751	0.6541	0.0784
0.1892	1.8982	1.2629	1.8173	0.9339	1.8154	-0.1106	1.1725	0.6469	0.0664
0.2062	1.8510	1.2599	1.7961	0.9270	1.8745	-0.1212	1.1718	0.6400	0.0573
0.2497	1.6218	1.2540	1.6673	0.8683	1.8863	-0.1234	1.1713	0.6389	0.0554
0.2583	1.5844	1.2514	1.6503	0.8586	1.9583	-0.1410	1.1680	0.6297	0.0432
0.3112	1.3283	1.2457	1.5004	0.7819	2.0306	-0.1468	1.1668	0.6266	0.0368
0.3651	1.0993	1.2274	1.3935	0.6981	2.1036	-0.1606	1.1641	0.6194	0.0237
0.4193	0.9858	1.2326	1.3071	0.6632	2.1770	-0.1711	1.1620	0.6139	0.0095
0.4746	0.8514	1.2203	1.2432	0.6141	2.1895	-0.1705	1.1621	0.6142	0.0071
0.4840	0.8303	1.2183	1.2331	0.5983	2.3258	-0.1845	1.1593	0.6068	-0.0106
0.5313	0.7437	1.2099	1.1911	0.5656	2.4760	-0.2017	1.1558	0.5976	-0.0325
0.5883	0.6281	1.2023	1.1262	0.5201	2.5518	-0.2093	1.1542	0.5935	-0.0444
0.5981	0.6013	1.1995	1.1129	0.5057	2.7059	-0.2233	1.1501	0.5872	-0.0492
0.6464	0.5466	1.1936	1.0856	0.4760	2.8230	-0.2344	1.1477	0.5812	-0.0591
0.6954	0.4801	1.1931	1.0397	0.4478	2.9412	-0.2282	1.1490	0.5846	-0.0632
0.7051	0.4660	1.1915	1.0327	0.4415	3.0814	-0.2321	1.1482	0.5825	-0.0681
0.7650	0.4133	1.1862	1.0045	0.4128	3.2024	-0.2340	1.1478	0.5814	-0.0659
0.8150	0.3446	1.1895	0.9504	0.3682	3.2632	-0.2345	1.1477	0.5812	-0.0712
0.8251	0.3344	1.1882	0.9452	0.3633	3.3842	-0.2392	1.1308	0.5950	-0.0795
0.8856	0.2829	1.1909	0.9045	0.3375	3.5056	-0.2452	1.1296	0.5916	-0.0948
0.9472	0.2430	1.1856	0.8843	0.3143	3.6269	-0.2468	1.1292	0.5907	-0.1002
1.0094	0.1934	1.1882	0.8453	0.2872	3.7486	-0.2523	1.1280	0.5876	-0.1094
1.0198	0.1798	1.1863	0.8384	0.2780	3.8199	-0.2514	1.1282	0.5881	-0.1137
1.0723	0.1368	1.1976	0.7926	0.2548					
1.1360	0.0968	1.1915	0.7725	0.2288					
1.2003	0.0654	1.1866	0.7567	0.2012					
1.2657	0.0470	1.1836	0.7473	0.1853					
1.3321	0.0187	1.1790	0.7329	0.1693					
1.3880	-0.0053	1.1750	0.7205	0.1493					
1.3992	-0.0060	1.1749	0.7201	0.1493					

Table C-11. Time histories of overpressure, sound speed, density and flow velocity from the reconstructed blast-wave flow field by the RCM for a 1-kg TNT equivalent ANFO surface explosion in a standard atmosphere. These signatures are for the specific radius r = 2.091 m, at which the blast-wave front arrives at time t = 1.447 ms.

t (ms)	$\Delta p/p_1$	a/a_1	ρ/ρ_1	u/a_1	t (ms)	$\Delta p/p_1$	a/a_1	ρ/ρ_1	u/a_1
0.0000	3.3997	1.2955	2.6214	1.2310	1.5612	-0.0373	1.1228	0.7635	0.1253
0.0417	2.9021	1.2792	2.3846	1.1412	1.6314	-0.0636	1.1295	0.7339	0.1056
0.0758	2.5824	1.2679	2.2286	1.0790	1.7020	-0.0776	1.1271	0.7261	0.0975
0.0928	2.5313	1.2653	2.2059	1.0698	1.7611	-0.0896	1.1340	0.7080	0.0865
0.1363	2.1845	1.2513	2.0338	0.9952	1.7730	-0.0921	1.1335	0.7066	0.0846
0.1450	2.1318	1.2483	2.0098	0.9838	1.8449	-0.1066	1.1309	0.6985	0.0668
0.1978	1.7321	1.2354	1.7902	0.8782	1.9173	-0.1159	1.1293	0.6933	0.0590
0.2517	1.5455	1.2257	1.6944	0.8349	1.9903	-0.1301	1.1266	0.6853	0.0401
0.3060	1.3037	1.2221	1.5424	0.7574	2.0636	-0.1400	1.1248	0.6797	0.0287
0.3613	1.0722	1.2069	1.4225	0.6788	2.0762	-0.1404	1.1247	0.6795	0.0287
0.3707	1.0575	1.2057	1.4153	0.6724	2.1380	-0.1452	1.1238	0.6768	0.0230
0.4179	0.9725	1.2040	1.3607	0.6395	2.2125	-0.1625	1.1206	0.6670	0.0045
0.4750	0.8402	1.2045	1.2684	0.5918	2.2876	-0.1705	1.1190	0.6624	0.0000
0.4847	0.8130	1.2019	1.2549	0.5796	2.3752	-0.1856	1.1161	0.6538	-0.0125
0.5330	0.7572	1.1966	1.2272	0.5572	2.5150	-0.2002	1.1132	0.6454	-0.0209
0.5821	0.6513	1.1860	1.1740	0.5127	2.6704	-0.2155	1.1101	0.6366	-0.0455
0.5918	0.6257	1.1834	1.1609	0.5014	2.7490	-0.2165	1.1099	0.6360	-0.0495
0.6516	0.5426	1.1829	1.1025	0.4668	2.9072	-0.2290	1.1074	0.6287	-0.0575
0.7017	0.4827	1.1822	1.0609	0.4418	3.0285	-0.2261	1.1080	0.6304	-0.0608
0.7118	0.4657	1.1803	1.0522	0.4337	3.1193	-0.2279	1.1076	0.6294	-0.0672
0.7723	0.3997	1.1725	1.0181	0.4018	3.2104	-0.2268	1.1078	0.6300	-0.0700
0.8338	0.3293	1.1639	0.9813	0.3591	3.3317	-0.2260	1.0992	0.6406	-0.0725
0.8960	0.2888	1.1588	0.9599	0.3385	3.4531	-0.2304	1.0875	0.6507	-0.0810
0.9065	0.2752	1.1570	0.9526	0.3252	3.5744	-0.2398	1.0856	0.6451	-0.0934
0.9590	0.2375	1.1561	0.9258	0.3078	3.6961	-0.2434	1.0841	0.6438	-0.0955
1.0226	0.2021	1.1514	0.9068	0.2862	3.7570	-0.2423	1.0843	0.6445	-0.0982
1.0869	0.1492	1.1440	0.8781	0.2530	3.8787	-0.2462	1.0835	0.6421	-0.1058
1.1523	0.1024	1.1372	0.8524	0.2187					
1.2187	0.0750	1.1398	0.8274	0.1983					
1.2747	0.0565	1.1370	0.8172	0.1799					
1.2858	0.0555	1.1369	0.8167	0.1799					
1.3536	0.0346	1.1336	0.8051	0.1691					
1.4221	0.0052	1.1290	0.7887	0.1547					
1.4798	-0.0225	1.1253	0.7719	0.1393					
1.4913	-0.0258	1.1248	0.7701	0.1372					

Table C-12. Time histories of overpressure, sound speed, density and flow velocity from the reconstructed blast-wave flow field by the RCM for a 1-kg TNT equivalent ANFO surface explosion in a standard atmosphere. These signatures are for the specific radius r = 2.137 m, at which the blast-wave front arrives at time t = 1.523 ms.

t (ms)	$\Delta p/p_1$	a/a_1	ρ/ρ_1	u/a_1	t (ms)	$\Delta p/p_1$	a/a_1	ρ/ρ_1	u/a_1
0.0000	3.1511	1.2757	2.5507	1.1733	1.6262	-0.0469	1.1099	0.7737	0.1139
0.0170	2.9573	1.2670	2.4651	1.1341	1.6853	-0.0633	1.1110	0.7588	0.1005
0.0605	2.6234	1.2601	2.2820	1.0739	1.6972	-0.0685	1.1102	0.7558	0.0964
0.0692	2.5454	1.2562	2.2468	1.0581	1.7691	-0.0772	1.1087	0.7508	0.0838
0.1220	2.1616	1.2450	2.0398	0.9772	1.8415	-0.0900	1.1065	0.7433	0.0715
0.1759	1.7945	1.2241	1.8650	0.8862	1.9145	-0.1059	1.1037	0.7340	0.0594
0.2302	1.5921	1.2150	1.7558	0.8317	1.9878	-0.1172	1.1017	0.7273	0.0477
0.2855	1.3511	1.2092	1.6081	0.7615	2.0004	-0.1177	1.1016	0.7271	0.0444
0.2949	1.2963	1.2051	1.5812	0.7412	2.0622	-0.1293	1.0995	0.7202	0.0374
0.3421	1.1262	1.1946	1.4900	0.6883	2.1367	-0.1401	1.0976	0.7139	0.0271
0.3992	0.9838	1.1904	1.3999	0.6413	2.2118	-0.1571	1.0944	0.7037	0.0183
0.4089	0.9767	1.1898	1.3963	0.6384	2.2869	-0.1696	1.0921	0.6963	0.0083
0.4572	0.9019	1.1891	1.3451	0.6148	2.2994	-0.1704	1.0919	0.6958	0.0079
0.5063	0.7834	1.1813	1.2779	0.5687	2.4392	-0.1820	1.0898	0.6888	-0.0122
0.5160	0.7603	1.1791	1.2661	0.5598	2.5946	-0.2004	1.0862	0.6777	-0.0303
0.5758	0.6802	1.1719	1.2233	0.5235	2.6732	-0.2092	1.0845	0.6723	-0.0397
0.6259	0.6067	1.1692	1.1752	0.4869	2.8314	-0.2166	1.0830	0.6679	-0.0488
0.6360	0.5790	1.1663	1.1607	0.4742	2.9527	-0.2207	1.0822	0.6654	-0.0584
0.6965	0.4869	1.1619	1.1014	0.4344	3.0435	-0.2238	1.0816	0.6635	-0.0644
0.7580	0.4175	1.1604	1.0527	0.4033	3.1346	-0.2203	1.0823	0.6657	-0.0638
0.8202	0.3651	1.1542	1.0247	0.3746	3.2559	-0.2232	1.0779	0.6686	-0.0706
0.8307	0.3557	1.1531	1.0197	0.3684	3.3773	-0.2213	1.0783	0.6697	-0.0714
0.8832	0.3124	1.1559	0.9823	0.3414	3.4986	-0.2296	1.0766	0.6646	-0.0778
0.9468	0.2581	1.1489	0.9531	0.3154	3.6203	-0.2339	1.0758	0.6620	-0.0853
1.0111	0.2160	1.1492	0.9208	0.2863	3.6812	-0.2370	1.0752	0.6600	-0.0911
1.0765	0.1787	1.1441	0.9005	0.2581	3.8029	-0.2405	1.0745	0.6579	-0.0940
1.1429	0.1333	1.1377	0.8756	0.2333	3.9246	-0.2449	1.0736	0.6551	-0.1032
1.1989	0.0892	1.1312	0.8511	0.2115					
1.2100	0.0880	1.1311	0.8505	0.2115					
1.2778	0.0556	1.1262	0.8323	0.1894					
1.3463	0.0350	1.1230	0.8207	0.1765					
1.4040	0.0128	1.1196	0.8081	0.1629					
1.4155	0.0089	1.1189	0.8058	0.1605					
1.4854	-0.0169	1.1148	0.7911	0.1433					
1.5556	-0.0298	1.1127	0.7836	0.1321					

Table C-13. Time histories of overpressure, sound speed, density and flow velocity from the reconstructed blast-wave flow field by the RCM for a 1-kg TNT equivalent ANFO surface explosion in a standard atmosphere. These signatures are for the specific radius r = 2.182 m, at which the blast-wave front arrives at time t = 1.583 ms.

t (ms)	$\Delta p/p_1$	a/a_1	ρ/ρ_1	u/a_1	t (ms)	$\Delta p/p_1$	a/a_1	ρ/ρ_1	u/a_1
0.0000	3.0015	1.2655	2.4987	1.1374	1.6367	-0.0363	1.1116	0.7799	0.1154
0.0087	2.9123	1.2614	2.4587	1.1209	1.7086	-0.0565	1.1083	0.7682	0.0972
0.0615	2.5077	1.2454	2.2617	1.0457	1.7810	-0.0698	1.1060	0.7604	0.0849
0.1154	2.2019	1.2351	2.0989	0.9822	1.8540	-0.0817	1.1040	0.7534	0.0733
0.1697	1.8006	1.2171	1.8907	0.8804	1.9273	-0.1023	1.1004	0.7414	0.0599
0.2250	1.5787	1.2097	1.7622	0.8187	1.9399	-0.1031	1.1003	0.7409	0.0587
0.2344	1.5576	1.2083	1.7519	0.8114	2.0017	-0.1111	1.0989	0.7361	0.0573
0.2816	1.4068	1.2022	1.6652	0.7731	2.0762	-0.1259	1.0962	0.7273	0.0461
0.3387	1.1823	1.1910	1.5384	0.7019	2.1513	-0.1418	1.0934	0.7179	0.0339
0.3484	1.1206	1.1861	1.5072	0.6734	2.2264	-0.1455	1.0927	0.7157	0.0214
0.3967	1.0231	1.1782	1.4574	0.6461	2.2389	-0.1505	1.0918	0.7127	0.0174
0.4458	0.9186	1.1745	1.3908	0.6106	2.3022	-0.1586	1.0903	0.7078	0.0106
0.4555	0.8975	1.1727	1.3798	0.6035	2.3787	-0.1645	1.0892	0.7043	0.0023
0.5153	0.7786	1.1645	1.3117	0.5599	2.5341	-0.1881	1.0847	0.6900	-0.0141
0.5654	0.7109	1.1655	1.2594	0.5302	2.6127	-0.1929	1.0838	0.6871	-0.0220
0.5755	0.6962	1.1641	1.2517	0.5250	2.7709	-0.2091	1.0807	0.6772	-0.0444
0.6360	0.5988	1.1600	1.1882	0.4785	2.8922	-0.2126	1.0800	0.6751	-0.0507
0.6975	0.4995	1.1524	1.1291	0.4324	2.9830	-0.2178	1.0790	0.6719	-0.0589
0.7597	0.4443	1.1469	1.0981	0.4051	3.0741	-0.2205	1.0784	0.6702	-0.0651
0.7702	0.4273	1.1496	1.0799	0.3954	3.1954	-0.2166	1.0792	0.6726	-0.0647
0.8227	0.3778	1.1439	1.0531	0.3715	3.3168	-0.2228	1.0780	0.6688	-0.0682
0.8863	0.3238	1.1373	1.0234	0.3382	3.4381	-0.2208	1.0784	0.6701	-0.0691
0.9506	0.2656	1.1418	0.9708	0.3104	3.5598	-0.2260	1.0774	0.6668	-0.0769
1.0160	0.2243	1.1364	0.9481	0.2953	3.6207	-0.2276	1.0770	0.6658	-0.0774
1.0824	0.1762	1.1299	0.9213	0.2660	3.7424	-0.2353	1.0755	0.6611	-0.0891
1.1384	0.1394	1.1248	0.9006	0.2431	3.8641	-0.2351	1.0701	0.6680	-0.0955
1.1495	0.1381	1.1246	0.8999	0.2431	3.9854	-0.2408	1.0614	0.6739	-0.1031
1.2173	0.0892	1.1176	0.8721	0.2129					
1.2858	0.0630	1.1216	0.8450	0.1975					
1.3435	0.0476	1.1250	0.8278	0.1852					
1.3550	0.0389	1.1236	0.8228	0.1792					
1.4249	0.0243	1.1214	0.8146	0.1646					
1.4951	-0.0010	1.1174	0.8002	0.1449					
1.5657	-0.0232	1.1138	0.7875	0.1291					
1.6248	-0.0282	1.1129	0.7845	0.1215					

Table C-14. Time histories of overpressure, sound speed, density and flow velocity from the reconstructed blast-wave flow field by the RCM for a 1-kg TNT equivalent ANFO surface explosion in a standard atmosphere. These signatures are for the specific radius r = 2.257 m, at which the blast-wave front arrives at time t = 1.699 ms.

t (ms)	$\Delta p/p_1$	a/a_1	ρ/ρ_1	u/a_1	t (ms)	$\Delta p/p_1$	a/a_1	ρ/ρ_1	u/a_1
0.0000	2.7744	1.2493	2.4181	1.0812	1.7385	-0.0496	1.0847	0.8077	0.1055
0.0542	2.3732	1.2347	2.2128	0.9985	1.8119	-0.0740	1.0807	0.7928	0.0885
0.1095	2.0448	1.2173	2.0547	0.9286	1.8244	-0.0751	1.0805	0.7922	0.0848
0.1189	2.0279	1.2164	2.0465	0.9199	1.8863	-0.0769	1.0802	0.7911	0.0779
0.1662	1.7403	1.2022	1.8960	0.8489	1.9607	-0.0921	1.0828	0.7744	0.0662
0.2232	1.5237	1.1922	1.7757	0.7924	2.0358	-0.1052	1.0806	0.7663	0.0531
0.2330	1.5091	1.1928	1.7635	0.7878	2.1109	-0.1188	1.0782	0.7580	0.0443
0.2813	1.3719	1.1860	1.6861	0.7534	2.1234	-0.1213	1.0777	0.7565	0.0431
0.3303	1.1660	1.1795	1.5569	0.6814	2.1867	-0.1320	1.0759	0.7499	0.0328
0.3401	1.0976	1.1741	1.5217	0.6568	2.2632	-0.1421	1.0741	0.7437	0.0260
0.3999	1.0043	1.1665	1.4730	0.6269	2.3408	-0.1549	1.0718	0.7357	0.0146
0.4499	0.9251	1.1602	1.4302	0.5951	2.4186	-0.1646	1.0700	0.7297	0.0031
0.4600	0.9052	1.1585	1.4196	0.5886	2.4972	-0.1664	1.0697	0.7286	-0.0038
0.5205	0.7734	1.1509	1.3389	0.5388	2.6554	-0.1843	1.0664	0.7174	-0.0240
0.5821	0.6837	1.1477	1.2782	0.5089	2.7768	-0.1971	1.0589	0.7160	-0.0395
0.6443	0.5789	1.1372	1.2209	0.4682	2.8675	-0.2032	1.0578	0.7122	-0.0487
0.6547	0.5523	1.1395	1.1954	0.4560	2.9586	-0.2079	1.0569	0.7091	-0.0502
0.7072	0.4986	1.1338	1.1657	0.4306	3.0800	-0.2139	1.0557	0.7053	-0.0586
0.7709	0.4396	1.1273	1.1328	0.4019	3.2013	-0.2165	1.0552	0.7036	-0.0644
0.8352	0.3749	1.1224	1.0913	0.3728	3.3227	-0.2178	1.0550	0.7028	-0.0631
0.9006	0.3159	1.1154	1.0577	0.3430	3.4444	-0.2177	1.0507	0.7087	-0.0677
0.9670	0.2658	1.1164	1.0156	0.3156	3.5052	-0.2160	1.0510	0.7098	-0.0674
1.0230	0.2242	1.1111	0.9916	0.2859	3.6269	-0.2177	1.0507	0.7086	-0.0770
1.0341	0.2226	1.1109	0.9907	0.2859	3.7486	-0.2197	1.0497	0.7081	-0.0813
1.1019	0.1852	1.1114	0.9595	0.2652	3.8700	-0.2305	1.0477	0.7011	-0.0939
1.1704	0.1475	1.1063	0.9376	0.2423	3.9917	-0.2291	1.0452	0.7057	-0.0957
1.2281	0.1219	1.1056	0.9177	0.2206					
1.2396	0.1030	1.1030	0.9067	0.2080					
1.3095	0.0813	1.0998	0.8939	0.1954					
1.3797	0.0515	1.0960	0.8753	0.1730					
1.4503	0.0310	1.0930	0.8631	0.1576					
1.5094	0.0136	1.0948	0.8457	0.1427					
1.5212	0.0154	1.0950	0.8468	0.1446					
1.5932	-0.0182	1.0898	0.8267	0.1240					
1.6655	-0.0280	1.0882	0.8208	0.1186					

Table C-15. Time histories of overpressure, sound speed, density and flow velocity from the reconstructed blast-wave flow field by the RCM for a 1-kg TNT equivalent ANFO surface explosion in a standard atmosphere. These signatures are for the specific radius r = 2.325 m, at which the blast-wave front arrives at time t = 1.818 ms.

t (ms)	$\Delta p/p_1$	a/a_1	ρ/ρ_1	u/a_1	t (ms)	$\Delta p/p_1$	a/a_1	ρ/ρ_1	u/a_1
0.0000	2.5122	1.2304	2.3199	1.0119	1.7674	-0.0397	1.0663	0.8446	0.1049
0.0473	2.2212	1.2173	2.1739	0.9524	1.8418	-0.0634	1.0625	0.8296	0.0868
0.1043	1.9827	1.2098	2.0380	0.8985	1.9169	-0.0773	1.0603	0.8208	0.0802
0.1140	1.8959	1.2057	1.9919	0.8760	1.9920	-0.0896	1.0582	0.8130	0.0678
0.1624	1.6758	1.1945	1.8754	0.8195	2.0045	-0.0932	1.0576	0.8106	0.0654
0.2114	1.4936	1.1828	1.7824	0.7731	2.0678	-0.1036	1.0559	0.8040	0.0540
0.2211	1.4757	1.1816	1.7733	0.7697	2.1443	-0.1135	1.0542	0.7977	0.0424
0.2809	1.2795	1.1680	1.6709	0.7103	2.2218	-0.1197	1.0532	0.7937	0.0356
0.3310	1.1357	1.1601	1.5868	0.6652	2.2997	-0.1356	1.0504	0.7834	0.0195
0.3411	1.1153	1.1586	1.5760	0.6595	2.3390	-0.1380	1.0500	0.7818	0.0180
0.4016	0.9747	1.1511	1.4903	0.6134	2.3783	-0.1412	1.0494	0.7798	0.0152
0.4631	0.8550	1.1451	1.4146	0.5724	2.4572	-0.1518	1.0476	0.7729	0.0034
0.5254	0.7419	1.1372	1.3469	0.5274	2.5365	-0.1572	1.0466	0.7694	-0.0044
0.5358	0.7262	1.1385	1.3318	0.5219	2.6579	-0.1740	1.0436	0.7584	-0.0172
0.5883	0.6620	1.1357	1.2886	0.4980	2.7486	-0.1836	1.0419	0.7521	-0.0250
0.6519	0.5748	1.1270	1.2400	0.4544	2.8397	-0.1907	1.0406	0.7474	-0.0338
0.7163	0.4899	1.1185	1.1910	0.4171	2.9611	-0.2020	1.0385	0.7400	-0.0467
0.7816	0.4311	1.1125	1.1564	0.3896	3.0824	-0.2053	1.0379	0.7378	-0.0521
0.8481	0.3726	1.1095	1.1150	0.3607	3.2038	-0.2113	1.0368	0.7338	-0.0615
0.9040	0.3344	1.1051	1.0927	0.3364	3.3255	-0.2108	1.0368	0.7341	-0.0656
0.9152	0.3324	1.1048	1.0915	0.3364	3.3863	-0.2094	1.0371	0.7351	-0.0632
0.9830	0.2762	1.0980	1.0585	0.3041	3.5080	-0.2116	1.0367	0.7336	-0.0696
1.0515	0.2315	1.0975	1.0224	0.2816	3.6297	-0.2091	1.0372	0.7352	-0.0708
1.1092	0.1995	1.0934	1.0033	0.2604	3.7511	-0.2140	1.0362	0.7320	-0.0779
1.1207	0.1922	1.0925	0.9989	0.2566	3.8728	-0.2215	1.0348	0.7270	-0.0826
1.1905	0.1587	1.0880	0.9788	0.2349	3.9944	-0.2256	1.0340	0.7243	-0.0909
1.2608	0.1181	1.0873	0.9457	0.2125	4.0856	-0.2279	1.0336	0.7227	-0.0954
1.3314	0.0798	1.0819	0.9224	0.1894					
1.3905	0.0567	1.0810	0.9043	0.1770					
1.4023	0.0470	1.0796	0.8984	0.1706					
1.4743	0.0267	1.0765	0.8858	0.1593					
1.5466	0.0123	1.0744	0.8770	0.1412					
1.6196	-0.0038	1.0719	0.8670	0.1308					
1.6930	-0.0264	1.0684	0.8529	0.1120					
1.7055	-0.0264	1.0684	0.8529	0.1114					

Table C-16. Time histories of overpressure, sound speed, density and flow velocity from the reconstructed blast-wave flow field by the RCM for a 1-kg TNT equivalent ANFO surface explosion in a standard atmosphere. These signatures are for the specific radius r = 2.393 m, at which the blast-wave front arrives at time t = 1.932 ms.

t (ms)	$\Delta p/p_1$	a/a_1	ρ/ρ_1	u/a_1	t (ms)	$\Delta p/p_1$	a/a_1	ρ/ρ_1	u/a_1
0.0000	2.3497	1.2187	2.2555	0.9693	1.8780	-0.0508	1.0526	0.8568	0.0892
0.0483	2.1402	1.2087	2.1493	0.9218	1.8905	-0.0579	1.0514	0.8521	0.0829
0.0974	1.9222	1.1985	2.0343	0.8748	1.9538	-0.0691	1.0497	0.8449	0.0750
0.1071	1.8520	1.1944	1.9993	0.8569	2.0303	-0.0792	1.0480	0.8383	0.0647
0.1669	1.5832	1.1795	1.8568	0.7839	2.1078	-0.0883	1.0514	0.8247	0.0558
0.2170	1.4589	1.1751	1.7806	0.7538	2.1857	-0.1044	1.0487	0.8143	0.0430
0.2271	1.4415	1.1739	1.7716	0.7504	2.2250	-0.1067	1.0483	0.8128	0.0383
0.2876	1.2039	1.1586	1.6419	0.6749	2.2643	-0.1124	1.0474	0.8091	0.0341
0.3491	1.0466	1.1496	1.5486	0.6244	2.3432	-0.1263	1.0450	0.8000	0.0245
0.4113	0.9399	1.1411	1.4898	0.5840	2.4225	-0.1354	1.0435	0.7941	0.0177
0.4218	0.9189	1.1393	1.4782	0.5771	2.4833	-0.1431	1.0421	0.7891	0.0084
0.4743	0.8462	1.1333	1.4373	0.5531	2.5438	-0.1510	1.0407	0.7839	0.0025
0.5379	0.7411	1.1266	1.3718	0.5099	2.6043	-0.1558	1.0399	0.7807	-0.0045
0.6022	0.6587	1.1190	1.3247	0.4792	2.6652	-0.1611	1.0390	0.7772	-0.0078
0.6676	0.5653	1.1098	1.2710	0.4405	2.7862	-0.1756	1.0364	0.7676	-0.0220
0.7340	0.4929	1.1075	1.2171	0.4064	2.9075	-0.1852	1.0346	0.7612	-0.0347
0.7900	0.4445	1.1049	1.1832	0.3817	3.0289	-0.1957	1.0327	0.7541	-0.0483
0.8011	0.4421	1.1047	1.1818	0.3817	3.1506	-0.1982	1.0275	0.7594	-0.0526
0.8689	0.3749	1.0994	1.1375	0.3508	3.2218	-0.2024	1.0267	0.7566	-0.0586
0.9374	0.3253	1.0963	1.1027	0.3263	3.3331	-0.2060	1.0261	0.7542	-0.0642
0.9951	0.2792	1.0940	1.0688	0.3053	3.4548	-0.2039	1.0265	0.7556	-0.0638
1.0066	0.2652	1.0923	1.0605	0.2978	3.5765	-0.2065	1.0260	0.7538	-0.0646
1.0765	0.2304	1.0879	1.0395	0.2798	3.6979	-0.2062	1.0260	0.7540	-0.0684
1.1467	0.1886	1.0826	1.0142	0.2552	3.8196	-0.2094	1.0254	0.7519	-0.0750
1.2173	0.1542	1.0784	0.9924	0.2299	3.9409	-0.2108	1.0252	0.7509	-0.0795
1.2764	0.1282	1.0749	0.9764	0.2144	4.0021	-0.2172	1.0240	0.7466	-0.0886
1.2883	0.1208	1.0739	0.9718	0.2101	4.1238	-0.2210	1.0199	0.7489	-0.0902
1.3602	0.0853	1.0690	0.9498	0.1841					
1.4326	0.0589	1.0656	0.9325	0.1703					
1.5056	0.0430	1.0668	0.9164	0.1604					
1.5789	0.0161	1.0629	0.8995	0.1459					
1.5915	0.0060	1.0614	0.8931	0.1391					
1.6533	0.0052	1.0612	0.8925	0.1361					
1.7278	-0.0244	1.0567	0.8737	0.1127					
1.8029	-0.0323	1.0555	0.8687	0.1055					

Table C-17. Time histories of overpressure, sound speed, density and flow velocity from the reconstructed blast-wave flow field by the RCM for a 1-kg TNT equivalent ANFO surface explosion in a standard atmosphere. These signatures are for the specific radius r = 2.446 m, at which the blast-wave front arrives at time t = 2.029 ms.

t (ms)	$\Delta p/p_1$	a/a_1	ρ/ρ_1	u/a_1	t (ms)	$\Delta p/p_1$	a/a_1	ρ/ρ_1	u/a_1
0.0000	2.1619	1.2061	2.1736	0.9166	1.8564	-0.0369	1.0505	0.8727	0.0937
0.0097	2.1313	1.2044	2.1585	0.9113	1.9329	-0.0570	1.0474	0.8597	0.0788
0.0695	1.9061	1.1927	2.0429	0.8593	2.0104	-0.0685	1.0459	0.8516	0.0674
0.1196	1.6563	1.1802	1.9072	0.7950	2.0883	-0.0848	1.0433	0.8409	0.0581
0.1297	1.6244	1.1781	1.8908	0.7874	2.1276	-0.0894	1.0425	0.8379	0.0548
0.1902	1.4487	1.1669	1.7982	0.7399	2.1669	-0.0936	1.0418	0.8351	0.0516
0.2517	1.2469	1.1562	1.6807	0.6801	2.2458	-0.1059	1.0398	0.8270	0.0389
0.3140	1.1039	1.1492	1.5929	0.6359	2.3251	-0.1158	1.0381	0.8204	0.0323
0.3244	1.0843	1.1477	1.5823	0.6303	2.3860	-0.1256	1.0365	0.8139	0.0229
0.3769	0.9607	1.1394	1.5103	0.5865	2.4465	-0.1346	1.0349	0.8079	0.0167
0.4405	0.8735	1.1330	1.4594	0.5560	2.5070	-0.1380	1.0344	0.8057	0.0111
0.5049	0.7587	1.1250	1.3897	0.5119	2.5372	-0.1454	1.0331	0.8007	0.0049
0.5702	0.6794	1.1176	1.3447	0.4832	2.5678	-0.1488	1.0325	0.7985	0.0022
0.6366	0.6086	1.1110	1.3032	0.4547	2.6888	-0.1547	1.0315	0.7945	-0.0076
0.6926	0.5119	1.1015	1.2462	0.4132	2.8102	-0.1678	1.0292	0.7857	-0.0204
0.7038	0.5091	1.1012	1.2446	0.4132	2.9315	-0.1781	1.0274	0.7787	-0.0328
0.7716	0.4519	1.0978	1.2048	0.3879	3.0532	-0.1863	1.0255	0.7737	-0.0439
0.8401	0.3860	1.0906	1.1652	0.3552	3.1245	-0.1934	1.0242	0.7688	-0.0507
0.8978	0.3546	1.0871	1.1463	0.3398	3.2358	-0.1970	1.0236	0.7664	-0.0539
0.9093	0.3396	1.0854	1.1372	0.3324	3.3575	-0.2025	1.0226	0.7627	-0.0589
0.9791	0.2901	1.0795	1.1070	0.3022	3.4791	-0.2048	1.0222	0.7611	-0.0642
1.0494	0.2472	1.0779	1.0733	0.2785	3.6005	-0.2039	1.0223	0.7617	-0.0674
1.1200	0.2095	1.0747	1.0471	0.2586	3.7222	-0.2027	1.0226	0.7625	-0.0696
1.1791	0.1800	1.0734	1.0240	0.2436	3.8435	-0.2045	1.0222	0.7613	-0.0734
1.1909	0.1730	1.0725	1.0197	0.2400	3.9047	-0.2081	1.0215	0.7588	-0.0752
1.2629	0.1381	1.0679	0.9979	0.2183	4.0264	-0.2108	1.0210	0.7570	-0.0836
1.3352	0.1057	1.0657	0.9735	0.2029	4.1478	-0.2159	1.0201	0.7535	-0.0910
1.4082	0.0723	1.0636	0.9479	0.1785					
1.4816	0.0443	1.0596	0.9301	0.1581					
1.4941	0.0430	1.0594	0.9293	0.1570					
1.5560	0.0343	1.0582	0.9237	0.1492					
1.6304	0.0097	1.0576	0.9027	0.1308					
1.7055	-0.0053	1.0554	0.8931	0.1206					
1.7806	-0.0235	1.0526	0.8813	0.1049					
1.7931	-0.0273	1.0520	0.8789	0.1025					

Table C-18. Time histories of overpressure, sound speed, density and flow velocity from the reconstructed blast-wave flow field by the RCM for a 1-kg TNT equivalent ANFO surface explosion in a standard atmosphere. These signatures are for the specific radius r = 2.514 m, at which the blast-wave front arrives at time t = 2.149 ms.

t (ms)	$\Delta p/p_1$	a/a_1	ρ/ρ_1	u/a_1	t (ms)	$\Delta p/p_1$	a/a_1	ρ/ρ_1	u/a_1
0.0000	2.0531	1.1969	2.1310	0.8850	1.9687	-0.0579	1.0321	0.8844	0.0761
0.0101	2.0267	1.1955	2.1178	0.8805	2.0080	-0.0659	1.0309	0.8790	0.0702
0.0706	1.7456	1.1803	1.9707	0.8114	2.0473	-0.0668	1.0307	0.8784	0.0669
0.1321	1.5158	1.1683	1.8432	0.7505	2.1262	-0.0832	1.0281	0.8673	0.0574
0.1944	1.3841	1.1594	1.7735	0.7150	2.2055	-0.0917	1.0267	0.8616	0.0478
0.2048	1.3411	1.1579	1.7463	0.7023	2.2663	-0.1032	1.0283	0.8481	0.0396
0.2573	1.1660	1.1463	1.6485	0.6497	2.3268	-0.1069	1.0277	0.8455	0.0350
0.3209	1.0576	1.1381	1.5886	0.6182	2.3874	-0.1142	1.0265	0.8406	0.0265
0.3853	0.9035	1.1274	1.4975	0.5648	2.4176	-0.1209	1.0254	0.8361	0.0209
0.4506	0.8168	1.1216	1.4441	0.5334	2.4482	-0.1215	1.0253	0.8357	0.0183
0.5170	0.7132	1.1160	1.3755	0.4924	2.5087	-0.1302	1.0239	0.8297	0.0123
0.5730	0.6578	1.1108	1.3436	0.4657	2.5692	-0.1338	1.0232	0.8273	0.0071
0.5841	0.6545	1.1105	1.3417	0.4657	2.6906	-0.1490	1.0207	0.8169	-0.0077
0.6519	0.5723	1.1050	1.2878	0.4300	2.8119	-0.1603	1.0187	0.8091	-0.0194
0.7204	0.4827	1.0958	1.2349	0.3888	2.9336	-0.1682	1.0139	0.8091	-0.0260
0.7782	0.4481	1.0942	1.2096	0.3755	3.0049	-0.1765	1.0125	0.8034	-0.0324
0.7896	0.4336	1.0926	1.2009	0.3689	3.1161	-0.1846	1.0110	0.7977	-0.0432
0.8595	0.3802	1.0867	1.1688	0.3441	3.2378	-0.1911	1.0099	0.7931	-0.0511
0.9298	0.3319	1.0812	1.1394	0.3233	3.3595	-0.1961	1.0090	0.7896	-0.0585
1.0004	0.2800	1.0753	1.1070	0.2958	3.4809	-0.1995	1.0084	0.7873	-0.0659
1.0595	0.2465	1.0712	1.0862	0.2778	3.6026	-0.1997	1.0083	0.7871	-0.0640
1.0713	0.2373	1.0701	1.0805	0.2730	3.7239	-0.1989	1.0085	0.7877	-0.0684
1.1433	0.2026	1.0660	1.0583	0.2522	3.7851	-0.1986	1.0085	0.7879	-0.0697
1.2156	0.1702	1.0619	1.0378	0.2318	3.9068	-0.1994	1.0084	0.7873	-0.0716
1.2886	0.1363	1.0600	1.0114	0.2104	4.0282	-0.2018	1.0080	0.7856	-0.0773
1.3620	0.1086	1.0563	0.9937	0.1925	4.1499	-0.2095	1.0066	0.7802	-0.0867
1.3745	0.0913	1.0539	0.9826	0.1811					
1.4364	0.0766	1.0518	0.9731	0.1702					
1.5108	0.0549	1.0489	0.9588	0.1541					
1.5859	0.0358	1.0462	0.9464	0.1418					
1.6610	0.0121	1.0427	0.9308	0.1236					
1.6735	0.0090	1.0423	0.9288	0.1211					
1.7368	-0.0035	1.0404	0.9205	0.1142					
1.8133	-0.0237	1.0374	0.9072	0.1027					
1.8908	-0.0324	1.0361	0.9014	0.0967					

Table C-19. Time histories of overpressure, sound speed, density and flow velocity from the reconstructed blast-wave flow field by the RCM for a 1-kg TNT equivalent ANFO surface explosion in a standard atmosphere. These signatures are for the specific radius r = 2.635 m, at which the blast-wave front arrives at time t = 2.353 ms.

t (ms)	$\Delta p/p_1$	a/a_1	ρ/ρ_1	u/a_1	t (ms)	$\Delta p/p_1$	a/a_1	ρ/ρ_1	u/a_1
0.0000	1.8590	1.1814	2.0486	0.8266	2.0616	-0.0472	1.0287	0.9004	0.0726
0.0525	1.6101	1.1662	1.9191	0.7603	2.1221	-0.0622	1.0263	0.8903	0.0615
0.1161	1.4671	1.1579	1.8403	0.7239	2.1826	-0.0675	1.0255	0.8867	0.0569
0.1805	1.3336	1.1510	1.7614	0.6916	2.2128	-0.0737	1.0245	0.8824	0.0505
0.2458	1.1336	1.1372	1.6498	0.6248	2.2434	-0.0776	1.0239	0.8798	0.0484
0.3122	1.0287	1.1291	1.5913	0.5940	2.3039	-0.0835	1.0230	0.8758	0.0433
0.3682	0.9136	1.1210	1.5228	0.5517	2.3644	-0.0934	1.0214	0.8690	0.0352
0.3793	0.9093	1.1206	1.5204	0.5517	2.4253	-0.1004	1.0203	0.8642	0.0317
0.4472	0.8122	1.1139	1.4605	0.5169	2.4858	-0.1080	1.0190	0.8590	0.0258
0.5156	0.7266	1.1071	1.4087	0.4837	2.5466	-0.1106	1.0186	0.8572	0.0211
0.5734	0.6687	1.1017	1.3748	0.4627	2.6071	-0.1217	1.0168	0.8495	0.0125
0.5848	0.6595	1.1009	1.3694	0.4598	2.6680	-0.1258	1.0161	0.8467	0.0074
0.6547	0.5894	1.0941	1.3278	0.4294	2.7288	-0.1309	1.0172	0.8400	0.0041
0.7250	0.4967	1.0862	1.2687	0.3875	2.8001	-0.1400	1.0157	0.8337	-0.0064
0.7956	0.4497	1.0823	1.2375	0.3660	2.9113	-0.1463	1.0146	0.8293	-0.0132
0.8547	0.4103	1.0783	1.2130	0.3478	3.0330	-0.1587	1.0125	0.8207	-0.0249
0.8665	0.3959	1.0767	1.2041	0.3410	3.1547	-0.1697	1.0106	0.8130	-0.0351
0.9385	0.3486	1.0716	1.1744	0.3154	3.2761	-0.1766	1.0094	0.8082	-0.0460
1.0108	0.3062	1.0683	1.1446	0.2925	3.3978	-0.1826	1.0064	0.8070	-0.0536
1.0838	0.2668	1.0637	1.1196	0.2722	3.5191	-0.1877	1.0055	0.8034	-0.0602
1.1572	0.2248	1.0602	1.0896	0.2511	3.5803	-0.1891	1.0052	0.8024	-0.0618
1.1697	0.2182	1.0594	1.0855	0.2481	3.7020	-0.1908	1.0050	0.8013	-0.0666
1.2316	0.1942	1.0564	1.0701	0.2348	3.8234	-0.1894	1.0052	0.8023	-0.0655
1.3060	0.1526	1.0537	1.0382	0.2095	3.9451	-0.1909	1.0049	0.8012	-0.0694
1.3811	0.1305	1.0517	1.0222	0.1974	4.0664	-0.1914	1.0039	0.8022	-0.0698
1.4562	0.1045	1.0482	1.0053	0.1798	4.1777	-0.1952	1.0033	0.7996	-0.0760
1.4687	0.0871	1.0458	0.9940	0.1694	4.2486	-0.1952	1.0033	0.7996	-0.0778
1.5320	0.0688	1.0433	0.9820	0.1598					
1.6085	0.0455	1.0400	0.9667	0.1418					
1.6860	0.0314	1.0394	0.9546	0.1334					
1.7639	0.0074	1.0360	0.9387	0.1168					
1.8032	0.0073	1.0360	0.9386	0.1145					
1.8425	-0.0050	1.0341	0.9304	0.1058					
1.9214	-0.0220	1.0325	0.9173	0.0931					
2.0007	-0.0293	1.0314	0.9125	0.0865					

Table C-20. Time histories of overpressure, sound speed, density and flow velocity from the reconstructed blast-wave flow field by the RCM for a 1-kg TNT equivalent ANFO surface explosion in a standard atmosphere. These signatures are for the specific radius r = 2.733 m, at which the blast-wave front arrives at time t = 2.534 ms.

t (ms)	$\Delta p/p_1$	a/a_1	ρ/ρ_1	u/a_1	t (ms)	$\Delta p/p_1$	a/a_1	ρ/ρ_1	u/a_1
0.0000	1.7061	1.1692	1.9795	0.7785	2.0323	-0.0268	1.0225	0.9309	0.0833
0.0654	1.4653	1.1540	1.8513	0.7115	2.0629	-0.0273	1.0224	0.9306	0.0827
0.1318	1.3444	1.1470	1.7821	0.6794	2.1234	-0.0397	1.0205	0.9221	0.0742
0.1878	1.2511	1.1416	1.7274	0.6526	2.1839	-0.0540	1.0183	0.9123	0.0621
0.1989	1.2185	1.1392	1.7095	0.6428	2.2448	-0.0644	1.0167	0.9051	0.0555
0.2667	1.0534	1.1268	1.6173	0.5866	2.3053	-0.0692	1.0160	0.9018	0.0491
0.3352	0.9581	1.1202	1.5605	0.5557	2.3661	-0.0776	1.0146	0.8960	0.0418
0.3929	0.8587	1.1133	1.4995	0.5218	2.4266	-0.0852	1.0134	0.8907	0.0360
0.4044	0.8399	1.1117	1.4887	0.5153	2.4875	-0.0917	1.0124	0.8862	0.0299
0.4743	0.7769	1.1069	1.4502	0.4906	2.5483	-0.0986	1.0115	0.8810	0.0246
0.5445	0.6775	1.0981	1.3911	0.4530	2.6092	-0.1070	1.0101	0.8752	0.0198
0.6151	0.6157	1.0929	1.3527	0.4310	2.6196	-0.1083	1.0099	0.8743	0.0182
0.6742	0.5734	1.0889	1.3271	0.4140	2.6700	-0.1097	1.0097	0.8733	0.0160
0.6860	0.5610	1.0876	1.3196	0.4092	2.7917	-0.1207	1.0079	0.8656	0.0028
0.7580	0.4839	1.0803	1.2714	0.3719	2.9134	-0.1352	1.0055	0.8553	-0.0098
0.8303	0.4284	1.0751	1.2358	0.3477	3.0348	-0.1441	1.0040	0.8491	-0.0188
0.9033	0.3767	1.0695	1.2035	0.3216	3.1565	-0.1522	1.0027	0.8433	-0.0284
0.9767	0.3354	1.0664	1.1744	0.3045	3.2782	-0.1626	1.0009	0.8359	-0.0383
0.9892	0.3305	1.0658	1.1713	0.3022	3.3693	-0.1714	0.9994	0.8296	-0.0456
1.0511	0.3024	1.0626	1.1535	0.2864	3.4607	-0.1763	0.9985	0.8261	-0.0530
1.1255	0.2538	1.0568	1.1226	0.2617	3.5821	-0.1803	0.9977	0.8235	-0.0551
1.2006	0.2171	1.0532	1.0974	0.2411	3.7038	-0.1841	0.9970	0.8208	-0.0612
1.2757	0.1857	1.0492	1.0771	0.2221	3.8251	-0.1863	0.9966	0.8192	-0.0656
1.2883	0.1749	1.0479	1.0700	0.2148	3.9468	-0.1830	0.9972	0.8215	-0.0660
1.3515	0.1598	1.0459	1.0602	0.2073	4.0077	-0.1833	0.9972	0.8213	-0.0670
1.4280	0.1279	1.0418	1.0393	0.1875	4.1290	-0.1810	0.9965	0.8248	-0.0691
1.5056	0.1076	1.0391	1.0259	0.1741	4.2504	-0.1867	0.9955	0.8206	-0.0746
1.5835	0.0698	1.0340	1.0006	0.1497					
1.6227	0.0552	1.0320	0.9908	0.1398					
1.6620	0.0504	1.0313	0.9876	0.1361					
1.7410	0.0330	1.0301	0.9734	0.1243					
1.8202	0.0181	1.0280	0.9634	0.1143					
1.8811	-0.0014	1.0262	0.9482	0.1004					
1.9416	-0.0159	1.0241	0.9384	0.0924					
2.0021	-0.0231	1.0230	0.9335	0.0878					

Table C-21. Time histories of overpressure, sound speed, density and flow velocity from the reconstructed blast-wave flow field by the RCM for a 1-kg TNT equivalent ANFO surface explosion in a standard atmosphere. These signatures are for the specific radius r = 2.831 m, at which the blast-wave front arrives at time t = 2.722 ms.

t (ms)	$\Delta p/p_1$	a/a_1	ρ/ρ_1	u/a_1	t (ms)	$\Delta p/p_1$	a/a_1	ρ/ρ_1	u/a_1
0.0000	1.5347	1.1553	1.8989	0.7213	1.9962	-0.0043	1.0205	0.9561	0.0922
0.0111	1.5026	1.1532	1.8816	0.7127	2.0570	-0.0193	1.0189	0.9447	0.0819
0.0789	1.3652	1.1442	1.8066	0.6757	2.1175	-0.0254	1.0180	0.9405	0.0797
0.1474	1.2370	1.1356	1.7347	0.6386	2.1784	-0.0296	1.0174	0.9376	0.0755
0.2051	1.1219	1.1282	1.6669	0.6045	2.2389	-0.0419	1.0155	0.9291	0.0641
0.2166	1.0762	1.1247	1.6412	0.5888	2.2997	-0.0541	1.0136	0.9207	0.0535
0.2865	0.9975	1.1196	1.5936	0.5616	2.3606	-0.0640	1.0122	0.9136	0.0469
0.3567	0.8673	1.1091	1.5181	0.5182	2.4214	-0.0744	1.0106	0.9063	0.0398
0.4273	0.7902	1.1035	1.4700	0.4900	2.4319	-0.0752	1.0105	0.9058	0.0374
0.4864	0.7470	1.0998	1.4444	0.4751	2.4823	-0.0786	1.0099	0.9034	0.0340
0.4983	0.7308	1.0983	1.4348	0.4693	2.5431	-0.0879	1.0084	0.8968	0.0266
0.5702	0.6498	1.0913	1.3852	0.4370	2.6040	-0.0928	1.0077	0.8934	0.0220
0.6426	0.5849	1.0857	1.3444	0.4108	2.6648	-0.0961	1.0072	0.8911	0.0200
0.7156	0.5043	1.0778	1.2950	0.3744	2.7257	-0.1023	1.0062	0.8867	0.0122
0.7889	0.4604	1.0742	1.2656	0.3551	2.7865	-0.1085	1.0052	0.8824	0.0073
0.8015	0.4422	1.0723	1.2543	0.3439	2.9079	-0.1187	1.0035	0.8751	-0.0015
0.8634	0.4164	1.0695	1.2382	0.3344	3.0296	-0.1316	1.0014	0.8660	-0.0120
0.9378	0.3589	1.0646	1.1989	0.3072	3.1509	-0.1413	0.9998	0.8591	-0.0196
1.0129	0.3289	1.0619	1.1784	0.2909	3.2121	-0.1476	0.9988	0.8545	-0.0259
1.0880	0.2873	1.0572	1.1517	0.2703	3.3338	-0.1556	0.9974	0.8488	-0.0352
1.1005	0.2740	1.0557	1.1432	0.2619	3.4552	-0.1603	0.9966	0.8454	-0.0427
1.1638	0.2509	1.0529	1.1284	0.2508	3.5769	-0.1708	0.9948	0.8379	-0.0525
1.2403	0.2139	1.0485	1.1042	0.2294	3.6982	-0.1719	0.9946	0.8371	-0.0567
1.3178	0.1832	1.0453	1.0828	0.2110	3.8095	-0.1775	0.9936	0.8331	-0.0625
1.3957	0.1555	1.0418	1.0646	0.1981	3.8804	-0.1782	0.9935	0.8327	-0.0663
1.4350	0.1348	1.0391	1.0510	0.1855	4.0021	-0.1762	0.9932	0.8351	-0.0658
1.4743	0.1258	1.0379	1.0450	0.1811	4.1234	-0.1777	0.9930	0.8340	-0.0691
1.5532	0.1044	1.0351	1.0308	0.1660	4.2448	-0.1751	0.9934	0.8359	-0.0690
1.6325	0.0689	1.0303	1.0070	0.1437	4.3661	-0.1791	0.9922	0.8338	-0.0728
1.6933	0.0518	1.0280	0.9954	0.1323					
1.7538	0.0407	1.0264	0.9878	0.1243					
1.8143	0.0312	1.0251	0.9814	0.1176					
1.8446	0.0237	1.0245	0.9753	0.1113					
1.8752	0.0177	1.0237	0.9711	0.1078					
1.9357	0.0052	1.0219	0.9626	0.0995					

Table C-22. Time histories of overpressure, sound speed, density and flow velocity from the reconstructed blast-wave flow field by the RCM for a 1-kg TNT equivalent ANFO surface explosion in a standard atmosphere. These signatures are for the specific radius r = 2.929 m, at which the blast-wave front arrives at time t = 2.927 ms.

t (ms)	$\Delta p/p_1$	a/a_1	ρ/ρ_1	u/a_1	t (ms)	$\Delta p/p_1$	a/a_1	ρ/ρ_1	u/a_1
0.0000	1.3876	1.1435	1.8261	0.6715	2.0337	-0.0017	1.0174	0.9645	0.0879
0.0115	1.3669	1.1420	1.8148	0.6664	2.0946	-0.0133	1.0157	0.9564	0.0791
0.0814	1.2652	1.1350	1.7584	0.6389	2.1554	-0.0205	1.0146	0.9515	0.0731
0.1516	1.1106	1.1244	1.6693	0.5920	2.2163	-0.0241	1.0141	0.9489	0.0701
0.2222	0.9996	1.1163	1.6046	0.5542	2.2267	-0.0262	1.0138	0.9475	0.0686
0.2813	0.9436	1.1124	1.5707	0.5373	2.2771	-0.0356	1.0124	0.9410	0.0620
0.2931	0.9096	1.1096	1.5510	0.5249	2.3380	-0.0507	1.0101	0.9304	0.0520
0.3651	0.8172	1.1019	1.4966	0.4904	2.3988	-0.0585	1.0089	0.9249	0.0445
0.4374	0.7452	1.0960	1.4529	0.4654	2.4597	-0.0642	1.0080	0.9209	0.0394
0.5104	0.6728	1.0894	1.4095	0.4382	2.5205	-0.0736	1.0066	0.9143	0.0337
0.5838	0.6143	1.0850	1.3712	0.4147	2.5814	-0.0810	1.0054	0.9091	0.0285
0.5963	0.6005	1.0837	1.3628	0.4066	2.6419	-0.0879	1.0044	0.9042	0.0234
0.6582	0.5682	1.0805	1.3432	0.3942	2.7027	-0.0929	1.0036	0.9006	0.0188
0.7326	0.4887	1.0735	1.2917	0.3581	2.7636	-0.0980	1.0028	0.8971	0.0138
0.8077	0.4286	1.0672	1.2543	0.3330	2.8244	-0.1010	1.0023	0.8949	0.0102
0.8828	0.3865	1.0629	1.2273	0.3145	2.9458	-0.1114	1.0006	0.8875	-0.0003
0.8953	0.3801	1.0622	1.2233	0.3115	3.0070	-0.1157	0.9999	0.8845	-0.0038
0.9586	0.3497	1.0588	1.2039	0.2953	3.1287	-0.1266	0.9982	0.8766	-0.0151
1.0351	0.3144	1.0559	1.1789	0.2789	3.2500	-0.1350	0.9968	0.8706	-0.0232
1.1127	0.2664	1.0503	1.1480	0.2525	3.3717	-0.1463	0.9949	0.8625	-0.0353
1.1905	0.2420	1.0479	1.1310	0.2397	3.4931	-0.1507	0.9942	0.8593	-0.0398
1.2298	0.2235	1.0457	1.1189	0.2286	3.6043	-0.1591	0.9928	0.8532	-0.0489
1.2691	0.2073	1.0437	1.1083	0.2204	3.6753	-0.1644	0.9919	0.8494	-0.0542
1.3481	0.1769	1.0405	1.0870	0.2029	3.7970	-0.1664	0.9915	0.8479	-0.0574
1.4273	0.1560	1.0379	1.0732	0.1900	3.9183	-0.1716	0.9906	0.8442	-0.0619
1.4882	0.1296	1.0346	1.0553	0.1753	4.0397	-0.1741	0.9902	0.8423	-0.0665
1.5487	0.1178	1.0330	1.0475	0.1699	4.1610	-0.1715	0.9899	0.8455	-0.0648
1.6092	0.0996	1.0306	1.0352	0.1589	4.2824	-0.1730	0.9896	0.8444	-0.0680
1.6394	0.0792	1.0280	1.0213	0.1453	4.3936	-0.1707	0.9900	0.8461	-0.0695
1.6700	0.0666	1.0262	1.0128	0.1370	4.4646	-0.1721	0.9898	0.8451	-0.0714
1.7305	0.0522	1.0243	1.0030	0.1255					
1.7910	0.0434	1.0230	0.9969	0.1186					
1.8519	0.0307	1.0221	0.9867	0.1113					
1.9124	0.0197	1.0205	0.9792	0.1049					
1.9732	0.0088	1.0189	0.9717	0.0951					

Table C-23. Time histories of overpressure, sound speed, density and flow velocity from the reconstructed blast-wave flow field by the RCM for a 1-kg TNT equivalent ANFO surface explosion in a standard atmosphere. These signatures are for the specific radius r = 3.065 m, at which the blast-wave front arrives at time t = 3.208 ms.

t (ms)	$\Delta p/p_1$	a/a_1	ρ/ρ_1	u/a_1	t (ms)	$\Delta p/p_1$	a/a_1	ρ/ρ_1	u/a_1
0.0000	1.2595	1.1328	1.7609	0.6253	1.9958	0.0188	1.0160	0.9870	0.0971
0.0118	1.2400	1.1314	1.7500	0.6201	2.0567	0.0045	1.0139	0.9771	0.0867
0.0838	1.1510	1.1251	1.6993	0.5949	2.1175	-0.0022	1.0130	0.9724	0.0812
0.1561	0.9958	1.1135	1.6098	0.5432	2.1784	-0.0171	1.0117	0.9603	0.0713
0.2291	0.9257	1.1078	1.5690	0.5210	2.2392	-0.0207	1.0112	0.9578	0.0673
0.3025	0.8307	1.0999	1.5132	0.4877	2.3001	-0.0242	1.0107	0.9553	0.0645
0.3150	0.8198	1.0990	1.5068	0.4818	2.3606	-0.0351	1.0090	0.9477	0.0567
0.3769	0.7658	1.0945	1.4740	0.4622	2.4214	-0.0426	1.0079	0.9424	0.0510
0.4513	0.7073	1.0900	1.4371	0.4408	2.4823	-0.0539	1.0062	0.9345	0.0402
0.5264	0.6180	1.0817	1.3829	0.4054	2.5431	-0.0592	1.0054	0.9307	0.0367
0.6015	0.5673	1.0769	1.3515	0.3859	2.6040	-0.0684	1.0040	0.9242	0.0298
0.6141	0.5638	1.0765	1.3493	0.3828	2.6645	-0.0737	1.0032	0.9204	0.0256
0.6773	0.5277	1.0730	1.3270	0.3696	2.6951	-0.0807	1.0021	0.9154	0.0181
0.7538	0.4515	1.0658	1.2777	0.3355	2.7257	-0.0810	1.0020	0.9153	0.0176
0.8314	0.4097	1.0614	1.2512	0.3174	2.7865	-0.0859	1.0013	0.9118	0.0137
0.9093	0.3673	1.0578	1.2219	0.2970	2.8474	-0.0885	1.0009	0.9099	0.0115
0.9485	0.3461	1.0555	1.2084	0.2843	2.9687	-0.1008	0.9989	0.9011	0.0005
0.9878	0.3356	1.0543	1.2016	0.2799	3.0904	-0.1084	0.9977	0.8956	-0.0067
1.0668	0.3021	1.0505	1.1799	0.2632	3.2118	-0.1183	0.9961	0.8886	-0.0147
1.1460	0.2571	1.0453	1.1505	0.2396	3.3230	-0.1271	0.9947	0.8822	-0.0223
1.2069	0.2365	1.0429	1.1368	0.2288	3.3940	-0.1328	0.9938	0.8781	-0.0280
1.2674	0.2210	1.0411	1.1266	0.2204	3.5157	-0.1416	0.9923	0.8718	-0.0358
1.3279	0.1944	1.0382	1.1082	0.2056	3.6370	-0.1462	0.9916	0.8684	-0.0414
1.3581	0.1777	1.0361	1.0971	0.1954	3.7584	-0.1530	0.9904	0.8634	-0.0493
1.3887	0.1709	1.0352	1.0926	0.1917	3.8797	-0.1584	0.9895	0.8595	-0.0556
1.4492	0.1568	1.0334	1.0831	0.1819	4.0011	-0.1597	0.9893	0.8586	-0.0591
1.5097	0.1365	1.0308	1.0695	0.1701	4.1123	-0.1629	0.9879	0.8578	-0.0637
1.5706	0.1181	1.0285	1.0570	0.1595	4.1833	-0.1658	0.9874	0.8557	-0.0669
1.6311	0.1051	1.0268	1.0483	0.1526	4.3046	-0.1641	0.9877	0.8570	-0.0666
1.6919	0.0847	1.0240	1.0344	0.1388	4.4256	-0.1619	0.9880	0.8585	-0.0681
1.7524	0.0661	1.0215	1.0217	0.1263	4.5470	-0.1627	0.9879	0.8579	-0.0695
1.8133	0.0502	1.0193	1.0108	0.1167					
1.8741	0.0377	1.0186	1.0001	0.1098					
1.9350	0.0283	1.0173	0.9936	0.1040					
1.9454	0.0228	1.0165	0.9898	0.1002					

Table C-24. Time histories of overpressure, sound speed, density and flow velocity from the reconstructed blast-wave flow field by the RCM for a 1-kg TNT equivalent ANFO surface explosion in a standard atmosphere. These signatures are for the specific radius r = 3.224 m, at which the blast-wave front arrives at time t = 3.523 ms.

t (ms)	$\Delta p/p_1$	a/a_1	ρ/ρ_1	u/a_1	t (ms)	$\Delta p/p_1$	a/a_1	ρ/ρ_1	u/a_1
0.0000	1.1359	1.1216	1.6980	0.5782	2.0456	0.0240	1.0132	0.9975	0.0907
0.0619	1.0808	1.1174	1.6665	0.5622	2.1064	0.0176	1.0123	0.9931	0.0851
0.1363	0.9561	1.1081	1.5929	0.5215	2.1673	0.0066	1.0107	0.9854	0.0776
0.2114	0.8805	1.1020	1.5486	0.4969	2.2281	-0.0017	1.0095	0.9796	0.0710
0.2865	0.8001	1.0954	1.5002	0.4670	2.2890	-0.0138	1.0078	0.9711	0.0627
0.2990	0.7883	1.0944	1.4931	0.4619	2.3495	-0.0181	1.0071	0.9681	0.0595
0.3623	0.7215	1.0887	1.4525	0.4374	2.3800	-0.0216	1.0066	0.9656	0.0577
0.4388	0.6795	1.0852	1.4261	0.4228	2.4106	-0.0222	1.0065	0.9651	0.0574
0.5163	0.5985	1.0776	1.3765	0.3899	2.4715	-0.0334	1.0049	0.9572	0.0505
0.5942	0.5580	1.0742	1.3503	0.3721	2.5323	-0.0408	1.0038	0.9520	0.0452
0.6335	0.5335	1.0718	1.3350	0.3621	2.5928	-0.0485	1.0026	0.9465	0.0381
0.6728	0.5207	1.0705	1.3270	0.3577	2.6537	-0.0563	1.0014	0.9410	0.0324
0.7517	0.4471	1.0631	1.2803	0.3248	2.7145	-0.0634	1.0004	0.9359	0.0274
0.8310	0.4160	1.0601	1.2599	0.3102	2.8359	-0.0736	0.9988	0.9286	0.0185
0.8919	0.3797	1.0562	1.2366	0.2925	2.9576	-0.0834	0.9973	0.9216	0.0088
0.9524	0.3430	1.0522	1.2131	0.2754	3.0184	-0.0889	0.9965	0.9176	0.0050
1.0129	0.3242	1.0501	1.2008	0.2672	3.1398	-0.0981	0.9950	0.9110	-0.0038
1.0431	0.3142	1.0490	1.1943	0.2629	3.2611	-0.1046	0.9940	0.9063	-0.0113
1.0737	0.2989	1.0472	1.1843	0.2548	3.3825	-0.1148	0.9923	0.8989	-0.0200
1.1342	0.2773	1.0447	1.1703	0.2433	3.5038	-0.1200	0.9915	0.8952	-0.0255
1.1947	0.2468	1.0411	1.1502	0.2266	3.6255	-0.1310	0.9897	0.8871	-0.0355
1.2556	0.2284	1.0389	1.1381	0.2161	3.7469	-0.1374	0.9887	0.8825	-0.0429
1.3161	0.2120	1.0370	1.1271	0.2084	3.8074	-0.1382	0.9885	0.8819	-0.0436
1.3769	0.1866	1.0341	1.1096	0.1942	3.9287	-0.1442	0.9876	0.8776	-0.0514
1.4374	0.1706	1.0321	1.0990	0.1831	4.0501	-0.1498	0.9866	0.8734	-0.0559
1.4983	0.1555	1.0302	1.0888	0.1747	4.1714	-0.1514	0.9864	0.8722	-0.0589
1.5591	0.1406	1.0283	1.0786	0.1669	4.2924	-0.1558	0.9856	0.8690	-0.0630
1.6200	0.1154	1.0254	1.0609	0.1516					
1.6304	0.1141	1.0252	1.0600	0.1492					
1.6808	0.1040	1.0239	1.0531	0.1426					
1.7417	0.0946	1.0229	1.0462	0.1378					
1.8025	0.0747	1.0202	1.0326	0.1252					
1.8634	0.0598	1.0182	1.0223	0.1157					
1.9242	0.0456	1.0162	1.0125	0.1042					
1.9851	0.0368	1.0150	1.0064	0.0986					

Table C-25. Time histories of overpressure, sound speed, density and flow velocity from the reconstructed blast-wave flow field by the RCM for a 1-kg TNT equivalent ANFO surface explosion in a standard atmosphere. These signatures are for the specific radius r = 3.367 m, at which the blast-wave front arrives at time t = 3.822 ms.

t (ms)	$\Delta p/p_1$	a/a_1	ρ/ρ_1	u/a_1	t (ms)	$\Delta p/p_1$	a/a_1	ρ/ρ_1	u/a_1
0.0000	1.0608	1.1149	1.6579	0.5490	2.0504	0.0359	1.0129	1.0097	0.0939
0.0633	0.9566	1.1069	1.5968	0.5130	2.0810	0.0334	1.0126	1.0079	0.0921
0.1398	0.8792	1.1006	1.5513	0.4881	2.1116	0.0274	1.0117	1.0037	0.0885
0.2173	0.8041	1.0945	1.5062	0.4622	2.1725	0.0193	1.0106	0.9981	0.0818
0.2952	0.7354	1.0885	1.4648	0.4360	2.2333	0.0086	1.0095	0.9898	0.0739
0.3345	0.6992	1.0852	1.4428	0.4214	2.2938	0.0029	1.0087	0.9857	0.0707
0.3738	0.6812	1.0836	1.4319	0.4145	2.3547	-0.0089	1.0070	0.9775	0.0616
0.4527	0.6131	1.0773	1.3899	0.3883	2.4155	-0.0153	1.0060	0.9729	0.0567
0.5320	0.5644	1.0726	1.3597	0.3674	2.4764	-0.0190	1.0055	0.9703	0.0538
0.5928	0.5391	1.0703	1.3436	0.3574	2.5369	-0.0284	1.0041	0.9636	0.0465
0.6533	0.5105	1.0674	1.3258	0.3466	2.5977	-0.0343	1.0033	0.9595	0.0415
0.7138	0.4606	1.0623	1.2943	0.3239	2.6586	-0.0390	1.0026	0.9561	0.0381
0.7441	0.4387	1.0605	1.2793	0.3139	2.7090	-0.0487	1.0011	0.9492	0.0299
0.7747	0.4213	1.0586	1.2682	0.3058	2.7194	-0.0487	1.0011	0.9492	0.0299
0.8352	0.4028	1.0567	1.2563	0.2972	2.7799	-0.0533	1.0004	0.9459	0.0266
0.8957	0.3752	1.0537	1.2387	0.2835	2.8408	-0.0617	0.9991	0.9399	0.0202
0.9565	0.3440	1.0502	1.2185	0.2684	2.9016	-0.0656	0.9985	0.9371	0.0169
1.0170	0.3204	1.0476	1.2030	0.2577	3.0230	-0.0770	0.9968	0.9290	0.0067
1.0779	0.2985	1.0452	1.1887	0.2471	3.1443	-0.0855	0.9955	0.9228	-0.0006
1.1384	0.2839	1.0435	1.1791	0.2381	3.2657	-0.0935	0.9942	0.9170	-0.0069
1.1992	0.2600	1.0407	1.1634	0.2255	3.3870	-0.1005	0.9931	0.9120	-0.0134
1.2601	0.2276	1.0371	1.1414	0.2083	3.4983	-0.1078	0.9920	0.9067	-0.0198
1.3209	0.2174	1.0359	1.1346	0.2035	3.5692	-0.1106	0.9915	0.9047	-0.0227
1.3314	0.2162	1.0357	1.1337	0.2016	3.6906	-0.1178	0.9904	0.8994	-0.0295
1.3818	0.2001	1.0338	1.1230	0.1933	3.8116	-0.1253	0.9891	0.8940	-0.0364
1.4426	0.1778	1.0312	1.1075	0.1806	3.9329	-0.1326	0.9880	0.8887	-0.0428
1.5035	0.1636	1.0294	1.0980	0.1712	4.0543	-0.1394	0.9869	0.8837	-0.0510
1.5643	0.1454	1.0274	1.0850	0.1618	4.1753	-0.1435	0.9862	0.8806	-0.0552
1.6252	0.1270	1.0251	1.0726	0.1508	4.2966	-0.1450	0.9859	0.8795	-0.0580
1.6860	0.1119	1.0231	1.0623	0.1426	4.4180	-0.1489	0.9853	0.8767	-0.0631
1.7465	0.0974	1.0212	1.0523	0.1351	4.5390	-0.1508	0.9846	0.8761	-0.0663
1.8074	0.0910	1.0203	1.0479	0.1300	4.6603	-0.1475	0.9851	0.8785	-0.0655
1.8682	0.0726	1.0179	1.0353	0.1174					
1.9291	0.0593	1.0161	1.0260	0.1089					
1.9899	0.0457	1.0142	1.0166	0.1004					

Table C-26. Time histories of overpressure, sound speed, density and flow velocity from the reconstructed blast-wave flow field by the RCM for a 1-kg TNT equivalent ANFO surface explosion in a standard atmosphere. These signatures are for the specific radius r = 3.526 m, at which the blast-wave front arrives at time t = 4.157 ms.

t (ms)	$\Delta p/p_1$	a/a_1	ρ/ρ_1	u/a_1	t (ms)	$\Delta p/p_1$	a/a_1	ρ/ρ_1	u/a_1
0.0000	0.9373	1.1037	1.5903	0.4991	1.9593	0.0632	1.0149	1.0322	0.1041
0.0393	0.8967	1.1004	1.5665	0.4857	2.0202	0.0569	1.0140	1.0278	0.1002
0.1182	0.8343	1.0951	1.5294	0.4654	2.0810	0.0452	1.0124	1.0197	0.0925
0.1975	0.7692	1.0898	1.4896	0.4401	2.1419	0.0367	1.0113	1.0137	0.0857
0.2583	0.7293	1.0863	1.4655	0.4265	2.2024	0.0240	1.0095	1.0049	0.0772
0.3188	0.6738	1.0813	1.4317	0.4048	2.2632	0.0170	1.0085	0.9999	0.0728
0.3793	0.6394	1.0781	1.4105	0.3920	2.3241	0.0097	1.0075	0.9948	0.0672
0.4096	0.6224	1.0766	1.3996	0.3857	2.3745	0.0049	1.0068	0.9915	0.0637
0.4402	0.6055	1.0750	1.3892	0.3783	2.3849	0.0048	1.0067	0.9913	0.0637
0.5007	0.5554	1.0707	1.3568	0.3574	2.4454	-0.0074	1.0050	0.9827	0.0557
0.5612	0.5349	1.0686	1.3441	0.3483	2.5063	-0.0136	1.0041	0.9784	0.0510
0.6220	0.4989	1.0653	1.3209	0.3328	2.5671	-0.0177	1.0036	0.9752	0.0485
0.6825	0.4676	1.0621	1.3011	0.3191	2.6276	-0.0214	1.0031	0.9726	0.0454
0.7434	0.4247	1.0576	1.2737	0.2999	2.6885	-0.0306	1.0017	0.9660	0.0387
0.8039	0.4046	1.0555	1.2608	0.2920	2.7490	-0.0361	1.0009	0.9621	0.0350
0.8647	0.3874	1.0536	1.2498	0.2834	2.8098	-0.0434	0.9998	0.9569	0.0286
0.9256	0.3540	1.0502	1.2276	0.2670	2.8703	-0.0504	0.9988	0.9520	0.0232
0.9864	0.3196	1.0464	1.2052	0.2497	2.9312	-0.0568	0.9978	0.9474	0.0185
0.9969	0.3182	1.0462	1.2044	0.2492	3.0525	-0.0635	0.9968	0.9425	0.0126
1.0473	0.3090	1.0452	1.1983	0.2452	3.1638	-0.0748	0.9951	0.9344	0.0032
1.1081	0.2904	1.0430	1.1861	0.2365	3.2347	-0.0765	0.9948	0.9331	0.0014
1.1690	0.2722	1.0409	1.1741	0.2274	3.3561	-0.0848	0.9935	0.9272	-0.0055
1.2298	0.2429	1.0375	1.1546	0.2118	3.4771	-0.0929	0.9921	0.9215	-0.0123
1.2907	0.2199	1.0348	1.1394	0.1978	3.5984	-0.1010	0.9909	0.9157	-0.0200
1.3515	0.2102	1.0336	1.1328	0.1931	3.7198	-0.1057	0.9901	0.9122	-0.0251
1.4120	0.1928	1.0316	1.1208	0.1837	3.8408	-0.1120	0.9891	0.9076	-0.0313
1.4729	0.1749	1.0294	1.1087	0.1736	3.9621	-0.1216	0.9876	0.9006	-0.0404
1.5337	0.1603	1.0276	1.0989	0.1645	4.0835	-0.1250	0.9871	0.8981	-0.0448
1.5946	0.1454	1.0257	1.0888	0.1562	4.2045	-0.1296	0.9863	0.8947	-0.0482
1.6554	0.1348	1.0244	1.0814	0.1500	4.3258	-0.1353	0.9854	0.8906	-0.0545
1.7159	0.1136	1.0216	1.0669	0.1367	4.3863	-0.1372	0.9851	0.8892	-0.0564
1.7465	0.1072	1.0208	1.0625	0.1319	4.5073	-0.1389	0.9848	0.8879	-0.0587
1.7771	0.1052	1.0205	1.0611	0.1311	4.6287	-0.1413	0.9844	0.8861	-0.0628
1.8380	0.0932	1.0189	1.0529	0.1238	4.7497	-0.1441	0.9839	0.8840	-0.0648
1.8988	0.0768	1.0168	1.0416	0.1134					

Table C-27. Time histories of overpressure, sound speed, density and flow velocity from the reconstructed blast-wave flow field by the RCM for a 1-kg TNT equivalent ANFO surface explosion in a standard atmosphere. These signatures are for the specific radius r = 3.700 m, at which the blast-wave front arrives at time t = 4.566 ms.

t (ms)	$\Delta p/p_1$	a/a_1	ρ/ρ_1	u/a_1	t (ms)	$\Delta p/p_1$	a/a_1	ρ/ρ_1	u/a_1
0.0000	0.8375	1.0944	1.5342	0.4571	1.9649	0.0687	1.0141	1.0391	0.1021
0.0306	0.8186	1.0928	1.5229	0.4509	1.9753	0.0684	1.0141	1.0389	0.1021
0.0911	0.7619	1.0879	1.4886	0.4307	2.0358	0.0601	1.0129	1.0332	0.0969
0.1516	0.7382	1.0858	1.4743	0.4217	2.0967	0.0546	1.0122	1.0294	0.0929
0.2124	0.6838	1.0811	1.4406	0.4015	2.1575	0.0407	1.0103	1.0196	0.0838
0.2729	0.6449	1.0775	1.4168	0.3861	2.2180	0.0329	1.0092	1.0141	0.0789
0.3338	0.6148	1.0747	1.3981	0.3753	2.2789	0.0228	1.0078	1.0070	0.0711
0.3943	0.5831	1.0717	1.3785	0.3618	2.3394	0.0182	1.0071	1.0038	0.0683
0.4551	0.5496	1.0685	1.3574	0.3480	2.4002	0.0108	1.0061	0.9986	0.0633
0.5160	0.5163	1.0654	1.3360	0.3342	2.4607	0.0040	1.0052	0.9937	0.0586
0.5768	0.4854	1.0624	1.3161	0.3220	2.5216	-0.0015	1.0044	0.9898	0.0543
0.5873	0.4794	1.0617	1.3123	0.3183	2.5824	-0.0120	1.0029	0.9824	0.0469
0.6377	0.4681	1.0606	1.3052	0.3138	2.6429	-0.0153	1.0024	0.9800	0.0439
0.6985	0.4284	1.0564	1.2798	0.2948	2.7038	-0.0179	1.0020	0.9782	0.0413
0.7594	0.3987	1.0533	1.2607	0.2815	2.7542	-0.0269	1.0007	0.9718	0.0347
0.8202	0.3758	1.0509	1.2459	0.2711	2.7643	-0.0270	1.0007	0.9717	0.0347
0.8811	0.3557	1.0486	1.2329	0.2608	2.8251	-0.0307	1.0001	0.9691	0.0319
0.9419	0.3257	1.0454	1.2129	0.2459	2.8856	-0.0389	0.9989	0.9632	0.0260
1.0024	0.3059	1.0432	1.2000	0.2363	2.9465	-0.0454	0.9979	0.9585	0.0202
1.0633	0.2906	1.0415	1.1899	0.2288	3.0675	-0.0552	0.9965	0.9515	0.0123
1.1241	0.2801	1.0402	1.1830	0.2228	3.1888	-0.0623	0.9955	0.9461	0.0066
1.1850	0.2631	1.0383	1.1718	0.2143	3.3102	-0.0711	0.9942	0.9398	-0.0002
1.2458	0.2351	1.0349	1.1531	0.1993	3.4312	-0.0791	0.9930	0.9340	-0.0069
1.3063	0.2103	1.0320	1.1364	0.1854	3.5525	-0.0869	0.9918	0.9283	-0.0134
1.3369	0.2063	1.0315	1.1338	0.1832	3.6739	-0.0925	0.9909	0.9243	-0.0189
1.3675	0.2029	1.0311	1.1315	0.1821	3.7949	-0.0999	0.9897	0.9189	-0.0253
1.4284	0.1922	1.0297	1.1243	0.1756	3.9162	-0.1051	0.9889	0.9150	-0.0294
1.4892	0.1691	1.0269	1.1087	0.1634	3.9767	-0.1100	0.9881	0.9115	-0.0340
1.5497	0.1551	1.0251	1.0992	0.1547	4.0977	-0.1169	0.9870	0.9064	-0.0400
1.6106	0.1475	1.0241	1.0940	0.1507	4.2191	-0.1198	0.9866	0.9043	-0.0443
1.6714	0.1344	1.0225	1.0851	0.1432	4.3401	-0.1234	0.9860	0.9017	-0.0484
1.7323	0.1179	1.0204	1.0738	0.1330	4.4614	-0.1280	0.9851	0.8985	-0.0534
1.7928	0.1044	1.0189	1.0639	0.1253	4.5828	-0.1308	0.9847	0.8965	-0.0571
1.8536	0.0936	1.0174	1.0564	0.1178	4.7041	-0.1345	0.9840	0.8938	-0.0604
1.9145	0.0866	1.0165	1.0516	0.1137	4.8255	-0.1361	0.9838	0.8926	-0.0639

Table C-28. Time histories of overpressure, sound speed, density and flow velocity from the reconstructed blast-wave flow field by the RCM for a 1-kg TNT equivalent ANFO surface explosion in a standard atmosphere. These signatures are for the specific radius r = 3.964 m, at which the blast-wave front arrives at time t = 5.153 ms.

t (ms)	$\Delta p/p_1$	a/a_1	ρ/ρ_1	u/a_1	t (ms)	$\Delta p/p_1$	a/a_1	ρ/ρ_1	u/a_1
0.0000	0.7293	1.0840	1.4718	0.4089	2.2378	0.0425	1.0092	1.0235	0.0775
0.0504	0.7076	1.0820	1.4585	0.4013	2.2983	0.0359	1.0083	1.0189	0.0723
0.1113	0.6712	1.0788	1.4360	0.3881	2.3592	0.0316	1.0077	1.0158	0.0692
0.1721	0.6304	1.0750	1.4108	0.3718	2.4197	0.0202	1.0061	1.0078	0.0620
0.2330	0.5946	1.0716	1.3886	0.3575	2.4802	0.0155	1.0055	1.0045	0.0592
0.2938	0.5699	1.0692	1.3732	0.3479	2.5410	0.0064	1.0042	0.9980	0.0530
0.3547	0.5396	1.0663	1.3542	0.3352	2.6015	0.0036	1.0038	0.9961	0.0508
0.4152	0.5107	1.0634	1.3359	0.3228	2.6620	-0.0062	1.0024	0.9891	0.0438
0.4760	0.4876	1.0613	1.3208	0.3137	2.7229	-0.0109	1.0017	0.9858	0.0406
0.5369	0.4653	1.0590	1.3066	0.3036	2.7834	-0.0139	1.0013	0.9836	0.0376
0.5977	0.4357	1.0559	1.2877	0.2901	2.8439	-0.0168	1.0008	0.9815	0.0355
0.6586	0.4069	1.0529	1.2692	0.2769	2.9047	-0.0247	0.9997	0.9759	0.0299
0.7191	0.3788	1.0499	1.2508	0.2644	2.9652	-0.0286	0.9991	0.9731	0.0267
0.7497	0.3719	1.0492	1.2463	0.2600	3.0261	-0.0321	0.9986	0.9706	0.0234
0.7803	0.3672	1.0487	1.2433	0.2586	3.0866	-0.0408	0.9973	0.9644	0.0167
0.8411	0.3535	1.0472	1.2343	0.2524	3.2076	-0.0496	0.9960	0.9581	0.0099
0.9020	0.3233	1.0438	1.2145	0.2375	3.3289	-0.0558	0.9951	0.9536	0.0048
0.9625	0.2941	1.0405	1.1953	0.2224	3.3894	-0.0628	0.9940	0.9485	-0.0003
1.0233	0.2860	1.0396	1.1899	0.2183	3.5104	-0.0670	0.9934	0.9455	-0.0044
1.0841	0.2701	1.0377	1.1794	0.2105	3.6318	-0.0737	0.9924	0.9407	-0.0101
1.1450	0.2620	1.0368	1.1741	0.2070	3.7528	-0.0816	0.9911	0.9349	-0.0163
1.2055	0.2481	1.0353	1.1645	0.2000	3.8741	-0.0864	0.9904	0.9314	-0.0209
1.2663	0.2287	1.0330	1.1516	0.1885	3.9955	-0.0933	0.9893	0.9264	-0.0268
1.3272	0.2027	1.0298	1.1341	0.1738	4.1168	-0.0974	0.9887	0.9234	-0.0307
1.3776	0.1949	1.0289	1.1288	0.1698	4.2382	-0.1044	0.9876	0.9183	-0.0375
1.3880	0.1944	1.0288	1.1284	0.1698	4.3595	-0.1082	0.9870	0.9155	-0.0413
1.4485	0.1877	1.0280	1.1239	0.1660	4.4805	-0.1120	0.9862	0.9129	-0.0453
1.5094	0.1711	1.0259	1.1126	0.1555	4.6019	-0.1179	0.9853	0.9086	-0.0507
1.5702	0.1552	1.0240	1.1018	0.1463	4.7232	-0.1212	0.9848	0.9062	-0.0543
1.6307	0.1461	1.0228	1.0955	0.1413	4.7837	-0.1217	0.9847	0.9059	-0.0550
1.6916	0.1337	1.0212	1.0870	0.1342	4.9051	-0.1225	0.9845	0.9052	-0.0574
1.7521	0.1246	1.0201	1.0808	0.1283					
1.8129	0.1121	1.0184	1.0722	0.1214					
1.8734	0.0995	1.0168	1.0635	0.1141					
1.9343	0.0891	1.0154	1.0563	0.1073					
1.9951	0.0825	1.0145	1.0517	0.1034					
2.0556	0.0704	1.0129	1.0433	0.0955					
2.1165	0.0584	1.0113	1.0349	0.0873					
2.1669	0.0539	1.0108	1.0315	0.0843					
2.1770	0.0537	1.0108	1.0313	0.0843					

Table C-29. Time histories of overpressure, sound speed, density and flow velocity from the reconstructed blast-wave flow field by the RCM for a 1-kg TNT equivalent ANFO surface explosion in a standard atmosphere. These signatures are for the specific radius r = 4.281 m, at which the blast-wave front arrives at time t = 5.903 ms.

t (ms)	$\Delta p/p_1$	a/a_1	ρ/ρ_1	u/a_1	t (ms)	$\Delta p/p_1$	a/a_1	ρ/ρ_1	u/a_1
0.0000	0.6344	1.0746	1.4155	0.3650	2.2764	0.0517	1.0094	1.0323	0.0760
0.0306	0.6287	1.0740	1.4119	0.3632	2.3369	0.0454	1.0085	1.0279	0.0721
0.0914	0.5913	1.0705	1.3887	0.3477	2.3974	0.0365	1.0073	1.0215	0.0662
0.1523	0.5589	1.0673	1.3684	0.3340	2.4579	0.0304	1.0065	1.0172	0.0617
0.2128	0.5308	1.0646	1.3506	0.3224	2.5184	0.0221	1.0053	1.0113	0.0555
0.2736	0.5087	1.0624	1.3366	0.3126	2.5793	0.0183	1.0048	1.0086	0.0530
0.3345	0.4900	1.0605	1.3248	0.3058	2.5894	0.0174	1.0046	1.0080	0.0525
0.3953	0.4652	1.0580	1.3090	0.2954	2.6398	0.0152	1.0043	1.0065	0.0508
0.4558	0.4461	1.0561	1.2966	0.2865	2.7003	0.0071	1.0032	1.0007	0.0452
0.5167	0.4267	1.0540	1.2842	0.2776	2.7608	0.0043	1.0028	0.9987	0.0433
0.5775	0.4008	1.0513	1.2675	0.2659	2.8213	-0.0047	1.0015	0.9923	0.0367
0.6280	0.3739	1.0484	1.2500	0.2529	2.8821	-0.0090	1.0009	0.9893	0.0337
0.6384	0.3731	1.0483	1.2495	0.2529	2.9426	-0.0124	1.0004	0.9868	0.0314
0.6989	0.3557	1.0464	1.2382	0.2449	3.0031	-0.0149	1.0000	0.9851	0.0293
0.7597	0.3445	1.0452	1.2309	0.2397	3.0640	-0.0210	0.9991	0.9807	0.0249
0.8206	0.3312	1.0437	1.2221	0.2341	3.1850	-0.0282	0.9981	0.9755	0.0191
0.8811	0.3093	1.0412	1.2076	0.2231	3.3063	-0.0390	0.9965	0.9678	0.0110
0.9419	0.2848	1.0384	1.1914	0.2104	3.4277	-0.0481	0.9951	0.9612	0.0042
1.0024	0.2725	1.0370	1.1833	0.2035	3.5490	-0.0538	0.9943	0.9571	-0.0006
1.0633	0.2611	1.0357	1.1757	0.1974	3.6704	-0.0614	0.9931	0.9516	-0.0061
1.1238	0.2501	1.0345	1.1681	0.1920	3.7917	-0.0662	0.9924	0.9481	-0.0100
1.1846	0.2375	1.0330	1.1597	0.1858	3.9127	-0.0732	0.9913	0.9431	-0.0166
1.2455	0.2311	1.0322	1.1555	0.1821	4.0139	-0.0760	0.9909	0.9410	-0.0189
1.3060	0.2090	1.0296	1.1406	0.1697	4.0946	-0.0800	0.9903	0.9381	-0.0224
1.3668	0.1940	1.0277	1.1304	0.1614	4.2159	-0.0849	0.9895	0.9345	-0.0268
1.4173	0.1857	1.0267	1.1248	0.1570	4.3373	-0.0895	0.9888	0.9312	-0.0307
1.4273	0.1832	1.0264	1.1231	0.1557	4.4583	-0.0946	0.9880	0.9275	-0.0353
1.4882	0.1779	1.0258	1.1195	0.1527	4.5796	-0.1003	0.9872	0.9233	-0.0411
1.5487	0.1653	1.0242	1.1109	0.1456	4.7010	-0.1031	0.9867	0.9212	-0.0441
1.6095	0.1503	1.0223	1.1006	0.1371	4.8220	-0.1056	0.9863	0.9194	-0.0467
1.6700	0.1425	1.0213	1.0953	0.1327	4.9433	-0.1104	0.9856	0.9158	-0.0514
1.7305	0.1343	1.0203	1.0897	0.1273					
1.7914	0.1228	1.0188	1.0817	0.1205					
1.8519	0.1137	1.0176	1.0754	0.1152					
1.9124	0.0994	1.0158	1.0656	0.1061					
1.9732	0.0935	1.0150	1.0615	0.1026					
2.0337	0.0835	1.0136	1.0545	0.0965					
2.0942	0.0775	1.0129	1.0503	0.0928					
2.1551	0.0666	1.0114	1.0427	0.0853					
2.2156	0.0551	1.0098	1.0347	0.0778					

Table C-30. Time histories of overpressure, sound speed, density and flow velocity from the reconstructed blast-wave flow field by the RCM for a 1-kg TNT equivalent ANFO surface explosion in a standard atmosphere. These signatures are for the specific radius r = 4.545 m, at which the blast-wave front arrives at time t = 6.531 ms.

t (ms)	$\Delta p/p_1$	a/a_1	ρ/ρ_1	u/a_1	t (ms)	$\Delta p/p_1$	a/a_1	ρ/ρ_1	u/a_1
0.0000	0.5689	1.0679	1.3758	0.3334	2.2542	0.0625	1.0103	1.0409	0.0788
0.0104	0.5679	1.0678	1.3752	0.3334	2.3147	0.0520	1.0089	1.0336	0.0715
0.0709	0.5322	1.0643	1.3527	0.3179	2.3752	0.0489	1.0085	1.0314	0.0697
0.1318	0.5202	1.0631	1.3451	0.3130	2.4360	0.0383	1.0070	1.0239	0.0627
0.1926	0.4955	1.0606	1.3294	0.3023	2.4965	0.0351	1.0066	1.0217	0.0601
0.2531	0.4727	1.0583	1.3150	0.2926	2.5570	0.0290	1.0057	1.0173	0.0561
0.3140	0.4523	1.0562	1.3019	0.2838	2.6179	0.0207	1.0046	1.0115	0.0505
0.3745	0.4377	1.0547	1.2926	0.2773	2.6784	0.0173	1.0041	1.0091	0.0480
0.4353	0.4164	1.0524	1.2788	0.2677	2.7392	0.0145	1.0037	1.0071	0.0462
0.4958	0.4024	1.0509	1.2698	0.2619	2.7997	0.0085	1.0028	1.0028	0.0421
0.5567	0.3797	1.0485	1.2550	0.2511	2.8606	0.0047	1.0023	1.0001	0.0392
0.6175	0.3555	1.0459	1.2392	0.2385	2.9211	-0.0001	1.0016	0.9967	0.0360
0.6780	0.3391	1.0440	1.2285	0.2309	2.9819	-0.0075	1.0005	0.9915	0.0304
0.7389	0.3261	1.0426	1.2200	0.2249	3.0424	-0.0107	1.0001	0.9891	0.0283
0.7893	0.3178	1.0417	1.2145	0.2212	3.1029	-0.0136	0.9997	0.9870	0.0262
0.7994	0.3160	1.0415	1.2133	0.2206	3.1638	-0.0156	0.9994	0.9857	0.0245
0.8602	0.3016	1.0398	1.2038	0.2135	3.2848	-0.0244	0.9981	0.9793	0.0177
0.9207	0.2834	1.0378	1.1918	0.2043	3.3860	-0.0328	0.9969	0.9733	0.0112
0.9816	0.2613	1.0352	1.1769	0.1918	3.4666	-0.0378	0.9961	0.9697	0.0079
1.0421	0.2546	1.0344	1.1724	0.1888	3.5880	-0.0453	0.9950	0.9643	0.0018
1.1026	0.2461	1.0334	1.1667	0.1843	3.7093	-0.0508	0.9942	0.9604	-0.0027
1.1634	0.2365	1.0324	1.1601	0.1797	3.8303	-0.0580	0.9931	0.9551	-0.0078
1.2239	0.2237	1.0309	1.1515	0.1730	3.9517	-0.0620	0.9925	0.9522	-0.0118
1.2844	0.2049	1.0286	1.1388	0.1625	4.0730	-0.0683	0.9915	0.9477	-0.0166
1.3453	0.1896	1.0267	1.1285	0.1537	4.1940	-0.0718	0.9910	0.9451	-0.0197
1.4058	0.1807	1.0256	1.1225	0.1488	4.3154	-0.0782	0.9900	0.9404	-0.0254
1.4663	0.1738	1.0248	1.1177	0.1453	4.4367	-0.0817	0.9895	0.9379	-0.0287
1.5271	0.1689	1.0242	1.1144	0.1427	4.5577	-0.0857	0.9889	0.9350	-0.0320
1.5876	0.1572	1.0227	1.1064	0.1359	4.6791	-0.0910	0.9881	0.9312	-0.0373
1.6485	0.1433	1.0209	1.0969	0.1277	4.8001	-0.0965	0.9872	0.9270	-0.0423
1.7090	0.1364	1.0201	1.0921	0.1232	4.9214	-0.0975	0.9870	0.9263	-0.0439
1.7695	0.1281	1.0190	1.0864	0.1185	5.0424	-0.0998	0.9867	0.9247	-0.0464
1.8300	0.1188	1.0178	1.0801	0.1132					
1.8905	0.1107	1.0167	1.0744	0.1082					
1.9513	0.1000	1.0153	1.0670	0.1019					
1.9614	0.0955	1.0147	1.0639	0.0987					
2.0118	0.0928	1.0144	1.0620	0.0972					
2.0723	0.0867	1.0136	1.0578	0.0937					
2.1328	0.0772	1.0123	1.0512	0.0875					
2.1933	0.0726	1.0117	1.0480	0.0851					

Table C-31. Time histories of overpressure, sound speed, density and flow velocity from the reconstructed blast-wave flow field by the RCM for a 1-kg TNT equivalent ANFO surface explosion in a standard atmosphere. These signatures are for the specific radius r = 4.862 m, at which the blast-wave front arrives at time t = 7.320 ms.

t (ms)	$\Delta p/p_1$	a/a_1	ρ/ρ_1	u/a_1	t (ms)	$\Delta p/p_1$	a/a_1	ρ/ρ_1	u/a_1
0.0000	0.4957	1.0602	1.3306	0.2969	2.3136	0.0589	1.0093	1.0394	0.0719
0.0101	0.4925	1.0599	1.3286	0.2958	2.3745	0.0490	1.0080	1.0325	0.0651
0.0709	0.4740	1.0580	1.3168	0.2878	2.4350	0.0461	1.0076	1.0304	0.0634
0.1314	0.4532	1.0559	1.3035	0.2788	2.4955	0.0422	1.0070	1.0277	0.0611
0.1923	0.4364	1.0541	1.2927	0.2717	2.5563	0.0354	1.0061	1.0229	0.0560
0.2528	0.4194	1.0523	1.2817	0.2634	2.5967	0.0328	1.0057	1.0211	0.0542
0.3133	0.4063	1.0509	1.2732	0.2580	2.6168	0.0300	1.0053	1.0191	0.0525
0.3741	0.3894	1.0491	1.2623	0.2504	2.6773	0.0266	1.0049	1.0166	0.0499
0.4346	0.3755	1.0476	1.2533	0.2441	2.7382	0.0188	1.0038	1.0112	0.0448
0.4951	0.3580	1.0457	1.2418	0.2361	2.7987	0.0155	1.0033	1.0088	0.0424
0.5560	0.3353	1.0432	1.2270	0.2243	2.8592	0.0137	1.0031	1.0075	0.0407
0.6165	0.3202	1.0415	1.2170	0.2169	2.9200	0.0065	1.0020	1.0024	0.0357
0.6770	0.3082	1.0402	1.2091	0.2111	2.9805	0.0045	1.0018	1.0010	0.0345
0.7378	0.2987	1.0391	1.2028	0.2069	3.0410	0.0003	1.0012	0.9980	0.0313
0.7983	0.2857	1.0376	1.1942	0.2000	3.1019	-0.0068	1.0001	0.9929	0.0262
0.8592	0.2723	1.0360	1.1853	0.1934	3.1624	-0.0099	0.9997	0.9908	0.0242
0.9197	0.2560	1.0341	1.1744	0.1847	3.2837	-0.0143	0.9991	0.9876	0.0206
0.9802	0.2417	1.0324	1.1649	0.1773	3.4047	-0.0227	0.9978	0.9815	0.0143
1.0407	0.2345	1.0316	1.1600	0.1735	3.5261	-0.0332	0.9963	0.9740	0.0066
1.1012	0.2262	1.0306	1.1544	0.1694	3.6474	-0.0364	0.9958	0.9717	0.0042
1.1620	0.2152	1.0293	1.1470	0.1637	3.7684	-0.0443	0.9947	0.9660	-0.0017
1.1721	0.2133	1.0291	1.1457	0.1627	3.8898	-0.0513	0.9936	0.9610	-0.0068
1.2225	0.2096	1.0286	1.1432	0.1609	4.0108	-0.0546	0.9931	0.9586	-0.0098
1.2830	0.1988	1.0273	1.1359	0.1549	4.1321	-0.0605	0.9922	0.9542	-0.0147
1.3435	0.1785	1.0248	1.1221	0.1432	4.2531	-0.0647	0.9916	0.9512	-0.0184
1.4040	0.1706	1.0238	1.1168	0.1383	4.3745	-0.0685	0.9910	0.9484	-0.0219
1.4649	0.1645	1.0231	1.1125	0.1351	4.4958	-0.0739	0.9902	0.9445	-0.0265
1.5254	0.1609	1.0226	1.1101	0.1335	4.6168	-0.0763	0.9898	0.9428	-0.0290
1.5859	0.1526	1.0216	1.1045	0.1286	4.6773	-0.0788	0.9894	0.9410	-0.0309
1.6467	0.1385	1.0198	1.0948	0.1202	4.7987	-0.0833	0.9887	0.9377	-0.0349
1.7072	0.1296	1.0186	1.0887	0.1152	4.9200	-0.0864	0.9883	0.9354	-0.0378
1.7677	0.1235	1.0178	1.0844	0.1112	5.0410	-0.0914	0.9875	0.9318	-0.0420
1.8286	0.1154	1.0168	1.0789	0.1065					
1.8891	0.1077	1.0158	1.0735	0.1020					
1.9499	0.1018	1.0151	1.0693	0.0985					
2.0104	0.0896	1.0134	1.0609	0.0909					
2.0713	0.0841	1.0127	1.0570	0.0878					
2.1318	0.0802	1.0122	1.0543	0.0856					
2.1926	0.0725	1.0112	1.0490	0.0803					
2.2531	0.0682	1.0106	1.0460	0.0779					

Table C-32. Time histories of overpressure, sound speed, density and flow velocity from the reconstructed blast-wave flow field by the RCM for a 1-kg TNT equivalent ANFO surface explosion in a standard atmosphere. These signatures are for the specific radius r = 5.338 m, at which the blast-wave front arrives at time t = 8.492 ms.

t (ms)	$\Delta p/p_1$	a/a_1	ρ/ρ_1	u/a_1	t (ms)	$\Delta p/p_1$	a/a_1	ρ/ρ_1	u/a_1
0.0000	0.4228	1.0523	1.2848	0.2589	2.3540	0.0638	1.0096	1.0436	0.0692
0.0504	0.4121	1.0512	1.2779	0.2544	2.4145	0.0552	1.0085	1.0376	0.0637
0.1109	0.3982	1.0497	1.2689	0.2476	2.4753	0.0506	1.0078	1.0344	0.0605
0.1714	0.3829	1.0481	1.2589	0.2407	2.5358	0.0449	1.0070	1.0304	0.0568
0.2319	0.3703	1.0467	1.2508	0.2351	2.5963	0.0414	1.0066	1.0279	0.0547
0.2928	0.3567	1.0452	1.2419	0.2289	2.6568	0.0375	1.0060	1.0252	0.0520
0.3533	0.3466	1.0441	1.2352	0.2243	2.7177	0.0325	1.0053	1.0216	0.0486
0.4138	0.3320	1.0425	1.2256	0.2169	2.7782	0.0279	1.0047	1.0183	0.0452
0.4746	0.3166	1.0408	1.2155	0.2093	2.8387	0.0245	1.0042	1.0160	0.0431
0.5351	0.3019	1.0391	1.2057	0.2019	2.8992	0.0175	1.0032	1.0110	0.0383
0.5956	0.2913	1.0379	1.1987	0.1964	2.9600	0.0144	1.0028	1.0088	0.0362
0.6565	0.2829	1.0370	1.1931	0.1926	3.0205	0.0124	1.0025	1.0073	0.0349
0.7170	0.2751	1.0360	1.1879	0.1890	3.0810	0.0075	1.0018	1.0038	0.0315
0.7778	0.2617	1.0345	1.1790	0.1821	3.1419	0.0043	1.0014	1.0016	0.0292
0.8383	0.2557	1.0338	1.1750	0.1791	3.2024	0.0013	1.0009	0.9995	0.0272
0.8992	0.2394	1.0319	1.1641	0.1703	3.2629	-0.0042	1.0001	0.9955	0.0231
0.9597	0.2258	1.0302	1.1549	0.1630	3.3842	-0.0100	0.9993	0.9914	0.0190
1.0205	0.2197	1.0295	1.1508	0.1601	3.4548	-0.0119	0.9990	0.9901	0.0172
1.0810	0.2131	1.0287	1.1463	0.1565	3.5661	-0.0183	0.9981	0.9855	0.0125
1.1415	0.2052	1.0277	1.1410	0.1529	3.6871	-0.0236	0.9973	0.9816	0.0083
1.2024	0.1958	1.0266	1.1346	0.1478	3.8084	-0.0316	0.9962	0.9759	0.0027
1.2629	0.1917	1.0261	1.1318	0.1460	3.9298	-0.0386	0.9951	0.9708	-0.0026
1.3234	0.1772	1.0243	1.1220	0.1372	4.0508	-0.0417	0.9947	0.9686	-0.0049
1.3842	0.1643	1.0227	1.1132	0.1295	4.1721	-0.0473	0.9938	0.9645	-0.0093
1.4246	0.1569	1.0218	1.1082	0.1255	4.2931	-0.0501	0.9934	0.9625	-0.0118
1.4447	0.1557	1.0216	1.1073	0.1246	4.4145	-0.0551	0.9927	0.9589	-0.0158
1.5052	0.1513	1.0210	1.1043	0.1224	4.5355	-0.0598	0.9920	0.9555	-0.0198
1.5661	0.1495	1.0208	1.1031	0.1215	4.6568	-0.0626	0.9915	0.9535	-0.0222
1.6266	0.1443	1.0202	1.0995	0.1187	4.7778	-0.0666	0.9909	0.9506	-0.0258
1.6871	0.1322	1.0186	1.0912	0.1111	4.8992	-0.0697	0.9905	0.9483	-0.0285
1.7479	0.1240	1.0176	1.0855	0.1063	5.0205	-0.0721	0.9901	0.9465	-0.0312
1.8084	0.1179	1.0168	1.0813	0.1026	5.1415	-0.0775	0.9893	0.9426	-0.0356
1.8689	0.1123	1.0161	1.0774	0.0993					
1.9298	0.1031	1.0149	1.0710	0.0937					
1.9903	0.0989	1.0143	1.0681	0.0909					
2.0508	0.0952	1.0138	1.0656	0.0889					
2.1116	0.0861	1.0126	1.0592	0.0832					
2.1721	0.0802	1.0118	1.0551	0.0795					
2.2326	0.0750	1.0111	1.0514	0.0764					
2.2935	0.0680	1.0102	1.0466	0.0718					

Table C-33. Time histories of overpressure, sound speed, density and flow velocity from the reconstructed blast-wave flow field by the RCM for a 1-kg TNT equivalent ANFO surface explosion in a standard atmosphere. These signatures are for the specific radius r = 5.904 m, at which the blast-wave front arrives at time t = 9.917 ms.

t (ms)	$\Delta p/p_1$	a/a_1	ρ/ρ_1	u/a_1	t (ms)	$\Delta p/p_1$	a/a_1	ρ/ρ_1	u/a_1
0.0000	0.3586	1.0452	1.2436	0.2242	2.3234	0.0696	1.0101	1.0483	0.0681
0.0202	0.3551	1.0448	1.2414	0.2226	2.3839	0.0630	1.0092	1.0437	0.0635
0.0807	0.3441	1.0436	1.2342	0.2176	2.4444	0.0603	1.0089	1.0417	0.0619
0.1415	0.3379	1.0429	1.2301	0.2150	2.5052	0.0547	1.0081	1.0378	0.0584
0.2020	0.3260	1.0416	1.2223	0.2090	2.5657	0.0504	1.0075	1.0348	0.0555
0.2625	0.3170	1.0406	1.2163	0.2048	2.6262	0.0459	1.0069	1.0316	0.0529
0.3234	0.3028	1.0390	1.2070	0.1977	2.6867	0.0408	1.0062	1.0280	0.0494
0.3839	0.2910	1.0376	1.1991	0.1914	2.7476	0.0377	1.0058	1.0258	0.0475
0.4444	0.2823	1.0366	1.1933	0.1872	2.8081	0.0342	1.0053	1.0234	0.0450
0.5052	0.2698	1.0352	1.1850	0.1809	2.8686	0.0296	1.0046	1.0201	0.0420
0.5657	0.2619	1.0343	1.1798	0.1768	2.9294	0.0253	1.0040	1.0171	0.0390
0.6262	0.2546	1.0334	1.1749	0.1732	2.9899	0.0228	1.0037	1.0153	0.0373
0.6871	0.2420	1.0319	1.1664	0.1665	3.0504	0.0164	1.0028	1.0107	0.0330
0.7476	0.2381	1.0314	1.1637	0.1648	3.1109	0.0139	1.0024	1.0089	0.0310
0.8081	0.2289	1.0303	1.1576	0.1602	3.1718	0.0117	1.0021	1.0074	0.0296
0.8689	0.2187	1.0291	1.1507	0.1545	3.2323	0.0084	1.0017	1.0051	0.0273
0.9294	0.2075	1.0278	1.1432	0.1480	3.2928	0.0055	1.0013	1.0030	0.0251
0.9899	0.2009	1.0270	1.1387	0.1450	3.4141	0.0004	1.0005	0.9993	0.0214
1.0508	0.1947	1.0262	1.1345	0.1418	3.5351	-0.0071	0.9994	0.9940	0.0160
1.1113	0.1887	1.0255	1.1304	0.1384	3.6565	-0.0106	0.9989	0.9915	0.0134
1.1718	0.1810	1.0245	1.1252	0.1343	3.7775	-0.0159	0.9982	0.9877	0.0094
1.2323	0.1765	1.0239	1.1221	0.1320	3.8988	-0.0212	0.9974	0.9839	0.0052
1.2931	0.1728	1.0235	1.1196	0.1304	4.0198	-0.0280	0.9964	0.9790	0.0004
1.3536	0.1583	1.0217	1.1097	0.1214	4.1412	-0.0315	0.9959	0.9765	-0.0023
1.4141	0.1476	1.0203	1.1024	0.1149	4.2118	-0.0352	0.9954	0.9738	-0.0047
1.4746	0.1422	1.0196	1.0986	0.1119	4.3230	-0.0378	0.9950	0.9720	-0.0068
1.5355	0.1387	1.0192	1.0963	0.1101	4.4444	-0.0443	0.9940	0.9672	-0.0117
1.5960	0.1369	1.0190	1.0950	0.1092	4.5654	-0.0452	0.9939	0.9666	-0.0129
1.6565	0.1320	1.0183	1.0916	0.1064	4.6867	-0.0496	0.9932	0.9634	-0.0166
1.7173	0.1210	1.0169	1.0840	0.0994	4.8077	-0.0540	0.9926	0.9603	-0.0201
1.7778	0.1163	1.0163	1.0808	0.0968	4.9329	-0.0565	0.9922	0.9584	-0.0222
1.8383	0.1108	1.0156	1.0770	0.0933	5.0588	-0.0604	0.9916	0.9556	-0.0252
1.8992	0.1046	1.0148	1.0726	0.0895	5.1843	-0.0627	0.9912	0.9539	-0.0275
1.9597	0.0991	1.0141	1.0688	0.0863	5.3102	-0.0653	0.9909	0.9520	-0.0298
2.0202	0.0927	1.0132	1.0644	0.0822					
2.0303	0.0908	1.0130	1.0631	0.0810					
2.0807	0.0885	1.0127	1.0615	0.0797					
2.1415	0.0853	1.0122	1.0593	0.0779					
2.2020	0.0786	1.0113	1.0545	0.0736					
2.2625	0.0731	1.0106	1.0507	0.0704					

Table C-34. Time histories of overpressure, sound speed, density and flow velocity from the reconstructed blast-wave flow field by the RCM for a 1-kg TNT equivalent ANFO surface explosion in a standard atmosphere. These signatures are for the specific radius r = 6.689 m, at which the blast-wave front arrives at time t = 11.947 ms.

t (ms)	$\Delta p/p_1$	a/a_1	ρ/ρ_1	u/a_1	t (ms)	$\Delta p/p_1$	a/a_1	ρ/ρ_1	u/a_1
0.0000	0.2950	1.0379	1.2022	0.1883	2.3533	0.0670	1.0096	1.0468	0.0612
0.0504	0.2896	1.0373	1.1987	0.1858	2.4141	0.0632	1.0091	1.0442	0.0588
0.1113	0.2779	1.0359	1.1908	0.1798	2.4746	0.0611	1.0088	1.0427	0.0575
0.1718	0.2714	1.0352	1.1865	0.1764	2.5351	0.0554	1.0080	1.0387	0.0539
0.2323	0.2648	1.0344	1.1820	0.1733	2.5956	0.0520	1.0075	1.0363	0.0518
0.2931	0.2569	1.0335	1.1768	0.1691	2.6565	0.0480	1.0070	1.0335	0.0492
0.3536	0.2467	1.0323	1.1699	0.1638	2.7170	0.0448	1.0066	1.0313	0.0472
0.4141	0.2381	1.0313	1.1642	0.1594	2.7775	0.0410	1.0060	1.0286	0.0447
0.4750	0.2322	1.0305	1.1602	0.1564	2.8397	0.0364	1.0054	1.0253	0.0417
0.5355	0.2266	1.0299	1.1564	0.1534	2.9027	0.0338	1.0050	1.0235	0.0398
0.5960	0.2163	1.0286	1.1495	0.1479	2.9656	0.0306	1.0046	1.0212	0.0378
0.6565	0.2129	1.0282	1.1472	0.1464	3.0285	0.0267	1.0040	1.0184	0.0349
0.7173	0.2051	1.0273	1.1420	0.1420	3.0911	0.0247	1.0038	1.0170	0.0335
0.7778	0.2004	1.0267	1.1388	0.1396	3.1540	0.0214	1.0033	1.0147	0.0314
0.8383	0.1924	1.0257	1.1334	0.1350	3.2170	0.0172	1.0027	1.0117	0.0284
0.8992	0.1843	1.0247	1.1278	0.1304	3.2799	0.0140	1.0023	1.0095	0.0263
0.9597	0.1795	1.0241	1.1245	0.1280	3.3428	0.0119	1.0020	1.0080	0.0248
1.0202	0.1742	1.0235	1.1210	0.1250	3.4687	0.0077	1.0014	1.0050	0.0218
1.0807	0.1682	1.0227	1.1169	0.1217	3.5946	0.0033	1.0007	1.0018	0.0186
1.1415	0.1620	1.0220	1.1126	0.1183	3.7201	-0.0038	0.9997	0.9967	0.0134
1.2020	0.1580	1.0214	1.1099	0.1162	3.8460	-0.0080	0.9991	0.9937	0.0104
1.2625	0.1553	1.0211	1.1081	0.1148	3.9719	-0.0103	0.9988	0.9921	0.0088
1.3230	0.1491	1.0203	1.1038	0.1112	4.0348	-0.0141	0.9982	0.9894	0.0061
1.3839	0.1403	1.0192	1.0977	0.1061	4.1603	-0.0181	0.9977	0.9865	0.0031
1.4444	0.1316	1.0181	1.0917	0.1007	4.2862	-0.0242	0.9968	0.9821	-0.0014
1.5049	0.1268	1.0175	1.0885	0.0980	4.4120	-0.0261	0.9965	0.9808	-0.0029
1.5657	0.1234	1.0170	1.0861	0.0961	4.5379	-0.0315	0.9957	0.9769	-0.0070
1.6262	0.1220	1.0168	1.0851	0.0953	4.6638	-0.0346	0.9953	0.9747	-0.0094
1.6867	0.1179	1.0163	1.0822	0.0930	4.7897	-0.0392	0.9946	0.9713	-0.0128
1.7472	0.1111	1.0154	1.0776	0.0887	4.9152	-0.0401	0.9944	0.9706	-0.0139
1.8081	0.1070	1.0149	1.0747	0.0863	5.0410	-0.0436	0.9939	0.9681	-0.0168
1.8686	0.1009	1.0141	1.0705	0.0826	5.1669	-0.0474	0.9934	0.9654	-0.0198
1.9291	0.0960	1.0135	1.0671	0.0796	5.2928	-0.0498	0.9930	0.9636	-0.0217
1.9896	0.0922	1.0129	1.0645	0.0773	5.4187	-0.0531	0.9925	0.9613	-0.0243
2.0504	0.0890	1.0125	1.0622	0.0753					
2.1109	0.0839	1.0119	1.0587	0.0719					
2.1714	0.0789	1.0112	1.0552	0.0688					
2.1815	0.0781	1.0111	1.0546	0.0683					
2.2323	0.0762	1.0108	1.0533	0.0672					
2.2928	0.0703	1.0100	1.0492	0.0633					

Table C-35. Time histories of overpressure, sound speed, density and flow velocity from the reconstructed blast-wave flow field by the RCM for a 1-kg TNT equivalent ANFO surface explosion in a standard atmosphere. These signatures are for the specific radius r = 7.512 m, at which the blast-wave front arrives at time t = 14.129 ms.

t (ms)	$\Delta p/p_1$	a/a_1	ρ/ρ_1	u/a_1	t (ms)	$\Delta p/p_1$	a/a_1	ρ/ρ_1	u/a_1
0.0000	0.2441	1.0319	1.1685	0.1586	2.4193	0.0601	1.0085	1.0422	0.0535
0.0508	0.2395	1.0313	1.1654	0.1563	2.4823	0.0584	1.0083	1.0410	0.0525
0.1113	0.2331	1.0305	1.1611	0.1531	2.5452	0.0557	1.0079	1.0391	0.0507
0.1718	0.2273	1.0299	1.1572	0.1500	2.6081	0.0512	1.0073	1.0360	0.0478
0.2326	0.2193	1.0289	1.1518	0.1456	2.6707	0.0481	1.0069	1.0338	0.0459
0.2931	0.2143	1.0283	1.1484	0.1429	2.7337	0.0443	1.0064	1.0311	0.0432
0.3536	0.2085	1.0276	1.1445	0.1399	2.7966	0.0423	1.0061	1.0297	0.0420
0.4141	0.2032	1.0269	1.1409	0.1370	2.8595	0.0397	1.0057	1.0279	0.0402
0.4750	0.1950	1.0259	1.1353	0.1324	2.9225	0.0359	1.0052	1.0252	0.0377
0.5355	0.1920	1.0256	1.1333	0.1310	2.9854	0.0328	1.0048	1.0230	0.0356
0.5960	0.1884	1.0251	1.1309	0.1291	3.0483	0.0304	1.0044	1.0213	0.0340
0.6582	0.1815	1.0243	1.1262	0.1253	3.1113	0.0276	1.0041	1.0193	0.0320
0.7211	0.1769	1.0237	1.1230	0.1229	3.1742	0.0240	1.0035	1.0167	0.0296
0.7841	0.1726	1.0232	1.1201	0.1205	3.2371	0.0222	1.0033	1.0154	0.0285
0.8470	0.1635	1.0220	1.1139	0.1152	3.3001	0.0198	1.0030	1.0138	0.0270
0.9096	0.1587	1.0214	1.1106	0.1126	3.3627	0.0172	1.0026	1.0120	0.0252
0.9725	0.1533	1.0207	1.1069	0.1097	3.4256	0.0128	1.0020	1.0088	0.0222
1.0355	0.1504	1.0204	1.1049	0.1080	3.5515	0.0094	1.0015	1.0064	0.0199
1.0984	0.1457	1.0198	1.1017	0.1052	3.6773	0.0056	1.0010	1.0037	0.0172
1.1613	0.1424	1.0194	1.0994	0.1035	3.8032	0.0027	1.0005	1.0016	0.0151
1.2243	0.1409	1.0192	1.0984	0.1028	3.9287	-0.0031	0.9997	0.9975	0.0108
1.2872	0.1379	1.0188	1.0963	0.1012	4.0546	-0.0068	0.9992	0.9948	0.0081
1.3501	0.1270	1.0174	1.0888	0.0945	4.1805	-0.0088	0.9989	0.9934	0.0067
1.4131	0.1218	1.0167	1.0852	0.0914	4.3063	-0.0134	0.9982	0.9901	0.0033
1.4760	0.1151	1.0158	1.0806	0.0873	4.4322	-0.0179	0.9976	0.9869	-0.0001
1.5386	0.1124	1.0155	1.0787	0.0859	4.5581	-0.0217	0.9970	0.9841	-0.0029
1.6015	0.1104	1.0152	1.0773	0.0847	4.6836	-0.0235	0.9968	0.9828	-0.0043
1.6645	0.1071	1.0148	1.0750	0.0829	4.8095	-0.0281	0.9961	0.9796	-0.0078
1.7274	0.1006	1.0139	1.0705	0.0788	4.9353	-0.0308	0.9957	0.9776	-0.0099
1.7903	0.0967	1.0134	1.0678	0.0764	5.0612	-0.0348	0.9951	0.9747	-0.0130
1.8216	0.0936	1.0130	1.0656	0.0744	5.1871	-0.0358	0.9950	0.9740	-0.0139
1.8533	0.0932	1.0130	1.0654	0.0743	5.3126	-0.0390	0.9945	0.9717	-0.0163
1.9162	0.0905	1.0126	1.0635	0.0727	5.3755	-0.0400	0.9944	0.9710	-0.0172
1.9788	0.0855	1.0119	1.0600	0.0696					
2.0417	0.0821	1.0115	1.0576	0.0675					
2.1047	0.0794	1.0111	1.0557	0.0658					
2.1676	0.0751	1.0106	1.0528	0.0632					
2.2305	0.0720	1.0101	1.0506	0.0612					
2.2935	0.0695	1.0098	1.0488	0.0596					
2.3564	0.0630	1.0089	1.0442	0.0554					

Table C-36. Time histories of overpressure, sound speed, density and flow velocity from the reconstructed blast-wave flow field by the RCM for a 1-kg TNT equivalent ANFO surface explosion in a standard atmosphere. These signatures are for the specific radius r = 8.189 m, at which the blast-wave front arrives at time t = 15.950 ms.

t (ms)	$\Delta p/p_1$	a/a_1	ρ/ρ_1	u/a_1	t (ms)	$\Delta p/p_1$	a/a_1	ρ/ρ_1	u/a_1
0.0000	0.2133	1.0281	1.1478	0.1401	2.4847	0.0555	1.0079	1.0391	0.0485
0.0316	0.2123	1.0280	1.1472	0.1397	2.5476	0.0538	1.0076	1.0379	0.0474
0.0946	0.2052	1.0271	1.1424	0.1358	2.6106	0.0512	1.0073	1.0361	0.0458
0.1572	0.1988	1.0264	1.1380	0.1324	2.6735	0.0471	1.0067	1.0332	0.0431
0.2201	0.1949	1.0259	1.1354	0.1303	2.7364	0.0448	1.0064	1.0316	0.0416
0.2830	0.1889	1.0251	1.1313	0.1270	2.7990	0.0425	1.0061	1.0299	0.0400
0.3460	0.1818	1.0243	1.1265	0.1230	2.8620	0.0391	1.0056	1.0275	0.0377
0.4089	0.1785	1.0238	1.1242	0.1213	2.9249	0.0365	1.0053	1.0257	0.0362
0.4718	0.1759	1.0235	1.1225	0.1200	2.9878	0.0335	1.0048	1.0236	0.0342
0.5348	0.1704	1.0228	1.1187	0.1170	3.0508	0.0323	1.0047	1.0227	0.0333
0.5977	0.1673	1.0225	1.1166	0.1153	3.1137	0.0292	1.0042	1.0205	0.0312
0.6606	0.1622	1.0218	1.1131	0.1124	3.1766	0.0272	1.0040	1.0192	0.0299
0.7236	0.1549	1.0209	1.1081	0.1081	3.2396	0.0226	1.0033	1.0159	0.0267
0.7865	0.1509	1.0204	1.1054	0.1059	3.3025	0.0207	1.0030	1.0145	0.0254
0.8491	0.1456	1.0197	1.1017	0.1029	3.3654	0.0202	1.0030	1.0142	0.0252
0.9120	0.1423	1.0193	1.0995	0.1010	3.4280	0.0176	1.0026	1.0124	0.0233
0.9750	0.1396	1.0190	1.0976	0.0996	3.4910	0.0159	1.0024	1.0111	0.0221
1.0379	0.1345	1.0183	1.0941	0.0967	3.5539	0.0119	1.0018	1.0082	0.0194
1.1008	0.1318	1.0180	1.0922	0.0951	3.6798	0.0088	1.0014	1.0060	0.0172
1.1638	0.1301	1.0177	1.0911	0.0944	3.8056	0.0053	1.0009	1.0036	0.0148
1.2267	0.1275	1.0174	1.0892	0.0929	3.9315	0.0031	1.0005	1.0020	0.0131
1.2896	0.1199	1.0164	1.0840	0.0882	4.0574	-0.0025	0.9998	0.9980	0.0092
1.3526	0.1163	1.0160	1.0815	0.0861	4.1829	-0.0056	0.9993	0.9958	0.0069
1.4155	0.1109	1.0152	1.0778	0.0827	4.3088	-0.0076	0.9990	0.9943	0.0054
1.4784	0.1060	1.0146	1.0744	0.0798	4.4346	-0.0115	0.9985	0.9915	0.0026
1.5410	0.1028	1.0142	1.0721	0.0779	4.5605	-0.0148	0.9980	0.9892	0.0001
1.6040	0.1015	1.0140	1.0712	0.0772	4.6235	-0.0172	0.9976	0.9874	-0.0017
1.6669	0.0997	1.0138	1.0700	0.0763	4.7490	-0.0202	0.9972	0.9853	-0.0038
1.7298	0.0948	1.0131	1.0666	0.0731	4.8748	-0.0213	0.9970	0.9845	-0.0047
1.7928	0.0894	1.0124	1.0628	0.0697	5.0007	-0.0257	0.9964	0.9814	-0.0081
1.8557	0.0860	1.0120	1.0604	0.0677	5.1266	-0.0272	0.9962	0.9803	-0.0093
1.9186	0.0836	1.0116	1.0588	0.0662	5.2525	-0.0306	0.9957	0.9778	-0.0119
1.9816	0.0803	1.0112	1.0565	0.0642	5.3780	-0.0323	0.9954	0.9766	-0.0133
2.0442	0.0771	1.0108	1.0542	0.0622					
2.1071	0.0745	1.0104	1.0524	0.0606					
2.1700	0.0727	1.0102	1.0512	0.0595					
2.2330	0.0681	1.0096	1.0479	0.0565					
2.2959	0.0650	1.0092	1.0458	0.0547					
2.3588	0.0629	1.0089	1.0443	0.0533					
2.4218	0.0580	1.0082	1.0408	0.0501					

Table C-37. Time histories of overpressure, sound speed, density and flow velocity from the reconstructed blast-wave flow field by the RCM for a 1-kg TNT equivalent ANFO surface explosion in a standard atmosphere. These signatures are for the specific radius r = 8.986 m, at which the blast-wave front arrives at time t = 18.120 ms.

t (ms)	$\Delta p/p_1$	a/a_1	ρ/ρ_1	u/a_1	t (ms)	$\Delta p/p_1$	a/a_1	ρ/ρ_1	u/a_1
0.0000	0.1858	1.0247	1.1293	0.1234	2.4426	0.0535	1.0076	1.0378	0.0452
0.0629	0.1815	1.0242	1.1264	0.1210	2.4534	0.0534	1.0075	1.0377	0.0452
0.1259	0.1767	1.0236	1.1230	0.1183	2.5160	0.0514	1.0073	1.0363	0.0440
0.1888	0.1706	1.0228	1.1189	0.1149	2.5789	0.0505	1.0071	1.0357	0.0434
0.2517	0.1654	1.0222	1.1154	0.1119	2.6419	0.0491	1.0069	1.0346	0.0425
0.3147	0.1629	1.0219	1.1137	0.1106	2.7048	0.0460	1.0065	1.0325	0.0405
0.3776	0.1611	1.0217	1.1124	0.1098	2.7677	0.0430	1.0061	1.0304	0.0385
0.4405	0.1563	1.0210	1.1091	0.1071	2.8307	0.0409	1.0058	1.0289	0.0372
0.5035	0.1534	1.0207	1.1072	0.1055	2.8936	0.0388	1.0055	1.0274	0.0357
0.5664	0.1497	1.0202	1.1046	0.1034	2.9565	0.0361	1.0052	1.0255	0.0340
0.6290	0.1461	1.0197	1.1021	0.1014	3.0195	0.0335	1.0048	1.0236	0.0321
0.6919	0.1401	1.0190	1.0980	0.0979	3.0824	0.0307	1.0044	1.0217	0.0303
0.7549	0.1367	1.0185	1.0956	0.0958	3.1450	0.0296	1.0042	1.0209	0.0295
0.8178	0.1327	1.0180	1.0929	0.0936	3.2079	0.0275	1.0040	1.0194	0.0282
0.8807	0.1287	1.0175	1.0902	0.0912	3.2709	0.0255	1.0037	1.0180	0.0268
0.9437	0.1267	1.0173	1.0888	0.0901	3.3338	0.0240	1.0035	1.0169	0.0257
1.0066	0.1215	1.0166	1.0852	0.0870	3.3967	0.0202	1.0029	1.0142	0.0231
1.0695	0.1202	1.0164	1.0843	0.0863	3.5226	0.0168	1.0025	1.0118	0.0208
1.1325	0.1181	1.0162	1.0829	0.0852	3.6485	0.0127	1.0019	1.0089	0.0180
1.1954	0.1167	1.0160	1.0819	0.0845	3.7744	0.0091	1.0014	1.0063	0.0154
1.2580	0.1110	1.0152	1.0780	0.0810	3.8999	0.0073	1.0011	1.0050	0.0142
1.3209	0.1071	1.0147	1.0752	0.0787	4.0257	0.0041	1.0007	1.0028	0.0120
1.3421	0.1048	1.0144	1.0736	0.0773	4.1516	0.0004	1.0001	1.0001	0.0093
1.3839	0.1016	1.0140	1.0714	0.0753	4.2775	-0.0035	0.9996	0.9973	0.0065
1.4468	0.0972	1.0134	1.0683	0.0725	4.4034	-0.0061	0.9992	0.9955	0.0047
1.5097	0.0942	1.0130	1.0663	0.0708	4.5289	-0.0077	0.9990	0.9944	0.0035
1.5727	0.0933	1.0129	1.0656	0.0703	4.6547	-0.0110	0.9985	0.9920	0.0011
1.6356	0.0922	1.0128	1.0649	0.0697	4.7806	-0.0141	0.9981	0.9898	-0.0012
1.6985	0.0893	1.0124	1.0628	0.0680	4.9065	-0.0180	0.9975	0.9869	-0.0041
1.7615	0.0848	1.0118	1.0597	0.0651	5.0324	-0.0194	0.9973	0.9859	-0.0052
1.8244	0.0816	1.0113	1.0575	0.0630	5.1582	-0.0230	0.9968	0.9834	-0.0078
1.8874	0.0787	1.0109	1.0554	0.0612	5.2837	-0.0247	0.9965	0.9822	-0.0092
1.9499	0.0765	1.0107	1.0539	0.0598	5.4096	-0.0270	0.9962	0.9805	-0.0110
2.0129	0.0728	1.0102	1.0513	0.0575					
2.0758	0.0699	1.0098	1.0493	0.0558					
2.1387	0.0679	1.0095	1.0479	0.0545					
2.2017	0.0666	1.0093	1.0470	0.0537					
2.2646	0.0633	1.0089	1.0447	0.0516					
2.3275	0.0607	1.0085	1.0428	0.0499					
2.3905	0.0586	1.0082	1.0414	0.0486					

Table C-38. Time histories of overpressure, sound speed, density and flow velocity from the reconstructed blast-wave flow field by the RCM for a 1-kg TNT equivalent ANFO surface explosion in a standard atmosphere. These signatures are for the specific radius r = 9.485 m, at which the blast-wave front arrives at time t = 19.463 ms.

t (ms)	$\Delta p/p_1$	a/a_1	ρ/ρ_1	u/a_1	t (ms)	$\Delta p/p_1$	a/a_1	ρ/ρ_1	u/a_1
0.0000	0.1718	1.0230	1.1198	0.1146	2.4322	0.0547	1.0077	1.0386	0.0451
0.0417	0.1687	1.0226	1.1177	0.1129	2.4948	0.0505	1.0071	1.0357	0.0424
0.1047	0.1648	1.0221	1.1150	0.1107	2.5577	0.0488	1.0069	1.0345	0.0413
0.1676	0.1587	1.0213	1.1108	0.1072	2.6207	0.0479	1.0068	1.0339	0.0408
0.2305	0.1558	1.0210	1.1088	0.1057	2.6836	0.0452	1.0064	1.0319	0.0390
0.2935	0.1537	1.0207	1.1074	0.1045	2.7465	0.0437	1.0062	1.0309	0.0380
0.3564	0.1517	1.0204	1.1060	0.1035	2.8095	0.0409	1.0058	1.0289	0.0362
0.4193	0.1477	1.0199	1.1033	0.1012	2.8724	0.0389	1.0055	1.0275	0.0349
0.4823	0.1451	1.0196	1.1015	0.0998	2.9353	0.0368	1.0052	1.0261	0.0335
0.5452	0.1395	1.0189	1.0976	0.0964	2.9983	0.0344	1.0049	1.0243	0.0319
0.6078	0.1351	1.0183	1.0946	0.0938	3.0612	0.0322	1.0046	1.0228	0.0304
0.6707	0.1316	1.0179	1.0922	0.0919	3.1241	0.0294	1.0042	1.0208	0.0287
0.7337	0.1299	1.0177	1.0910	0.0909	3.1867	0.0280	1.0040	1.0198	0.0280
0.7966	0.1261	1.0172	1.0884	0.0887	3.2497	0.0258	1.0037	1.0182	0.0268
0.8595	0.1224	1.0167	1.0858	0.0865	3.3126	0.0242	1.0035	1.0171	0.0259
0.9225	0.1204	1.0164	1.0845	0.0854	3.3755	0.0220	1.0032	1.0155	0.0246
0.9854	0.1162	1.0159	1.0816	0.0829	3.5014	0.0169	1.0025	1.0119	0.0215
1.0483	0.1143	1.0156	1.0802	0.0818	3.6273	0.0139	1.0020	1.0098	0.0199
1.1005	0.1124	1.0154	1.0790	0.0808	3.7531	0.0090	1.0014	1.0063	0.0169
1.1113	0.1124	1.0154	1.0789	0.0808	3.8790	0.0064	1.0010	1.0044	0.0154
1.1739	0.1110	1.0152	1.0780	0.0800	4.0045	0.0033	1.0005	1.0022	0.0136
1.2368	0.1070	1.0147	1.0752	0.0776	4.1304	0.0003	1.0001	1.0001	0.0119
1.2997	0.1040	1.0143	1.0731	0.0758	4.2563	-0.0026	0.9997	0.9980	0.0102
1.3627	0.0979	1.0135	1.0688	0.0720	4.3821	-0.0068	0.9991	0.9950	0.0075
1.4256	0.0944	1.0130	1.0664	0.0698	4.5080	-0.0090	0.9988	0.9935	0.0062
1.4885	0.0909	1.0126	1.0640	0.0677	4.6335	-0.0108	0.9985	0.9922	0.0053
1.5515	0.0891	1.0123	1.0627	0.0666	4.7594	-0.0141	0.9980	0.9898	0.0031
1.6144	0.0880	1.0122	1.0620	0.0660	4.8853	-0.0172	0.9976	0.9875	0.0011
1.6773	0.0859	1.0119	1.0605	0.0648	5.0111	-0.0206	0.9971	0.9851	-0.0010
1.7403	0.0813	1.0113	1.0573	0.0619	5.1370	-0.0226	0.9968	0.9837	-0.0023
1.8029	0.0779	1.0108	1.0549	0.0597	5.2629	-0.0261	0.9963	0.9812	-0.0046
1.8658	0.0750	1.0104	1.0529	0.0579	5.3888	-0.0280	0.9960	0.9798	-0.0058
1.9287	0.0744	1.0104	1.0524	0.0577					
1.9917	0.0701	1.0098	1.0495	0.0549					
2.0546	0.0676	1.0095	1.0477	0.0533					
2.1175	0.0658	1.0092	1.0465	0.0523					
2.1805	0.0640	1.0090	1.0452	0.0511					
2.2434	0.0632	1.0088	1.0446	0.0507					
2.3063	0.0601	1.0084	1.0424	0.0487					
2.3693	0.0565	1.0079	1.0399	0.0464					

Table C-39. Time histories of overpressure, sound speed, density and flow velocity from the reconstructed blast-wave flow field by the RCM for a 1-kg TNT equivalent ANFO surface explosion in a standard atmosphere. These signatures are for the specific radius r = 9.880 m, at which the blast-wave front arrives at time t = 20.563 ms.

t (ms)	$\Delta p/p_1$	a/a_1	ρ/ρ_1	u/a_1	t (ms)	$\Delta p/p_1$	a/a_1	ρ/ρ_1	u/a_1
0.0000	0.1620	1.0217	1.1131	0.1085	2.4638	0.0471	1.0067	1.0333	0.0444
0.0108	0.1619	1.0217	1.1130	0.1085	2.5268	0.0435	1.0062	1.0308	0.0421
0.0734	0.1562	1.0210	1.1091	0.1051	2.5897	0.0428	1.0061	1.0303	0.0419
0.1363	0.1525	1.0205	1.1066	0.1030	2.6527	0.0420	1.0059	1.0297	0.0415
0.1992	0.1498	1.0202	1.1047	0.1015	2.7156	0.0393	1.0056	1.0278	0.0399
0.2622	0.1477	1.0199	1.1033	0.1004	2.7785	0.0378	1.0054	1.0268	0.0391
0.3251	0.1458	1.0197	1.1020	0.0995	2.8411	0.0350	1.0050	1.0248	0.0373
0.3880	0.1419	1.0192	1.0993	0.0972	2.9040	0.0334	1.0048	1.0236	0.0364
0.4510	0.1383	1.0187	1.0969	0.0952	2.9670	0.0309	1.0044	1.0219	0.0349
0.5139	0.1340	1.0182	1.0939	0.0926	3.0299	0.0285	1.0041	1.0202	0.0333
0.5768	0.1292	1.0176	1.0905	0.0898	3.0928	0.0263	1.0038	1.0186	0.0320
0.6398	0.1265	1.0172	1.0887	0.0882	3.1558	0.0237	1.0034	1.0167	0.0303
0.7024	0.1249	1.0170	1.0876	0.0874	3.2187	0.0224	1.0032	1.0159	0.0296
0.7653	0.1201	1.0164	1.0843	0.0846	3.2817	0.0204	1.0029	1.0144	0.0283
0.8282	0.1174	1.0160	1.0824	0.0832	3.3446	0.0189	1.0027	1.0134	0.0274
0.8912	0.1154	1.0158	1.0810	0.0823	3.4705	0.0138	1.0020	1.0097	0.0241
0.9541	0.1109	1.0152	1.0779	0.0798	3.5960	0.0117	1.0017	1.0082	0.0229
1.0170	0.1094	1.0150	1.0769	0.0792	3.7218	0.0079	1.0012	1.0056	0.0204
1.0800	0.1072	1.0147	1.0753	0.0781	3.8477	0.0042	1.0006	1.0029	0.0180
1.1429	0.1057	1.0145	1.0743	0.0775	3.9736	0.0017	1.0003	1.0011	0.0165
1.2058	0.1017	1.0140	1.0715	0.0753	4.0995	-0.0013	0.9999	0.9990	0.0145
1.2688	0.0967	1.0133	1.0681	0.0724	4.2253	-0.0033	0.9996	0.9976	0.0132
1.3317	0.0927	1.0128	1.0653	0.0700	4.3512	-0.0077	0.9989	0.9944	0.0102
1.3943	0.0892	1.0123	1.0628	0.0681	4.4767	-0.0102	0.9986	0.9926	0.0086
1.4572	0.0863	1.0119	1.0608	0.0665	4.6026	-0.0121	0.9983	0.9912	0.0073
1.5202	0.0842	1.0117	1.0593	0.0654	4.7285	-0.0149	0.9979	0.9892	0.0053
1.5831	0.0829	1.0115	1.0584	0.0648	4.8543	-0.0164	0.9977	0.9881	0.0043
1.6460	0.0814	1.0113	1.0574	0.0642	4.9802	-0.0200	0.9972	0.9856	0.0018
1.7090	0.0793	1.0110	1.0559	0.0631	5.1061	-0.0228	0.9968	0.9835	-0.0002
1.7719	0.0750	1.0104	1.0529	0.0605	5.2316	-0.0242	0.9966	0.9826	-0.0012
1.8348	0.0719	1.0100	1.0508	0.0587	5.3575	-0.0275	0.9961	0.9802	-0.0035
1.8978	0.0692	1.0097	1.0488	0.0572					
1.9607	0.0656	1.0092	1.0464	0.0550					
2.0237	0.0636	1.0089	1.0449	0.0539					
2.0862	0.0614	1.0086	1.0434	0.0527					
2.1492	0.0592	1.0083	1.0418	0.0515					
2.2121	0.0578	1.0081	1.0409	0.0508					
2.2750	0.0560	1.0079	1.0396	0.0498					
2.3380	0.0522	1.0073	1.0369	0.0474					
2.4009	0.0502	1.0071	1.0355	0.0463					

UTIAS Technical Note No. 251

Institute for Aerospace Studies, University of Toronto
4925 Dufferin Street, Downsview, Ontario, Canada, M3H 5T6

NUMERICAL RECONSTRUCTION OF PART OF AN ACTUAL BLAST-WAVE FLOW FIELD
TO AGREE WITH AVAILABLE EXPERIMENTAL DATA

Lau, S. C. M., Gottlieb, J. J.

1. Blast wave 2. Shock wave 3. Flow-field reconstruction
4. Random-choice method 5. Piston-driven flow

I. Lau, S. C. M., Gottlieb, J. J. II. UTIAS Technical Note No. 251

A new method of solution is presented and validated for the numerical reconstruction of a certain part of an actual blast-wave flow field of interest for planar, cylindrcal and spherical explosions, away from the explosion source where the blast-wave has become sufficiently weak that real-gas effects are unimportant. This method involved, essentially, a trial-and-error process of constructing the best possible path of a fluid particle or equivalent piston at the upstream side of the flow field of interest such that the resulting flow field constructed numerically in front of the equivalent moving piston agrees as well as possible with all available although limited experimental data. For this study, the relatively new random-choice method has been suitably modified to easily handle the numerical computations of the nonstationary flow in front of the moving piston. Finally, the present method is used to reconstruct the flow field for past TNT and ANFO surface explosions, for which the blast-wave amplitudes are less than about 1 MPa. These new results are presented in convenient graphical and tabular form, scaled for the case of a 1-kg TNT surface explosion or its equivalent in a standartd atmosphere, so that they can be utilized readily for different sized explosions at the same or other atmospheric conditions.

Available copies of this report are limited. Return this card to UTIAS if you require a copy.

UTIAS Technical Note No. 251

Institute for Aerospace Studies, University of Toronto
4925 Dufferin Street, Downsview, Ontario, Canada, M3H 5T6

NUMERICAL RECONSTRUCTION OF PART OF AN ACTUAL BLAST-WAVE FLOW FIELD
TO AGREE WITH AVAILABLE EXPERIMENTAL DATA

Lau, S. C. M., Gottlieb, J. J.

1. Blast wave 2. Shock wave 3. Flow-field reconstruction
4. Random-choice method 5. Piston-driven flow

I. Lau, S. C. M., Gottlieb, J. J. II. UTIAS Technical Note No. 251

A new method of solution is presented and validated for the numerical reconstruction of a certain part of an actual blast-wave flow field of interest for planar, cylindrcal and spherical explosions, away from the explosion source where the blast-wave has become sufficiently weak that real-gas effects are unimportant. This method involved, essentially, a trial-and-error process of constructing the best possible path of a fluid particle or equivalent piston at the upstream side of the flow field of interest such that the resulting flow field constructed numerically in front of the equivalent moving piston agrees as well as possible with all available although limited experimental data. For this study, the relatively new random-choice method has been suitably modified to easily handle the numerical computations of the nonstationary flow in front of the moving piston. Finally, the present method is used to reconstruct the flow field for past TNT and ANFO surface explosions, for which the blast-wave amplitudes are less than about 1 MPa. These new results are presented in convenient graphical and tabular form, scaled for the case of a 1-kg TNT surface explosion or its equivalent in a standartd atmosphere, so that they can be utilized readily for different sized explosions at the same or other atmospheric conditions.

Available copies of this report are limited. Return this card to UTIAS if you require a copy.

UTIAS Technical Note No. 251

Institute for Aerospace Studies, University of Toronto
4925 Dufferin Street, Downsview, Ontario, Canada, M3H 5T6

NUMERICAL RECONSTRUCTION OF PART OF AN ACTUAL BLAST-WAVE FLOW FIELD
TO AGREE WITH AVAILABLE EXPERIMENTAL DATA

Lau, S. C. M., Gottlieb, J. J.

1. Blast wave 2. Shock wave 3. Flow-field reconstruction
4. Random-choice method 5. Piston-driven flow

I. Lau, S. C. M., Gottlieb, J. J. II. UTIAS Technical Note No. 251

A new method of solution is presented and validated for the numerical reconstruction of a certain part of an actual blast-wave flow field of interest for planar, cylindrcal and spherical explosions, away from the explosion source where the blast-wave has become sufficiently weak that real-gas effects are unimportant. This method involved, essentially, a trial-and-error process of constructing the best possible path of a fluid particle or equivalent piston at the upstream side of the flow field of interest such that the resulting flow field constructed numerically in front of the equivalent moving piston agrees as well as possible with all available although limited experimental data. For this study, the relatively new random-choice method has been suitably modified to easily handle the numerical computations of the nonstationary flow in front of the moving piston. Finally, the present method is used to reconstruct the flow field for past TNT and ANFO surface explosions, for which the blast-wave amplitudes are less than about 1 MPa. These new results are presented in convenient graphical and tabular form, scaled for the case of a 1-kg TNT surface explosion or its equivalent in a standartd atmosphere, so that they can be utilized readily for different sized explosions at the same or other atmospheric conditions.

Available copies of this report are limited. Return this card to UTIAS if you require a copy.

UTIAS Technical Note No. 251

Institute for Aerospace Studies, University of Toronto
4925 Dufferin Street, Downsview, Ontario, Canada, M3H 5T6

NUMERICAL RECONSTRUCTION OF PART OF AN ACTUAL BLAST-WAVE FLOW FIELD
TO AGREE WITH AVAILABLE EXPERIMENTAL DATA

Lau, S. C. M., Gottlieb, J. J.

1. Blast wave 2. Shock wave 3. Flow-field reconstruction
4. Random-choice method 5. Piston-driven flow

I. Lau, S. C. M., Gottlieb, J. J. II. UTIAS Technical Note No. 251

A new method of solution is presented and validated for the numerical reconstruction of a certain part of an actual blast-wave flow field of interest for planar, cylindrcal and spherical explosions, away from the explosion source where the blast-wave has become sufficiently weak that real-gas effects are unimportant. This method involved, essentially, a trial-and-error process of constructing the best possible path of a fluid particle or equivalent piston at the upstream side of the flow field of interest such that the resulting flow field constructed numerically in front of the equivalent moving piston agrees as well as possible with all available although limited experimental data. For this study, the relatively new random-choice method has been suitably modified to easily handle the numerical computations of the nonstationary flow in front of the moving piston. Finally, the present method is used to reconstruct the flow field for past TNT and ANFO surface explosions, for which the blast-wave amplitudes are less than about 1 MPa. These new results are presented in convenient graphical and tabular form, scaled for the case of a 1-kg TNT surface explosion or its equivalent in a standartd atmosphere, so that they can be utilized readily for different sized explosions at the same or other atmospheric conditions.

Available copies of this report are limited. Return this card to UTIAS if you require a copy.